

**DEVELOPMENT AND CHARACTERISATION OF  
MEDICATED WOUND DRESSINGS FOR CHRONIC WOUND  
HEALING**

**By**

**HARSHAVARDHAN VILASRAO PAWAR {BPharm, MRes (Pharm. Sci.)}**

**A thesis submitted in partial fulfilment of the requirements of the University of  
Greenwich for the degree of Doctor of Philosophy**

**July, 2013**



**UNIVERSITY  
of  
GREENWICH**

**DECLARATION**

“I certify that this work has not been accepted in substance for any degree, and is not concurrently being submitted for any degree other than that of Doctor of Philosophy being studied at the University of Greenwich. I also declare that this work is the result of my own investigations except where otherwise identified by references and that I have not plagiarised the work of others”.

.....

**HARSHAVARDHAN PAWAR (CANDIDATE)**



**PHD SUPERVISORS**

**DR. JOSHUA BOATENG** .....

**DR JOHN TETTEH** .....

**FEBRUARY 2014**

## ACKNOWLEDGEMENTS

First and foremost, I would like to take this opportunity to thank the almighty God for His loving kindness and faithfulness in sustaining my life all these years. To the greatest extent thanks to Dr. Joshua Boateng for giving me such opportunity to work on this project and thanks for your steadfast support, encouragement, understanding and guidance. Your insight was pivotal in allowing me to complete my PhD. I would like to extend my deepest gratitude and appreciation to my second supervisor Dr. John Tetteh for his advice, guidance and many critical discussions. I would like to thank my parents who always provided constant love, freedom and support for doing the PhD.

I would also like to acknowledge the University of Greenwich for nominating me for ORSAS funding and the School of Science for making up the difference in my tuition fees to complete my PhD. I am grateful to Dr Isaac Ayensu and Dr Farnoosh Kianfar, for being my second pair of eyes giving me suggestions in exploring new ideas. I would like to acknowledge Dr Concetta Giovino, Dr Nazanin Zand and Dr Arun Kumar Kotha for their selfless help throughout my PhD. I am also grateful to Dr. Ian Slipper for all the SEM and XRPD techniques and Devyani Amin for the HPLC analysis and troubleshooting of the HPLC and Samantha Lewis for her help during microbiological studies. Thanks also to all other staff and technicians for supporting me during the experimental work.

Last but not least I would like to thank to Amit Patil, Vilas Beloshe, Nilesh Manikwar, Anniruddha Bhagurkar, Shankar Manjare and Prithviraj Patil and roommates who have given me constant support and financial help when I asked. Big thanks to Amit Bhosale for cheering me up every time throughout my PhD. You guys are amazing, without all of you it will not be possible to pass this journey. I am obliged to express my gratitude to my research group members and all the persons who met me on the path of this journey and helped me directly and indirectly to complete my studies.

## ABSTRACT

Chronic wounds are difficult to heal and exhibit physiological features including prolonged inflammatory phase, mixed bacterial flora resistance and formation of biofilms, ineffectiveness of topical antimicrobials and high volumes of wound exudate. Polymeric gels of Polyox (POL) and blends of POL with carrageenan (CAR), chitosan (CS), hydroxypropylmethylcellulose (HPMC) and sodium alginate (SA) in different weight ratios were used to prepare films by the solvent casting technique and evaluated using scanning electron microscopy (SEM), X-ray powder diffraction (XRPD), differential scanning calorimetry (DSC) and Fourier transform spectroscopy (FTIR). The same gels were analysed using DSC to develop an optimum lyophilisation cycle with or without an annealing step to obtain freeze dried wafers of POL-CAR and POL-SA. Films prepared from POL were non-transparent and showed spherulitic crystallisation, however POL blends with CAR and SA (75/25 and 50/50 weight ratios respectively) showed improved flexibility and transparency with reduced spherulitic crystallisation (i.e. homogeneous surface) through hydrogen bonding between POL and/or CAR and SA. Addition of annealing step  $-25^{\circ}\text{C}$  resulted in formulations with porous surface morphology for both POL-CAR and POL-SA wafers. Annealing (wafers) and addition of glycerol (GLY) (films) resulted in improved mechanical properties expected to withstand the mechanical stresses occurring during day-to-day activities and whilst flexible enough to prevent potential damage to newly formed tissue. Tough and flexible films were obtained by the addition of 9%w/w and 20% w/w GLY in POL-SA and POL-CAR respectively. Further, the POL-CAR and POL-SA films and wafers were loaded with 5-15%w/w of diclofenac (DLF) and 15-30% w/w of streptomycin (STP). Furthermore POL-CAR and POL-SA blank (BLK) and drug loaded (DL) films and wafers were analysed for swelling, mucoadhesion (in presence of normal and viscous simulated wound fluid), *in vitro* drug dissolution and anti-bacterial activity and compared against marketed medicated wound dressings. Addition of drug (STP and DLF) resulted in fair transparency of films and decreased porosity of wafers with existence of sodium sulphate which affected general performance of the films and wafers in terms of swelling, mucoadhesion, and antimicrobial activity. BLK plasticised (GLY) films and BLK annealed wafers showed higher swelling capacities compared to DL films and wafers. Neither DL films nor wafers showed 100 % release of the incorporated STP and DLF due to the formation of sodium sulphate which reduced hydration. Findings also showed that POL-SA films and wafers were effective against normal exudate whereas POL-CAR films and wafers were effective for

viscous exudate to achieve better bioavailability and prolonged retention time. Multivariate data analysis of mucoadhesion showed slower rate of mucin diffusion into POL-CAR films and wafers compared to POL-SA films and wafers. The formulated films, wafers and marketed dressing showed antibacterial efficacy against  $10^5$  CFU/ml of *S. aureus*, *P. aeruginosa* and *E. coli*. STP and DLF present in both films and wafers acted synergistically and showed better antimicrobial activity than marketed dressings. Film dressing allows ease of application and due to fair transparency and flexibility whereas wafer dressings are useful to control exudate and both can maintain a moist environment. Combination of STP and DLF within a single dressing is expected to help to treat and prevent wound infections whereas DLF can help to relieve pain and inflammation associated with injury.

## TABLE OF CONTENTS

DECLARATION.....	ii
ACKNOWLEDGEMENTS.....	iii
ABSTRACT .....	iv
TABLE OF CONTENTS .....	vi
LIST OF FIGURES .....	xv
LIST OF TABLES.....	xxi
ABBREVIATIONS .....	XXII
LIST OF PUBLICATIONS AND CONFERENCE PROCEEDINGS .....	xxv
CHAPTER 1 : GENERAL INTRODUCTION AND LITERATURE REVIEW .....	1
1.1 OVERVIEW .....	1
1.2 TYPES OF WOUNDS .....	3
1.2.1 Clinical context .....	4
1.2.1.1 Simple wounds .....	4
1.2.1.2 Complex wounds .....	4
1.2.2 Nature of repair process .....	5
1.2.2.1 Acute wounds .....	5
1.2.2.2 Chronic wounds .....	5
1.2.2.3 Exuding wounds .....	7
1.2.3 Skin layers and area of skin layers.....	8
1.2.3.1 Superficial wounds .....	8
1.2.3.2 Partial thickness wounds .....	8

1.2.3.3	Full thickness wounds .....	8
1.2.4	Wounds based on contamination .....	9
1.2.4.1	Clean wounds .....	9
1.2.4.2	Clean contaminated wounds .....	10
1.2.4.3	Contaminated wounds .....	10
1.2.4.4	Dirty wounds .....	10
<b>1.3</b>	<b>WOUND HEALING AND STAGES INVOLVED IN HEALING .....</b>	<b>10</b>
1.3.1	Moist wound healing .....	10
1.3.2	Haemostasis .....	11
1.3.3	Inflammation .....	12
1.3.4	Proliferation .....	13
1.3.5	Remodelling and scar maturation .....	14
<b>1.4</b>	<b>BACTERIAL WOUND INFECTION .....</b>	<b>14</b>
1.4.1	Management of wound infection .....	17
1.4.2	Role of topical antimicrobials .....	17
1.4.3	Exudate associated with acute and chronic wounds .....	25
<b>1.5</b>	<b>WOUND DRESSINGS .....</b>	<b>27</b>
1.5.1	Traditional wound dressings .....	27
1.5.2	Modern wound dressings .....	29
1.5.2.1	Film dressings .....	30
1.5.2.2	Hydrogel dressings .....	30
1.5.2.3	Foam dressings .....	30

1.5.2.4	Hydrocolloid dressings .....	31
1.5.2.5	Alginate dressings.....	31
1.5.2.6	Medicated dressings .....	32
1.5.2.7	Freeze dried wafers.....	33
1.5.3	Biological wound dressings .....	35
<b>1.6</b>	<b>FUNCTIONAL PROPERTIES OF MOIST WOUND DRESSINGS .....</b>	<b>35</b>
1.6.1	Bio (muco)adhesion .....	35
1.6.2	Swelling and drug release .....	37
1.6.2.1	Theories of polymer erosion.....	37
1.6.2.2	Theories of polymer erosion/degradation.....	38
1.6.2.3	Drug release mechanisms .....	39
<b>1.7</b>	<b>POLYMERS, EXCIPIENTS AND DRUGS USED IN THIS PROJECT .....</b>	<b>39</b>
1.7.1	Polyethylene oxide (Polyox <sup>TM</sup> ) .....	39
1.7.2	Carrageenan (CAR) .....	40
1.7.3	Sodium alginate (SA).....	41
1.7.4	Chitosan (CS).....	42
1.7.5	Hydroxypropylmethylcellulose (HPMC).....	43
1.7.6	Plasticizer .....	43
1.7.7	Model drugs .....	45
1.7.7.1	Diclofenac sodium (DLF).....	45
1.7.7.3	Streptomycin sulphate (STP).....	45
<b>1.8</b>	<b>FORMULATION AND CHARACTERISATION .....</b>	<b>46</b>

1.8.1	Freeze drying .....	46
1.8.2	Solvent film casting .....	47
1.8.3	Texture analysis characterisation .....	48
1.8.4	Spectroscopic and chemometric data analysis .....	50
<b>1.9</b>	<b>AIMS AND OBJECTIVES.....</b>	<b>51</b>
<b>CHAPTER 2 : PREPARATION AND PHYSICO-CHEMICAL CHARACTERISATION OF POLYOX™ BASED SOLVENT CAST FILMS.....</b>		<b>53</b>
<b>2.1</b>	<b>INTRODUCTION .....</b>	<b>53</b>
<b>2.2</b>	<b>MATERIALS.....</b>	<b>54</b>
<b>2.3</b>	<b>METHODS.....</b>	<b>55</b>
2.3.1	Preliminary formulation development .....	55
2.3.2	Preparation of blank (BLK) POL-CAR and POL-SA films .....	56
2.3.3	Preparation of drug loaded (DL) POL-CAR and POL-SA films.....	56
2.3.4	Scanning electron microscopy (SEM) .....	57
2.3.5	Differential scanning calorimetry (DSC).....	58
2.3.6	X-ray powder diffraction (XRPD) .....	58
2.3.7	Attenuated total reflectance Fourier transform infrared spectroscopy (ATR-FTIR).....	59
2.3.8	Texture analysis (TA) .....	59
<b>2.4</b>	<b>RESULTS AND DISCUSSION.....</b>	<b>61</b>
2.4.1	Preliminary formulation development .....	61
2.4.2	Scanning electron microscopy (SEM) .....	66
2.4.3	Differential scanning calorimetry (DSC).....	69
2.4.4	X-ray powder diffraction (XRPD) .....	73

2.4.5	Attenuated total reflectance Fourier transform infrared spectroscopy (ATR-FTIR).....	75
2.4.6	Texture analysis (TA) .....	80
<b>2.5</b>	<b>CONCLUSIONS.....</b>	<b>84</b>
<b>CHAPTER 3 : DEVELOPMENT, OPTIMISATION AND PHYSICO-CHEMICAL CHARACTERISATION OF MEDICATED LYOPHILISED WAFER DRESSING.....</b>		<b>86</b>
<b>3.1</b>	<b>INTRODUCTION .....</b>	<b>86</b>
<b>3.2</b>	<b>MATERIALS.....</b>	<b>87</b>
<b>3.3</b>	<b>METHODS.....</b>	<b>87</b>
3.3.1	Preparation of POL-CAR and POL-SA [blank (BLK) and drug loaded (DL)] gels .....	87
3.3.2	Freeze drying cycle development with annealing step .....	87
3.3.3	Lyophilisation .....	88
3.3.4	Scanning electron microscopy (SEM) .....	89
3.3.5	Mechanical properties of wafers (TA).....	90
3.3.6	X-ray diffraction (XRD) .....	90
3.3.7	Differential scanning calorimetry (DSC).....	91
3.3.8	Attenuated total reflectance-Fourier transform infrared spectroscopy (ATR-FTIR) .....	91
<b>3.4</b>	<b>RESULTS AND DISCUSSION.....</b>	<b>92</b>
3.4.1	Freeze drying cycle development with annealing step .....	92
3.4.2	Freeze-drying formulation development and optimisation.....	93
3.4.3	Scanning electron microscopy (SEM) .....	94
3.4.4	Mechanical properties of wafers (TA).....	96
3.4.5	X-ray diffraction (XRD) .....	99
3.4.6	Differential scanning calorimetry (DSC).....	100

3.4.7	Attenuated total reflection-Fourier transform infrared spectroscopy (ATR-FTIR).....	102
<b>3.5</b>	<b>CONCLUSIONS.....</b>	<b>104</b>
<b>CHAPTER 4 : <i>IN VITRO</i> SWELLING AND DRUG DISSOLUTION STUDIES OF</b>		
<b>SOLVENT CAST FILMS AND FREEZE DRIED WAFERS .....</b>		
		<b>105</b>
<b>4.1</b>	<b>INTRODUCTION .....</b>	<b>105</b>
<b>4.2</b>	<b>MATERIALS .....</b>	<b>107</b>
4.2.2	<i>In vitro</i> swelling studies of POL-CAR films .....	107
4.2.3	<i>In vitro</i> drug dissolution studies.....	108
4.2.3.1	Drug dissolution studies for POL-CAR films using phosphate buffer.....	108
4.2.3.2	<i>In vitro</i> drug dissolution studies of films and wafers using SWF .....	109
4.2.4	HPLC analysis .....	110
4.2.5	Drug release kinetics.....	111
<b>4.3</b>	<b>RESULTS AND DISCUSSION .....</b>	<b>111</b>
4.3.1	Swelling capacity of POL-CAR films .....	113
4.3.2	Swelling capacity of POL-SA films .....	115
4.3.3	Swelling capacity of POL-CAR and POL-SA wafers .....	116
4.3.4.2	Release of STP and DLF from the POL-CAR films (SWF).....	121
4.3.4.3	Release of STP and DLF from POL-SA films (SWF).....	122
4.3.4.4	Release of STP and DLF from the POL-CAR and POL-SA wafers (SWF).....	124
4.3.5	Kinetic mechanism.....	125
4.3.6	Comparison of release profiles .....	130
<b>4.4</b>	<b>CONCLUSIONS.....</b>	<b>131</b>

<b>CHAPTER 5 : <i>IN VITRO</i> MUCOADHESION STUDIES OF SOLVENT CAST FILMS AND FREEZE DRIED WAFERS USING TA AND ATR-FTIR .....</b>	<b>133</b>
<b>5.1 INTRODUCTION .....</b>	<b>133</b>
<b>5.2. MATERIALS .....</b>	<b>134</b>
<b>5.3 METHODS.....</b>	<b>135</b>
5.3.1 Mucoadhesion studies by TA [SWF (2% and 5%w/w BSA) and 2%w/w mucin] .....	135
5.3.2 Mucoadhesion studies by ATR-FTIR (2% w/w mucin) .....	136
5.3.3 Chemometric analysis .....	136
5.3.3.1 Overview of target factor analysis (TFA).....	138
<b>5.4 RESULTS AND DISCUSSION.....</b>	<b>147</b>
5.4.1 Mucoadhesion studies by TA [SWF (2% and 5%w/w BSA)] .....	147
5.4.1.1 Unplasticised films .....	147
5.3.1.2 Plasticised films .....	150
5.3.1.3 Drug loaded (DL) films .....	152
5.3.1.4 Freeze-dried wafers (BLK and DL).....	152
5.4.2 Mucoadhesion studies by TA (2%w/w mucin).....	155
5.4.3 ATR-FTIR analysis of mucin diffusion into films and wafers .....	157
5.4.3.1 Diffusion profiles for POL-CAR and POL-SA films .....	161
5.4.3.2 Diffusion profiles POL-CAR and POL-SA wafers .....	163
5.4.3.3 Comparison of BLK films and wafers.....	164
5.4.3.4 Comparison of DL films and wafers .....	165
<b>5.5 CONCLUSIONS.....</b>	<b>167</b>

<b>CHAPTER 6 : EVALUATION AND COMPARISON OF <i>IN VITRO</i> ANTIBACTERIAL EFFICACY OF FILM, WAFER AND COMMERCIAL WOUND DRESSINGS .....</b>	<b>169</b>
<b>6.1 INTRODUCTION .....</b>	<b>169</b>
<b>6.2 MATERIALS .....</b>	<b>170</b>
<b>6.3 FORMULATIONS .....</b>	<b>171</b>
<b>6.3 METHODS.....</b>	<b>172</b>
6.3.1 Bacterial storage and preparation.....	172
6.3.2 Minimum inhibitory concentration (MIC) of STP and DLF .....	172
6.3.3 <i>In vitro</i> antibacterial study .....	173
6.3.3.1 Disk diffusion assay of POL-CAR-DL films using $10^9$ CFU/ml .....	173
6.3.3.2 Disk diffusion assay of films and wafers and marketed dressing using $10^5$ CFU/ml . .....	174
6.3.4 Statistical analysis .....	175
<b>6.4 RESULTS AND DISCUSSION.....</b>	<b>175</b>
6.4.1 Minimum inhibitory concentration (MIC) of STP and DLF .....	175
6.4.2 Antimicrobial efficacy of control pure STP and DLF .....	177
6.4.3 Antibacterial efficacy of POL-CAR films ( $10^9$ CFU/ml) .....	178
6.4.4 Antibacterial activity of POL-CAR films ( $10^5$ CFU/ml) .....	181
6.4.5 Antibacterial activity of POL-SA films ( $10^5$ CFU/ml) .....	182
6.4.6 Antibacterial activity of POL-CAR and POL-SA wafers ( $10^5$ CFU/ml).....	184
6.4.7 Antimicrobial efficacy of marketed wound dressings ( $10^5$ CFU/ml) .....	186
6.4.8 Comparison of antibacterial activity of the film, wafer and marketed wound dressings ... .....	188

<b>6.5</b>	<b>CONCLUSIONS.....</b>	<b>191</b>
	<b>CHAPTER 7 : SUMMARY CONCLUSIONS AND FUTURE WORK .....</b>	<b>193</b>
<b>7.1</b>	<b>SUMMARY CONCLUSIONS.....</b>	<b>193</b>
<b>7.2</b>	<b>FUTURE WORK.....</b>	<b>196</b>
	<b>CHAPTER 8 : REFERENCES .....</b>	<b>198</b>
	<b>CHAPTER 9 : APPENDIX.....</b>	<b>224</b>
	<b>Appendix A: Manuscript in preparation.....</b>	<b>224</b>
	<b>Appendix B: Abstract and posters from conference proceedings.....</b>	<b>225</b>
	1 <sup>st</sup> UK Hydrocolloids Symposium, Yorkshire, UK (2013): Abstract#.....	225
	UKICRS Reading UK (2013): Poster# 29.....	227
	AAPS, San Antonio, Texas (2013): Abstract# 654.....	228
	AAPS Chicago Illinois (2012): Abstarct# 1307 .....	229
	APS-UK-PharmaSci- Nottingham, UK (2012): Poster# 46 .....	230
	SAWC Spring Atlanta, Georgia (2012): Abstract# WHS20120035 .....	231
	APS-UK-PharmaSci- Nottingham, UK (2011): Poster# .....	232
	APS-UK-PharmaSci- Nottingham, UK-(2011): Poster#.....	233
	APS-UK-PharmaSci- Nottingham, UK-2010: Poster# .....	234

## LIST OF FIGURES

Figure 1.1 (A) Arterial ulcer at the cross malleolus of the leg with sharp margins and a punched out appearance; (B) Venous stasis ulcer with irregular border and shallow base, (C) Diabetic foot ulcer with surrounding callus, severe ulcer caused by diabetic neuropathy and bony deformity; (D) Pressure ulcer in a paraplegic (impairment of motor or sensory function in the lower extremities) patient, causing full-thickness skin loss (Adapted from Fonder <i>et al.</i> , 2008).	7
Figure 1.2: Partial dermal thickness wound with the irregular and patchy surface and islets of epithelium (Adapted from Beldon, 2010).	9
Figure 1.3: Schematic representation of different stages involved in the wound healing process (a) wound or injury (b) haemostasis (c) inflammatory phase (d) proliferation (e) remodelling and scar maturation (Beanes <i>et al.</i> , 2003).	13
Figure 1.4: A prolonged inflammatory response due to infection or presence of foreign material delays the progression through normal phases of acute wound healing (Franz <i>et al.</i> , 2007).	16
Figure 1.5: A typical example of a high exuding wound (adapted from CiniMed, 2012).	25
Figure 1.6: Schematic representation of drug release mechanism from films and wafers (Siepmann and Siepmann, 2008).	37
Figure 1.7: Chemical structure of polyethylene oxide.	40
Figure 1.8: Typical structure of CAR.	41
Figure 1.9: Chemical structure of alginate containing mannuronate and guluronates residue.	42
Figure 1.10: Chemical structure of CS.	42
Figure 1.11: Chemical structure of hydroxypropylmethylcellulose (HPMC). [Adapted from <a href="http://www.tschem.com.cn/5.htm">http://www.tschem.com.cn/5.htm</a> ]	43
Figure 1.12: Chemical structure of glycerol.	44
Figure 1.13: Structural illustration of DLF and phenothiazine and similarities between the two drugs.	45
Figure 1.14: Chemical structure of STP containing streptobiosamine and streptidine units.	46
Figure 2.1: Illustration of preparation method for polymeric films (BLK and DL).	56
Figure 2.2: Representation of sample cell used for XRPD analysis of the polymeric films.	59
Figure 2.3: Schematic representation of texture analyser for the evaluation of mechanical properties of the films.	60
Figure 2.4: POL films prepared from gels of different concentrations based on total polymer weight.	61

Figure 2.5: Blended films of POL with SA, CAR, CS and HPMC.....	63
Figure 2.6: POL-CAR (BLK and DL) films with or without 20% GLY .....	65
Figure 2.7: Digital images of POL-SA (50/50) BLK and DL films with or without GLY.....	66
Figure 2.8: SEM image of POL film containing spherulitic crystals radially oriented chains.....	67
Figure 2.9: SEM topography of POL blended films with SA, HPMC, CAR or CS (75/25).....	67
Figure 2.10: SEM images of POL-CAR-BLK-20%GLY, POL-CAR-DL and POL-CAR-DL-20%GLY.....	68
Figure 2.11: SEM morphology of POL-SA (BLK and DL) films .....	69
Figure 2.12: Comparison of DSC profiles of pure polymers and drugs.....	70
Figure 2.13: DSC profiles of films prepared from blends of POL with CAR, CS, SA and HPMC. ....	71
Figure 2.14: DSC thermograms of POL-CAR-BLK-20%GLY, POL-SA-BLK-9%GLY, POL-CAR-DL, POL-CAR-DL-20% GLY, POL-SA-DL and POL-SA-DL-9%GLY.....	72
Figure 2.15: XRPD patterns of pure polymers (POL, CS, SA, CAR and HPMC), DLF and STP .....	74
Figure 2.16: XRPD patterns of blended films combining POL with either CS, SA, CAR or HPMC (All in the ratio of 75/25 based on total polymer weight except POL-SA-BLK which was in 50/50 wt ratio). ....	74
Figure 2.17: XRPD patterns of films of POL-CAR-BLK-20%GLY, POL-CAR-DL, POL-CAR-DL-20%GLY, POL-SA-BLK-9%GLY, POL-SA-DL-9%GLY. ....	75
Figure 2.18: FTIR spectra of pure polymers and drugs from bottom POL, CAR, HPMC, CS, SA, STP and DLF (n=3). ....	78
Figure 2.19: FTIR spectra of the blended films from bottom POL-SA, POL-CAR, POL-CS, POL-HPMC in ratio of 75/25wt and top POL-SA in 50/50wt ratio [Inset - shifting of peak of C-O-C stretch of POL chains at 1100 cm <sup>-1</sup> ] (n=3). ....	79
Figure 2.20: FTIR spectra of POL-CAR-BLK-20%GLY, POL-CAR-DL, and POL-CAR-DL-20% GLY films (n=3).....	80
Figure 2.21: Mechanical properties (Toughness, elongation at break, elastic modulus and tensile strength) of POL-CAR (BLK and DL) films (mean±SD, n=3).....	83
Figure 2.22: Mechanical properties (Toughness, elongation at break, elastic modulus and tensile strength) of POL-SA (BLK and DL) films (mean± SD, n=3).....	84
Figure 3.1: Schematic diagram of the lyophilisation cycles used for the preparation of wafers...89	
Figure 3.2: DSC thermogram of the POL-CAR and POL-SA gels (NAn and An) at -25°C.....	93

Figure 3.3: SEM images of POL-CAR-BLK-NAn, POL-CAR-BLK-An, POL-CAR-DL-An, POL-SA-BLK-NAn, POL-SA-BLK-An, POL-SA-DL-An. ....	95
Figure 3.4: Effect of depth of the compression of POL-CAR and POL-SA BLK NAn and An wafers and DL POL-CAR and POL-SA An wafers (at a speed of 1mm/sec, mean± SD, n=5)....	97
Figure 3.5: Effect of speed of compression on POL-CAR and POL-SA BLK (NAn and An) wafers and POL-CAR-DL and POL-SA-DL-An wafers (depth 2.0 mm, mean± SD, n=5).....	98
Figure 3.6: Hardness profiles of POL-CAR-BLK and POL-SA-BLK (An and NAn) and POL-CAR-DL, POL-SA-DL (An) wafers (at a speed of 1mm/sec, depth 2.0mm, mean± SD, n=5)....	98
Figure 3.7: XRD patterns of POL-CAR and POL-SA (BLK-An and DL-An) wafers. ....	100
Figure 3.8: DSC profiles of the pure polymers, drugs and POL-CAR and POL-SA (BLK-An and DL-An) wafers. ....	101
Figure 3.9: FTIR spectra showing peaks for different components within freeze dried POL-CAR and POL-SA (BLK-An and DL-An) wafers.....	103
Figure 4.1: Digital photograph of modified Franz-type diffusion cell as set up for drug release experiments in the current project. ....	110
Figure 4.2: Swelling profiles of POL-CAR films in PBS of pH 7.3 showing plot of % swelling index against time (mean± SD, n=4).....	112
Figure 4.3: Swelling index of POL-CAR films in presence of SWF (mean± SD, n=4). ....	113
Figure 4.4: Swelling profiles showing the change in % swelling index with time of POL-SA films in the presence of SWF (mean ±SD, n=4).....	116
Figure 4.5: Swelling index of POL-CAR and POL-SA wafers in presence of SWF (mean ±SD, n=4).....	118
Figure 4.6: Standard HPLC calibration curves for DLF and STP for determining the release of STP and DLF during the drug dissolution study for the films and wafers.....	119
Figure 4.7: <i>In vitro</i> drug release profiles of (A) DLF and (B) STP from POL-CAR-DL and POL-CAR-DL-20% GLY films showing mean percent cumulative release (mean ±SD, n = 3) against time in presence of phosphate buffer pH 7.3.....	120
Figure 4.8: <i>In vitro</i> drug release profiles of (A)DLF and (B) STP from POL-CAR-DL and POL-CAR-DL-20% GLY films showing plot of mean percent cumulative release (n = 3;±SD) against time in presence of SWF. ....	121
Figure 4.9: <i>In vitro</i> drug release profiles of (A) DLF and (B) STP from POL-SA-DL and POL-SA-DL-9% GLY films showing plot of mean percent cumulative release (n = 3;±SD) against time in presence of SWF. ....	123

Figure 4.10: <i>In vitro</i> drug release profiles of STP and DLF from POL-SA-DL-wafer and POL-CAR-DL-wafer showing plot of mean percent cumulative release (n = 3; $\pm$ SD) against time in presence of SWF.....	125
Figure 4.11: Representative plots of experimental release data of films and wafers fitted into different kinetic models, showing (a) first order (b) zero order (c) Higuchi (d) Hixon-Cromwell cube root law and (e) Korsmeyer-Peppas.....	126
Figure 5.1: ATR assembly for in situ measurement of inter-diffusion of mucin solution through the films and wafers.....	136
Figure 5.2: Schematic layout of the target factor analysis process: (1) complex data matrix (D); (2) chemometric factor analysis; (3) significant factors affecting data matrix; (4) target reference spectra (Rt) used in combination with the R and C; (5) target transformation through least square regression; (6) predicted spectrum (Rp) and concentration profile (Cp).....	140
Figure 5.3: (a) shows a typical ATR-FTIR 3D spectral profile for the selected window 1400-1700 $\text{cm}^{-1}$ (b) overlay plot of raw ATR-FTIR spectral profile (c) significant factor calculated using factor indicator function (IND) (d) percentage significant level (%SL) plotted against the number of factors (e) cumulative percentage variance (CPV) accounted for the abstract factor reproduction. The arrow indicates the cutoff point for the selection of number of significant factors. ....	142
Figure 5.4: Ten abstract factors of the row domain R (spectral profiles) from that only 1, 2 and 3 are significant whereas rest of the factors are experimental noise. ....	143
Figure 5.5: Visual inspection of ten abstract factors corresponding column domain C from that only 1, 2 and 3 are significant whereas rest of the factors are experimental noise. ....	144
Figure 5.6: An example of a match between the reference spectra of mucin (black dotted line) and the predicted spectral profiles of the targets (black solid line) with correlation coefficient of R=0.99915 of diffusion of mucin across the formulation. ....	145
Figure 5.7: The deconvoluted diffusion output of the 2% mucin and other factors within the spectrum window 1400-1700 $\text{cm}^{-1}$ used for the analysis. ....	146
Figure 5.8: Mucoadhesion profiles of unplastised POL-CAR and POL-SA films with SWF containing 2% w/w BSA. ....	149
Figure 5.9: Mucoadhesion characteristics of POL-CAR and POL-SA films with SWF containing 5% w/w BSA. ....	151
Figure 5.10: Mucoadhesion studies of POL-CAR and POL-SA wafers with SWF containing 2% w/w BSA.....	154

Figure 5.11: Mucoadhesion characteristics of POL-CAR and POL-SA wafers with SWF containing 5% w/w BSA. ....	155
Figure 5.12: Mucoadhesion performance of POL-CAR and POL-SA films and wafers showing stickiness, WOA and cohesiveness. ....	157
Figure 5.13: FTIR spectra of mucin powder, 2% mucin (PBS) and PBS solution. ....	158
Figure 5.14: Representative plots of the POL-SA-BLK films showing reproducibility. ....	160
Figure 5.15: Normalised diffusion of mucin across POL-CAR films (mean±SD, n=3).....	162
Figure 5.16: Normalised diffusion of mucin across POL-SA (BLK and DL) films (mean±SD, n=3).....	163
Figure 5.17: Normalised diffusion of mucin across POL-SA (BLK and DL) films (mean±SD, n=3).....	164
Figure 5.18: Normalised diffusion of mucin across BLK films and wafers (mean±SD, n=3)....	165
Figure 5.19: Normalised diffusion of mucin across DL films and wafers (mean±SD, n=3). ....	166
Figure 6.1: Graphical representation of disk diffusion assay .....	175
Figure 6.2: ZOI of (N) control STP (O) control DLF for <i>S. aureus</i> , <i>P. aeruginosa</i> and <i>E. coli</i> . The inset of control DLF shows the absence of bacteria around the applied area of the disk (mean ± SD, n = 3). ....	177
Figure 6.3: Antibacterial activity of STP, DLF and combined (STP + DLF) within film at bacterial load of 10 <sup>9</sup> CFU/ml for (a) <i>S aureus</i> (b) <i>E coli</i> (c) <i>P aeruginosa</i> . (I-DLF reference, II-STP reference, III- POL-CAR-DL films, IV-POL-CAR-DL-20% GLY).....	179
Figure 6.4: ZOI of <i>S. aureus</i> , <i>P. aeruginosa</i> and <i>E. coli</i> for the POL-CAR (DL and DL-20%GLY) films and STP and DLF (mean ± SD, n = 3). ....	181
Figure 6.5: The digital images of ZOI of (A) POL-CAR-BLK, (B) POL-CAR-DL, (C) POL-CAR-DL-20%GLY observed for <i>S. aureus</i> , <i>P. aeruginosa</i> and <i>E. coli</i> (mean ± SD, n=3).....	182
Figure 6.6: ZOI of <i>S. aureus</i> , <i>P. aeruginosa</i> and <i>E. coli</i> for the POL-SA-DL and POL-SA-DL-9%GLY films and control STP and DLF (mean ± SD, n = 3). ....	183
Figure 6.7: The digital images of ZOI of (D) POL-SA-BLK, (B) POL-SA-DL, (C) POL-SA-DL-9%GLY observed for <i>S. aureus</i> , <i>P. aeruginosa</i> and <i>E. coli</i> (mean ± SD, n = 3). ....	184
Figure 6.8: ZOI of <i>S. aureus</i> , <i>P. aeruginosa</i> and <i>E. coli</i> for POL-CAR-DL-An and POL-SA-DL-An wafers and control STP and DLF (mean ± SD, n = 3). ....	185
Figure 6.9: Digital images of ZOI of (G) POL-CAR-BLK-An, (H) POL-CAR-DL-An, (I) POL-SA-BLK-An, (J) POL-SA-DL-An, observed for <i>S. aureus</i> , <i>P. aeruginosa</i> and <i>E. coli</i> (mean ± SD, n = 3). ....	186

Figure 6.10: ZOI of *S. aureus*, *P. aeruginosa* and *E. coli* for the marketed dressings (Aquacel<sup>®</sup> Ag, Melgisorb<sup>®</sup> Ag, Allevyn<sup>®</sup> Ag (mean  $\pm$  SD, n=3). .....187

Figure 6.11: Digital images of ZOI observed for *S. aureus*, *P. aeruginosa* and *E. coli* of (K) Aquacel<sup>®</sup> Ag; (L) Melgisorb<sup>®</sup> Ag; and (M) Allevyn<sup>®</sup> Ag. Inset shows the absence of bacteria at the applied area of dressing (mean  $\pm$  SD, n = 3). .....188

## LIST OF TABLES

Table 1.1: Topical antibiotics and antiseptics products available on the market with their bacterial spectrum, advantages and disadvantages for wound healing (Lipsky and Hoey 2009).	19
Table 1.2: Different types, colours and significance of exudates present at wound site (Cutting, 2004).....	26
Table 1.3: The desirable characteristics of wound dressings required for wound healing and their clinical significance (Wittaya-arekul and Prahsarn, 2006; Khan <i>et al.</i> , 2000; Boateng <i>et al.</i> , 2008).....	28
Table 1.4: Types of wound dressings and their indications of use (Moon and Crabtree, 2003; Stashak <i>et al.</i> , 2004). ....	29
Table 1.5: List of medicated dressing currently available in the market and their available sizes (O'Brien 2008). ....	34
Table 2.1: Quantities used during preparation of polymeric gels of POL and blends of POL with other polymers (CAR, SA, HPMC, and CS). ....	55
Table 2.2: Quantities of the polymers, drugs and GLY (varying amounts based on total solid weight) used for formulation of POL-CAR and POL-SA (BLK and DL) films. ....	57
Table 2.3: Parameters used to evaluate tensile properties of films (n=3).....	60
Table 2.4: The observed FTIR peaks (n=3) for pure polymers and drugs with their characteristic bands (Çaykara <i>et al.</i> , 2005; Azevedo <i>et al.</i> , 2006; Fuller <i>et al.</i> , 2001; Khan <i>et al.</i> , 2000) .....	76
Table 2.5: The effect of drug and plasticizer on mechanical (tensile) properties of selected optimised POL-CAR and POL-SA films (mean $\pm$ SD, n=3). ....	81
Table 3.1: Composition of polymers and drugs (varying quantity) present in gels used to produce freeze dried wafers.....	87
Table 3.2: Lyophilised wafers used to analyse surface morphology.....	90
Table 4.1: Different drug release kinetic models with their respective equation, definition of terms and its implications (Shoeb <i>et al.</i> , 2006).....	106
Table 4.2: Release parameters obtained from fitting experimental drug dissolution (release) data to different kinetic equations for films and wafer containing STP.....	128
Table 4.3: Release parameters obtained from fitting experimental drug dissolution (release) data to different kinetic equations for films and wafers containing DLF. ....	129
Table 4.4: Model independent difference ( $f_1$ ) and similarity ( $f_2$ ) factors for release profiles of STP and DLF and pure drug (STP and DLF) are used as reference batch ( $R_j$ ). ....	130

Table 5.1: Optimised formulations used for the <i>in vitro</i> mucoadhesion study.....	135
Table 5.2: Settings used for mucin diffusion through films and wafers.....	137
Table 5.3: Relative absorption values of the diffusion of mucin for the POL-CAR and POL-SA BLK and DL films and wafers. ....	159
Table 5.4: Diffusion coefficient values for mucin through the optimised films and wafers. ....	161
Table 5.5: Descending order of diffusion of mucin through films and wafers .....	166
Table 6.1: Formulations used to evaluate antimicrobial efficacy against <i>S. aureus</i> , <i>P. aeruginosa</i> and <i>E. coli</i> . ....	171
Table 6.2: Stock solutions of STP and DLF used to evaluate MIC of <i>S. aureus</i> , <i>E. coli</i> and <i>P.</i> <i>aeruginosa</i> (mean $\pm$ SD, n=3). ....	173
Table 6.3: MIC values for STP and DLF for <i>S. aureus</i> , <i>P. aeruginosa</i> and <i>E. coli</i> (mean $\pm$ SD, n = 3).....	176
Table 6.4: ZOI of film, wafer and marketed dressings with the positive control of STP and DLF for <i>S. aureus</i> , <i>P. aeruginosa</i> and <i>E. coli</i> (mean $\pm$ SD, n = 3). ....	178
Table 6.5: The diameter and percentage increase in the ZOI of <i>S. aureus</i> , <i>E. coli</i> and <i>P.</i> <i>aeruginosa</i> using bacterial load of $10^9$ CFU/ml (mean $\pm$ SD, n = 3). ....	180
Table 6.6: Description of the silver containing dressings used for antimicrobial study (Hamberg <i>et al.</i> , 2012).....	187

## ABBREVIATIONS

<b>Abbreviation</b>	<b>Meaning</b>
AIDS	Acquired immune deficiency syndrome
ATR-FTIR	Attenuated total reflection-Fourier transform infra-red
BHT	Butylated hydroxytoluene
BLK	Blank
CAR	$\kappa$ -carrageenan
CMC	Carboxymethylcellulose
CS	Chitosan
DL	Drug loaded
DLF	Diclofenac sodium
DSC	Differential scanning calorimetry
FDA	Food and drug administration
GLY	Glycerol
HPLC	High-performance liquid chromatography
HPMC	Hydroxypropylmethylcellulose
ICH	International Conference on Harmonisation
KI	Potassium iodide
MCT	Mercury-cadmium-telluride
MRSA	Methicilline resistant <i>Staphylococcus aureus</i> ;
PAF	Peak adhesive force
PBS	Phosphate buffered saline
POL	Polyox
SEM	Scanning electron microscopy

SA	Sodium alginate
STP	Streptomycin sulphate
SWF	Simulated wound fluid
TA	Texture analyser
WOA	Work of adhesion
XRPD	X-ray powder diffraction

## **FORMULATIONS**

## **MEANING**

POL-CAR	Polyox-carrageenan
POL-CS	Polyox-chitosan
POL-HPMC	Polyox-hydroxypropylmethylcellulose
POL-SA	Polyox-sodium alginate
POL-CAR-BLK	Blank polyox-carrageenan film
POL-CAR-BLK-GLY	Blank and plasticised polyox-carrageenan film
POL-CAR-DL	Drug loaded polyox-carrageenan film
POL-CAR-DL-GLY	Drug loaded and plasticised polyox-carrageenan film
POL-SA-BLK	Blank polyox-sodium alginate film
POL-SA-BLK-GLY	Blank and plasticised polyox-sodium alginate film
POL-SA-DL	Drug loaded polyox-sodium alginate film
POL-SA-DL-GLY	Drug loaded and plasticised polyox-sodium alginate film
POL-CAR-BLK-An	Blank polyox-carrageenan annealed wafer
POL-CAR-BLK-NAn	Blank polyox-carrageenan non-annealed wafer
POL-CAR-DL-An	Drug loaded polyox-carrageenan annealed wafer
POL-SA-BLK-An	Blank polyox-sodium alginate annealed wafer
POL-SA-BLK-NAn	Blank polyox-sodium alginate non-annealed wafer
POL-SA-DL-An	Drug loaded polyox-sodium alginate annealed wafer

## LIST OF PUBLICATIONS

- Boateng J. S., Ayensu I., **Pawar H. V.** Chitosan, in *Mucoadhesive Materials and Drug Delivery Systems*, Ed Khutoryanskiy V. Wiley (In Press, 2013)
- Boateng J. S., Mitchell J.C., **Pawar H. V.**, Ayensu I. Physico-chemical characterisation and in-vitro / ex vivo permeation studies of insulin loaded thiolated chitosan xerogels, *Peptide and Protein Letters*, (In Press 2014).
- Pawar, H. V.**, Tetteh, J. and Boateng, J. S. (2013) 'Preparation, optimisation and characterisation of novel wound healing film dressings loaded with streptomycin and diclofenac', *Colloids and surfaces. B, Biointerfaces*, 102, 102-10.
- Boateng, J. S., **Pawar, H. V.** and Tetteh, J. (2013) 'Polyox and carrageenan based composite film dressing containing anti-microbial and anti-inflammatory drugs for effective wound healing', *International Journal of Pharmaceutics*, 441(1–2), 181-191.
- Pawar, H.**, Douroumis, D. and Boateng, J. S. (2012) 'Preparation and optimization of PMAA–chitosan–PEG nanoparticles for oral drug delivery', *Colloids and Surfaces B: Biointerfaces*, 90, 102-108.
- Pawar H. V.** Tetteh J., Boateng J. S. (2012), Preparation and evaluation of streptomycin and diclofenac loaded mucoadhesive films for wound healing SAWC-SPRING 2012, *Wound Repair and Regeneration*, 20 (2), A34.

## CONFERENCE PROCEEDINGS

- H. V. Pawar**, J. Tetteh, J. Boateng. 2013. Multi-targeted Alginate Based Medicated Wafers for Chronic Wound Healing, AAPS, San Antonio, Texas
- H. V. Pawar**, J. Tetteh, J. Boateng. 2013. Preparation and characterisation of novel medicated dressings for chronic wound healing, UKICRS, Reading, UK.
- H. V. Pawar**, J. Tetteh, J. Boateng. 2012. Preparation and evaluation of solvent cast film dressings containing streptomycin and diclofenac for wound healing. AAPS, Chicago.
- H.V. Pawar**, J. Tetteh, J.S. Boateng. 2012. Preparation and characterization of Polyox-carrageenan films containing antimicrobial and anti-inflammatory drugs for wound healing UKPHARMSCI, Nottingham (**Podium presentation**).
- H. V. Pawar**, J. Tetteh, J.S. Boateng. 2011. Preparation and optimization of anti-infective mucoadhesive films for wound healing applications. UKPHARMSCI, Nottingham.
- H. V. Pawar**, J. Tetteh, J.S. Boateng. 2011. Preparation and characterization of novel mucoadhesive films comprising polyox for wound healing applications UKPHARMSCI Nottingham.
- H. V. Pawar**, D. Douroumis, J. S. Boateng, (2010). Preparation and optimization of PMAA-Chitosan-PEG nanoparticles for oral drug delivery. *Journal of Pharmacy and Pharmacology*. 62 (10) S1463 (**Podium presentation**).

## CHAPTER 1: GENERAL INTRODUCTION AND LITERATURE REVIEW

### 1.1 Overview

Over the years, numerous attempts have been made to accelerate wound healing by improving the nature and functional components of wound dressings. There are number of wound care products available on the market applied to aid the healing of wounds (Bradley *et al.*, 1999; Thu *et al.*, 2012). Their primary function is to keep the wound moist, clean and avoiding entry of harmful bacteria into the wound (Boateng *et al.*, 2008).

In the past, traditional dressings such as natural or synthetic bandages, cotton wool, lint and gauzes all with varying degrees of absorbency were used for the management of wounds. These dry conventional dressings provide passive wound protection and one of their limitations is the inability to maintain a moist environment for effective wound healing (Boateng *et al.*, 2008). Furthermore, other conventional semi-solid formulations such as creams and gels cannot maintain effective drug concentrations for a prolonged period of time at moist wound surfaces due to their short retention times. They are also associated with leakage and messiness in highly exuding wounds which leads to inconvenience and poor patient compliance (Dobaria *et al.*, 2009). Subsequently, there was a desire for modern wound dressings which keep the wound moist and helps more rapid healing of the wound (Ross, 1971). These modern dressings offer an optimum microenvironment for healing (Wittaya-areekul and Prahsarn, 2006; Hanna and Giacobelli, 1997). For example, Dobaria *et al.*, (2009) found that bioadhesive polymers have the capacity to stick to the mucosal epithelial surface whilst at the same time maintaining a moist wound environment, therefore overcoming limitations associated with semi-solid formulations and dry traditional dressings (Dobaria *et al.*, 2009).

Beneficial effects of moist wounds over a dry wound environment include prevention of tissue dehydration and cell death, accelerated angiogenesis, increased breakdown of dead tissue and fibrin (Field and Kerstein, 1994). Optimum wound healing also requires adequate blood supply, tissue perfusion (Albritton, 1991; Robson *et al.*, 1990) and white blood cells for debridement and decontamination (Hanna and Giacobelli, 1997; Albritton, 1991). Oxygen perfusion assists collagen synthesis and angiogenesis which improves wound healing (Ross, 1971). There are other factors which significantly affect wound healing including nutritional status, age, systemic disease [e.g. diabetes and acquired immune deficiency syndrome (AIDS),

medication (e.g. chemotherapy) and bacterial infection along with size, depth, cause and etiology of the wound (Guo and Dipietro, 2010).

Solvent cast films and lyophilised wafers prepared from bioadhesive polymers have been used for delivering drugs to moist surfaces such as wounds, vagina, nasal, and buccal cavities due to their biocompatible and biodegradable properties (Ayensu *et al.*, 2012; Boateng *et al.*, 2009, 2010; Kianfar *et al.*, 2012, 2013). An ideal film dressing is required to be flexible, possess homogeneous and smooth surfaces (Boateng *et al.*, 2009). Film dressings provide a simple and effective method of creating a moist wound environment and promote healing in shallow wounds (Sussman, 2010). Films have the advantage of ease of application especially around joints and other difficult areas due to their flexibility. In low exuding wounds, transparent films help to examine the wound bed without the need for removal of the dressing. However, highly exuding chronic wounds such as diabetic foot and venous ulcers limit the application of films. This has resulted in the need for other modern dressings which can absorb higher amounts of exudate and prevent maceration of healthy skin tissue around the wound site (Boateng *et al.*, 2009). Polymeric gels (and solutions) loaded with therapeutic agents and freeze dried to form lyophilised wafers, can be applied to the surface of exuding wounds (Matthews *et al.*, 2005). Wafers are useful to control exudate and maintain a moist environment without damage to newly formed tissue (Matthews *et al.*, 2006). Freeze dried wafers have been developed and proposed as vehicles for the delivery of various therapeutic compounds to mucosal surfaces including exuding wounds (Labovitiadi *et al.*, 2012; Ayensu *et al.*, 2012). They also offer higher drug loading capacity compared with solvent cast films and other semi-solid polymer gels (Boateng *et al.*, 2009).

Antimicrobial agents such as antibiotics and antiseptics are useful for managing wound infections as they reduce the infection rate and ultimately improve wound healing (Forbes, 1961). However, the persistent emergence of resistant microbial strains has resulted in the need for alternative treatments for wound infections. Systemic antibiotic treatment can also be difficult in certain ulcers such as diabetic ulcers due to the poor blood circulation at the extremities (Bowler *et al.*, 2001). Combined therapy using drugs with different therapeutic effects is an effective way in disease therapy and tissue repair. Streptomycin sulphate (STP) in combination with diclofenac sodium (DLF) has been reported to demonstrate synergistic antimicrobial activity systemically (Dutta *et al.*, 2004, 2007). Combination of STP and DLF within a single dressing can act on two phases of wound healing with STP preventing as well as

treating wound infections whilst the anti-inflammatory drug DLF can target the inflammatory phase of wound healing and relieve pain associated with injury.

This thesis describes the formulation design, optimisation and physico-mechanical characterisation of solvent cast films and freeze dried wafers from Polyox<sup>®</sup> 301 (POL) combined with known hydrophilic polymers [carrageenan (CAR), hydroxypropylmethylcellulose (HPMC), sodium alginate (SA) and chitosan (CS)] as potential wound dressing containing antimicrobial and anti-inflammatory drugs for rapid wound healing. The nature and types of wounds as well as the complex processes involved in wound healing are reviewed. The ideal characteristics and different types of wound dressings available, their advantages and challenges have been critically discussed. The role of topical antimicrobials used in the management of wound infections, their advantages and disadvantages are also discussed in detail. Exudate associated with wounds and different types of dressings and their applications are reviewed. Bio analytical characterisation such as mucoadhesion, swelling and drug release mechanisms in addition to multivariate data analysis are described in detail. Films and wafers have been prepared and characterised for morphology, thermal behaviour, mucoadhesion and mechanical properties using scanning electron microscopy (SEM), differential scanning calorimetry (DSC), and texture analysis (TA) respectively as these affect functional characteristics such as residence (retention at wound site) and moisture absorption capacity. The data obtained from characterisation of wafers has been used to compare morphology and mechanical strength of non-annealed and annealed wafers whereas films were analysed for the effect of glycerol (GLY) and model drugs (STP and DLF). Both formulations have been further evaluated using swelling, *in vitro* drug release (by Franz diffusion cell at 37°C) studies and mucoadhesion studies using TA and attenuated total reflectance Fourier transform infrared spectroscopy (ATR-FTIR) in combination with multivariate data analysis. *In vitro* antibacterial study of optimised films, wafers and commercial wound dressings was carried out using disk diffusion method. Finally, the optimised formulations were compared with selected commercially available medicated dressings.

## **1.2 Types of wounds**

According to the Wound Healing Society (WHS), a wound is the consequence of disruption of normal anatomic structure and function. It usually describes the rupture or defect in skin or body tissue due to physical or thermal damage or a consequence of underlying physiological and medical conditions (Boateng *et al.*, 2008). A wound can also be defined as a

discontinuity in the body which can be restored quickly by maintaining homeostasis (Enoch and Leaper, 2008). Wounds are classified into different categories depending upon their clinical perspective (context), nature of the repair process, skin layers affected and contamination occurring in the wound. These are discussed in brief as follows.

### **1.2.1 Clinical context**

Wounds are classified according to their complication and provide useful clinical information for effective wound management. It can be simple, complex (or complicated) wounds (Kumar and Leaper, 2005).

#### **1.2.1.1 Simple wounds**

A simple wound is one without much complication and involves only skin and subcutaneous tissue without major tissue loss. Simple wounds appear cosmetically aesthetic after healing (Enoch and Leaper, 2005; Kumar and Leaper, 2005).

#### **1.2.1.2 Complex wounds**

The Surgical Infection Study Group (SISG) described characteristics of wound infection in complicated wounds as ‘a purulent discharge in, or exuding from the wound and spreading of erythema indicative of cellulitis’ (Wilson, 1995). Complex wounds include traumatic and orthopaedic, blunt or penetrating injuries, open fracture, laparotomy and wounds particularly in the extremities with extensive loss of the integument and soft tissue infections (Park *et al.*, 2010; Schatzker and Tile, 2005; Enoch and Leaper, 2005; Kumar and Leaper, 2005; Percival, 2002). The above are all complex whether they are acute or chronic wounds (Ferreira *et al.*, 2006). Further, complex wounds concerned with secondary complications include wound infection, compartment syndrome or necrosis (Enoch and Leaper, 2005). Gas gangrene is another example of complex wound which is a rapid progressive infection of muscle and soft tissue found mainly in contaminated traumatic wounds by anaerobic, gram-positive, spore-forming bacillus of *Clostridium septicum*, *Clostridium sporogenes*, and *Clostridium novyi* (Parvizi, 2010). Compartment syndrome is a complex condition which involves muscle and nerve ischemia due to bleeding or oedema in closed muscle compartment (Gourgiotis *et al.*, 2007). Complex wounds are also associated with signs of circulation impairment either localized or more extensive (usually in the limbs), leading to extensive loss of subcutaneous tissue (Ferreira *et al.*, 2006).

## **1.2.2 Nature of repair process**

The wound healing process is a complex phenomenon and involves different phases which are discussed in a later section. Based on the nature of the repair process wounds are classified as acute or chronic wounds.

### **1.2.2.1 Acute wounds**

Wounds that completely heal within 8-12 weeks with minimal scarring are known as acute wounds (Boateng *et al.*, 2008) and usually involve tissue injuries such as trauma or inflammation. Principal causes of acute wounds include mechanical injuries which are caused by external factors such as abrasion, incision, laceration, degloving injury and ulceration. It also includes penetrating wounds (knives or gunshot), surgical cuts, chemical injuries (burns) and thermal burns (Kumar and Leaper, 2005).

### **1.2.2.2 Chronic wounds**

All chronic wounds arise from tissue injuries and usually take beyond 12 weeks to heal and often reoccur. Such wounds fail to heal due to repeated tissue insults or underlying physiological conditions (Boateng *et al.*, 2008). Compared with acute wounds, chronic wounds represent a medical challenge due to various complicating factors connected with the wound. These factors include diabetes, malignancies, chronic systemic inflammation, persistent infection (e.g. sepsis), and destruction of neighbouring tissues, poor primary treatment and other patient related factors such as poor nutrition. These result in a disruption of normal orderly sequence of events during the wound healing process (Boateng *et al.* 2008; Kirketerp-Moller *et al.*, 2011). Chronic wounds are traditionally divided into three major groups due to similarities in their pathogenesis, venous leg ulcers, diabetic foot ulcers, and pressure ulcers. Additionally, there are other subgroups such as ischemic and inflammatory ulcers (Kirketerp-Moller *et al.*, 2011). Venous leg ulcers are triggered by malfunction of venous valves causing venous hypertension in the crural veins (veins supplying the leg), which increases the pressure in capillaries and results in oedema. Venous pressure exceeding 45 mmHg certainly leads to development of a venous leg ulcer. Diabetic foot ulcer is triggered by monotonous load on the neurophatic and often ischemic foot while pressure ulcers are caused by sustained or repetitive load on often vulnerable areas such as the sciatic (spinal nerve roots), tuberculum, sacral area, heels, and shoulders in the immobilized patient (Bjarnsholt *et al.*, 2008). Patients with chronic ulcers usually present with

underlying complicated factors caused by immunological defects, dysfunction in diabetic fibroblasts and the effect of local infection or critical colonization and disruptive effects of bacteria in the form of increased cytokine cascades that prolong the inflammatory phase by continuous influx of polymorphonuclear neutrophils which release cytotoxic enzymes, free oxygen radicals, and inflammatory mediators. These factors are responsible for cellular dysfunction and damage to the host tissue (Carter *et al.*, 2010), which cause delays or stop completely, the wound healing process (Falanga, 2000). Figure 1.1 represents the different types of chronic wounds. Chronic wounds associated with the skin are usually in a permanent state of inflammation; though, there is no simple theory that clearly describes the mechanism of this inflammation (Wild *et al.*, 2010). Chronic and severe wounds are the most difficult wounds to heal and have been the focus of significant research and product innovation in recent years. Chronic wounds, including pressure sores, leg ulcers, diabetic foot ulcers and other kinds of wounds, which heal by secondary intention are common in the community (hospitals, social wound care) surroundings. The prevention and treatment of chronic wounds involve many strategies, including the use of various wound dressings, bandages, antimicrobial agents, footwear, physical therapies and educational approaches (O'Meara *et al.*, 2000). Lifestyle diseases such as diabetes, obesity, and cardiovascular diseases are increasing day by day which is expected to result in an increase in the number of cases of chronic wounds. Globally, the projected number of diabetic patients was 246 million people in the year 2007 and is expected to rise to 380 million people by the year 2025 (Diabetes Atlas *cited in* Kirketerp-Moller *et al.*, 2011). Wound care alone costs the United States healthcare system more than \$20 billion each year, including more than \$4 billion spent on wound management products (Jackson and Stevens, 2006). The management of chronic wounds places an enormous drain on healthcare resources with studies revealing the calculated cost of wound care to the NHS to be about £1 billion a year. In the United Kingdom, around 24,000 admissions a year are for patients with diabetic foot ulceration alone, which costs the NHS some £17 million (Harding *et al.*, 2002).



## Common chronic wounds

Figure 1.1 (A) Arterial ulcer at the cross malleolus of the leg with sharp margins and a punched out appearance; (B) Venous stasis ulcer with irregular border and shallow base, (C) Diabetic foot ulcer with surrounding callus, severe ulcer caused by diabetic neuropathy and bony deformity; (D) Pressure ulcer in a paraplegic (impairment of motor or sensory function in the lower extremities) patient, causing full-thickness skin loss (Adapted from Fonder *et al.*, 2008).

### 1.2.2.3 Exuding wounds

Exudate is the fluid that leaches from wounds whilst exuding wounds are the wounds that significantly produce high volumes of exudate. Highly exuding wounds are difficult to manage which leads to skin maceration, delayed healing, bad odour, infection and frequent dressing change (Sweeney *et al.*, 2012). Surgically created wounds which are deliberately left open for the

normal healing process (healing by secondary intention) or large pressure ulcers and burns are examples of exuding wounds (Adderley, 2008).

### **1.2.3 Skin layers and area of skin layers**

#### **1.2.3.1 Superficial wounds**

Wounds which occur in the epidermal skin surface and papillary dermis are referred to as superficial wounds (Boateng *et al.*, 2008). They heal by epithelialization from surviving pilosebaceous units such as sebaceous glands, sweat glands and hair follicles. No substantial scar formation and wound contraction takes place. Wound healing occurs within 10 days if infection is avoided and an appropriate wound environment is maintained (Percival, 2002).

#### **1.2.3.2 Partial thickness wounds**

Wounds affecting the epidermal and deeper dermal layers alongside blood vessels, sweat glands and hair follicles are called partial thickness wounds (Boateng *et al.*, 2008). Figure 1.2, represents an example of partial thickness wounds with an irregular shape. These wounds heal with a mixture of re-epithelisation from pilosebaceous (also known as sebaceous gland) units and a degree of wound contraction and scar formation. These wounds heal within 10-20 days (Percival, 2002).

#### **1.2.3.3 Full thickness wounds**

This involves damage to the underlying subcutaneous fat or deeper tissues in addition to the epidermis and dermal layers (Boateng *et al.*, 2008). Healing of such wounds occur in two ways: primary healing or secondary healing (Percival, 2002). Primary healing involves closure of surgical wounds by approximation of wound edges using sutures, staples, glue or Steristrips™ which accelerate the healing process with fewer scars. Secondary healing involves normal healing process where the wounds are usually not amenable to surgical closure and left open to granulate and epithelialize from the wound bed and edges (Moon and Crabtree, 2003; Percival, 2002).



Figure 1.2: Partial dermal thickness wound with the irregular and patchy surface and islets of epithelium (Adapted from Beldon, 2010).

#### **1.2.4 Wounds based on contamination**

The USA National Research Council classified wounds into clean, clean-contaminated, contaminated and dirty wounds and are discussed briefly below:

##### **1.2.4.1 Clean wounds**

Clean wounds occur through optional surgery that are neither infected nor involves the respiratory, alimentary or genitourinary tracts (where there is increased risk of infection and contamination). Vital care is taken using antiseptic techniques to avoid infection during primary closure and patients are therefore at low risk for developing a postoperative infection at the surgical site. Examples of clean wounds are vascular and endocrine procedures, eye surgery and simple orthopaedic and surgical procedures involving the skin (Seeley, 1964; Gottrup *et al.*, 2005; Enoch and Leaper, 2008).

#### **1.2.4.2 Clean contaminated wounds**

When wounds closed by adhesive tape or sutures are reopened for drainage or to remove wires, pins or for other surgical reasons, then they are known as clean contaminated wounds. These are clean wounds with a high risk of developing postoperative infection. Examples of clean contaminated wounds are ear surgeries, thoracic, nasal, oropharynx and genitourinary procedures (Gottrup *et al.*, 2005; Enoch and Leaper 2008).

#### **1.2.4.3 Contaminated wounds**

Contaminated wounds involve open accidental wounds, surgeries without acceptable sterile and aseptic techniques and gross leakage from the gastrointestinal tract. Wounds indicating presence of any foreign body such as bullet or knife blade are also known as contaminated wounds. Patients with contaminated wounds are at a high risk of infection and therefore require urgent attention (Enoch and Leaper 2008; Seeley 1964; Gottrup *et al.*, 2005).

#### **1.2.4.4 Dirty wounds**

Wounds having foreign body, devitalized tissue or wounds occurring through postoperative damage of tracheal, bronchial, gastrointestinal and genitourinary tracts are categorised as dirty wounds. These wounds often involve purulent inflammation and abscess formation (Enoch and Leaper, 2008; Gottrup *et al.*, 2005; Seeley, 1964).

### **1.3 Wound healing and stages involved in healing**

Healing of wounds involves complex, dynamic and organised series of biological (biochemical, molecular, physiological) as well as cellular events which internally communicate between cells and related to growth and tissue regeneration (Boateng *et al.*, 2008). A healed wound is one in which the connective tissues have been repaired and the wound area is completely re-epithelialized by regeneration and that has returned to its anatomical structure and functions without the need for continued drainage or dressing (Enoch and Leaper, 2008).

#### **1.3.1 Moist wound healing**

In 1962, George Winter demonstrated that epithelialization occurs twice as fast in moist wounds using polyurethane film compared to dry wounds exposed to air in wounded pigs. He described the latter as “dry healing” which involves formation of clot containing fibrin mesh, red

blood cells, platelets and wound debris. The debris dehydrates to form a hard protective covering known as scab. This results in cell desiccation and death which consumes energy and requires a longer time for the wound to heal. However, in a moist environment, epithelial cells migrate freely at vascular wound surfaces. Winter's theory of moist wound healing was supported by other studies (Winter 1962; *cited in* Bryan 2004). Hinman and Maibach's (1963) research on humans found a similar result of increased rate of epithelialization in obstructed wounds (Hinman and Maibach 1963; *cited in* Bryan 2004). Dyson *et al.*, (1988) examined cellular changes in 42 moist and 42 dry full-thickness wounds in animals. By the third day moist wounds contained almost twice as many macrophages as dry wounds. By day five, they contained significantly fewer inflammatory cells and more proliferative cells, and on day seven had virtually re-epithelialized. In dry wounds large numbers of inflammatory cells remained and epithelialization was still incomplete on day 14 (Dyson *et al.*, 1988). This principle of moist wound healing formed the basis for the introduction of a new range of modern occlusive wound dressings that prevent escape of too much water vapour from the wound surface allowing the maintenance of adequate moisture around the wound environment and these are discussed later in this chapter.

Wound healing is mainly divided into four stages as shown in figure 1.3 which are haemostasis, inflammation, proliferation, remodelling and scar maturation (Enoch and Leaper, 2005; 2008; Boateng *et al.*, 2008).

### **1.3.2 Haemostasis**

This stage is characterised by micro-vascular injury and release of blood components at the wound site. Platelets come in contact with and adhere to the wall of the injured blood vessels. This adherence activates the platelets to release cytokines, growth factors and numerous pro-inflammatory mediators, resulting in platelet aggregation and triggers the intrinsic and extrinsic coagulation pathways to form a fibrin clot which limits further blood loss. Growth factors produced by the platelets initiate the healing cascade. Platelet-derived growth factors (PDGF) activate the chemotaxis of neutrophils and macrophages, smooth muscle cells and fibroblasts. Transforming growth factor-beta (TGF- $\beta$ ) attracts macrophages into the wound area and stimulates them to produce additional cytokines, including fibroblast growth factor (FGF), PDGF, tumour necrosis factor alpha (TNF- $\alpha$ ) and interleukin-1 (IL-1). In addition, TGF- $\beta$

further enhances the fibroblast and smooth muscle chemotaxis and controls the expression of collagen and collagenase (Hantash *et al.*, 2008; Beldon 2010).

### **1.3.3 Inflammation**

The inflammatory phase starts at the same time as haemostasis sometime between a few minutes after injury to 24 h and lasts for about three days. Aggregated platelets store vasoactive amines such as prostaglandins and histamine while other amines from granules released by mast cells, in response to injury, results in increased micro-vascular permeability and vasodilation, leading to exudation of fluid into the extravascular space. This allows the migration of monocytes and protein-rich exudate into the wound and surrounding tissue, resulting in oedema. These are typical signs of the inflammation process and patients start complaining about pain at the site of injury within 24 h. This raises the need for appropriate analgesic provision (Beldon, 2010). Neutrophils infiltrate the wound within an hour of the insult and migrate in sustained levels for the first 48 hours. This is mediated through various chemical signalling mechanisms, including the complement cascade, interleukin activation and TGF- $\beta$  signalling, which leads to neutrophils passing down a chemical gradient towards the wound for destroying debris and bacteria by phagocytosis (Young and McNaught, 2011). This appears as pus or slough at the wound surface. Neutrophils begin to disappear from the wound site through the process of apoptosis. The process of wound cleansing continues with the monocytes which pass to the wound bed through the inflammatory phase. Macrophages are much larger phagocytic cells which reach peak concentration in a wound within 2-3 days after injury. They are attracted to the wound by chemical messengers released from platelets and damaged cells. Macrophages are highly phagocytic and engulf dead cells, bacteria-filled neutrophils, damaged extracellular matrix, debris and any bacteria from the wound site. Macrophages also attract vascular endothelial cells into the wound bed for angiogenesis and production of extracellular matrix by fibroblast (Young and McNaught, 2011). However, if the wound is contaminated with non-viable or necrotic tissue or become infected, then inflammation will be prolonged (Beldon 2010; Hantash *et al.*, 2008; Boateng *et al.*, 2008; Enoch and Leaper 2005). This consequently increases the cost of wound management and can affect the patient's mental health (Beldon 2010).

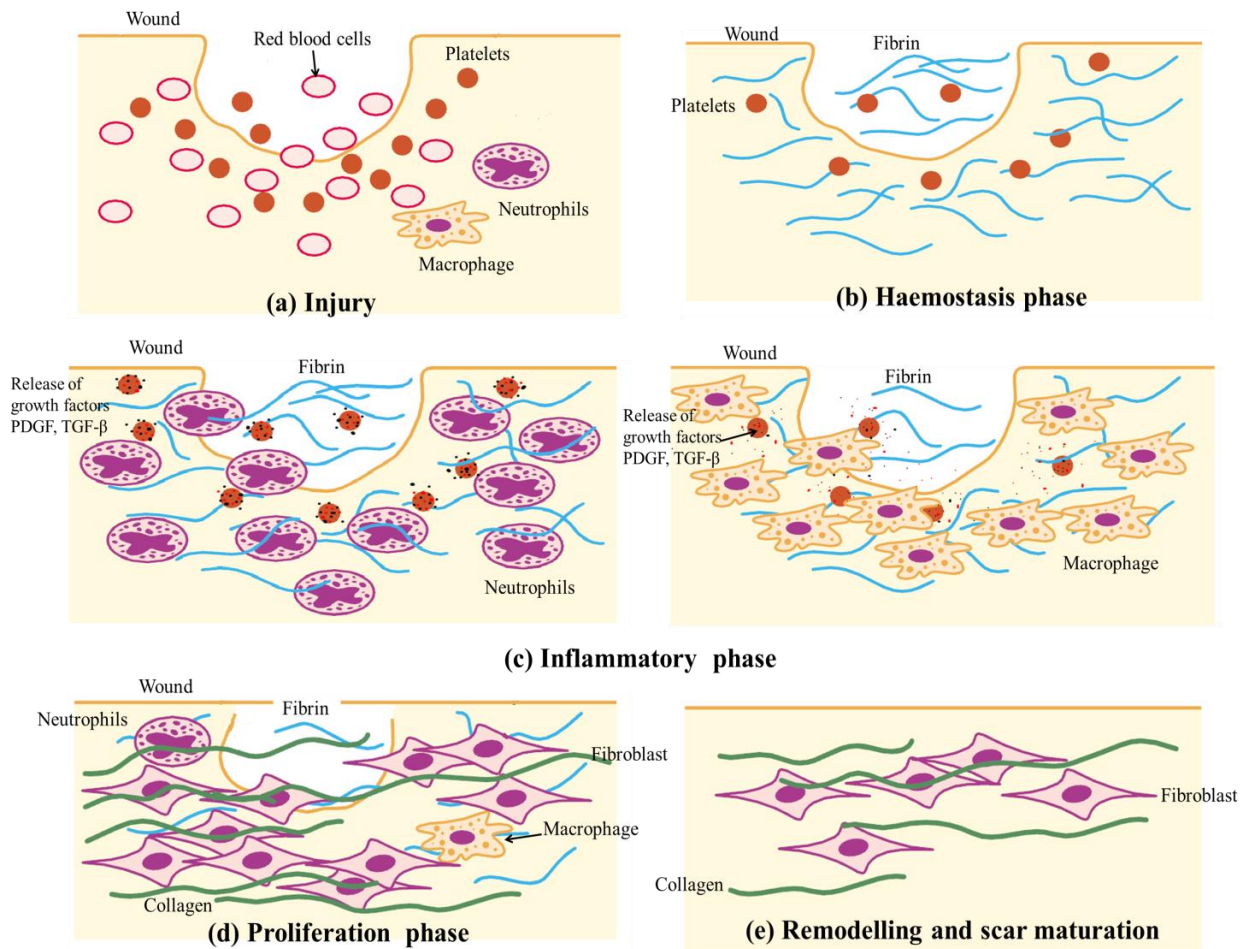


Figure 1.3: Schematic representation of different stages involved in the wound healing process (a) wound or injury (b) haemostasis (c) inflammatory phase (d) proliferation (e) remodelling and scar maturation (Beanes *et al.*, 2003).

### 1.3.4 Proliferation

The proliferative phase starts at about day 3 and lasts for 2-4 weeks after wounding and is characterized by fibroblast migration, deposition of extracellular matrix and formation of highly vascular connective tissue commonly referred as granulation tissue. In this phase, vascular endothelial growth factor (VEGF), basic fibroblast factor (bFF) and TGF- $\beta$  are released which activate neovascularisation (or angiogenesis). Endothelial cells in the venules adjacent to the wound bed initiate capillary production by projecting pseudopods into the wound bed. The low oxygen tension caused by lack of blood supply actually initiates the release of hypoxia-inducible factor (HIF), which regulates the expression of VEGF. As new blood vessels are introduced into the wound environment, the oxygen tension rises and oxygen binds to the HIF, blocking its activity which in turn leads to decreased production of VEGF. The predominant cell responsible

for the formation of the extracellular matrix is the fibroblast; these are attracted into the wound bed by a number of factors, including cytokines produced by macrophages, PDGF and TGF- $\beta$ . Fibroblasts attach to the provisional fibrin matrix and begin the production of collagen which provides tensile strength to the wound bed (Hantash *et al.*, 2008; Enoch and Leaper 2005; Beldon 2010).

### **1.3.5 Remodelling and scar maturation**

Synthesis and remodelling of the extracellular matrix is initiated concurrently with the development of granulation tissue and continues over prolonged periods. Remodelling involves continuous synthesis and breakdown of collagen as extracellular matrix and starts at about 3-4 weeks after wounding. Wound contraction occurs through the interactions between fibroblasts and the surrounding extracellular matrix and is influenced by a number of cytokines and growth factors including TGF- $\beta$ , PDGF, and bFF (Enoch and Leaper, 2005). As scar matures, fibronectin and hyaluronan are broken down and collagen bundles increase in diameter, corresponding with increasing tensile strength of the wound. However, these collagen fibres never regain the original strength of unwounded skin, and a maximum of 80% strength of unwounded skin can be achieved (Enoch and Leaper, 2005).

### **1.4 Bacterial wound infection**

Infection occurs in wounds when one or more microorganisms compete with the host natural immune system. Subsequent invasion of these microorganisms in viable tissue provokes a series of local and systemic host responses such as purulent discharge, painful spreading erythema or symptomatic cellulitis around a wound. Wound infection involves a multitude of microbial and host factors, including type, size, site and depth of wound, extent of non-viable exogenous contamination, level of blood perfusion to the wound, general health and immune status of the host, microbial load and combined level of virulence expressed by types of microorganisms. Most wound infections involve both aerobic and anaerobic microorganisms (Duerden, 1994). Postoperative infection occurs in clean and complicated surgical wounds and the risk of infection is generally based on the susceptibility of a surgical wound to microbial contamination. The former carries a 1-5% risk of infection due to the presence of *Staphylococcus aureus* from a patient's skin flora whereas complicated surgical wounds are more susceptible to endogenous contamination of microorganisms from the gastrointestinal, gynaecologic, or respiratory tracts and involve a 27% of risk of infection (Nichols, 1998). It is estimated that up to

75% of burn injuries present a risk of infection through the contamination by microorganisms from the sweat glands and hair follicles (Church *et al.*, 2006), gastrointestinal and upper respiratory tracts (Revathi *et al.*, 1998; Vindenes and Bjerknes, 1995; Bowler, *et al.*, 2001).

Chronic wounds associated with ulcers and diabetes mellitus are susceptible to infection due to a high incidence of microorganisms and inability of polymorphonuclear leukocytes to deal with impaired migration, phagocytosis and intracellular killing of microorganisms (Oncul *et al.*, 2007). Almost all open injuries are contaminated with different microbes, however, this usually has no clinical significance since they express no evidence of infection and heal as expected. Several wounds are apparently infected and they have pus-filled exudations or some of the cardinal appearances of inflammation such as erythema, warmth, pain or tenderness that have characteristically defined the host response to soft tissue destruction caused by pathogenic and invasive microorganisms (White *et al.*, 2006; 2001). Figure 1.4 shows an example of an infected wound showing the presence of foreign material that delays wound healing. The development of wound infection is directly associated with the inoculum extent and virulence of the colonizing microorganism and inversely associated with local and systemic host resistance (Heinzelmann *et al.*, 2002).

Wound colonisation is defined as presence of multiplying micro-organisms on the surface of a wound, but with no immune response from the host (Ayton, 1985) and with no associated clinical signs and symptoms. Quantitative determination of microbial load has a valid role in predicting the risk of infection and ultimately helps in the management of wounds. High microbial load has a clinical significance in delaying wound healing and has been reported by several authors (Hickey *et al.*, 1997; Bendy *et al.*, 1964; Levine *et al.*, 1976; Bowler *et al.*, 2001) noting that “acute or chronic wound infection exists when the microbial load is  $10^6$  CFU/ml of wound fluid or  $10^5$  CFU/g of tissue”. Breidenbach and Trager (1995) demonstrated that a microbial bio-burden of  $10^4$  CFU/g of tissue is the critical level of bacteria in complex wounds (Breidenbach and Trager, 1995). Distribution of microorganisms within the wound is an important factor which may impact on wound healing. Qualitatively, majority of wounds are poly-microbial containing aerobes (*E. coli*, *S. aureus*, and *Strep. pyogenes*) and anaerobes (*P. aeruginosa*, *B. fragilis* spp, *Peptostreptococcus* spp, *Clostridium* spp, *Prevotella* spp, and *Fusobacterium* spp,) (Brook and Frazier 1998; Bikowski 1999; Gorbach 1994). *S. aureus*, *P. aeruginosa*, and *beta-haemolytic streptococci* are the most common causes of infection and most frequently cited as the reason for delayed wound healing (Brook 1996; Halbert *et al.*, 1992; Sehgal and Arunkumar 1992; Twumdanso *et al.*, 1992; Bowler *et al.*, 2001). A meeting of the

European Tissue Repair Society and the European Wound Management Association in 1998 provided a general opinion that the presence of *beta-haemolytic streptococci* or *P. aeruginosa* in a chronic wound was an indicator for antimicrobial therapy (Bowler *et al.*, 2001). *P. aeruginosa* isolated from burned patients showed resistance to silver based topical antimicrobials and gentamicin due to natural resistance determinants (Japoni *et al.*, 2009). Furthermore, wound healing therapy failures are associated within appropriate initial antibiotic administration with insufficient treatment of multi-drug resistant pathogens. The underlying principle of using combinations of antibiotics is to cover multidrug resistant Gram-negative microorganisms, however, clinical data supporting this strategy are limited (Japoni *et al.*, 2009). Additional factors which influence delayed wound healing due to infection is the efficacy of the host immune response in dealing with microbial infection at the wound site. Other factors involve tissue necrosis, hypoxia, ischemia and other immune deficiencies such as Human immunodeficiency virus (HIV) patients and those undergoing chemotherapy (Bowler *et al.*, 2001). To overcome this problem, a novel dressing containing non-antibiotic compounds which have antibacterial activity and can act through different mechanisms to enhance the antibiotic activity (Mazumdar *et al.*, 2009; Dutta *et al.*, 2004; 2007; 2008; 2009) and reduce the resistance to the microorganisms is needed.

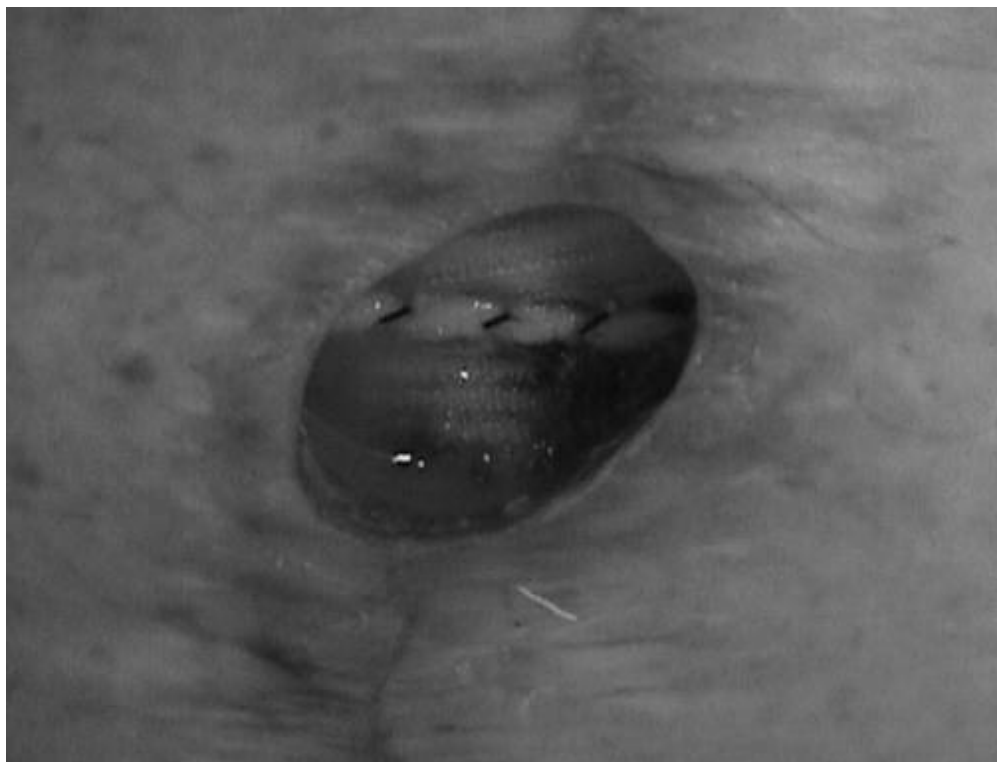


Figure 1.4: A prolonged inflammatory response due to infection or presence of foreign material delays the progression through normal phases of acute wound healing (Franz *et al.*, 2007).

#### **1.4.1 Management of wound infection**

Effective management of wound infection requires reduced exogenous microbial contamination (bio-burden) by using topical and systemic broad-spectrum antimicrobial agents, debridement of devitalized tissue, appropriate dressing and maximization of immune resistance and provision of adequate nutrition (Macmillan, 1980; Hunt, 1981; *cited in Bowler et al., 2001*).

#### **1.4.2 Role of topical antimicrobials**

Topical antimicrobials are compounds which are used to either kill or control the growth of micro-organisms in wounds (White, 2002). Topical antimicrobials are mainly classified as antiseptics and antibiotics and have high specificity to treat wound infection. However, persistent emergence of microbial resistant strains has resulted in the need for alternative treatments for wound infections. Table 1.1 shows the commonly used antiseptics and antibiotics in wound care practice with their advantages and disadvantages. Antiseptics are disinfectants that can be used on intact skin and some open wounds to kill or inhibit microorganisms. They often have multiple microbial targets, a broad antimicrobial spectrum, and residual anti-infective activity but are often toxic to host tissues and cell components (e.g. fibroblasts, keratinocytes, and possibly leukocytes) (Lipsky and Hoey 2009). Antibiotics are potent antimicrobial agents or chemicals with high specificity, produced either naturally (e.g. by a microorganism) or synthetically which in dilute concentrations, inhibit or kill other microorganisms. They usually act on one specific cell target, and are relatively non-toxic as well as being more susceptible to losing their effectiveness to bacterial resistance (Lipsky and Hoey, 2009). However, the relentless emergence of antibiotic-resistant strains of pathogens, together with the retarded discovery of novel antibiotics has led to the need to find alternative treatments for wound infections. Commonly used topical antiseptic agents include iodine-releasing agents (e.g. povidone iodine [PVP-I]), chlorine-releasing solutions (e.g. Dakin's and sodium hypochlorite solutions), hydrogen peroxide, chlorhexidine, silver-releasing agents, and acetic acid. In terms of efficacy, acetic acid (1%) has limited activity but has been used with great success in the management of wounds heavily colonized with *P. aeruginosa* (Phillips and Davey, 1997; Bowler *et al.*, 2001). Honey and sugar paste are considered useful as topical antimicrobial agents, primarily as a consequence of their high osmolarity and ability to minimize water availability to bacteria (Molan 1999).

In modern wound care practice, iodine, silver and broad spectrum germicidal agents such as neomycin, bacitracin, polymyxin, streptomycin (STP), gentamycin and/or combinations are

used to control and treat bacterial infection in chronic wounds. Local delivery of these antibiotics in the form of dressings is more convenient over systemic administration since they deliver a higher concentration of medication directly to the desired area and are less frequently implicated in causing bacterial resistance (Spann *et al* 2003; Pielesz *et al.*, 2011; Howes, 1947; Bowler *et al.*, 2001; Hwang *et al.*, 2010). Antibiotics, such as aminoglycosides that inhibit protein synthesis in bacteria release lower amounts endotoxin than those targeting the bacterial cell wall which helps to reduce the adverse effects on the infected wound (Periti *et al.*, 1998; Bowler *et al.*, 2001). Topical treatments may also prove helpful with the increasing problem of multidrug-resistant organisms that are untreatable with most systemic agents. A recent study of 47 multidrug-resistant organisms from burn wounds found that most were susceptible to 11 commonly used topical antibiotics and antiseptics, although the rates of resistance were higher than non-multidrug-resistant organisms (Lipsky and Hoey, 2009). McHugh and co-authors have reported in their review, that high levels of topical antibiotic use for prophylaxis and several surgical procedures have been shown to be significantly beneficial than peri-operative topical prophylaxis (McHugh *et al.*, 2011). The main arguments against using topical antiseptics are the lack of adequate proof of efficacy and residual concerns about their potential toxicity to healing wounds. A compound's toxicity risk depends on the particular formulation, concentration of active ingredient, and duration of exposure. Newer formulations and methods of applying topical antiseptics appear to reduce the risk. Antiseptics should not be used in solutions, because they are more likely to cause cell damage. Newer topical creams, ointments, gels, and dressings provided adequate, sustained, and apparently non-toxic levels of antiseptics and demonstrated benefit over saline irrigation (White *et al.*, 2001).

Table 1:1: Topical antibiotics and antiseptics products available on the market with their bacterial spectrum, advantages and disadvantages for wound healing (Lipsky and Hoey 2009).

Product name and /or formulation	Bacterial spectrum	Advantages	Disadvantages
<b>Topical antiseptic products available for treating chronic wounds</b>			
Acetic acid	Bactericidal against most (G+ve) and (G-ve), including <i>P. aeruginosa</i>	Inexpensive; eliminate <i>P. aeruginosa</i> colonization from burns	Cytotoxic <i>in vitro</i> although may not be <i>in vivo</i> ; limited activity against biofilms.
Cadexomer iodine	Polysaccharide starch lattice; active agent is slowly released (free iodine); broad spectrum of activity (same as iodine)	Reduced local toxicity compared to iodine; elemental iodine released on exposure to exudate	Causes stinging and erythema but less tissue damage than other iodine products; effect may not persist.
Cetrimide	Active against bacteria and fungi; not active against <i>P. aeruginosa</i>	May be less toxic to wound tissues than other antiseptics	May be corrosive and is potentially harmful if swallowed.
Chlorhexidine gluconate	Active against (G+ve) bacteria (e.g. <i>S. aureus</i> ) and (G-ve) bacteria, including <i>P. aeruginosa</i>	Persistent activity up to 6 h after application; few adverse effects	Hypersensitivity, including anaphylaxis, generalized urticaria, bronchospasm, cough, dyspnoea, wheezing and malaise; may cause serious injury to the eye and

			middle ear; avoid contact with face.
Hexachlorophene	Biguanide that is bacteriostatic against <i>Staphylococcus</i> species and other (G+ve) bacteria	May retain residual effect on skin for several days	Rapidly absorbed and may result in toxic blood levels; application to burns has resulted in neurotoxicity and death; may cause central nervous system stimulation and convulsions, dermatitis, and hypersensitivity reactions
Iodine compounds and iodine tincture	Microbicidal against bacteria, fungi, viruses, spores, protozoa, and yeasts	Broad spectrum	Highly toxic if ingested or significantly absorbed; do not use with occlusive dressings; causes pain and stains skin and clothing; use cautiously in patients within thyroid disorders
Povidone iodine	Broad spectrum includes <i>S. aureus</i> and <i>Enterococci</i> ; active ingredient is liberated free iodine; shares spectrum but is less potent than iodine	Less irritating to skin and less allergenic than iodine. Can be covered with dressings. Clinically significant resistance is very rare	Antibacterial action requires at least 2 min contact; may cause stinging and erythema; effect may not persist, and efficacy may be reduced in body fluids; prolonged use may cause metabolic acidosis; stains skin and clothing.
Sodium hypochlorite	Vegetative bacteria, viruses, and some spores and fungi	Inexpensive. No known systemic toxicity	May require prolonged contact for antibacterial action; inactivated by pus;

			toxic to fibroblasts and keratinocytes, and may cause pain or may lyse blood clots
Hydrogen peroxide	Oxidizing agent active against many (G+ve) and (G-ve) bacteria	Broad-spectrum, bactericidal, inexpensive; no known resistance	May cause some discomfort
Silver nitrate	Silver ions are bactericidal against a broad spectrum of (G+ve) and (G-ve) bacteria	Low cost; easily applied	Painful on application; stains tissues; may delay healing; concentrations 10.5% cause cauterization; inactivated by wound exudates and chlorine
Sliver dressings	Slowly released silver ions have broad-spectrum,	Sustained levels of active silver ions; rare resistance; less painful and few adverse effects than silver nitrate; variety of products available; infrequent application need	Levels of silver ions at wound interface not well defined; may cause silver staining of tissues; may delay epithelialization; relatively expensive; few published comparative trials

---

**Topical antibiotics products available for treating chronic wounds**

---

Bacitracin	Many (G+ve) organisms, including aerobic <i>Staphylococci</i> and <i>Streptococci</i> , <i>Corynebacteria</i> , anaerobic <i>cocci</i> , and <i>clostridia</i> ; inactive against most (G-ve)	Activity not impaired by blood, pus, necrotic tissue, or large bacterial inoculate; resistance is rare but increasing among staphylococci; no cross-resistance with other antibiotics; minimal absorption	May cause allergic reactions, contact dermatitis, and (rarely) anaphylactic reactions; may lead to overgrowth of drug-resistant organisms, including fungi
------------	---	---	--

---

	organisms		
Fusidic acid	<i>S. aureus</i> , <i>Streptococci</i> (in topical concentrations), <i>corynebacteria</i> , and well as crust and cellular debris <i>clostridia</i>	Penetrates intact and damaged skin as	Occasional hypersensitivity reactions; resistance among <i>staphylococci</i> is emerging; must apply 3 times daily
Gentamicin	<i>Streptococci</i> , <i>Staphylococci</i> , <i>P. aeruginosa</i> , <i>Enterobacter aerogenes</i> , <i>E. coli</i> , and <i>Klebsiella pneumoniae</i>	Broad spectrum; inexpensive	Must be applied 3–4 times daily; may cause resistance, toxic
Mafenide acetate	A sulphonamide that is bacteriostatic against many (G-ve) organisms, including <i>P. aeruginosa</i> , and some (G+ve) organisms, but minimal activity against <i>Staphylococci</i> and some obligate anaerobes	Remains active in the presence of pus and serum, and its activity is not affected by acidity of environment	Systemic absorption; drug and metabolites may inhibit carbonic anhydrase, causing metabolic acidosis; use cautiously in patients with renal impairment; pain on application; hypersensitivity reactions
Metronidazole	Many clinically important anaerobic bacteria	May reduce odour associated with anaerobic infections; application only 1–2 times daily	Relatively expensive; systemic formulations available; could drive resistance to these

Mupirocin and mupirocin calcium	(G+ve) aerobes, including <i>S. aureus</i> (most MRSA*), <i>S. epidermidis</i> , <i>S. saprophyticus</i> , and <i>streptococci</i> but not enterococci, some (G-ve) aerobes (not <i>P. aeruginosa</i> ), <i>Corynebacteria</i> , and obligate anaerobes	Minimal potential for allergic reactions	Rare local burning and irritation; applying ointment to large wounds in azotemic patients can cause accumulation of polyethylene glycol; long-term use can lead to resistance among <i>staphylococci</i> .
Neomycin sulphate	Good for (G-ve) organisms but not <i>P. aeruginosa</i> ; active against some (G+ve) bacteria, including <i>S. aureus</i> , but <i>streptococci</i> are generally resistant; inactive against obligate anaerobes	Low cost; applied only 1–3 times daily; may enhance re-epithelialization	Irrigating solution may cause systemic toxicity (FDA banned); use other formulations cautiously on large wounds, especially with azotaemia; hypersensitivity reaction in 1%–6%, often with chronic use or history of allergies
Nitrofurazone	Broad gram-positive and gram-negative activity, including <i>S. aureus</i> and <i>streptococci</i> , but not <i>P. aeruginosa</i>	Used mainly for burn wounds	Hypersensitivity reactions; polyethylene glycols (in some formulations) may be absorbed and can cause problems in azotemic patients
Polymyxin B	Bactericidal against many (G-ve) organisms, including <i>P. aeruginosa</i> ; minimal activity against (G+ve) gram-positive bacteria; activity may	Inexpensive	Some hypersensitivity and neurological or renal adverse reactions reported; may show cross-reaction with bacitracin

be neutralized by divalent cations

Retapamulin	Active against <i>staphylococci</i> (but uncertain for MRSA) and <i>streptococci</i> and some obligate anaerobes	May be active against some mupirocin-resistant <i>Staphylococcus aureus</i> strains; broader activity than mupirocin	Not evaluated for use on mucosal surfaces; may cause local irritation
Silver sulfadiazine	A sulphonamide; the released silver ions are the primary active ingredient; active against many (G+ve) and (G –ve) organisms,	Applied only once or twice daily; soothing application; low rate of hypersensitivity reaction	Potential cross-reaction with other sulphonamides; may rarely cause skin staining
Sulphacetamide Na+	Bacteriostatic against many (G+ve) and (G–ve) pathogens	Broad spectrum; can be combined with sulphur	Systemic absorption and rarely severe side effects occur with application to large, denuded areas; hypersensitivity reactions.
Streptomycin	Effective against (G –ve) bacilli,	Broad spectrum; does not interfere with granulation at 100 0 units per cc.	Toxic, hypersensitivity reaction

---

Note: (G+ve) and (G–ve) stand for gram-positive and gram negative, KI stands for potassium iodide,\*MRSA-methylene resistant *Staphylococcus aureus*

### 1.4.3 Exudate associated with acute and chronic wounds

Exudate is defined as fluid leaking from a wound. It plays an important role in maintaining a moist environment and ultimately wound healing (Boateng *et al.*, 2008; Thomas *et al.*, 2007; Romanelli *et al.*, 2011). Effective management of exudate is necessary to create an optimal moist environment for rapid wound healing and to protect the surrounding skin from the risk of maceration (White and Cutting 2006). Figure 1.5 is an example of a high exuding wound which caused maceration at wound site. It is composed of mainly water, and also contains electrolytes, nutrients, proteins, inflammatory mediators, protein digesting enzymes such as matrix metalloproteinase, growth factors and debris. Exudate also contains various types of cells (e.g. neutrophils, macrophages and platelets) and microorganisms. Generally, the nature of exudates is clear, pale amber and of watery consistency (Vowden and Vowden 2004). Small amounts of thin, pale yellow or straw-coloured exudate is normal in acute wounds. Colour, consistency and amount of exudate may change as a result of various physiological processes in chronic wounds. Table 1.2 shows the different types and colour of exudates produced and their significance to healing. Initially, wound exudate is modified serum which is contaminated with tissue debris and micro-organisms as it arrives at the wound surface (White and Cutting, 2006). Production of wound exudate decreases as it progresses through the healing process (Thomas 1997 *cited in* Romanelli *et al.*, 2011).

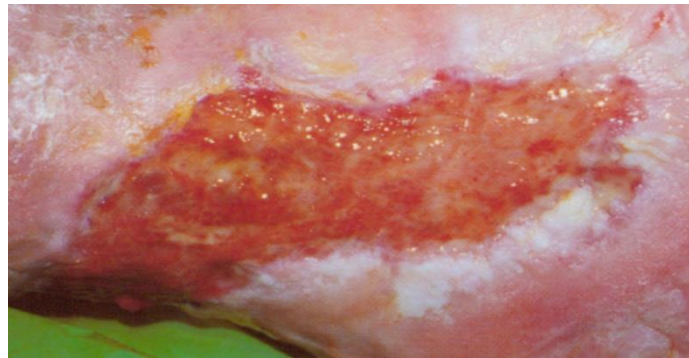


Figure 1.5: A typical example of a high exuding wound (adapted from CiniMed, 2012).

Table 1.2: Different types, colours and significance of exudates present at wound site (Cutting, 2004)

Type	Colour	Consistency	Significance
Serous	Clear, straw-coloured	Thin, watery	Normal. Possibly a sign of infection. Some bacteria produce fibrinolysis, which degrade fibrin clots or coagulated plasma. Some strains of <i>S. aureus</i> , $\beta$ -haemolytic group <i>Streptococci</i> and <i>Bacteroides fragilis</i> produce fibrinolysis. <i>P. aeruginosa</i> produces a non-specific enzyme that degrades fibrin.
Fibrinous	Cloudy	Thin	Contains fibrin protein strands.
Serosanguinous	Clear, pink	Thin, watery	Normal.
Sanguinous	Red	Thin, watery	Trauma to blood vessels.
Seropurulent	yellow, cream-coffee	Thicker, creamy	Infection
Purulent	Yellow, grey, green	Thick	Infection. Contains pyogenic organisms and other inflammatory cells.
Haemopurulent	Dark, blood-stained	Viscous, sticky	Contains neutrophils, dead/dying bacteria and inflammatory cells. This means an established infection is present. Consequent damage to dermal capillaries leads to blood leakage.
Haemorrhagic	Red	Thick	Infection. Trauma. Capillaries are so friable they readily break down and spontaneous bleeding occurs. Not to be confused with bloody exudate produced by over-enthusiastic debridement.

The volume of exudate is relatively dependent on the surface area of the wound and therefore large wounds such as burns, venous leg ulcers and skin donor sites often produce

higher volumes of exudates (Romanelli *et al.*, 2011). Production of too high or too low amounts of exudate may adversely affect the healing process. High exudate volumes are produced due to inflammation, bacterial contamination whereas low exudates indicate dehydration, hypovolaemic shock, micro-angiopathy, or may be a feature of ischaemic ulcers (World Union of Wound Healing Societies *cited in* Romanelli *et al.*, 2011). In chronic wounds, the inflammatory response is altered owing to elevated levels of inflammatory mediators and activated matrix metalloproteinase with a concurrent increase in vascular permeability and the amount of extravascular fluid (White and Cutting, 2006; Vowden and Vowden, 2004).

## **1.5 Wound dressings**

Several factors including the type of wound dressing need to be considered to achieve successful wound healing. It is important to select the most appropriate dressing for effective wound management. The choice of optimum dressing for effective healing depends upon the type, place and exudate volume of wound. Table 1.3 describes the desired ('ideal') characteristics of wound dressing with their clinical significance (Boateng *et al.*, 2008). Wound dressings are designed to keep the wound in a moist (but not wet) condition.

As noted earlier, a moist wound environment makes the migration of epithelial cells from the edge of the wound to the injured area progress faster than in a dry state (Chen *et al.*, 2006; Jones *et al.*, 2006). This requirement and corresponding advantage for rapid healing has resulted in an increased demand for developing modern wound dressings. Wound dressings can be categorized as either (i) traditional (ii) modern or (iii) biological. Table 1.4 above illustrates the different types of wound dressings available for the management of wounds with their indications of use.

### **1.5.1 Traditional wound dressings**

For majority of the past years of wound management, gauze, lint silk, linen or cellulose-based substances and cotton have been used as traditional dressings and commonly been made of natural, synthetic or semi synthetic materials. These are used as passive or secondary dressings in minimal and low exuding wounds and are limited to simple, clean, superficial wounds and minor burns. Gauze has been used for debridement of heavily contaminated exudative and necrotic wounds. These dressings may lead to maceration in highly exuding wounds as the water vapour and exudation may not pass through and be trapped within the wound. It has

disadvantages such as adherence to the wound surface, necrosis of newly formed tissue and requires frequent changes (Stashak *et al.*, 2004; Boateng *et al.*, 2008). Readily available marketed traditional wound dressings include Band-Aids<sup>®</sup>, Telfa<sup>®</sup> pads and Exu-dry<sup>®</sup> dressings.

Table 1.3: The desirable characteristics of wound dressings required for wound healing and their clinical significance (Wittaya-areekul and Prahsarn, 2006; Khan *et al.*, 2000; Boateng *et al.*, 2008).

<b>Desirable Characteristics</b>	<b>Clinical significance to wound healing</b>
<b>1 Debridement (wound cleansing)</b>	1. Enhances migration of leucocytes into the wound bed and supports the accumulation of enzymes. Necrotic tissue, foreign bodies and particles prolong the inflammatory phase and serve as a medium for bacterial growth.
<b>2 Provide or maintain a moist wound environment</b>	Prevents desiccation and cell death, enhances epidermal migration, promotes angiogenesis and connective tissue synthesis and supports autolysis by rehydration of desiccated tissue.
<b>3 Absorption and removal of excess exudate</b>	In chronic wounds, there is excess exudate containing tissue degrading enzymes that block the proliferation and activity of cells and break down extracellular matrix materials and growth factors, thus delaying wound healing. Excess exudates can also macerate surrounding healthy skin.
<b>4 Gaseous exchange (water vapour and air)</b>	Permeability to water vapour controls the management of exudate levels. Low tissue oxygen levels stimulate angiogenesis. Raised tissue oxygen stimulates epithelialization and fibroblasts.
<b>5 Prevent infection: Protect the wound from bacterial invasion</b>	Infection prolongs the inflammatory phase and delays collagen synthesis, inhibits epidermal migration and induces additional tissue damage. Infected wounds can give an unpleasant odour.
<b>6 Provision of thermal insulation</b>	Normal tissue temperature improves the blood flow to wound bed and enhances epidermal migration.
<b>7 Low adherence. Protects the wound from trauma</b>	Adherent dressings may be painful and difficult to remove and cause further tissue damage or re-injury.
<b>8 Cost effective, low frequency of dressing change</b>	Dressing comparisons based on treatment costs rather than unit or pack costs should be made (cost-benefit-ratio). Although many dressings are more expensive than traditional materials, a more rapid response to treatment may save considerably on total cost

Table 1.4: Types of wound dressings and their indications of use (Moon and Crabtree, 2003; Stashak *et al.*, 2004).

<b>Product type</b>	<b>Indications of use</b>	<b>Example of commercial product</b>
<b>Gauze dressing</b>	Debridement of heavily contaminated, exudative and necrotic wounds. Applied dry when wound fluids are of low viscosity or moistened	Paranet™
<b>Films</b>	Dry, superficial wounds. Can be used as a secondary dressing. Acute partial- or full-thickness wounds with minimal exudates. Non-draining primarily closed wounds.	Tegaderm™, Hydrofilm™, Opsite™
<b>Films and pads</b>	Post-operative wounds	Hydrofilm Plus™, Tegaderm Film™
<b>Foams</b>	Moderate to heavily exuding wounds. Can be used as primary and secondary dressing. Can be used as a cavity filter.	Allevyn™, Biatain™, Mepilex™
<b>Hydrogel</b>	Indicated for dry, necrotic and thick sloughy wounds	Activeheal™, Intrasite™, Activeform cool™
<b>Hydrocolloid</b>	Low to moderately exuding wound. They promote debridement of slough and necrosis. Can reduce pain through hydration of nerve endings	Comfeel™, Granuflex™

### 1.5.2 Modern wound dressings

These are more recent wound care products which provide a moist environment for rapid wound healing processes. They consist of new elastomeric polymers capable of forming a protective layer which covers the wound and provides optimum conditions required to heal the wound (Szycher and Lee, 1992). Wiechula (2003) in his review compared moist wound-healing dressings against traditional non-moist dressings which favoured moist wound-healing approaches in terms of healing rates, pain and infection. These moist dressings have distinct

clinical advantages over non-moist products in the management of skin graft donors (Wiechula, 2003). Modern dressings are classified into films, wafers, hydrogels, foam, hydrocolloids and alginates.

#### **1.5.2.1 Film dressings**

These dressings are made up of thin polymeric films coated with an adhesive. Film dressings allow high levels of comfort, flexibility and transparency which permits inspection and monitoring of the wound bed without the need for removal of the dressing. Films absorb wound exudates and maintain moist environment at the site of injury. Films are suitable for superficial, lightly exuding or epithelializing wounds. They are however, avoided for heavily exuding wounds because fluid tends to accumulate underneath the film, leading to maceration of the surrounding healthy skin (Watson and Hodgkin, 2005). Hydrofilm Plus™, Opsite post op™, Tegaderm Film™, Mepore ultra™ are commonly marketed film dressing available for postoperative wounds.

#### **1.5.2.2 Hydrogel dressings**

A hydrogel can be described as a three-dimensional network of hydrophilic polymers (Sedlarik *et al.*, 1995). Hydrogels are capable of absorbing additional liquid due to the presence of hydrophilic chains which allows them to swell extensively without changing their gelatinous nature, allowing them to function as moist absorbent wound dressings (Jones and Vaughan, 2005). They can be used in dry, sloughy or necrotic wounds but usually need a secondary dressing to hold it close against the wound bed (Watson and Hodgkin, 2005). These dressings are conventional for unusual shapes of wounds due to their jelly-like nature. Hydrogels are non-particulate, non-toxic and non-adherent (Jones and Vaughan, 2005). They also assist in providing a moist environment to dehydrated tissue to prevent them from desiccation and absorb exudates from wounds. Intrasite™, Nu-gel™, Aquaform™ are some of examples of marketed hydrogel products available for wound healing.

#### **1.5.2.3 Foam dressings**

Foam dressings are constructed from polyurethane and absorb exudate without interacting with the wound bed. Foam rapidly absorbs and distributes the wound exudate within the structure of wound dressing due to presence of horizontal tapering which provides moist environment to the wound bed (Fletcher, 2003). They help to absorb low-to-moderate amounts

of fluid and usually have a semi-permeable backing to allow the escape of moisture (Watson and Hodgkin, 2005). Foam dressings have the ability to apply pressure and decrease the mobility of skin and due to this property they are widely used as postoperative dressings. They help to minimize inflammation, oedema, and ecchymosis (David, 1981; Lehnert and Jhala, 2005). Popular foam dressings available in the market for wound healing are Lyofoam™, Allevyn™, and Tielle™.

#### **1.5.2.4 Hydrocolloid dressings**

Hydrocolloid dressings are made from colloidal materials such as carboxymethylcellulose, gelatine and pectin in combination with elastomers and adhesives. Examples of hydrocolloid dressings include Granuflex™, Aquacel™, Comfeel™ and Tegaserb™. These dressings are available in form of thin sheets or film. They are useful to cover light to moderately exuding wounds including minor burns and trauma. In their intact state, hydrocolloid dressings are impermeable to water vapour but on absorption of wound exudate, a change in physical state occurs with the formation of a gel covering the wound. They become progressively more permeable to water and air as the gel forms. Some studies have shown that the use of hydrocolloid dressing reduces pain associated with injury, and also need less analgesia (Heenan, 1998). Hydrocolloid dressings generally have an occlusive outer cover that prevents water vapour exchange between the wound and its surroundings. This can be disadvantageous for infected wounds that require a certain amount of oxygen to heal rapidly (Heenan 1998; Thomas and Loveless, 1997; Boateng *et al.*, 2008).

#### **1.5.2.5 Alginate dressings**

Alginate dressings are made from calcium and sodium salts of alginic acid which is a polysaccharide consisting of mannuronic and guluronic acid units. Alginate dressing containing high amount of mannuronic acid forms soft gel whereas high amount of guluronic acid units forms a firm gel. Sorbsan™, Kaltostat™, Tegagen™ are few examples of alginate dressings which are available on the market. It has high absorbency due to hydrophilic nature of alginate and forms a gel upon contact with wound exudates and these dressing also helps to minimize bacterial infection.

When alginate dressings are applied to wounds, ions present in alginate fibres are exchanged with those present in exudate and blood to form a protective film of gel. This helps to

maintain the wound at an optimum moisture content and temperature which promotes healing and the formation of granulation tissue. Lansdown (2002) reported the role of  $\text{Ca}^{2+}$  ions released from  $\text{Ca}^{2+}$  alginate fibres, in the normal homeostasis of mammalian skins serving as a modulator in keratinocyte proliferation and differentiation, which promotes the initial stage of wound healing (Lansdown, 2002). It has been reported that alginates with high mannuronate content were immunogenic and approximately ten times more potent in inducing cytokine production compared with alginates having high guluronate content. Khanna and co workers demonstrated sustained release of the growth factor encapsulated in the multi-layered alginate beads (Khanna *et al.*, 2010). Alginate dressings are useful for moderate to heavily exuding wounds (Kim *et al.*, 2008). The high absorption is achieved via strong hydrophilic gel formation which limits wound secretions and minimizes bacterial contamination. Alginate dressings are readily biodegradable in nature and can be easily applied in the form of fibres and rinsed away with saline solution which does not destroy granulation tissue and makes dressing change virtually painless (Gilchrist and Martin, 1983; Boateng *et al.*, 2008). They have been successfully applied to cleanse a wide variety of secreting lesions (Paşcalău *et al.*, 2011; Lee, and Mooney 2012).

#### **1.5.2.6 Medicated dressings**

The use of topical pharmaceutical agents in the form of solutions, creams and ointments to wound sites has been in existence for quite some time (Boateng *et al.*, 2008). Examples of such dressings are povidone–iodine solution, creams, ointments, dry spray, low-adherent dressing or dressings containing concentrated cadexomer, iodine paste and silver sulphadiazine gel (Ovington, 2007). The modern dressings used to deliver active agents to wounds include hydrocolloids, hydrogels, alginates, polyurethane foam/films and silicone gels (Heenan, 1998). Medicated dressings contain pharmacological agents which have therapeutic value. They play an active role in the wound healing process directly or indirectly as cleansing and debriding agents for removing necrotic tissue, antimicrobials to prevent or treat infection, and growth factors to aid tissue regeneration (Boateng *et al.*, 2008, Matthews *et al.*, 2008). Antimicrobial dressings refer to medicated wound dressings which contain an antiseptic agent (e.g. silver, iodine and chlorhexidine) incorporated into the wound dressing. Recently, a trend towards the use of wound dressings containing silver has been evident, and today, a selection of foam, film, hydrocolloid, gauze and dressings with Hydrofiber<sup>®</sup> technology impregnated with silver are commercially available (Percival *et al.*, 2005). Silver sulfadiazine incorporated bilayer chitosan wound dressing showed excellent oxygen permeability, controlled water vapour transmission

rate, and water-uptake capability. It exhibited excellent antibacterial activity in an *in vitro* culture for one week (Paul and Sharma, 2004). However, concerns are being expressed regarding the overuse of silver and the possible emergence of bacterial resistance to silver, particularly within a clinical environment (Percival *et al.*, 2005).

Sterculia-cl-poly(vinyl alcohol) polymeric films containing tetracycline and sterculia-cl-poly(vinyl alcohol) polymeric film containing gentamycin were prepared to improve wound healing as compared to the non-medicated hydrogel because of the potential healing effect of drug (Singh and Pal 2012). Bilayer hydrocolloid alginate films impregnated with model drug (ibuprofen) showed faster rate of wound closure and well-formed epidermis with faster granulation tissue formation. The bilayer film dressing can be potentially exploited as a slow-release wound dressing for low to medium suppurating wounds (Thu *et al.*, 2012). Hypertonic saline dressings are cotton or synthetic gauze impregnated with 20% sodium chloride and are available in sheet, rope or ribbon form. These dressings create osmotic action to cleanse the wound by reducing necrotic or infected purulent debris. Bacterial growth is inhibited by hypertonic properties. A hydrogel sheet composed of chitosan, honey and gelatin (0.5:20:20, w/w) was developed as a medicated burn wound dressing which showed powerful antibacterial efficacy against *S. aureus* and *E. coli*. Such hydrogel sheets had a significant effect on wound contraction which repaired the intact epidermis within twelve days. Table 1.5 shows the different types of medicated dressings containing antimicrobial agents and their available sizes for the treatment of chronic wounds (O'Brien 2008).

#### **1.5.2.7 Freeze dried wafers**

Lyophilised wafers have potential as drug delivery systems for suppurating wounds. They are produced by freeze-drying polymer solutions and gels to yield solid porous structures that can easily be applied to exuding wound surfaces. Their physical architecture resembles those of foam dressings which are made of porous polyurethane. Stability of drugs should be better in a lyophilised dosage form than a semi-solid hydrogel based formulation. It is anticipated that a lyophilised polymer matrix would preserve the size, shape and form of contained compounds unlike a conventional gel suspension, where crystal ripening, agglomeration and polymorphic changes may occur (Matthews *et al.*, 2008; Ayensu *et al.*, 2012). Wafers provide a potential means of delivering pharmacological agents to wound surfaces to aid healing (Matthews *et al.*, 2005; 2006). Lyophilized wafers also have the ability to incorporate soluble and insoluble

antimicrobial compounds greater than their minimum bactericidal concentration for antibacterial activity against pathogenic bacteria (Labovitiadi *et al.*, 2012). Wafers have the capacity to absorb large amounts of exudate due to their porous nature and thereby maintain a moist environment without damage of newly formed tissue. Wafers also offer high drug loading capacity compared to solvent cast films (Boateng *et al.*, 2010).

Table 1.5: List of medicated dressing currently available in the market and their available sizes (O'Brien 2008).

<b>Medicated dressings</b>	<b>Size</b>
Chlorhexidine Tulle Gras	(10 x 10 cm) and (20 x 10 cm)
Povidone-iodine Tulle Gras	(5 x 5 cm) and (10 x 10 cm)
Cadexomer iodine	10 gm tube or 5 gm sachets
Silver impregnated Tulle Gras	(5 x 5 cm) and (10 x 10 cm)
Silver impregnated hydrocolloid	(10 x 10 cm)
Hypertonic saline gel	5 gm tube
Silver impregnated foam	(10 x 10 cm)
Silver impregnated hydro fibre	(10 x 10 cm) and (10 x 20 cm)
Silver charcoal	(10 x 10 cm) and (10 x 20 cm)
Nanocrystalline silver	(10 x 10 cm) and (10 x 20 cm)
Nanocrystalline silver calcium alginate	(10 x 10 cm)
Zinc oxide paste bandage	80 cm, 4 each per box
Silver sulphadiazine 1% / chlorhexidine 0.2% (100 mg) Cream	
Metronidazole 0.75% gel	10 gm
Bacitracin/neomycin/ polymyxin B (Neosporin) ointment	(15 gm Tube)

### **1.5.3 Biological wound dressings**

A recent advance is the development of bioengineered skin substitutes, which have been approved by the Food and Drug Administration (FDA) for the treatment of recalcitrant diabetic foot ulcers and venous leg ulcers (Coulthard *et al.*, 2010). Engineered scaffolds either from natural or synthetic sources are potentially useful for the delivery of additional bioactive materials such as growth factors and genetic materials to a wound. They are usually of natural source commonly comprising collagen, elastin and lipids (Sai and Babu, 2000). Alloskin and pig skin are biologic dressings commonly used clinically for clean partial-thickness burns as temporary coverage (Jayakumar *et al.*, 2011). Collagen is involved in scar tissue formation, cell proliferation, cell migration, cell differentiation and interactions between different tissues which progresses to wound healing. Collagen wound dressings are available in the form of films, extruded fibres and sponges (Sai and Babu, 2000). Biobrane<sup>®</sup> is a bi-laminate membrane consisting of fabric nylon mesh bonded to a thin layer of silicone and is recommended in superficial partial-thickness burns within first 6 h of injury. Apligraf<sup>®</sup> is derived by combining a gel of type I bovine collagen with living neonatal allogeneic fibroblasts. It accelerates the healing rate and is used to treat deep and chronic wound ulcers and is effectively used in the treatment of venous ulcers. Dermagraft<sup>®</sup> is a cryo-preserved new allogeneic fibroblasts loaded onto a polymer scaffold (polyglycolic acid or polyglactin-910). These fibroblasts within the polymer mesh secrete growth factors and dermal matrix proteins (collagens, glycosaminoglycan) to create the living dermal structure in chronic diabetic foot ulcers for rapid healing (Jones *et al.*, 2002).

## **1.6 Functional properties of moist dressings**

### **1.6.1 Bio (muco)-adhesion**

Bioadhesion is a state in which two materials at least one of which is biological in nature are held together for extended periods of time by interfacial forces. In pharmaceutical sciences, when adhesive attachment is to mucus or mucus membrane, then the phenomenon is referred as mucoadhesion (Smart, 2005). For mucoadhesion, the key mechanism is diffusivity of polymer network which depends upon molecular weight and degree of cross-linking (Peppas and Sahlin, 1996). Over the last two decades mucoadhesion, has attracted significant interest for its potential to optimise localised drug delivery by retaining a dosage form at the absorption site (e.g. wound surface, vaginal, nasal and eye cavities) for prolonged periods. In early 1947, carboxymethylcellulose (CMC) and petroleum jelly were used for the formulation development

of an adhesive penicillin ointment based drug delivery system. Sodium CMC, pectin and gelatine have been used as a vehicle in mucoadhesive drug delivery. Other polymers such as sodium alginate (SA), guar gum, chitosan (CS), hydroxypropylmethylcellulose (HPMC), carrageenan (CAR), polyethylene glycol (PEG), poly (acrylic acid) and polyox (POL) have been found to exhibit mucoadhesive properties (Kianfar *et al.*, 2013; Smart, 2005; Morales, and McConville, 2011). Today there is wide range of polymers used in mucoadhesive formulation development. Such novel mucoadhesive polymers have an advantage over conventional drug delivery devices for site specific or targeted drug delivery for optimal release of the drug. Particularly, hydrophilic polymers containing numerous hydrogen bond sites are the most suitable in this mucoadhesive category (Salamat-Miller *et al.*, 2005; Smart, 2005).

Mucus interacts with the mucoadhesive polymer through physical entanglement and secondary bonding such as hydrogen bonding and van der Waals attraction. This interaction may be associated with the chemical structure of the polymers. Functional groups such as hydroxyl, carboxyl, amine and amides are responsible for mucoadhesion. Peppas and Buri, (1985) suggested the polymer characteristics which are necessary for mucoadhesion as strong hydrogen bonding groups, strong anionic charges, high molecular weight, sufficient chain flexibility and surface energy properties favouring spreading on to the mucous (Peppas and Buri, 1985).

Mucoadhesive wound drug delivery systems work by increasing the drug residence time and bioavailability at the wound site by localizing the drug to open wound tissue. This can help to improve overall performance of wound dressing by reducing frequent dressing changes and controlled release of the drug at wound site with improved bioavailability of the drug and enhanced patient compliance (Gombotz, and Wee 2012). Singh and Pal (2012) evaluated the mucoadhesive performance of sterculia-cl-poly(VA) film which allowed adherence and afforded protection against external environment and therefore fulfils one of the primary requirements for a polymeric material to function as a wound dressing (Singh and Pal, 2012). There are several factors which need to be considered during mucoadhesion testing such as type of wound, extent of exudate, presence of salts and ions, temperature and pH. These factors can affect *in vitro* residence of the wound dressing.

## 1.6.2 Swelling and drug release

### 1.6.2.1 Theories of polymer erosion

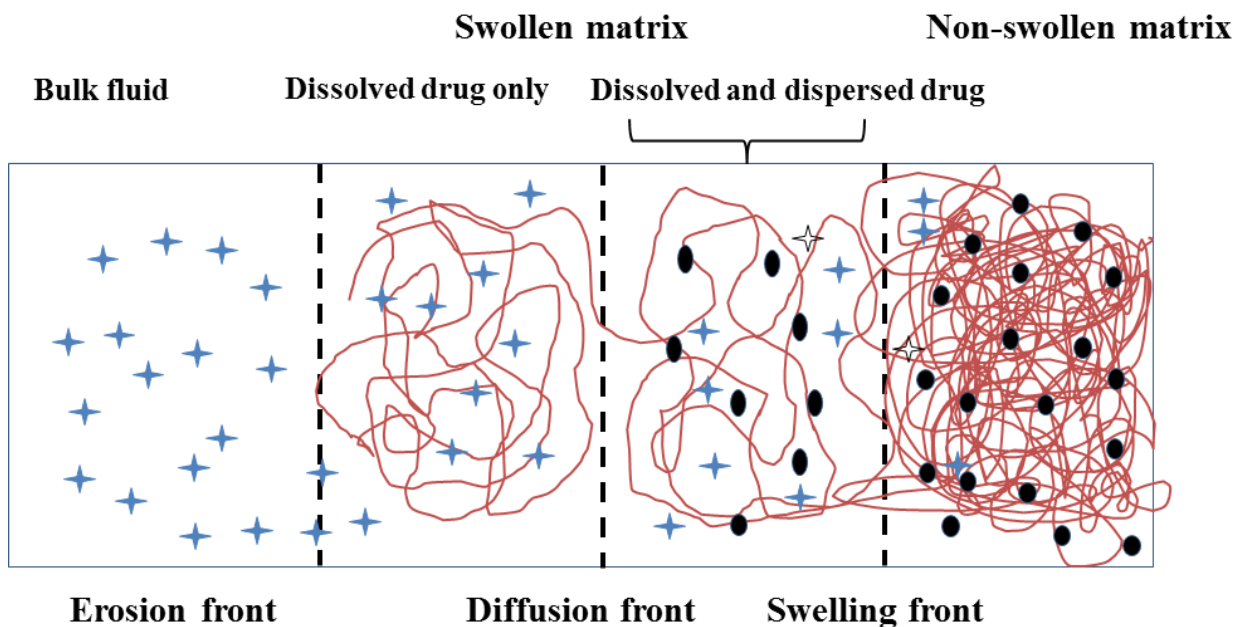


Figure 1.6: Schematic representation of drug release mechanism from films and wafers (Siepmann and Siepmann, 2008).

Increased or decreased drug release rates potentially depend on the type of polymer and type of drug delivery system. Figure 1.6 schematically represents the physical phenomena which can be involved in the control of drug release from a swellable matrix system. This might represent a thin film in which one surface is exposed to an aqueous fluid in an outward direction. On the other end (right hand side), top layer is still in the dry and glassy state (non-swollen), on the left hand side the bulk fluid is located. Upon contact with the release medium, water diffuses into the system and with increasing water content, the mobility of the polymer chains (and, also drug molecules) increases. As soon as a certain polymer-specific water concentration is reached, the macromolecular mobility increases steeply. This phenomenon is called “polymer chain relaxation” or “glassy-to-rubbery-phase-transition”. The front at which polymer chain relaxation process takes place is called “swelling front”, which separates the swollen matrix from the non-swollen matrix and this is moving boundary, and not a stationary boundary. If the initial drug concentration in the delivery system exceeds drug solubility then dissolved and non-dissolved drug is exist together within the matrix. Furthermore dissolved drug molecules start to diffuse

out of the swollen matrix into the dissolution medium due to concentration gradients and significantly increased mobility. As long as non-dissolved excess of drug exists, the concentration of dissolved drug in this part of the system is constant (drug molecules that are released are replaced by the dissolution of non-dissolved drug, providing a saturated solution). However, as soon as all excess drug is dissolved the concentration within the swollen matrix decreases. The front which separates ‘dissolved drug’ and ‘dissolved and dispersed drug’ in the swollen matrix is called the diffusion front (Figure 1.6) (Colombo *et al.*, 1999; Siepmann and Siepmann 2008) which is also known as the moving front. Furthermore, a third front can be distinguished, which separates the drug delivery system from the dissolution medium and which is also moving. In the case of water-soluble matrix formers, this front is called “erosion front”.

### **1.6.2.2 Theories of polymer erosion/degradation**

Unfortunately, the terms “erosion” and “degradation” are not uniformly used in the literature (Goepferich, 1996). Polymer degradation is the chain scission process by which polymer chains are cleaved into oligomers and monomers. In contrast, erosion is defined as the process of material loss from the polymer bulk. Such materials may be monomers, oligomers, parts of the polymer backbone or even parts of the polymer bulk. Thus, the degradation of water-insoluble polymers is part of their erosion process. Depending on the relative rates of water penetration into such systems and polymer chain cleavage, two extreme types of erosion can be distinguished: surface (or heterogeneous) erosion and bulk (or homogeneous) erosion (Langer and Peppas, 1983). In the first case, the polymer chain cleavage is much faster than the water penetration into the system. Consequently, degradation process is mostly restricted to the outermost polymer layers and erosion predominantly affects the surface, and not the inner parts of device. In contrast, if water penetration is much more rapid than polymer chain cleavage, the entire system is rapidly wetted and degradation occurs throughout the device (bulk erosion). Generally, drug delivery systems which are based on polymers with highly reactive bonds (e.g., polyanhydrides) in their backbone structure undergo surface erosion, whereas devices that are based on polymers with less reactive functional groups tend to be bulk eroding. It should be noted however, that the dimensions of the drug delivery system affect the relative water penetration rate into the matrix for example film drug delivery systems show surface erosion (Siepmann and Goepferich, 2001).

### 1.6.2.3 Drug release mechanisms

Drug delivery systems are often classified on the basis of their design or their rate-controlling release mechanism (such as diffusion, erosion/chemical reactions, swelling) (Frenning 2011). The timely and reproducible release of active pharmaceutical ingredients from delivery vehicles of various kinds is, of paramount importance for safe and efficient treatment of disease (Frenning 2011). The study of drug release from polymeric systems usually involves the uptake of water by the glassy polymer and subsequent swelling to form a gel layer which controls drug release by viscous resistance to drug diffusion (Boateng *et al.*, 2009). Control of drug release from a dosage form such as tablet, films and wafers, depends on the type of drug(s), the dose, types and amounts of polymers and excipients, preparation method and environmental circumstances during drug release as well as geometry of the drug delivery system. Siepmann and Siepmann, (2008) outlined some phenomena which might be involved in the control release of drug. These include: wetting by water and its diffusion into the system, phase transitions (e.g., glassy-to rubbery) of polymer, excipients and drugs. Others include changes in the micro-environmental pH due to variations in the rate of drugs and/or excipients degradation, physical drug-drug and or drug-polymer or excipients interactions, changes in drugs and/or excipients solubility, diffusion of drugs and/or excipients out of the dosage form (Gallagher and Corrigan, 2000; Grassi *et al.*, 2003; Zhou *et al.*, 2005; Berchane *et al.*, 2007; Bertrand *et al.*, 2007; Chirico *et al.*, 2007; Abdekhodaie and Wu, 2008, Siepmann and Siepmann, 2008). To date, numerous kinetic models have been reported in the literature to describe the release kinetics of drugs from pharmaceutical dosage forms based on the drug dissolution or release data. These are zero order, first order, Hixson-Crowell cube root law, Higuchi square root and Korsmeyer-Peppas kinetic release equations. These are summarised in a later part of the report (Chapter four).

## 1.7 Polymers, excipients and drugs used in this project

### 1.7.1 Polyethylene oxide (Polyox™)

Polyox™ (POL) is polyethylene oxide, a synthetic non-ionic polymer with the molecular formula  $(-\text{CH}_2\text{CH}_2\text{O}-)_n$  (Figure 1.7). It is non-toxic, semi-crystalline, bio (muco) adhesive, because of its water solubility, hydrophilicity, high viscosity, ability to form hydrogen bonds, and biocompatibility with other bioactive substances (Zivanovic *et al.*, 2007; Çaykara *et al.*, 2005). It has been shown that POL exhibits increased mucoadhesive capacity and can be used as carriers for improved mucoadhesion (De Ascentiis *et al.*, 1995). POL can undergo chain

cleavage via auto-oxidation. Therefore, storage stability is an important issue for POL. The rate of auto-oxidation can be minimized through the addition of antioxidants since POL water-soluble resins contain some level of butylated hydroxytoluene (BHT) antioxidant.

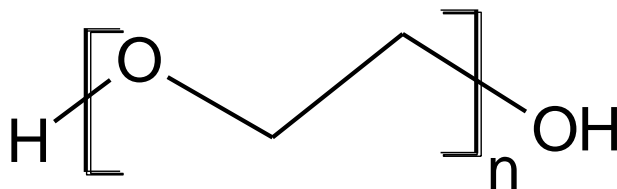


Figure 1.7: Chemical structure of polyethylene oxide.

### 1.7.2 Carrageenan (CAR)

CAR is a natural polymer obtained from intercellular matrix of seaweed plant tissue. Carrageenan is commercially available in three different types of iota (I), kappa ( $\kappa$ ) and lambda ( $\lambda$ ) carrageenan which differ in the sulfate content, the position of the sulfate ester group in the repeating galactose units and the molecular weight. This results in different solubility and gelling properties (Bornhöft *et al.*, 2005). It is a high molecular weight polysaccharide with 15% to 40% of ester-sulphate content.  $\kappa$ -CAR which is one of the common grades has an ester sulphate content of about 25 to 30%. It is formed by alternate units of D-galactose and 3, 6 anhydrogalactose (Figure 1.8).  $\kappa$ -CAR is soluble in hot water; with the normal solubility temperature between 40° and 70° C. It has excellent gel and film forming properties which produces pliable, cohesive and uniform films such films exhibits high tensile strength (Pielesz *et al.*, 2011a). Kianfar and co-authors have reported the use of  $\kappa$ -CAR combined with poloxamer for films (Kianfar *et al.*, 2012) and wafers (Kianfar *et al.*, 2013) for the delivery of small molecules via the buccal mucosa membrane. Sulphate concentration and molecular weight of seaweed polysaccharides influence biological activities such as antitumor, antiviral and anti-hyperlipidaemia (Silva *et al.*, 2010). CAR, as a prominent natural marine sulphated polysaccharide, exhibits potent anticoagulant, antithrombotic and anti-inflammatory activities (Fan *et al.*, 2011; Mourão, 2004; Silva *et al.*, 2010). CAR has good gelling capacity which has been extensively used in the form of hydrogel and micro/nanoparticles as controlled drug delivery vehicles. It has been found that the drug release rate is strongly dependent on the characteristics of the gel structure (Mangione *et al.*, 2007). Micro beads of CAR crosslinked by epichlorohydrin has been studied as potential drug carrier (Keppeler *et al.*, 2009). Hydrogels based on radiation induced copolymerisation of N-isopropylacrylamide and CAR has also been

investigated as controlled release vehicle (Zhai *et al.*, 2004). Basic butylated methacrylate copolymer/ CAR inter-polyelectrolyte complex has been studied for the release of ibuprofen (Prado *et al.*, 2008). The good film forming ability of CAR has been explored for the development of wound healing patches for the treatment of topical burn wounds (Dalafu *et al.*, 2010). Hydrogel dressings containing polyvinyl alcohol, CAR and agar has been used in clinical trials on human patients which showed safety and efficacy of the dressing. Such dressing has been used in treatment of burns, non-healing ulcers of diabetes, leprosy and other external wounds. This dressing is now being marketed in India under different brand names (Varshney, 2007). CAR film formation includes gelation mechanism during moderate drying, leading to a three-dimensional network formed by polysaccharide double helices and to a solid film after solvent evaporation (Skurtys *et al.*, 2010). Such property can help to absorb wound exudate to form a three dimensional network which can help water vapour and oxygen transmission which is helpful especially in angiogenesis.

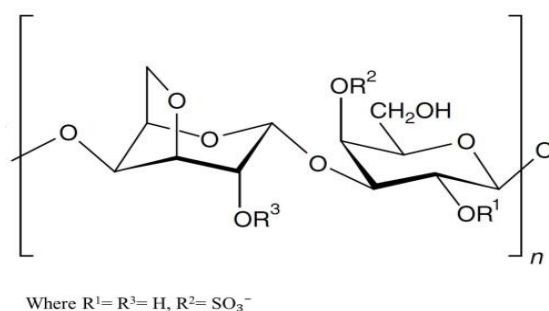


Figure 1.8: Typical structure of CAR.

### 1.7.3 Sodium alginate (SA)

Alginates are a naturally occurring anionic linear polysaccharide obtained from marine brown algae and are composed of 1,4-linked  $\beta$ -D-mannuronate residues and 1, 4-linked  $\alpha$ -L-guluronates (Figure 1.9) (Rees and Welsh, 1977 *cited in* Çaykara *et al.*, 2005). Alginate is hydrophilic, biocompatible, and relatively economical and exhibits excellent bioadhesive properties (Tonnesen and Karlsen, 2002). It has been extensively exploited and studied in detail for biomedical applications and drug delivery due to its biocompatibility, biodegradability, immunogenicity and non-toxicity (George and Abraham, 2006). It has been widely used in medical applications such as wound dressings, scaffolds for hepatocyte culture and surgical or dental impression material, even if allergic reaction to skin has occurred (Paşcalău *et al.*, 2011).

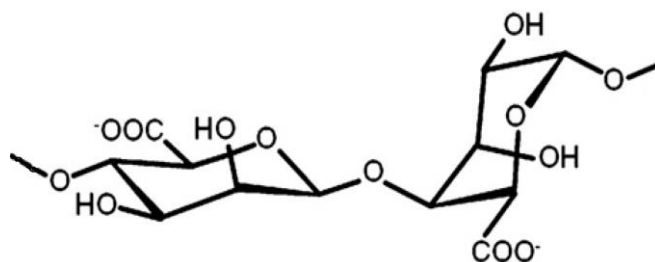


Figure 1.9: Chemical structure of alginate containing mannuronate and guluronates residue.

#### 1.7.4 Chitosan (CS)

CS is a linear cationic copolymer of  $\beta$ -(1-4) linked 2-acetamido-2-deoxy-  $\beta$  -d-glucopyranose and 2-amino-2-deoxy-  $\beta$  -d-glycopyranose (Figure.1.10). It is obtained by alkaline deacetylation of its parent polymer chitin, a polysaccharide widely distributed in nature (e.g. crustaceans, insects and certain fungi) (Dash *et al.*, 2011). CS has found wide application in the biomedical field in the form of hydrogels, films, fibres or sponges, due to its interesting biological properties that include: biocompatibility, biodegradability, haemostatic activity and bacteriostatic effect (Rinaudo 2006; Paul and Sharma 2004). CS also exhibits numerous other interesting properties, such as anti-tumour, immune-adjuvant, haemostatic and antibacterial activities (Kurita 1998). Moreover, it has been shown to facilitate wound healing (Berger *et al.*, 2004). CS solutions have been used for the treatment of skin wounds, such as skin ulcers, burns and surgical wounds (Campos *et al.*, 2006). Its film forming ability makes it a promising biomaterial for application in burn wounds (Azevedo *et al.*, 2006). CS has a potential to be used as artificial tissue and organ replacement material, however, its poor mechanical properties has limited its use in this regard (Kim *et al.*, 2008).

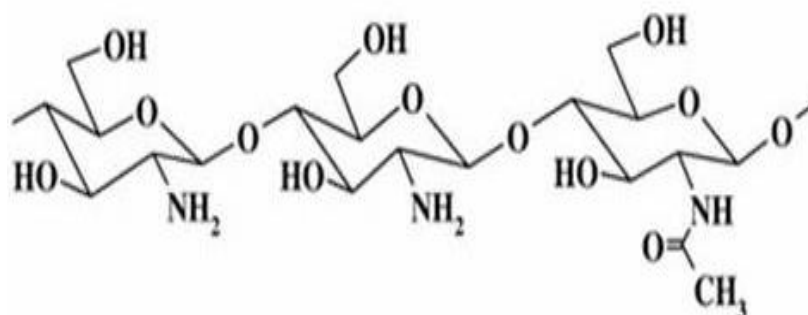


Figure 1.10: Chemical structure of CS.

### 1.7.5 Hydroxypropylmethylcellulose (HPMC)

Cellulose derivatives are used in a wide variety of industrial applications such as food, pharmaceutical, textile, and adhesive industries. Hydroxypropylmethylcellulose (HPMC) consists of the polymeric backbone of cellulose, a natural carbohydrate that contains a basic repeating structure of 1-4  $\beta$  o-anhydroglucose units, and methyl and hydroxypropyl substitutions (Figure 1.11) (Greiderer *et al.*, 2011). It is a most favourable polymer used in the production of film coatings (Fahs *et al.*, 2010) due to its ease of use, availability, water solubility, and non-toxicity (Ford, 1999). HPMC is the most important hydrophilic carrier material used for the preparation of oral controlled drug delivery systems (Siepmann and Peppas 2001). It has high swellability which controls drug release through the hydrated systems by diffusion. HPMC forms a gelatinous layer at the surface of the matrix which causes relaxation of polymer chain and volume expansion and ultimately allows diffusion of drug through the matrix (Fahs *et al.*, 2010). HPMC is soluble in cold water and some organic solvents and over the entire biological pH range and forms transparent and flexible films from aqueous solutions (Fahs *et al.*, 2010).

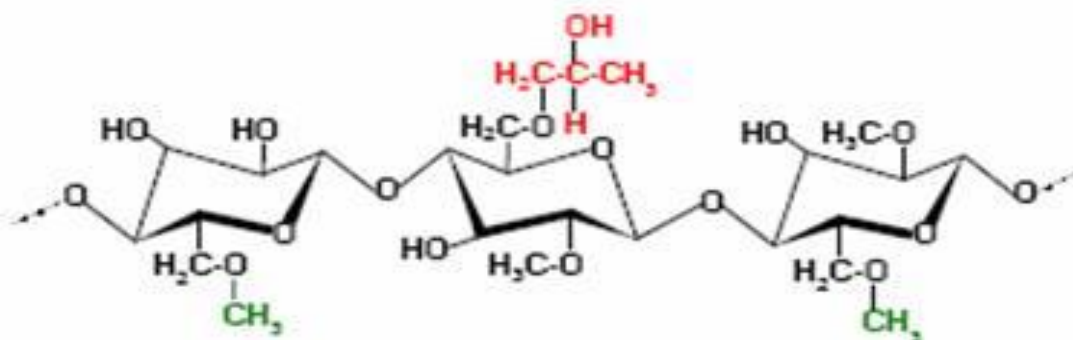


Figure 1.11: Chemical structure of hydroxypropylmethylcellulose (HPMC).

### 1.7.6 Plasticizer

Plasticizers are mainly used for the purpose of processing and modifying the properties of polymeric systems particularly films to overcome brittleness and improve flexibility and extensibility (López *et al.*, 2008) and depends upon type and concentration of plasticizers. Plasticizers are an important class of low molecular weight non-volatile compounds and act by reducing glass transition temperature ( $T_g$ ) and intermolecular forces between the chains of polymers and improves handling of films and enhance the performance by avoiding pores and cracks in the polymeric film matrix (Jagannath *et al.*, 2003; Adeodato Vieira *et al.*, 2011). The

council of the International Union of Pure and Applied Chemistry (IUPAC) defined a plasticizer as a substance incorporated in a material (usually a plastic or elastomer) to increase its flexibility, workability, or distensibility (Adeodato Vieira *et al.*, 2011). These substances reduce the tension of deformation, resistance to fracture, hardness and degree of crystallinity.

The selection of a plasticizer is normally based on its compatibility with the polymer, the amount required for plasticization, processing characteristics, desired thermal and mechanical properties of the final product (Cao *et al.*, 2009; Adeodato Vieira *et al.*, 2011; Cheng *et al.*, 2006). Hydrogen bonding, polarity and solubility parameter are also significant for effective plasticization (Choi and Park, 2004; Adeodato Vieira *et al.*, 2011). Increased concentration of plasticizer affects the compatibility of polymers resulting in a phase separation with the leaching of plasticizer usually observed (Silva *et al.*, 2009; Adeodato Vieira *et al.*, 2011).

Cheng and co-authors (2006) have postulated that an ideal plasticizer should have characteristics such as small size, high polarity and more polar groups per molecule. They reported that the plasticizing effect of a plasticizer on the polymeric system increases as the distance between the polar groups within a molecule increases (Cheng *et al.*, 2006). Generally, hydroxyls and polyols are cited as good plasticizers due to their ability to reduce the intermolecular hydrogen bonding while increasing intermolecular spacing (Audic and Chaufer, 2005). Water is a naturally occurring plasticizer which reduces  $T_g$  and increases free volume in hydrophilic polymers (Karbowiak *et al.*, 2006; Cheng *et al.*, 2006).

Glycerol (GLY) readily absorbs moisture and changes the film moisture content at room temperature and also prevents film brittleness (Karbowiak *et al.*, 2006; Kristo and Biliaderis 2006). GLY contains three hydroxyl groups (Figure 1.12) which imparts its solubility in water. GLY fills up the void spaces within three-dimensional rigid polymer network and interacts with the polymer chain through weak secondary forces (van der Waals forces or hydrogen bonding) and acts as a lubricant to reduce the intermolecular forces which imparts flexibility to the polymer (Di Gioia and Guilbert 1999).

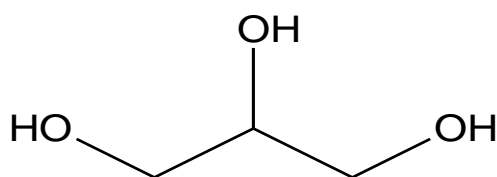


Figure 1.12: Chemical structure of glycerol.

## 1.7.7 Model drugs

### 1.7.7.1 Diclofenac sodium (DLF)

Diclofenac sodium (DLF) is a synthetic compound belonging to the non-steroidal anti-inflammatory drugs (NSAID) class. It is a well-known analgesic and anti-inflammatory agent which inhibit the synthesis of prostaglandins by inhibiting cyclooxygenase (COX) enzyme 1 and 2. It is commercially available on the market in various pharmaceutical dosage forms such as enteric coated and sustained release oral tablets, topical preparations and injections (Tudja *et al.*, 2001). DLF was found to possess antibacterial activity against both drug-sensitive and drug resistant clinical isolates of *S. aureus*, *Listeria monocytogenes*, *E. coli*, and *Mycobacterium spp.* in addition to its potent anti-inflammatory activity. It also has an antibacterial activity both *in vitro* and *in vivo* due to its ability to inhibit DNA synthesis of *E. coli* (Mazumdar *et al.*, 2009, Dutta *et al.*, 2004; 2007; 2008; 2009). DLF possesses anti-plasmid activity and reported to act as a ‘helper compound’ in synergistic combination with streptomycin (STP) against *E. coli* (Mazumdar *et al.*, 2009, Dutta *et al.*, 2004). The antibacterial action comes through the incomplete phenothiazine ring as shown in figure 1.13. DLF also consists of a secondary amino group and a phenyl ring, both ortho positions of which are occupied by chlorine atoms, causing an angle of torsion between the two aromatic rings, which might play a key role in imparting antimicrobial activity to this compound (Mazumdar *et al.*, 2009, Dutta *et al.*, 2007).

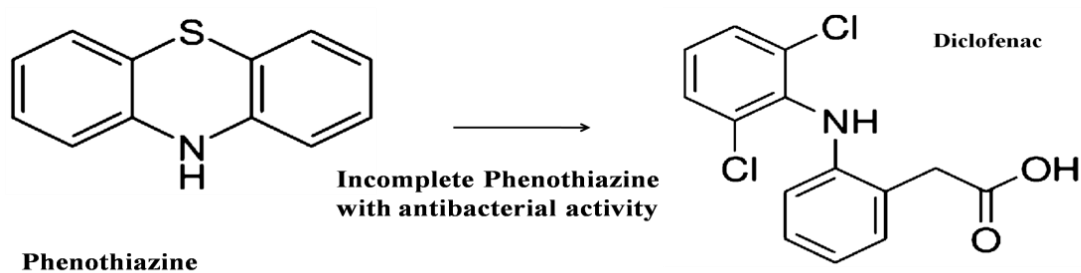


Figure 1.13: Structural illustration of DLF and phenothiazine and similarities between the two drugs.

### 1.7.7.3 Streptomycin sulphate (STP)

Streptomycin (STP) is an aminoglycoside antibiotic discovered by Schatz, Bugie and Waksman in 1944. It acts by inhibiting the initiation phase of protein synthesis by binding to the 30S subunit of ribosomes. In the initial uptake, the polycationic streptomycin binds to negative

charges on the cell surface or passes through water filled pores (Kornder, 2002). Streptomycin is actively transported across the cell wall but it may be affected by presence of abscess where the oxygen tension is very low. Overall, STP is most active against Gram-negative organisms (Smith and Jarvis, 1999). STP functions as a triacidic base because of the presence of two characteristic chemical entities, such as (a) two strongly basic guanido moieties and (b) relatively weakly basic methyl amino functional group (Figure 1.14).

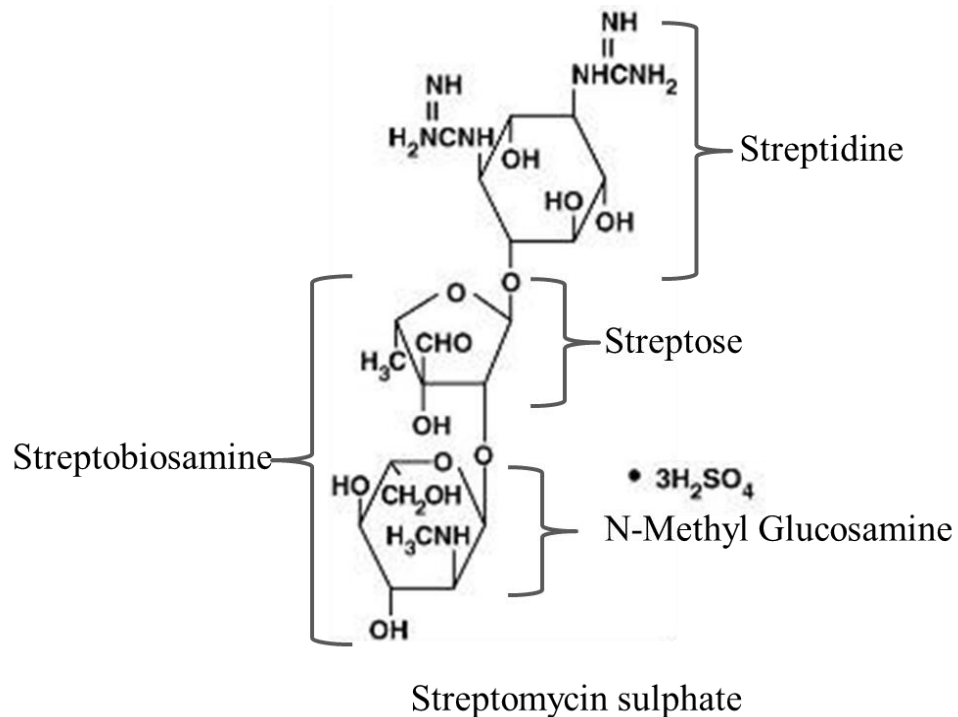


Figure 1.14: Chemical structure of STP containing streptobiosamine and streptidine units.

## 1.8 Formulation and characterisation

### 1.8.1 Freeze drying

Freeze-drying is also known as lyophilisation where water or another solvent is removed from a frozen solution by sublimation under high vacuum, thus obtaining a porous and friable structure that can be easily re-hydrated (Boateng *et al.*, 2009). This drying method involves lower operating temperatures which are particularly suitable for heat sensitive materials and proteins. This process is an alternative to overcoming the disadvantages of traditional drying methods (e.g. oven drying) by avoiding the degradation of the compound of interest and increases the stability of the final product at elevated temperature (Barresi *et al.*, 2009).

Lyophilisation involves three different, unique and interdependent stages where a sample is frozen to form an ice cake (freezing) and quantity of solvent is reduced by sublimation (primary drying) with consecutive stage of desorption (secondary drying) to achieve final product. In the freezing step, the temperature of the sample is reduced to or below the freezing point of water which converts the water into ice crystals in a random network referred to as a freeze concentrate (Tang and Pikal, 2004). Freeze drying depends upon the initial freezing step which fixes the sample structure, size and shape and its final characteristics (Tang and Pikal, 2004). Primary drying is typically the most time consuming stage of the freeze-drying cycle and optimization of this stage will have greatest impact on process economics (Tang and Pikal, 2004). In primary drying, vacuum is used to control pressure (Tang and Pikal, 2004) and a given product temperature (i.e. given ice vapour pressure), the smallest chamber pressure gives the highest ice sublimation rate. However, very low chamber pressure may cause problems, such as contamination of product with volatile stopper components or pump oil. During the initial phase of primary drying, 95% water should be removed after sublimating the compound. In secondary drying, a stable and dried product is formed at room temperature by the removal of residual moisture i.e. bound, unfrozen water. This is because small amounts of residual water remaining after the primary drying stage can damage the product. This step is performed by the application of heat and higher vacuum to remove bound water at lower temperatures (Tang and Pikal, 2004).

### **1.8.2 Solvent film casting**

Films as dosage forms have gained relevance in the pharmaceutical arena as novel, patient friendly, convenient products (Morales and McConville, 2011). Solvent cast films can be formulated to release the drug towards moist mucosal surfaces such as buccal, vaginal and wounds all of which exhibit the advantage of avoiding the first pass effect by direct absorption through the mucosal membranes or to achieve a local effect (Squier and Wertz, 1996). The film casting method is undoubtedly the most widely used manufacturing process found in the literature for making films including edible hydrocolloids films. This is mainly due to the ease of the process and the low cost that the system set up requires at the research laboratory scale. The process consists of at least six steps: preparation of the casting solution, removal of entrapped air bubbles from the solution, transfer of the appropriate volume of solution onto the casting surface, drying the casting of solution, cutting the final dosage form to contain the desired amount of drug, and packaging (Scott, 2008). Water or water-ethanol solutions or dispersions of the polymeric materials are spread on a suitable casting container and later dried in the ventilated

oven. During drying of the solution, solvent evaporation leads to a decrease in solubility of the polymer until polymer chains align themselves to form films. The choice of the substrate is important to obtain films, which can be easily peeled without any damage after the solvent is evaporated (Skurtys *et al.*, 2010). Throughout the manufacture of films, particular importance is given to the rheological properties of the solution or suspension, entrapped air bubbles, content uniformity and residual solvents in the final dosage form. The rheology of the liquid to be cast will determine the drying rates and uniformity in terms of the active content as well as the physical appearance of the films. During the mixing steps of the manufacturing process, air bubbles are inadvertently introduced to the liquid and removal of air is a critical step for homogeneity reasons (Morales and McConville, 2011).

Solvent cast films possess some principal advantages and drawbacks. The main advantage of solvent cast technology is the unique process of drying a liquid on a surface without applying further mechanical or thermal stress. Additionally, it offers a variety of specific features such as homogeneous thickness, distribution, high optical purity, free specks, transparency and flatness. Very thin films can be produced which is not possible by extrusion. There are some limitations on the types of polymer films for which solvent casting technology cannot be used. These include (a) proteins or any biological materials cannot be processed into films by solvent casting, (b) very thick films are very costly to produce by solvent casting technique, (c) slow production speed depending on a slow solvent evaporation process and requires high costs and energy for the recovery of organic solvents and the associated environmental concerns (Siepmann *et al.*, 2006).

### **1.8.3 Texture analysis characterisation**

#### **1.8.3.1 Tensile properties**

Film dressings are required to exhibit certain mechanical properties which provide valuable information on functional properties such as durability, stress resistance, softness, flexibility, pliability and elasticity. Such mechanical properties describe the stresses exerted by different parts of the body having various shapes, especially around the joints such as knees and elbows (Wittaya-areekul *et al.*, 2006; Khan *et al.*, 2000). These properties play a crucial role in maintaining the integrity of the dosage form (Morales and McConville, 2011). Tensile test helps to evaluate the flexibility and brittleness of a film when subjected to tension. The measurement of the above properties can be carried out by the use of texture analyser (TA). The American

Society for Testing and Materials (ASTM) specifies test methods for evaluating the tensile properties of films less than 1 mm in thickness (ASTM, 1997).

*Percentage elongation at break* is the increase in length relative to the initial length of sample by a tensile force. The tensile stress increases from zero to a peak force value at which it begins to break and rapidly drops to zero. The % elongation can be written as (Boateng *et al.*, 2009),

$$\text{Elongation at break (\%)} = \frac{\text{Yield break distance}}{\text{Original length}} \times 100 \quad (\text{Equation 1.1})$$

*Elastic modulus* or *Youngs modulus* is the stiffness of films or deformation of the film in elastic region. It is determined by the slope of initial linear portion of stress-strain curve by using the following equation (Perumal *et al.*, 2008; Boateng *et al.*, 2009; Morales and McConville, 2011):

$$\text{Elastic modulus (MPa)} = \frac{\text{Slope of stress-strain curve}}{\text{Film thickness} \times \text{cross head speed}} \quad (\text{Equation 1.2})$$

*Tensile strength* of a film is the resistance of the material to force tending to tear it apart, which is maximum (peak) stress on the stress-strain curve and given by equation 1.3 (Perumal *et al.*, 2008). Films containing plasticizer has significant reduction in both tensile strength and elastic modulus with increasing concentration plasticizer (Elgindy and Samy, 2009).

$$\text{Tensile strength (MPa)} = \frac{\text{Force at failure}}{\text{Initial cross sectional area of the film}} \quad (\text{Equation 1.3})$$

### 1.8.3.2 Mucoadhesion

Recently, texture analyser has been used for studying properties of mucoadhesive polymers and dosage forms using tensile mode of testing. The mucoadhesion of polymeric formulations by using tensile test technique was evaluated by measuring maximum force required to separate the polymeric formulation (films or wafers) from the surface of a mucosal substrate (Peppas and Sahlin, 1996). These *in vitro* experiments involve attaching films or wafers to a probe and force applied to bring the sample in contact with the substrate for a specific time (contact time) and a mechanical force applied to detach the probe from the mucosal substrate (Morales and McConville, 2011). The adhesive strength is evaluated by the force (*Fmax*)

required to detach the sample from the model mucosal substrate after mucoadhesive bonding has been established. Total work of adhesion (WOA) represents the total amount of energy involved in the probe withdrawal from the mucosal surface and determined through the area under the force versus distance curve. Cohesiveness determines the ability of the sample to resist the separation from the mucosal (wound) substrate due to the intermolecular forces (such as those from hydrogen bonding and van der Waals forces). It is determined through the distance travelled by sample before being detached (Thirawong *et al.*, 2007).

#### **1.8.4 Spectroscopic and chemometric data analysis**

Mucoadhesion by texture analyser usually involves measurement of mechanical force required to fracture the interface between substrate or mucin and polymer and depends upon the fracture theory of mucoadhesion (Jabbari *et al.*, 1993). Saiano and co-worker in (2002) reported that variations in the experimental parameters such as contact time, force, test speed and rate of removal from bioadhesive surface produces variations in experimental results of bioadhesive properties. This variation makes it very difficult to compare data between investigators to assign exact values representing bioadhesive properties (Saiano *et al.*, 2002). Jabbari and co-workers in 1993 reported that mucoadhesion studies by texture analyser is advantageous for classification of polymers for mucoadhesion, it is however not an accurate technique and cannot focus on mechanisms of adhesion at the biointerface (Jabbari, *et al.*, 1993). Hence, as an alternative, spectroscopic analysis techniques have been implemented and adopted to evaluate mucoadhesion mechanisms to investigate the interaction between substrate and polymer. In particular, ATR-FTIR has been applied effectively to study the interpenetration and entanglement of polymer chains and mucous which is fundamentally based on the diffusion theory of mucoadhesion (Jabbari *et al.*, 1993; Saiano *et al.*, 2002). It can be used to study mucoadhesion properties and diffusion profiles of solvent through different membranes (biological tissues, films, silicon membranes etc. (Tetteh *et al.*, 2009; Saiano *et al.*, 2002). It can provide real time information of diffusion of mucin through the membrane. Such kinetic diffusion data of mucin solution across the polymer based on FTIR spectroscopy generally produces large quantities of often complex multivariate data sets that requires appropriate chemometric analysis. The employment of chemometric techniques generally involves calibration, validation and extraction of maximum chemical information from the analytical data and its usefulness has been reviewed previously in pharmaceutical field (Gabrielsson *et al.*, 2002). Among the chemometric techniques used to resolve complex spectral data, factor analysis (FA) or principal component analysis (PCA)

(Malinowski, 1991; Wold *et al.*, 1987a), based on singular value decomposition (SVD) (Golub and Van Loan, 1989). Factor analysis is a multivariate technique for reduction of data matrices into its lowest dimensionality by the use of orthogonal factor space and transformation that yields predictions and/or recognisable factors which are influencing the data matrix. Due to possible spectral overlap, multivariate curve resolution (MCR) techniques are particularly very efficient in the analysis and modelling of such data sets. The basic principle of MCR is based on the fact that each component in the multivariate spectral data contributes additively and linearly to the absorbance at each spectral wavenumber. Also, the observed absorbance is directly proportional to the concentration based on the Beer Lambert law. In this study the MCR technique used is based on target factor analysis (TFA) described in full theoretical detail elsewhere (Malinowski 1991; Gemperline *et al.*, 1990). The advantage of this approach is that models of real factors can be systematically pieced together.

## **1.9 Aims and objectives**

This project aims to develop, formulate, characterise and optimise novel composite solvent cast films and freeze-dried wafers to deliver antimicrobial and anti-inflammatory drugs to chronic wound sites. The formulation development will be based on optimisation of films and wafers using different blends of hydrophilic polymers with optimised drug loading and *in vitro* release properties with their potential to act on two different phases of wound healing with low toxicity to maximise the effect by shortening wound healing times.

The main objectives are as follows:

1. Identification and characterisation of biocompatible and biodegradable polymeric systems and pre-formulation studies of the selected polymers. The work will also include formulation of polymer gels and optimising formulation parameters such as the concentration of polymer in the gel, based on their ease of handling, concentration of plasticizer for the flexibility of films and wafers, appropriate drug (STP and DLF) loading to inhibit bacteria and reduce inflammation at site of injury and evaluate the latter by *in vitro* antibacterial and other studies.
2. Formulation and lyophilisation cycle development (using DSC) of selected polymeric systems and drugs to obtain an optimised formulation exhibiting desirable characteristics of a wound dressing with controlled release of drug for rapid wound healing.

3. Physico-chemical and bio-analytical methods (SEM, XRD, DSC, ATR-FTIR, HPLC, texture analyser, Franz diffusion and *in vitro* antibacterial, adhesion and swelling studies) will be used to characterise functional physico-chemical properties of blank and drug loaded films and wafers to help in the selection of optimised formulation(s).
4. For *in vitro* mucoadhesion studies, ATR-FTIR technique will be used to monitor the entrapment of the mucin into drug-polymer cross-linking. The technique will also help to determine the rate of diffusion of mucin solution into the films and wafers using chemometric technique of principal component analysis (PCA) and multivariate curve resolution. Texture analyser will help to evaluate the adhesive strength, total energy involved in mucoadhesive bonding between the sample and wound substrate and affinity of the sample to resist the separation from a model wound substrate. *In vitro* mucoadhesion studies using ATR-FTIR spectroscopy and texture analyser will be compared for predictive mucoadhesive performance of films and wafers.
5. *In vitro* drug release study by Franz diffusion cell will be carried out using simulated wound fluid and its drug release kinetics will be evaluated to predict possible *in vivo* performance
6. Disk diffusion assay using three different microorganisms (*P. aeruginosa*, *E. coli* and *S. aureus*) will be evaluated for the zone of inhibition. Statistical t-test will be performed to determine the inhibition sensitivity for each bacterium to the drugs based on replicates.
7. The selected optimised film and wafer dressings will be compared with medicated marketed film and foam dressings.

## CHAPTER 2: PREPARATION AND PHYSICO-CHEMICAL CHARACTERISATION OF POLYOX™ BASED SOLVENT CAST FILMS

### 2.1 Introduction

Wound care is often labour intensive, requiring frequent attention by skilled professionals. Severe wounds (injury or burning) and chronic non-healing wounds damage the epithelium or even the endothelium of skin which is the barrier of the body and causes millions of deaths each year all around the world (Loke *et al.*, 2000 *cited in* Zaman *et al.*, 2011). The different types of the wounds and ideal characteristics required to heal these wounds have already been discussed previously (*in chapter 1 section 1.2 and 1.5*). Films prepared from aqueous solutions are widely used in pharmaceutical dosage forms and as drug delivery systems. Film-forming polymeric solutions are also well known in the field of surgery, wound care and skin protection. In surgery, film forming preparations are used as tissue glue for the thread-free closing of incisions or as disinfectants for preoperative skin preparation. Film-forming aqueous polymeric solutions are also utilized with or without antimicrobials substances for the non-surgical care of minor cuts and abrasions or in ostomy care for the protection of the skin surrounding the ostomy wound against the aggressive body fluids (Zurdo Schroeder *et al.*, 2007). Films prepared from such solutions will be advantageous in wound care management while films prepared in organic solvents, are considered undesirable because of the difficulty in removing the solvents completely, stringent regulations on exposure to these organic solvents, and more severe guidelines on discharge of organic solvents due to increased environmental concerns (Boateng *et al.*, 2009; Zurdo Schroeder *et al.*, 2007). Films must be bioadhesive to achieve controlled drug delivery to moist surfaces such as wound, nasal cavity and vagina (Silva *et al.*, 2008). Film dressings have ease of application (due to flexibility) around joints and other difficult areas, and their transparency enables examination of the wound bed without the removal of the dressing. At the same time, it must have enough strength to resist abrasion (Boateng *et al.*, 2009). Film dressings can be used as primary or secondary dressings and often form part of the construction of other dressings such as hydrocolloids, hydrogel sheets and are used to protect the skin from shearing forces. Films are also used as covering or seal in negative pressure wound therapy systems and as a protective cover over intravenous catheter sites to prevent infection. Film dressings are indicated for the management of minor burns and simple wounds such as scalds abrasions, lacerations and lightly exuding wounds. Their flexibility also means that they can be used to cover sutures following surgery. Even after sutures or clips are removed, film

dressings can still be applied over an incision site for a few months and are especially good at reducing the skin tension on surfaces (Sussman, 2010).

The increasing interest in polymer blends of synthetic with natural ones in biomedical applications has been observed from the last three decades. Such a composite system has improved biocompatibility, physical and mechanical properties compared with those of the individual components. Blends of synthetic and natural polymers can form a new class of materials with improved mechanical properties and also known as bio-artificial or biosynthetic polymeric materials (Sionkowska, 2011). Natural polymers are usually biocompatible, whereas synthetic polymers have good mechanical properties and thermal stability, much better than several naturally occurring polymers (Sionkowska 2011).

In this study, we report on film dressings formulated by blending a synthetic polymer Polyox<sup>®</sup> (POL) with four different hydrophilic polymers, namely carrageenan (CAR), sodium alginate (SA), chitosan (CS) and hydroxypropylmethylcellulose (HPMC). All the polymers were chosen due to their well-known bioadhesive and film forming properties (Crowley *et al.*, 2004; Kianfar *et al.*, 2012; Boateng *et al.*, 2009; Giovino *et al.*, 2012; Rai *et al.*, 2010). Films were prepared by the solvent casting approach from polymeric gels of the polymers and characterised for functional properties expected for wound dressings. The films were characterised using scanning electron microscopy (SEM), differential scanning calorimetry (DSC), Fourier transform infrared spectroscopy (FTIR) and X-ray diffraction (XRD). Further, films plasticized with glycerol (GLY) (9-50% w/w) were characterised by measuring their tensile properties on a texture analyser. Two model drugs streptomycin sulphate (STP) and diclofenac sodium (DLF) which target two different stages of wound healing were incorporated into the optimised plasticised films.

## 2.2 Materials

Polyox<sup>®</sup> WSR 301 LEO NF ( $\approx 4000$  KDa) polyethylene oxide (POL) was obtained from Colorcon Ltd; (Dartford, UK), kappa carrageenan (CAR) (Gelcarin GP 812 NF) IMCD Ltd; (Sutton, UK), chitosan (CS) (medium molecular weight 9413) 75-85% deacetylated, glycerol (GLY) (approximately 98%), hydroxypropylmethylcellulose (HPMC), diclofenac sodium (DLF) and streptomycin sulphate (STP) were all purchased from Sigma Aldrich, (Gillingham, UK). Acetic acid, sodium alginate (SA), ethanol (laboratory grade), were all purchased from Fisher Scientific, (Leicestershire, UK).

## 2.3 Methods

### 2.3.1 Preliminary formulation development

Polymeric films were prepared using solvent casting technique. Prior to the preparation of films, experiments were performed to produce 0.7-1.2% w/w aqueous gels of POL to determine concentrations suitable for further formulation development. This was based on clear uniform solutions with no lumps of undissolved polymer, ease of pouring and the release of air bubbles entrapped during stirring (Boateng *et al.*, 2009). polymeric gels comprising only POL (1% w/w) and blends of POL separately with CAR, SA, CS and HPMC in a different weight ratios, based on total polymer content of 1% w/w were prepared by stirring on a magnetic stirrer with heating at 70°C to assist complete dissolution. Table 1 shows the amount (weight) of the polymers used for the preparation of films. For CS, which is insoluble in water, the pH of the gel was subsequently adjusted using 1% v/v acetic acid solution. The resulting gels were poured into Petri dishes (86 mm diameter) and kept in an oven at 40°C for 18 h to dry. Figure 2.1 shows the schematic representation of the preparation of blank (BLK) and drug loaded (DL) films. These films were further examined visually for morphological defects.

Table 2.1: Quantities used during preparation of polymeric gels of POL and blends of POL with other polymers (CAR, SA, HPMC, and CS).

<b>Formulation</b>	<b>POL (gm)</b>	<b>CAR (gm)</b>	<b>SA (gm)</b>	<b>CS (gm)</b>	<b>HPMC (gm)</b>	<b>Total weight<sup>†</sup> (gm)</b>
POL	1.00	-	-	-	-	1.00
POL-CAR	0.75	0.25	-	-	-	1.00
POL-SA	0.75	-	0.25	-	-	1.00
POL-CS*	0.75	-	-	0.25	-	1.00
POL-HPMC	0.75	-	-	-	0.25	1.00
POL-SA	0.50	-	0.50	-	-	1.00

<sup>†</sup> Quantities reported were for 100 ml of the solvent (distilled water).

\* 1% v/v acetic acid was used to dissolve the chitosan.

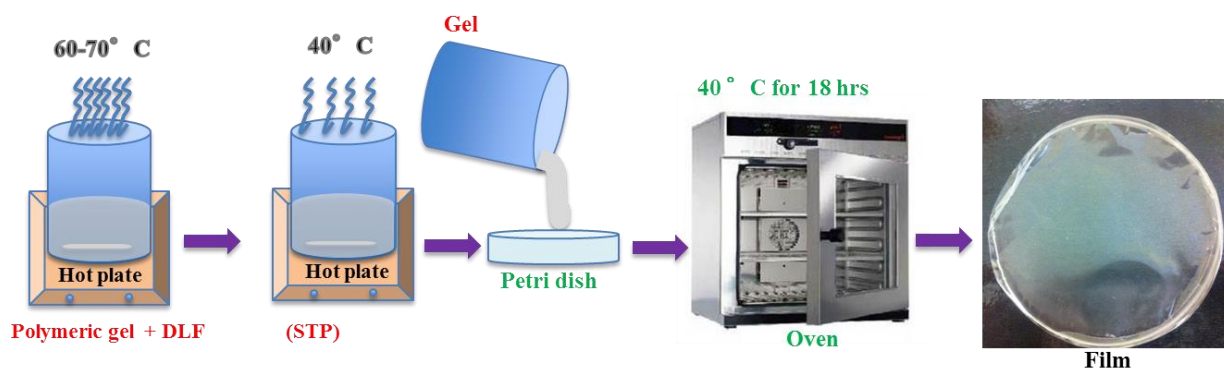


Figure 2.1: Illustration of preparation method for polymeric films (BLK and DL).

### 2.3.2 Preparation of blank (BLK) POL-CAR and POL-SA films

Based on the results of the preliminary film development using POL and all the four hydrophilic polymers, blends of POL with CAR and SA in the ratio of (75/25) and (50/50) respectively, based on 1% total polymer weight, were prepared by dissolving in distilled water with continuous stirring at 70°C. The resultant gels were poured into Petri dishes and dried in a hot air oven for 18h for complete drying. Furthermore, these formulations (gels) were subsequently loaded with GLY based on the total polymer weight (w/w) as plasticiser to optimise the mechanical properties of the formulations. The total dry weight (% w/w) of the individual polymers, drug and plasticiser present in films are shown in table 2.2.

### 2.3.3 Preparation of drug loaded (DL) POL-CAR and POL-SA films

POL-SA and POL-CAR gels were loaded with 4 ml ethanolic solution of DLF containing 50 mg and 100 mg of the drug (1.25% w/v and 2.50% w/v solution respectively) in the gel to achieve a final concentration of 5-10% w/w DLF in the polymeric gel. These gels were subsequently cooled to 40°C with constant stirring. Similarly, a 4 ml aqueous solution containing 150 mg and 300 mg of STP (3.75% w/v and 7.50% w/v solution) was subsequently added to achieve a final STP concentration of 15-30% w/w in the DL gels. The DL gels were dried in an oven at 40°C for 18 h as above to obtain DL films. All the dried films were carefully peeled off from the Petri dish, wrapped into a Parafilm<sup>®</sup> and kept in desiccators over silica at room temperature (23°C). These films were analysed for their physico-chemical (SEM, XRD, DSC and FTIR) and mechanical (tensile) properties.

Table 2.2: Quantities of the polymers, drugs and GLY (varying amounts based on total solid weight) used for formulation of POL-CAR and POL-SA (BLK and DL) films.

<b>Formulation</b>	<b>POL (gm)</b>	<b>CAR (gm)</b>	<b>SA (gm)</b>	<b>GLY (gm)</b>	<b>DLF (gm)</b>	<b>STP (gm)</b>	<b>Total weight (gm)</b>	<b>% GLY Content</b>
POL-CAR-BLK	0.75	0.25	-	0.00	-	-	1.00	0.00
POL-CAR-BLK	0.75	0.25	-	0.10	-	-	1.10	9.09
POL-CAR-BLK	0.75	0.25	-	0.25	-	-	1.25	20.00
POL-CAR-BLK	0.75	0.25	-	0.50	-	-	1.50	33.33
POL-CAR-BLK	0.75	0.25	-	0.75	-	-	1.75	42.86
POL-CAR-BLK	0.75	0.25	-	1.00	-	-	2.00	50.00
POL-CAR-DL	0.75	0.25	-	0.00	0.10	0.30	1.40	0.00
POL-CAR-DL	0.75	0.25	-	0.10	0.10	0.30	1.50	6.67
POL-CAR-DL	0.75	0.25	-	0.25	0.10	0.30	1.65	15.15
POL-CAR-DL	0.75	0.25	-	0.50	0.10	0.30	1.90	26.32
POL-CAR-DL	0.75	0.25	-	0.75	0.10	0.30	2.15	34.88
POL-CAR-DL	0.75	0.25	-	1.00	0.10	0.30	2.40	41.67
POL-SA-BLK	0.50	-	0.50	0.00	-	-	1.00	0.00
POL-SA-BLK	0.50	-	0.50	0.10	-	-	1.10	9.09
POL-SA-BLK	0.50	-	0.50	0.25	-	-	1.25	20.00
POL-SA-BLK	0.50	-	0.50	0.50	-	-	1.50	33.33
POL-SA-DL	0.50	-	0.50	0.00	0.05	0.15	1.20	0.00
POL-SA-DL	0.50	-	0.50	0.10	0.05	0.15	1.30	7.69
POL-SA-DL	0.50	-	0.50	0.25	0.05	0.15	1.45	17.24
POL-SA-DL	0.50	-	0.50	0.50	0.05	0.15	1.70	34.48

### 2.3.4 Scanning electron microscopy (SEM)

Surface morphology of the prepared POL, POL-CAR, POL-SA, POL-CS, POL-HPMC (all are in a ratio of 75/25 except POL only films) and optimised formulation POL-CAR (75/25) and POL-SA (50/50) (BLK and DL) with or without GLY films were analysed by a Hitachi SU 8030, (Hitachi High-Technologies, Germany) scanning electron microscope at low accelerating

voltage (1 kV). Films were cut into small pieces and mounted onto aluminium stubs (15 mm diameter) with ‘Agar Scientific G3347N’ double sided adhesive carbon tape. Images of the films were acquired using *i-scan 2000* software at a working distance of 8-15 mm at different magnifications.

### **2.3.5 Differential scanning calorimetry (DSC)**

Differential scanning calorimetry analysis of the films [POL, POL-CAR, POL-SA, POL-CS, POL-HPMC (all are in a ratio of 75/25 except POL) and optimised formulation POL-CAR (75/25) and POL-SA (50/50) (BLK and DL)] and starting materials [pure polymers and drug (DLF and STP)] was carried on a DSC1 Mettler Toledo instrument (Leicester, UK) calibrated with indium (based on heating range). Films were cut into small pieces and 3-5 mg of sample was placed into 40 $\mu$ l aluminium pans with lids (Mettler Toledo, Leicester, UK) and sealed using crucible sealing press (Metler Toledo Leicester, UK). An empty aluminium pan sealed with a lid was used as a reference. *STAR<sup>e</sup>* software program was used to run the samples. This involved initially cooling a sample from 25°C to -50°C and then heated from (-50°C to 350°C) at the rate of 10°C/min under constant purge of nitrogen (100 ml/min) to evaluate the glass transition, melting and crystallisation temperatures and any possible interaction between different polymers and drugs (STP and DLF).

### **2.3.6 X-ray powder diffraction (XRPD)**

A D8 Advantage X-ray diffractometer (Bruker AXS GmbH, Karlsruhe, Germany) was used to investigate the crystallisation or amorphous forms of drugs (STP and DLF) and polymers at the surface of films as well as the effect of the plasticizer (GLY). X-ray patterns of films and starting materials were obtained with a DIFFRAC plus XRD commander over a start to end diffraction angle of  $2\theta = 2^\circ - 45^\circ$  step size of 0.01 and a scan speed of 0.4 s. A Goebel mirror was used as monochromator which produced a focused monochromatic  $\text{CuK}\alpha_{1\&2}$  primary beam ( $\lambda=1.54184 \text{ \AA}$ ) with exit slits of 0.6 mm and a Lynx eye detector for performing the experiment. The operating conditions during the experiment were 40 kV and 40 mA. Figure 2.2 shows the graphical representation of the sample cell used for analysis of the polymeric films. The films were cut into 2 cm<sup>2</sup> strips and stuck to the square tiles of the holder by adhesive tape to acquire diffractograms. The Goebel mirror produces a divergent beam at different locations on the mirror to produce diffracted parallel beam. It generate high intensity  $\text{K}\alpha_{1\&2}$  and used in high resolution diffraction for samples having low absorption such as pharmaceuticals and biomaterials. A

background spectrum of the adhesive tape with the tile was always subtracted to get the pure spectra of the films.

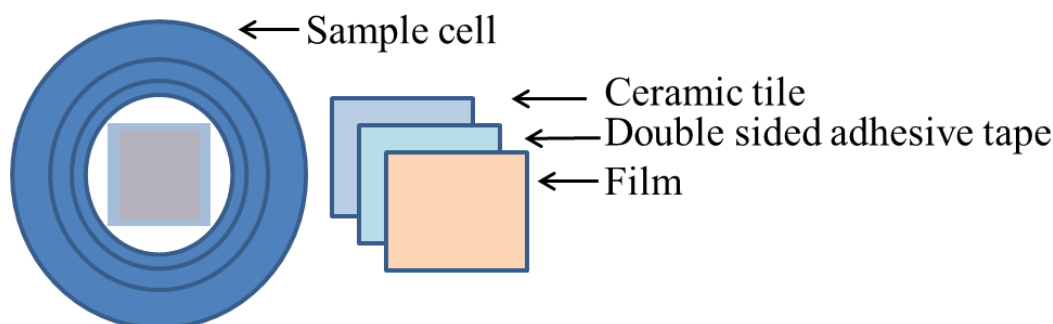


Figure 2.2: Representation of sample cell used for XRPD analysis of the polymeric films.

### 2.3.7 Attenuated total reflectance Fourier transform infrared spectroscopy (ATR-FTIR)

An ATR-FTIR spectrophotometer (Thermo Nicolet, Thermo Scientific, UK), connected with SMART arc accessory was used in combination with zinc selenide (ZnSe) ATR crystal to characterise uniformity and polymer interaction in the films. Films were placed on the ATR crystal and maximum pressure was applied by using a pressure clamp accessory to ensure intimate contact of the films with the ATR crystal. The FTIR was equipped with *OMNIC*<sup>®</sup> software, KBr beam splitter and mercury-cadmium-telluride (MCT) detector. Spectra were recorded at 4 cm<sup>-1</sup> resolution within a wavenumber range of 650-4000 cm<sup>-1</sup> with 256 scans to achieve better resolution. True absorbance of the films was obtained by subtracting background spectral information of both air and crystal.

### 2.3.8 Texture analysis (TA)

The mechanical (tensile) properties of POL-CAR and POL-SA (BLK and DL) films plasticized with varying concentrations of GLY were evaluated by a TA HD plus (Stable Micro System, Surrey, UK) texture analyser equipped with 5 kg load cell and Texture *Exponent-32*<sup>®</sup> software program. Figure 2.3 shows an illustration of texture analysis of BLK and DL films. The amount of GLY used as plasticizer is shown in table 2.2. Prior to testing, the average thickness of each sample was measured using a micrometer screw gauge. The films (n=3) devoid of any physical defects were selected for testing and cut in the shape of a dumb-bell (80 mm long, 30 mm gauge length and 3.5 mm width) and stretched between two tensile grips at (2-6 mm/sec) to a distance of 50-300 mm before returning to the starting position. A trigger force of 0.09N was

applied during the testing until the films broke and the tensile strength (force), elastic modulus, work done to break films representing the toughness (area under the force-distance curve) and % elongation at break were determined. The various instrument parameters used to carry out the mechanical testing are shown in table 2.3. Three replicates were carried out for each type of film. The effect of varying concentrations based on polymer weight (as shown in table 2.2) of GLY was evaluated for POL-CAR and POL-SA films.

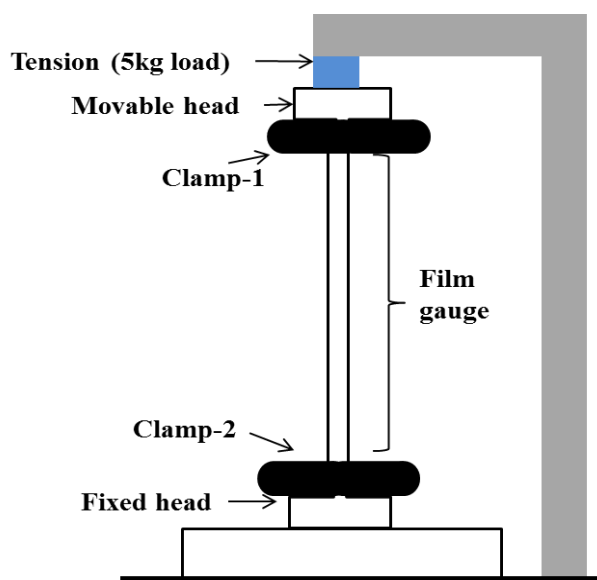


Figure 2.3: Schematic representation of texture analyser for the evaluation of mechanical properties of the films.

Table 2.3: Parameters used to evaluate tensile properties of films (n=3).

Test mode	Tension	
Pre-test speed	2-6 mm/sec	Speed of probe before stretching
Test speed	2-6 mm/sec	Stretching speed of the film
Post-test speed	10 mm/sec	Speed at which probe returns to the start position
Distance	50-300 mm	Distance to which grips separate from their starting position after stretching
Trigger type	Auto (Force=0.09 N)	Force achieved before profile is plotted

## 2.4 Results and discussion

### 2.4.1 Preliminary formulation development

POL is a synthetic polymer which has high viscosity, water solubility, compatibility with other bioactive substances and exhibits increased mucoadhesive capacity and can be used as a drug carrier with improved bioadhesion in biomedical applications (Zivanovic *et al.*, 2007; De Ascentiis *et al.*, 1995). Among the different concentrations of POL gels prepared, 1% w/w was easy to handle and pour from the container when compared to 0.7% w/w and 1.2% w/w. Figure 2.4 shows the digital images of POL films prepared from different gel concentrations (% w/w). Constant stirring with heat was chosen to help dissolve and disperse the POL into the water which prevented the formation of lumps which may not be possible through just hydration of polymer due to its high viscosity (1650-5500 cP). Boateng and co-authors reported that the use of vortex hydration with heat helps to disperse the polymer quickly without formation of lumps, and ultimately forming a clear solution. Heat helps in the reduction of the viscosity of the solution and facilitates the removal of entrapped air bubbles as well as ease of pouring into a Petri-dish (casting container) (Boateng *et al.*, 2009). Films prepared from only POL were difficult to remove from the Petri dish owing to strong adhesion and high viscosity.

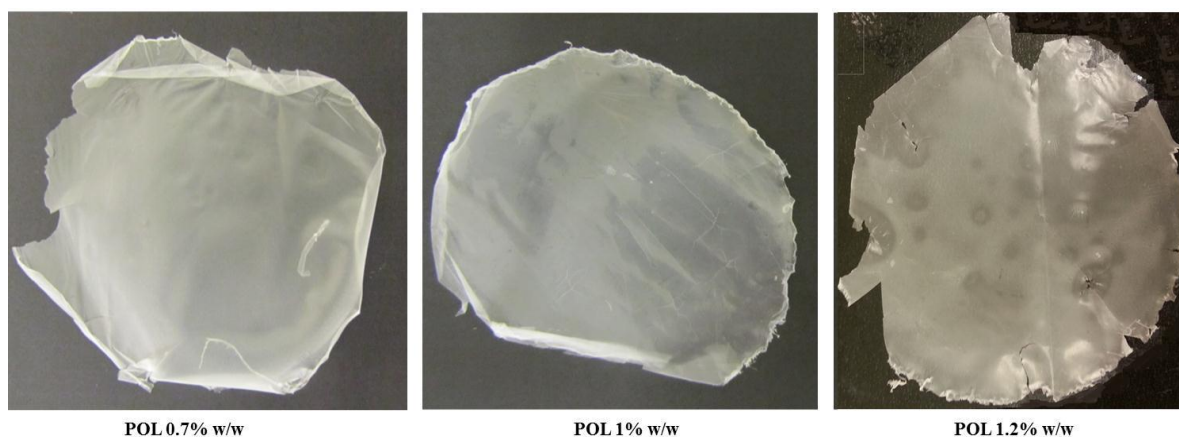


Figure 2.4 POL films prepared from gels of different concentrations based on total polymer weight.

It was also observed that the films prepared from POL were non-transparent. Transparency is a key advantage of film dressings which allows the inspection of the wound bed without the need to remove the dressing (Boateng *et al.*, 2008) and it was important to maintain this critical characteristic. It has been reported from previous research that increased opacity of

films was observed when more than 50% (based on total polymer weight) polyethylene oxide was used (Zivanoic *et al.*, 2007) as was the case for films prepared from only POL. This was attributed to spherulitic crystallisation of POL which appeared as monoclinic units cells of crystals with four radially oriented chains (Li *et al.*, 2010), though it should be noted that they used POL with a lower molecular weight. To overcome this problem, blended films of POL (synthetic) with natural and semi-synthetic hydrophilic polymers (CAR, CS, SA and HPMC) were prepared to improve the mechanical properties and biocompatibility.

It has been previously demonstrated that the use of synthetic and natural polymers helps to improve the physical properties which makes them suitable for applications in the biomedical field (Sionkowska, 2011). All the blended films were generally relatively more transparent due to the reduction in the crystallisation associated with POL by intermolecular interaction. This miscibility of the blend is associated with hydrogen bonding between the ether oxygen of POL and hydroxyl group of the polysaccharide. Figure 2.5 shows the digital images of the POL blended films with other polymers (CAR, CS, SA and HPMC). POL-CAR (75/25) films were smooth, homogeneous and flexible. Addition of CAR improved the mechanical strength as well as ease of removal for the flexible films (Alves *et al.*, 2006; Campo *et al.*, 2009). CAR exhibits potent anticoagulant, antithrombotic and anti-inflammatory activities (Fan, 2011) and its carboxy-methyl derivative has similarities with heparin which has shown a potential role in wound healing with beneficial effects on angiogenic and fibrogenic growth factors *in vitro* (Galvan, 1996). CAR has been previously used as a hydrogel wound dressing with polyvinyl alcohol and polyethylene glycol which showed improved properties of the dressing material (Silva *et al.*, 2011). Films associated with CS showed a 'scaly' surface which may be due to the acetic acid present in the polymeric gel. Giovino and co-workers used 1% w/v sodium hydroxide solution to neutralise the acidified chitosan films (Giovino *et al.*, 2012) and the same process was implemented to remove the scaly surface and obtain transparent films. On visual inspection phase separation occurred in the films due to the water solubility of POL and needs further investigation. Films prepared from POL-HPMC and POL-SA gels were thin in nature. Furthermore, films prepared with POL-SA in weight ratio of 50/50 were transparent, appeared clear and were flexible. SA has a wide range of applications in the biomedical field including its gel forming property which maintains a moist environment at the wound site. In addition, it is biocompatible, biodegradable, haemostatic and assists in fibroblast formation, activating the macrophages to produce growth factors (fibroblast growth factor [FGF], TGF- $\beta$ , and PDGF).

Films [POL-CAR (75/25) and POL-SA (50/50)] plasticized with GLY were transparent and flexible. All the drug loaded films (POL-CAR and POL-SA) were fairly transparent and translucent due to the added drug in the film. Figure 2.6 and 2.7 shows the digital images of POL-CAR (75/25) and POL-SA (50/50) (BLK and DL) plasticized with or without GLY.

Film dressings are required to exhibit certain mechanical properties which provide valuable information on functional properties such as durability, stress resistance, softness, flexibility, pliability and elasticity (Khan *et al.*, 2000). Unplasticised films of POL with CAR, CS, SA and HPMC were thin ( $0.05-0.07 \pm 0.01$  mm) as compared to POL-CAR-BLK-20%GLY, POL-CAR-DL; POL-CAR-DL-20%GLY films (0.09-0.13 mm). POL-CAR-BLK and POL-SA-BLK films prepared from 1.0% w/w solutions were too thin for easy removal without any damage and were too brittle and deformed or cracked for effective application.

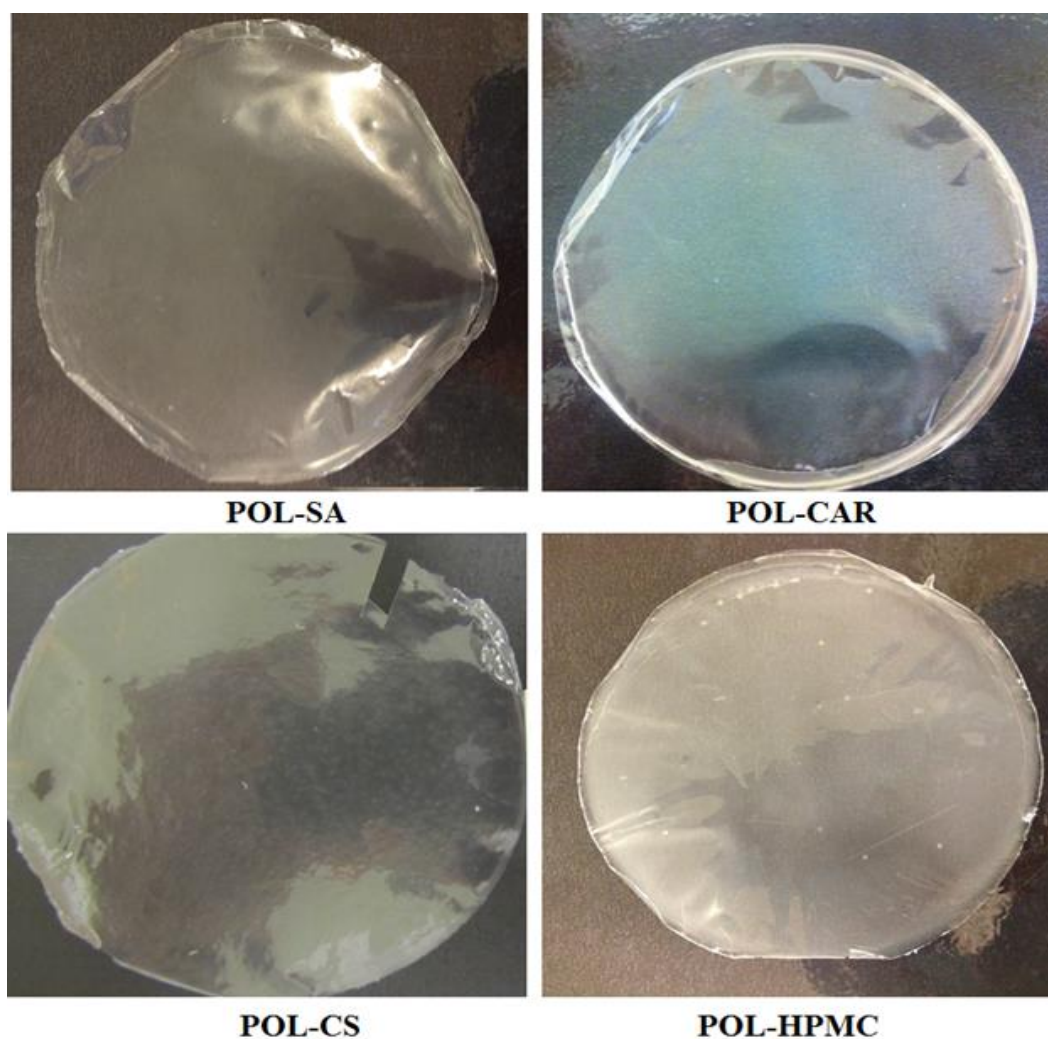
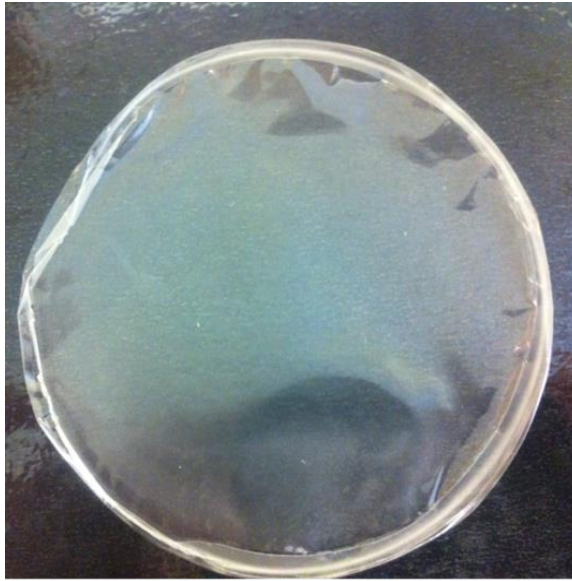


Figure 2.5: Blended films of POL with SA, CAR, CS and HPMC.

However, addition of GLY imparted flexibility to the films with increased thickness, therefore rendering them easier to remove (Chung and Rubner, 2002). All films without GLY and drug showed thickness between 0.05 to 0.07 mm which was increased with the addition of plasticizer and added drug (0.07 - 0.13mm). This increase in thickness consequently results in the ease of removal from the casting container. Thickness of films significantly affects their swelling as it determines concentration and depth of penetration of solvent molecules into a film. Previous studies also reported that the highest loading capacity was achieved with the thickest films (Burke and Barrett 2004; 2005). Laohakunjit and Noomhorm (2004) explained the relationship between the thickness of films and water vapour transmission rate. They reported that the addition of plasticizer increases the thickness which ultimately increases the water vapour transmission rate and oxygen transmission rate of starch plasticized edible films (Laohakunjit and Noomhorm, 2004). That was the case when films were plasticized with GLY (0.05-0.13) which is expected to help to increase water vapour transmission rate and oxygen transmission rate. These properties can help to manage the wound exudate released from wounds and also promote angiogenesis with improved wound healing. Lrotonda (2007) reported that CAR films plasticized with GLY improved almost all their physical properties (hygroscopic, mechanical, barrier) due to their deformable nature. In our case, GLY imparted thickness as well as overall appearance (flexibility, mechanical strength, ease of removal) (Lrotonda, 2007) although increased thickness in the films could be associated with increasing total weight due to GLY and added drug. It was observed that thickness of POL-CAR films was high (0.07-0.13) when compared with POL-SA (0.05-0.09) which may be associated with the formation of compact arrangements of SA when the gel collapsed during drying to form thinner films. Sriamornsak, and Kennedy reported that the thickness of films is associated with the molecular weight of the individual polymers, where molecular weight of the polymers and weight ratios could have had an added effect on the thickness of the films (Sriamornsak, and Kennedy, 2008).



**POL-CAR-BLK Films**



**POL-CAR-BLK-20% GLY**



**POL-CAR-DL Films**



**POL-CAR-DL-20% GLY Films**

Figure 2.6: POL-CAR (BLK and DL) films with or without 20% GLY



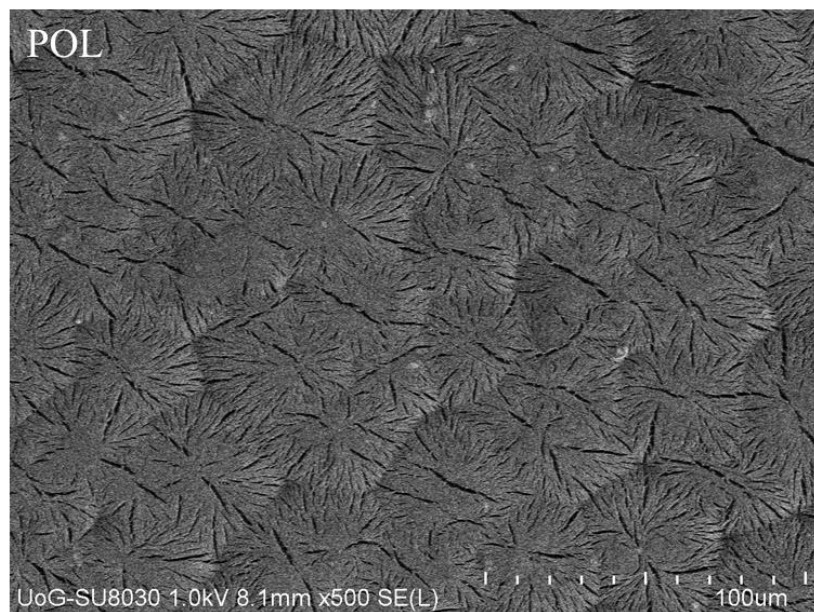


Figure 2.8: SEM image of POL film containing spherulitic crystals radially oriented chains.

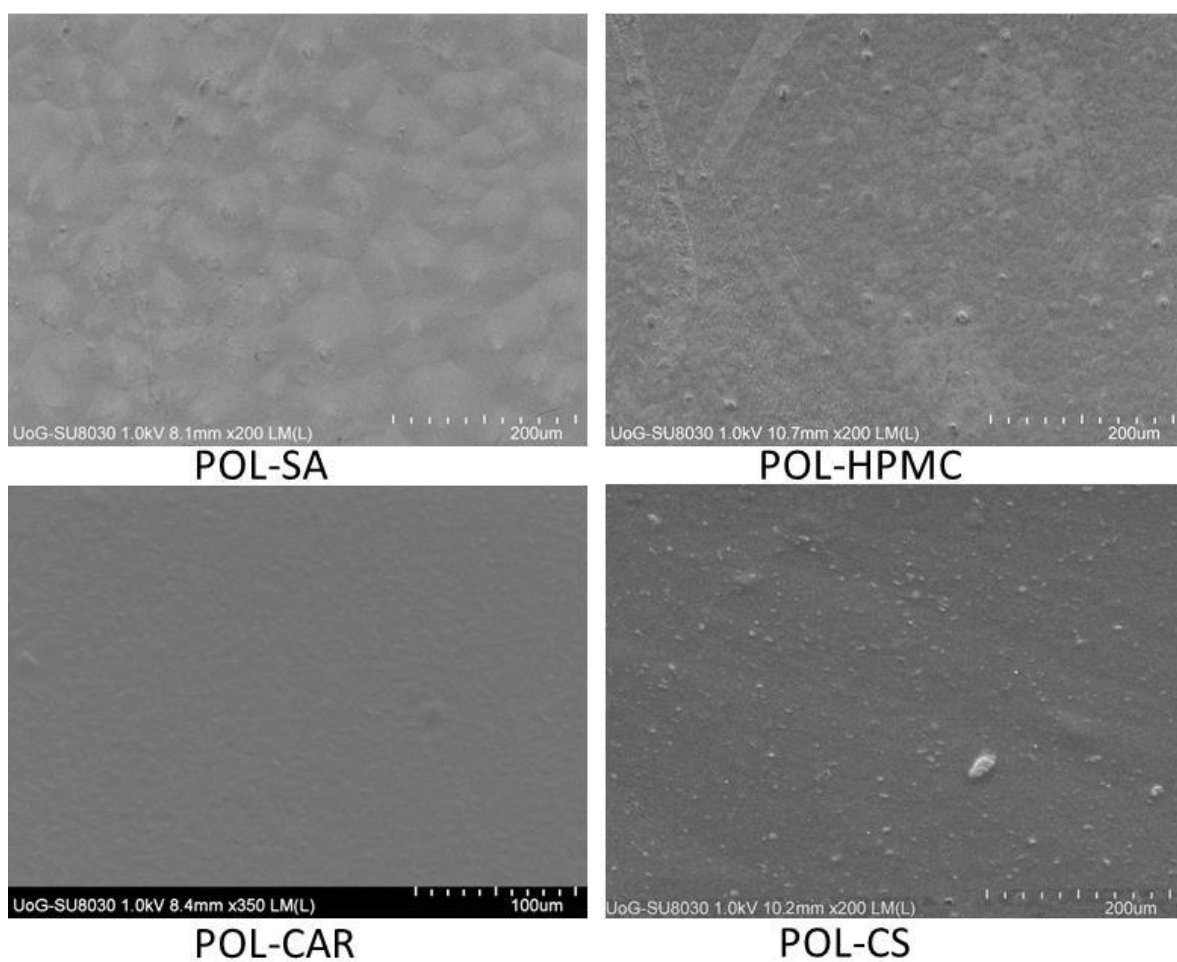


Figure 2.9: SEM topography of POL blended films with SA, HPMC, CAR or CS (75/25).

Figure 2.10 shows the SEM morphology of POL-CAR (BLK and DL) films with or without plasticizer (20%GLY). POL-CAR-BLK-20%GLY showed a smooth surface due to interpenetration of GLY into the polymeric network. There were crystals present on the surface of POL-CAR-DL films which decreased after plasticizing with 20% GLY. This is because; GLY produced flexibility in the films by reducing the crystallinity. Such flexibility of the films prevents re-injury to the surrounding skin in orthopaedic wounds, which are prone to swelling and have an increased risk of friction between the wound and dressing (Ousey *et al.*, 2012).

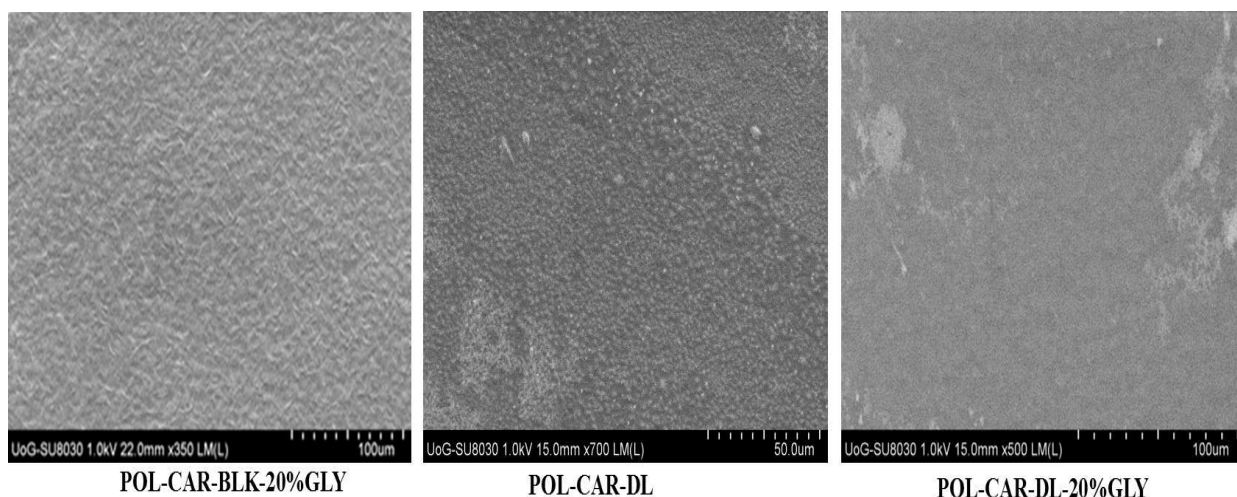


Figure 2.10: SEM images of POL-CAR-BLK-20%GLY, POL-CAR-DL and POL-CAR-DL-20%GLY.

Further, BLK films prepared from POL-SA (50/50 w/w ratio) with (9%GLY) and without GLY showed smooth homogeneous surface (as shown in figure 2.11) which showed further decreased spherulitic crystallisation whereas POL-CAR-DL film with (9%GLY) and without GLY showed a rough surface with the presence of some particles observed on the surface. This may be associated with added drug in the formulation. POL-SA-BLK-9% GLY showed a smooth surface and this may be due to the added GLY in the films but addition of drug showed fractures on the surface of the films.

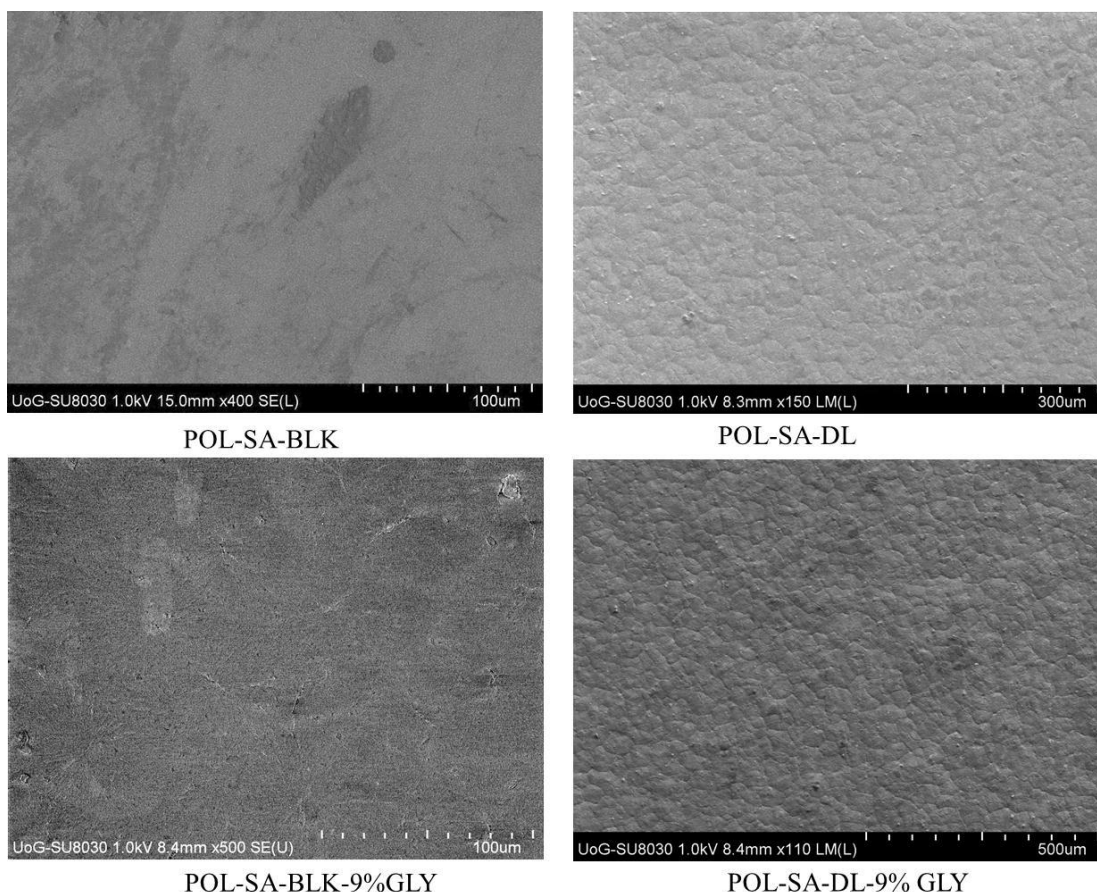


Figure 2.11: SEM morphology of POL-SA (BLK and DL) films

### 2.4.3 Differential scanning calorimetry (DSC)

Figures 2.12, 2.13 and 2.14 show the DSC thermograms for pure polymers, pure drugs and their corresponding films. STP showed endothermic peaks due to its amorphous nature, however, the thermograms seem to indicate recrystallization and then eventual melting which was difficult to attribute to a particular compound. This may be associated with the presence of other compounds such as salts or possible STP degradation products but this needs further investigation. The observed glass transition temperatures of SA and HPMC were 60.28°C and 64.42°C respectively. SA, CS and HPMC showed broad endothermic peaks at 152.73°C, 139.48°C and 166.69°C respectively, whereas CAR showed broad endothermic peak at 148.76°C which was quickly decomposed at 192.56°C. Observations for these four polymers were due to their amorphous nature. DLF showed melting peaks at 293.96°C in addition to immediate decomposition. POL showed an endothermic peak at 70.22°C with an exothermic peak at 177.21°C which could be attributed to the recrystallization from the melt.

DSC curves of all POL-CAR films showed a suppression of the POL melting peak ( $61\pm 4.5^\circ\text{C}$ ) due to the molecular chain of CAR which has a significant effect on the overall chain mobility in the mixture and retards the rate of crystal growth of POL. The melting temperature decreased from  $70.22^\circ\text{C}$  to  $65.22^\circ\text{C}$ , suggesting that the equilibrium characteristics of POL are significantly altered by the presence of CAR, resulting in more transparent films. There was no considerable suppression of POL's melting point in POL-CS, POL-SA and POL-HPMC films (Figure 2.13). POL-SA (50/50) films showed further decrease in the melting temperature which may be due to the decrease in the spherulitic crystallisation of POL in these films. Çaykara *et al.*, (2005) reported that the use of SA decreases the melting temperature and crystallinity of polyethylene oxide (POL) when used at 33% based on total polymeric weight (Çaykara *et al.*, 2005). This may be due to the POL which is semi-crystalline in nature and contains a two phase material consisting of spherulitic crystals embedded in an amorphous part in a continuous configuration. Maclaine and Booth (1975) reported that the crystallinity of POL is in the range of 45–55% when the molecular weight is 1,000,000 or more (Maclaine and Booth 1975).

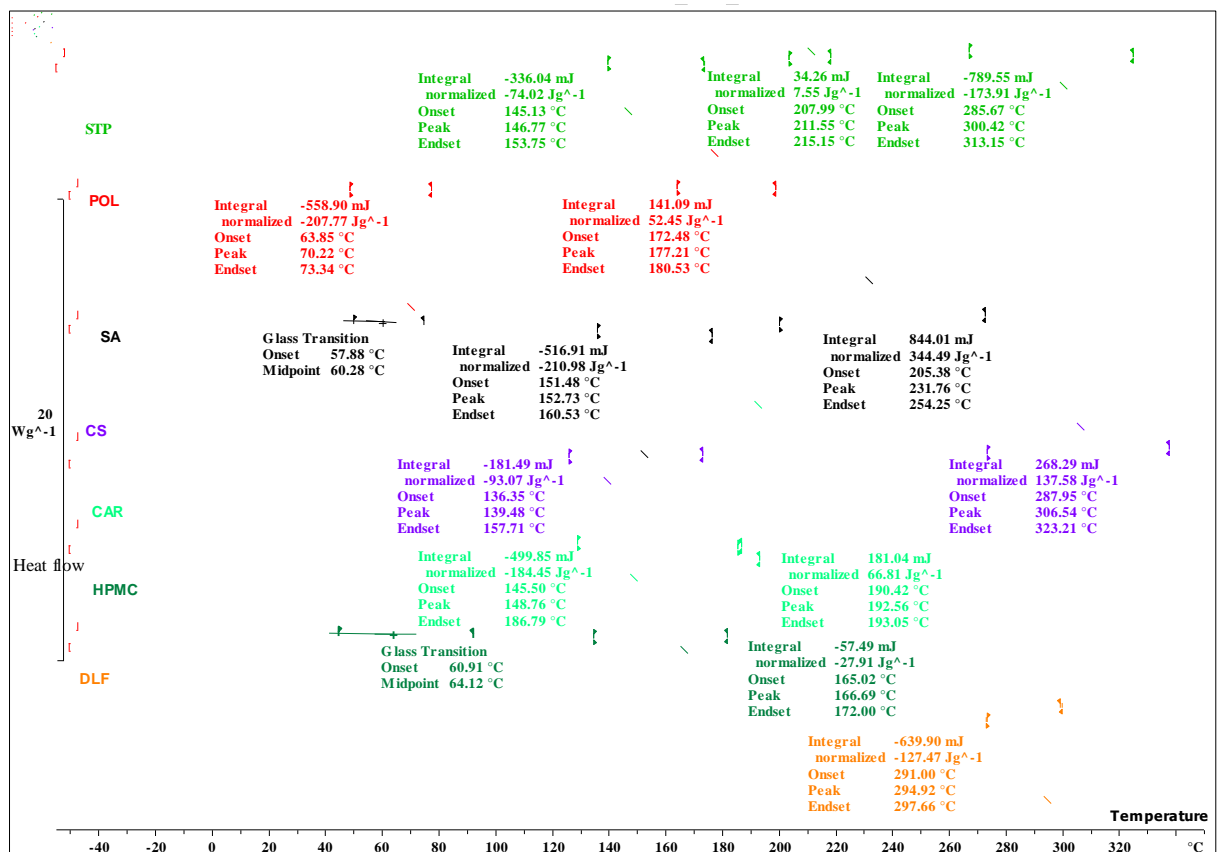


Figure 2.12: Comparison of DSC profiles of pure polymers and drugs.

POL-Car-BLK film results in the melting of the crystalline part at 70.22°C and the amorphous part further crystallises to give an exothermic peak at 135.66°C which subsequently melts to produce an endothermic peak at 207.70°C.

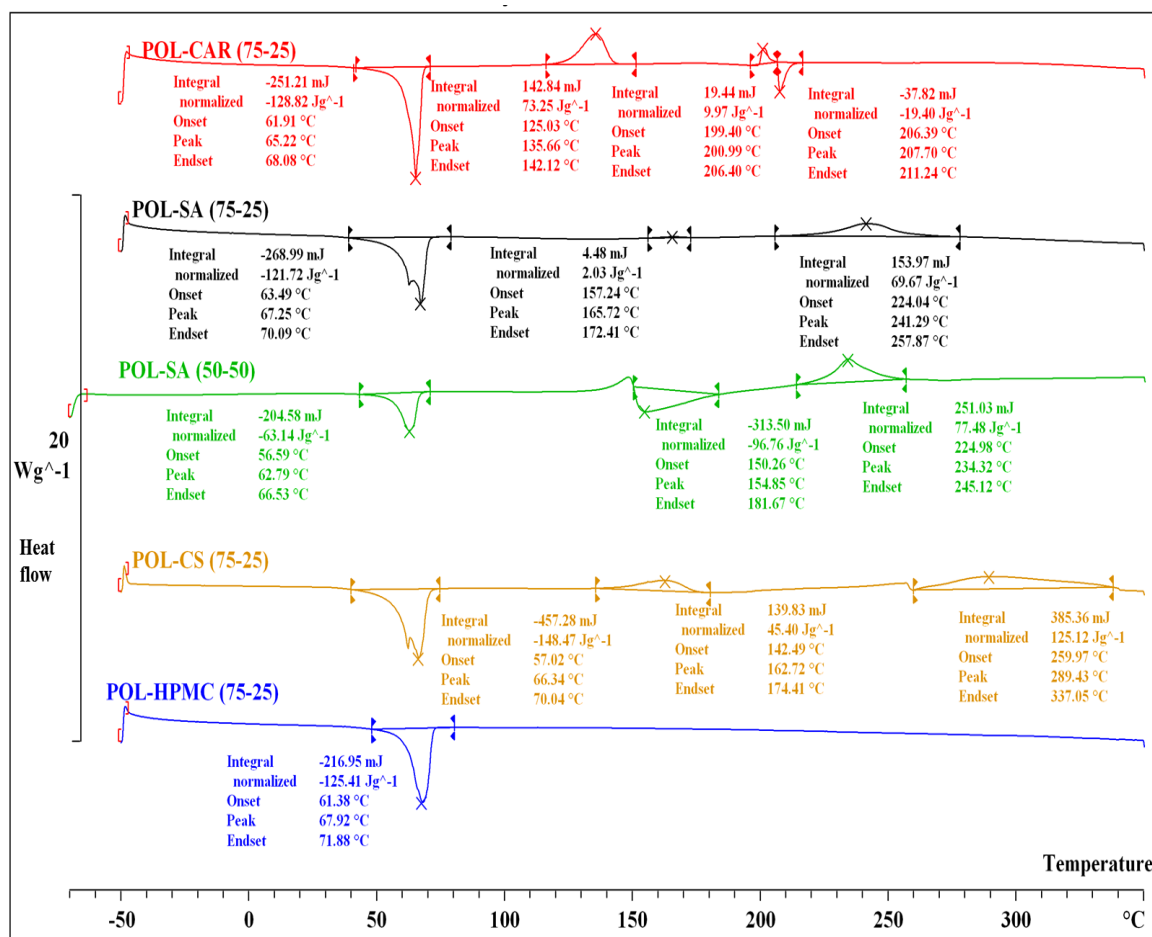


Figure 2.13: DSC profiles of films prepared from blends of POL with CAR, CS, SA and HPMC.

All the POL blended films except POL-HPMC showed exothermic peak which is associated with crystallisation of POL. POL-CAR films further showed an exothermic and endothermic peak between 199-211°C which may be associated with CAR. POL-SA (75/25) and POL-SA (50/50) films showed an endothermic peak at 154.85°C due to the augmented effect of SA. POL-SA (75/25) and POL-SA (50/50) films also showed exothermic peak between 224-245°C which is associated with recrystallization of SA. POL-CS films showed a step change in the baseline of the thermogram around 259°C which immediately recrystallized at 289°C, as some part of CS was melted but undergoes immediate recrystallization and may affect the stability of the films.

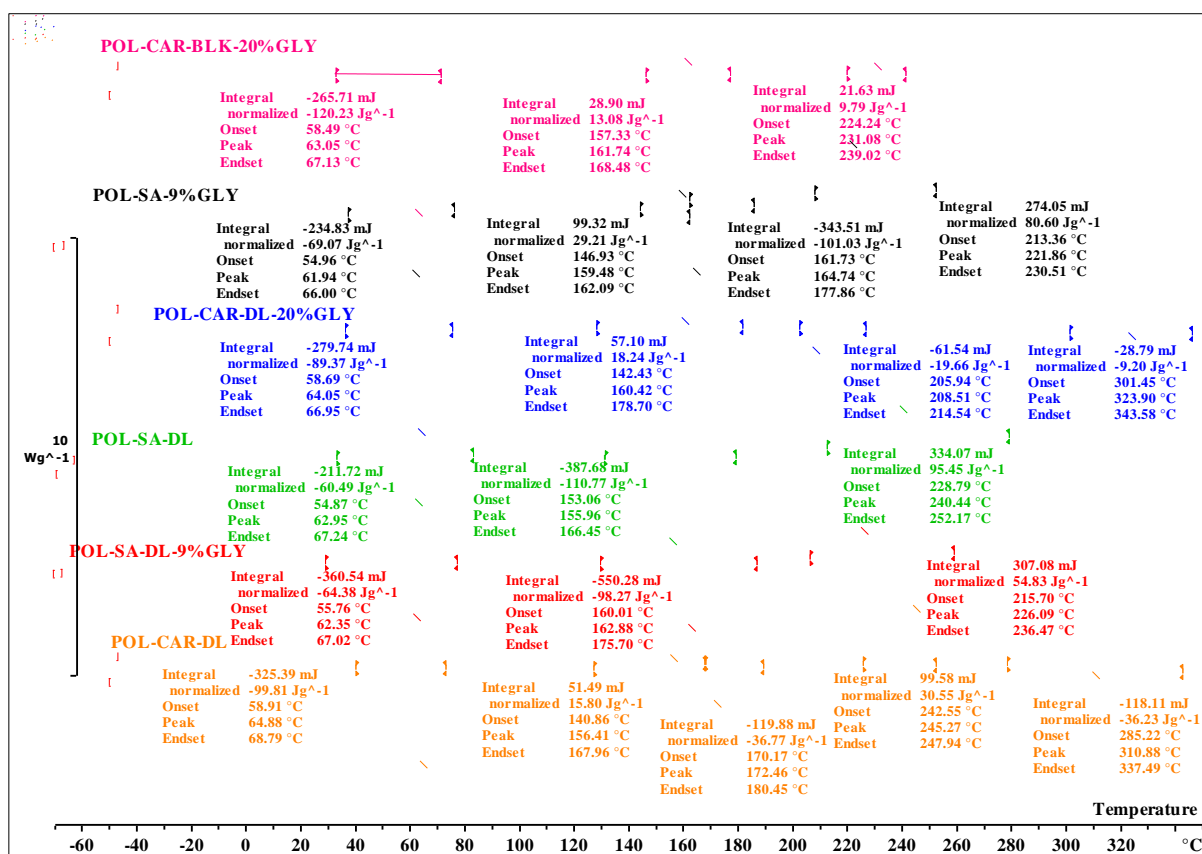


Figure 2.14: DSC thermograms of POL-CAR-BLK-20%GLY, POL-SA-BLK-9%GLY, POL-CAR-DL, POL-CAR-DL-20% GLY, POL-SA-DL and POL-SA-DL-9%GLY.

All the POL-CAR and POL-SA (BLK and DL) films showed a melt peak around 62-65°C which was accompanied by the POL melting. POL-CAR-BLK-20%GLY films showed an exothermic peak at 168°C whereas POL-SA-BLK-9%GLY showed an exothermic peak at 159°C due to the presence of POL and subsequent melt (166.7°C) and recrystallization peak at 221.0°C may be associated with the SA. Furthermore, POL-CAR-DL and POL-CAR-DL-20% GLY films showed an exothermic peak (156-160°C) and endothermic peak (172.46-208.51°C) respectively. The endothermic peak was shifted to a higher temperature which may be associated with improved stability of the films by addition of GLY. It was observed that the addition of GLY resulted in a step change in the baseline of the thermogram of POL-CAR-DL20%GLY whilst there was an exothermic peak at 245°C in POL-CAR-DL films. This may be due to the rearrangement of crystals of POL-CAR-DL films from the melt which is inhibited by the presence of GLY in POL-CAR-DL-20%GLY film. In the case of POL-SA-DL and POL-SA-DL-9%GLY) the exothermic peak associated with the POL was suppressed by the SA endothermic peak (155-163°C). None of the films showed any covalent interaction (except hydrogen bonding)

to form a new complex entity which implies the polymer blends were compatible with each other. All the optimised drug loaded films (POL-CAR-DL, POL-CAR-DL-20%GLY, POL-SA-DL and POL-SA-9%GLY) did not show any peaks for DLF and STP which suggests the molecular dispersion of the drugs within the film matrix which can help to release both drugs in a controlled manner (Boateng *et al.*, 2013; ).

#### **2.4.4 X-ray powder diffraction (XRPD)**

Pure POL films showed sharp distinct peaks at 14.62°, 15.05°, 19.11°, 23.22°, 26.23° and 26.91° (Figure 2.15) which explains the helical crystalline geometry of POL (polyethylene oxide) whose structure completes two turns around an axis every seven repeating units, due to trans (C-C-O-C), trans (C-O-C-C), gauche (O-C-C-O) conformational arrangements (Pereira *et al.*, 2009). Due to the absence of large side groups, the POL molecular chain is considered as more flexible and intermolecular forces act on the main-chain atoms more strongly (Takahashi and Tadokoro, 1973). CAR showed an amorphous nature with the presence of additional peaks at 28.39°, and 40.58° which may be attributed to inorganic salt impurities from KCl (Prasad *et al.*, 2009) whereas SA and HPMC did not show any distinct sharp peaks but CS had two broad peaks suggesting their amorphous nature (Figure 2.15). Films prepared by blending of POL with the other polymers showed a reduction in the crystallisation in descending order of CS > HPMC > SA > CAR respectively (Figure 2.16). This could probably be due to interruption of POL chain interactions because of formation of hydrogen bonds between the ether oxygen of POL and side chain hydroxyl groups of the other polymers (Zivanovic *et al.*, 2007). Further, the intensities of POL crystalline peaks at 19.11° and 23.22° were reduced which confirms the DSC results that crystallinity of POL was reduced after film formation in the presence of CAR (Figure 2.17). It was observed that the formation of sodium sulphate in POL-CAR-DL and POL-CAR-DL-20%GLY due to the salts of the drugs (STP and DLF). However, there were no distinct peaks of DLF and STP, suggesting that the addition of these drugs did not change the nature of the original polymer blends which confirms molecular dispersity of both drugs within the film. GLY increases the spaces between the crystal lattice and decreases the crystallinity of the films. Such films have higher hydration capacity compared to those with the crystallised films (). Films with lower crystallinity can help to absorb and retain large quantities of wound exudate containing pro-inflammatory cytokines and neutrophils which prevents maceration around the wound bed and subsequently promote wound healing (Kramer and Maassen, 2012).

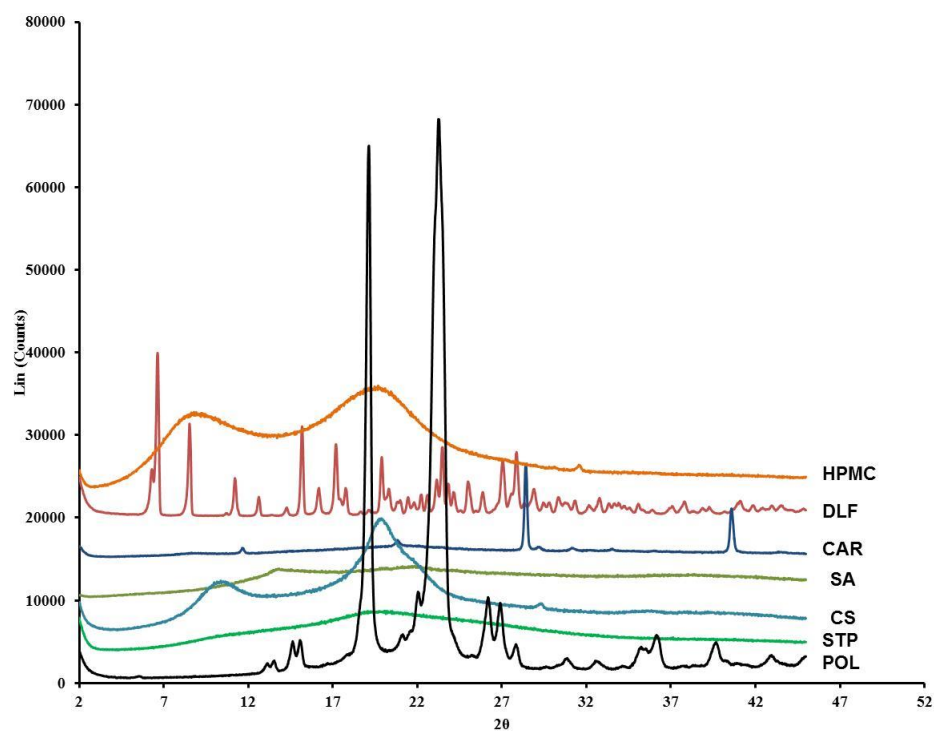


Figure 2.15: XRPD patterns of pure polymers (POL, CS, SA, CAR and HPMC), DLF and STP

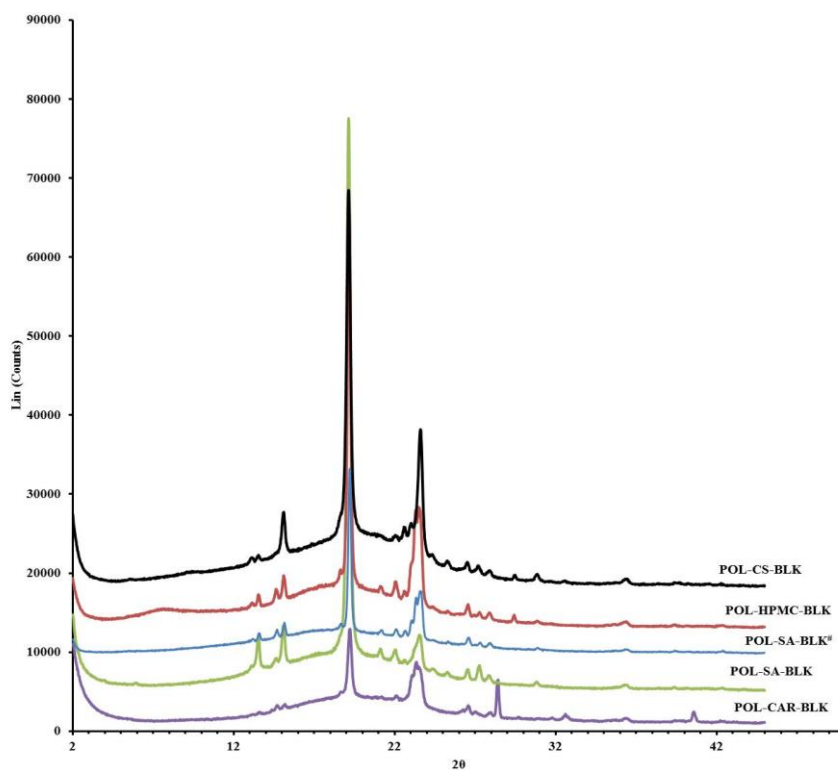


Figure 2.16: XRPD patterns of blended films combining POL with either CS, SA, CAR or HPMC (All in the ratio of 75/25 based on total polymer weight except POL-SA-BLK which was in 50/50 wt ratio).

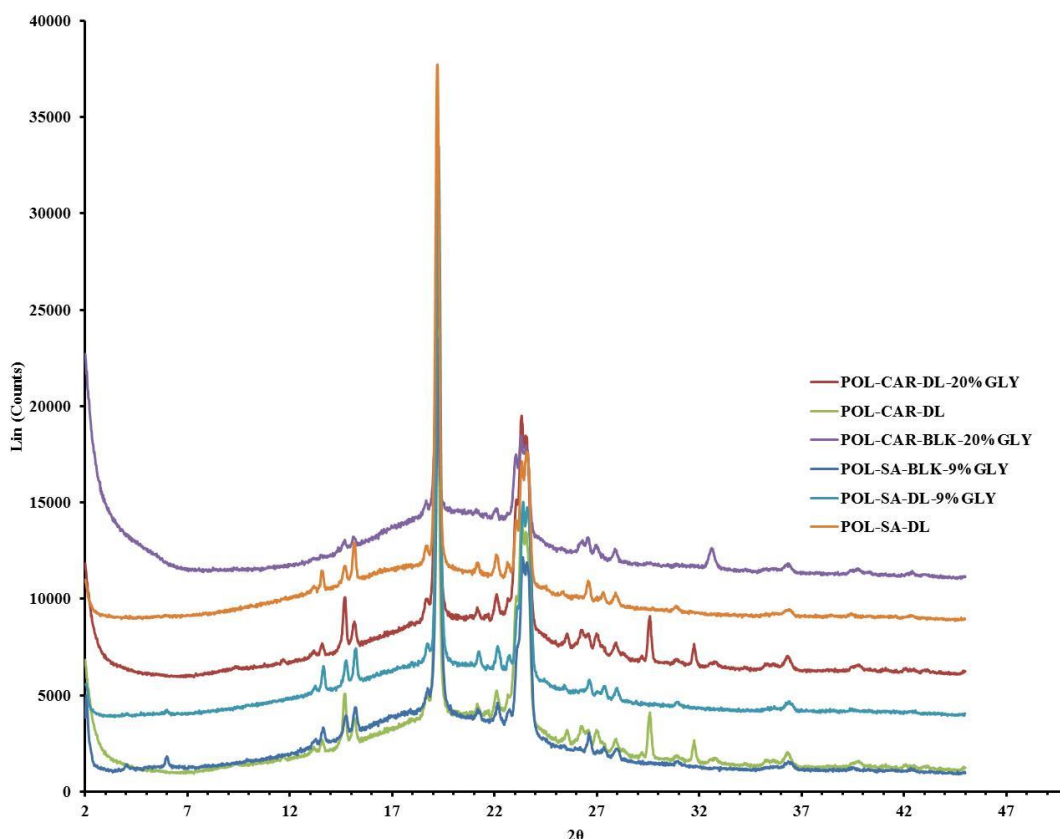


Figure 2.17: XRPD patterns of films of POL-CAR-BLK-20%GLY, POL-CAR-DL, POL-CAR-DL-20%GLY, POL-SA-BLK-9%GLY, POL-SA-DL-9%GLY.

#### 2.4.5 Attenuated total reflectance Fourier transform infrared spectroscopy (ATR-FTIR)

Table 2.4 shows characteristic peaks for pure polymers and drugs whilst figures 2.18, 2.19 and 2.20 show FTIR spectra of starting materials (pure polymers and drugs), BLK films and DL films with or without plasticizer. FTIR spectral analysis of BLK blended films is a direct method to evaluate the molecular interaction such as hydrogen bonding or complexation by monitoring the band shift of a given functional group (Liu *et al.*, 2013).

The interaction occurring in a specific region of a FTIR system can be distinctively reflected in changes in the wavenumbers of spectral peaks. Hydrogen bonds are formed between the proton-donor and proton-acceptor molecules which shifts the bands to a lower wavenumber. This may be due to the intensity of the hydrogen bond band which depends on the acidity of the hydrogen in the proton-donor and the alkalinity of the proton-acceptor in addition to their possible close contacts (Caykara *et al.*, 2005).

Table 2.4: The observed FTIR peaks (n=3) for pure polymers and drugs with their characteristic bands (Çaykara *et al.*, 2005; Azevedo *et al.*, 2006; Fuller *et al.*, 2001; Khan *et al.*, 2000)

Polymers	Average peaks (cm <sup>-1</sup> )	Characteristics
POL	2885	C-H symmetric stretching
	1465	CH <sub>2</sub> scissoring
	1242	CH <sub>2</sub> asymmetric twisting
	1278	CH <sub>2</sub> asymmetric twisting
	1100	C-O-C asymmetric stretching
	958	CH <sub>2</sub> wagging
	840	CH <sub>2</sub> twisting
	CS	1573
1652		(CO-NH) amide group
3429		O-H stretching
3354		N-H stretching
2877		CH <sub>2</sub> stretching of pyranose ring
1409		OH/CH vibration of pyranose ring
1153		C-O-C glycosidic linkage
1062		C-O-C glycosidic linkage
1028		C-O-C glycosidic linkage
SA		3287
	1595	Asymmetric -COO <sup>-</sup> stretching
	1400	C-OH deformation vibration
	1084	C-O stretching
	1024	C-C stretching
	929	C-O stretching of uronic acid in alginate
CAR	1232	sulphate ester
	1155	C-O stretching of pyranose ring
	924	3,6 anhydrogalactose residue
	844	Galactose 4-sulphate
	890	C-H stretching of β-galactopyranosyl residue
HPMC	3255	O-H stretching
	1056	C-O stretching
	2904	C-H stretching
DLF	3452	O-H stretching
	1573	O-C-O asymmetric stretching
	1556	Ring 1 stretching
	1602	Ring stretching
	1585	Ring stretching (both)
	1498	CH rocking, NH deformation
	1469	CN stretch + CH rock (ring 1)
	1450	CN stretch + CH rock (ring 2)
STP	1402	O-C-O symmetric stretch
	3365	Primary NH <sub>2</sub> group
	3201	O-H stretching
	1035	C-O-C stretching
	1458	C-N stretching
	1618,1654	C=N and N-H stretching

As a consequence of hydrogen bonding, the covalent bonds in the donor and acceptor groups are weaker, while the energy barrier for angle deformation becomes higher. Hence, in the groups which are involved in hydrogen bonding formation, the frequency of the valence

vibrations decreases with the simultaneous increase in the frequency of the deformation vibrations (Caykara *et al.*, 2005).

The FTIR peak of interest is the C–O–C asymmetric stretch at  $1100\text{ cm}^{-1}$ . The spectra of the blended films showed significant differences in the region of C-O-C asymmetric stretch at  $1100\text{ cm}^{-1}$ . The results show that the blended films have undergone a step transition resulting in a band shift to a lower wave number. The change in the C-O-C band in the spectrum, suggests that hydrogen bonding is the underlying mechanism in the interaction which causes shifting of absorption maxima of stretching towards lower wavenumbers. Hydrogen bonding can form between the ether oxygen atoms of POL and hydroxyl groups of CAR, CS, SA and HPMC (Kondo and Sawatari 1994; Çaykara *et al.*, 2005; Azevedo *et al.*, 2006; Fuller *et al.*, 2001; Khan *et al.*, 2000). POL showed C-O-C asymmetric stretch at  $1100\text{ cm}^{-1}$  which was shifted to  $1095\text{--}1097\text{ cm}^{-1}$  for POL-CAR, POL-SA, POL-CS and POL-HPMC films (Figure 2.19).

The expanded view of the peak at  $1100\text{ cm}^{-1}$  is shown in the inset of figure 2.19. POL and other polymers (CAR, CS, SA, and HPMC) are certainly cross-linked through hydrogen bonding without any significant change in the chemical property and contribute towards achieving the homogeneous texture of the film. In addition, POL-SA (50/50) films showed further decrease in the intensity of the peaks at  $1100\text{ cm}^{-1}$  in films which is shown in the inset of figure 2.19. POL-CAR-BLK-20%GLY and POL-CAR-DL-20%GLY films showed a band shift to  $1097\text{ cm}^{-1}$  whilst it was  $1099\text{ cm}^{-1}$  for the POL-CAR-DL films (Figure 2.20). Films of (POL-SA-BLK, POL-SA-BLK-9%GLY and POL-SA-DL and POL-SA-DL-9%GLY) films showed the C-O-C band shifted to the  $1097\text{ cm}^{-1}$  wavenumber.

In summary, blending of polymers are responsible for the high intermolecular interaction and formation of hydrogen bonding which could be responsible for the enhanced physical stability of the [POL-CAR and POL-SA (BLK and DL)] films, with or without plasticizer. After blending of the polymers, these interactions did not deteriorate or degrade the chemical constituents of the individual polymer entity and can assist the added drug (STP and DLF) in the POL-CAR-DL, POL-CAR-DL-20%GLY, POL-SA-DL, POL-SA-DL-9%GLY films (Liakos *et al.*, 2013). All DL films did not show any characteristic peaks of DLF in FTIR due to the homogeneous mixing into the POL-CAR and POL-SA DL films. However, the presence of C=N and N-H stretching band at  $1618\text{--}1654$  confirms the presence of streptomycin in all POL-CAR (DL) films.

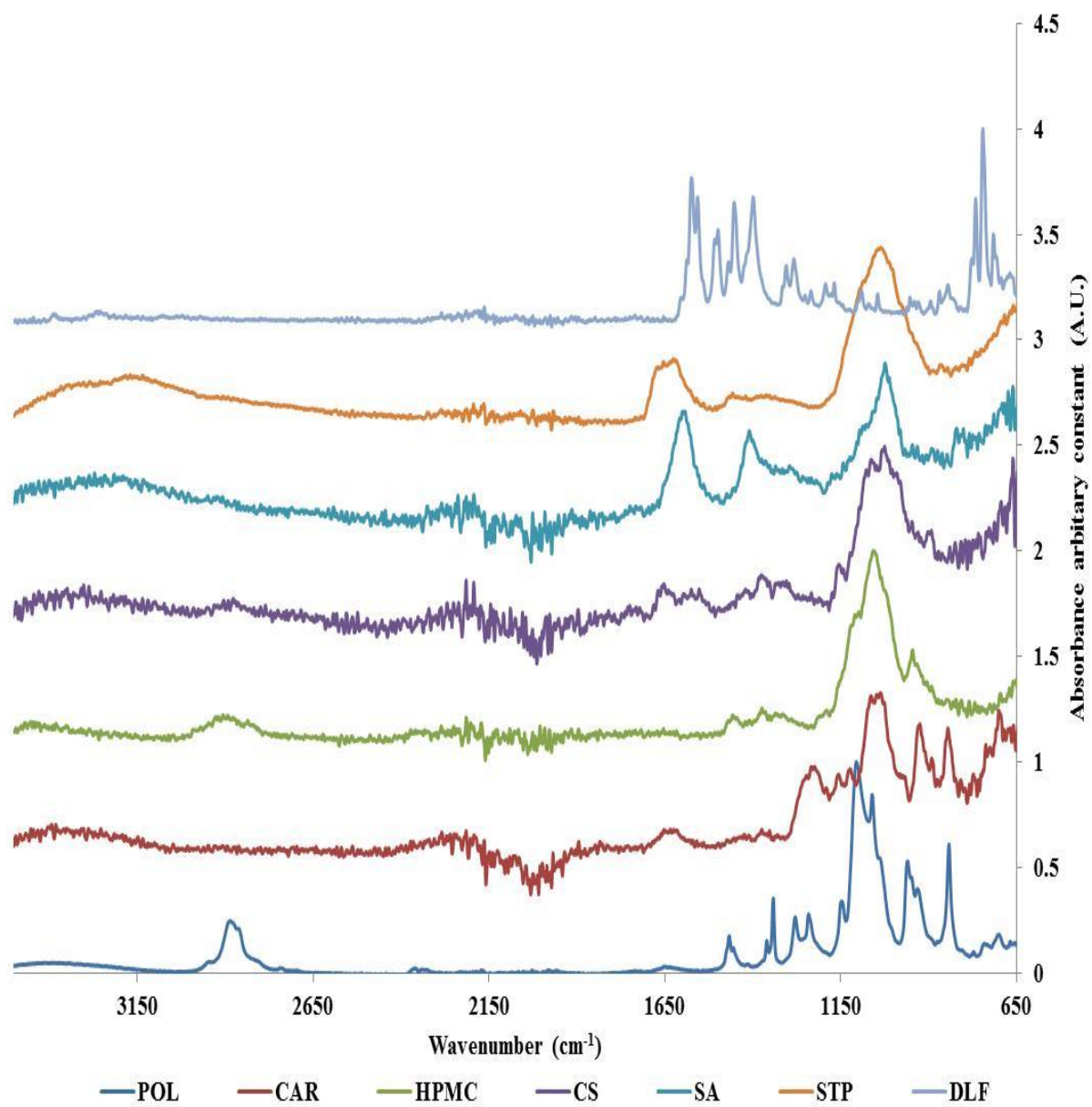


Figure 2.18: FTIR spectra of pure polymers and drugs from bottom POL, CAR, HPMC, CS, SA, STP and DLF (n=3).

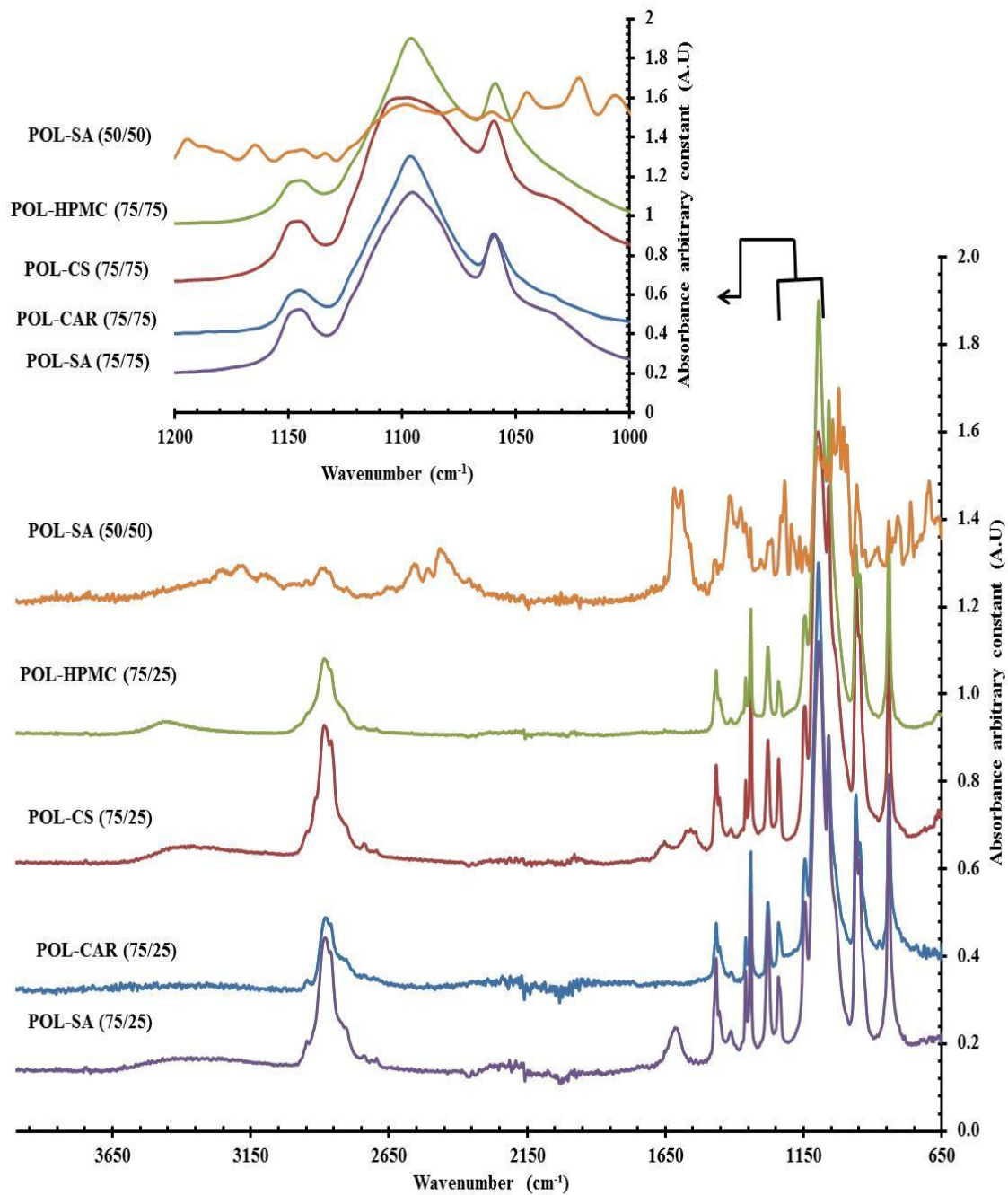


Figure 2.19: FTIR spectra of the blended films from bottom POL-SA, POL-CAR, POL-CS, POL-HPMC in ratio of 75/25wt and top POL-SA in 50/50wt ratio [Inset - shifting of peak of C-O-C stretch of POL chains at 1100 cm<sup>-1</sup>] (n=3).

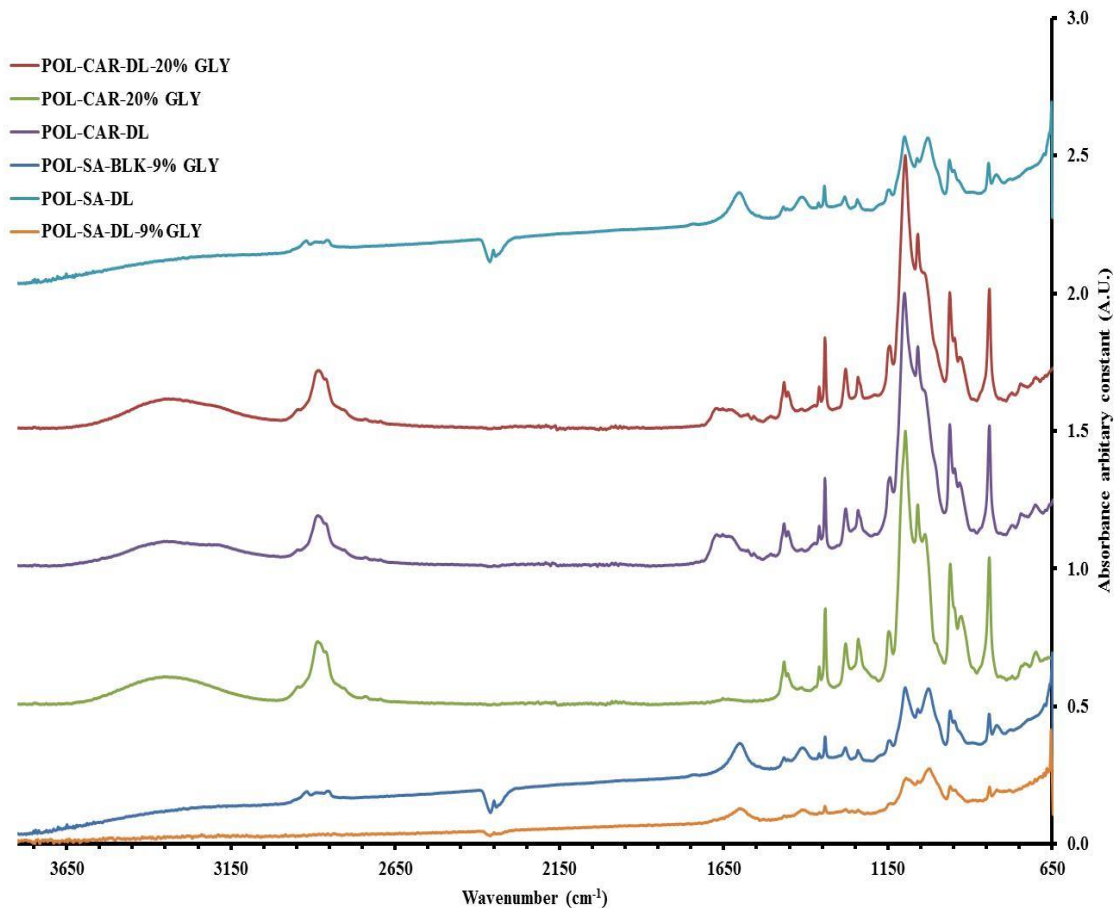


Figure 2.20: FTIR spectra of POL-CAR-BLK-20%GLY, POL-CAR-DL, and POL-CAR-DL-20% GLY films (n=3).

#### 2.4.6 Texture analysis (TA)

Ideal mechanical properties of a wound dressing include durability, flexibility, elasticity, pliability and stress resistance to cope with the stresses exerted by different parts of the body, especially around the joints such as knees and elbows (Khan *et al.*, 2000). Such properties also help to protect the wound and have clinical significance in effective routine handling. Such flexibility of the wound dressing is essential, especially for orthopaedic wounds that are prone to swelling and have an increased risk of friction between the wound and dressing (Peles and Zilberman, 2012).

Table 2.5: The effect of drug and plasticizer on mechanical (tensile) properties of selected optimised POL-CAR and POL-SA films (mean  $\pm$  SD, n=3).

<b>Films</b>	<b>GLY % w/w</b>	<b>Tensile strength MPa</b>	<b>Elastic modulus MPa</b>	<b>Elongation at break (%)</b>	<b>Area under curve AUC N.mm</b>
POL-CAR-BLK	0	12.32 $\pm$ 1.40	7.89 $\pm$ 0.01	117.24 $\pm$ 15.21	27.98 $\pm$ 2.12
	9.1	6.12 $\pm$ 0.90	5.71 $\pm$ 0.60	135.25 $\pm$ 42.31	62.15 $\pm$ 11.70
	20.0	2.74 $\pm$ 1.11	1.96 $\pm$ 0.07	151.11 $\pm$ 16.25	49.84 $\pm$ 14.23
	33.3	2.34 $\pm$ 1.22	2.04 $\pm$ 0.44	1031.92 $\pm$ 85.26	78.86 $\pm$ 16.58
	42.9	1.91 $\pm$ 0.98	1.46 $\pm$ 0.15	783.8 $\pm$ 35.12	42.46 $\pm$ 7.07
	50.0	1.13 $\pm$ 0.76	1.27 $\pm$ 0.02	709.78 $\pm$ 30.21	124.73 $\pm$ 15.46
POL-CAR-DL	0	9.52 $\pm$ 1.12	7.00 $\pm$ 2.31	106.11 $\pm$ 10.21	14.13 $\pm$ 11.01
	9.1	4.21 $\pm$ 0.19	3.51 $\pm$ 1.26	750.9 $\pm$ 8.25	50.49 $\pm$ 13.83
	20.0	1.02 $\pm$ 0.28	1.11 $\pm$ 0.15	1031.33 $\pm$ 16.23	114.69 $\pm$ 12.42
	33.3	0.70 $\pm$ 0.17	0.48 $\pm$ 0.02	1372.14 $\pm$ 28.36	54.68 $\pm$ 7.69
	42.9	0.82 $\pm$ 0.12	0.49 $\pm$ 0.06	1139.72 $\pm$ 36.21	37.80 $\pm$ 1.61
	50.0	0.74 $\pm$ 0.08	0.28 $\pm$ 0.04	1514.06 $\pm$ 12.26	50.55 $\pm$ 9.94
POL-SA-BLK	0	0.06 $\pm$ 0.02	466.15 $\pm$ 62.69	101.39 $\pm$ 0.55	0.47 $\pm$ 0.38
	9.1	0.01 $\pm$ 0.01	278.79 $\pm$ 67.29	102.42 $\pm$ 0.86	3.17 $\pm$ 1.32
	20.0	0.03 $\pm$ 0.01	93.46 $\pm$ 30.17	107.05 $\pm$ 1.98	6.74 $\pm$ 3.57
	33.3	0.03 $\pm$ 0.01	20.13 $\pm$ 5.29	148.89 $\pm$ 5.98	36.88 $\pm$ 4.99
POL-SA-DL	0	0.10 $\pm$ 0.01	262.37 $\pm$ 70.80	117.61 $\pm$ 0.18	4.55 $\pm$ 1.91
	9.1	0.09 $\pm$ 0.02	212.20 $\pm$ 2.01	128.72 $\pm$ 0.65	7.61 $\pm$ 1.00
	20.0	0.03 $\pm$ 0.01	77.56 $\pm$ 17.03	137.89 $\pm$ 0.25	3.66 $\pm$ 1.39
	33.3	0.07 $\pm$ 0.01	75.17 $\pm$ 13.64	137.09 $\pm$ 7.38	13.98 $\pm$ 1.64

Figures 2.21 and 2.22 show the results for elastic modulus, tensile strength, work done to break (area under the curve) and elongation at break for the POL-CAR and POL-SA (BLK and DL) films. The determination of tensile properties of the different POL-CAR and POL-SA films showed differences in the behaviour based on the varying concentrations of GLY. For POL-CAR and POL-SA films, tensile strength and elastic modulus decreased and elongation at break increased with increasing concentration of GLY (Table 2.5). Films prepared from gels plasticized with 42.8% and 50.0% GLY were tackier owing to exuding of excess GLY from both the BLK and DL films. Such higher amounts of GLY (42.8-50.0% w/w) can lead to the collection of exudate in highly exuding wounds or create wet conditions instead of maintaining a moist environment in low exuding wounds and may lead to the maceration of healthy skin around the wound area which is undesirable (Ousey *et al.*, 2012; Prudencioferreira and Areas 1993; Siepmann *et al.*, 2006). Mechanical testing of POL-SA-BLK and DL films containing high amounts (42.8-50.0%) were not tested further. Elastic modulus measures the film stiffness and rigidity and is calculated from the slope of the initial linear portion (region of linear elastic deformation) of stress-strain curve (Boateng *et al.*, 2009). Both POL-CAR and POL-SA (BLK and DL) films without GLY were hard, strong and brittle and stretched over a shorter distance resulting in a high elastic modulus as compared to higher content of GLY which had high elasticity and flexibility. Tensile strength is the tension which is determined by the maximum force per unit area needed to break a sample. Tensile strength measures the ability of film to withstand rupture, mechanical pressures or the force required to break the film. POL-CAR and POL-SA (BLK and DL) showed higher tensile strength. Since GLY has multiple -OH groups that penetrated into the polymeric network and forms hydrogen bonds with the -OH groups of the polymers, this created enlarged spaces between the polymeric chains and resulted in reduced brittleness, improved flow, flexibility and increased thickness of the films. Plasticization with GLY showed differences in the mechanical properties of both POL-CAR and POL-SA-BLK films. This may be associated with the macromolecular polymer complexes formed due to the non-covalent hydrogen bonding between the POL and SA or CAR.

Generally, films prepared from SA were very strong and brittle which may be due to the presence of high guluronic acid side chains which could not dissipate stresses generated during the solvent casting of the films resulting in small volumes between the polymeric chains (Boateng *et al.*, 2009) which results in brittle and hard films. Addition of GLY reduces the glass transition temperature ( $T_g$ ) leading to conversion of a rigid polymer into a rubbery state which

increases the mobility (relaxation) and dissipates stresses generated by the polymer. Due to the variations between the  $T_g$  of these two natural polymers, differences in the mechanical properties were observed. It was also noted that the POL and CAR had lower glass transition temperatures ( $-50^\circ\text{C}$  and  $-2^\circ\text{C}$ ) whilst SA had a glass transition temperature around  $60.28^\circ\text{C}$ . This can explain the differences in the mechanical properties.

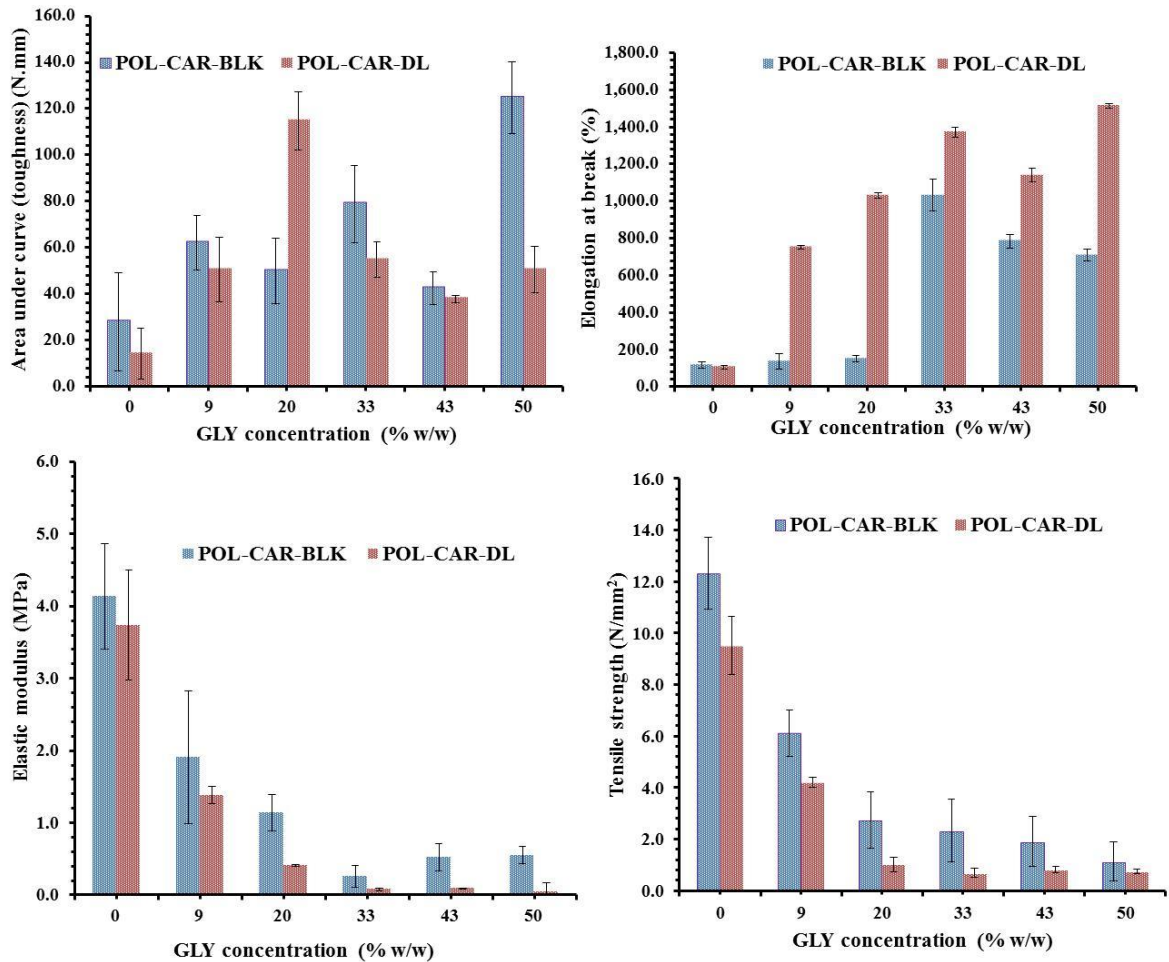


Figure 2.21: Mechanical properties (Toughness, elongation at break, elastic modulus and tensile strength) of POL-CAR (BLK and DL) films (mean $\pm$ SD, n=3).

The observed tensile behaviour of the POL-CAR BLK films containing 33.3% w/w of GLY and DL film containing 20.0% GLY could be associated with those of ductile polymers since elastic modulus ( $1.14\pm 0.25$  MPa,  $0.41\pm 0.01$  MPa), tensile stress ( $2.34 \pm 1.2$  MPa,  $1.01 \pm 0.3$  MPa) decreased and elongation at break, ( $1031.92\pm 85.3$ ,  $1031.33\pm 16.2$  % strain) increased significantly ( $p < 0.001$ , student T-test). This may be associated with the STP which has an additive plasticizing effect due to the presence of multiple hydroxyl groups and its amorphous

nature. In the case of POL-SA films, BLK and DL films containing 9.1 % GLY are associated with those of ductile polymer since elastic modulus ( $278.79\pm67.3$ ,  $212.20\pm2.0$  MPa), tensile strength ( $0.01\pm0.01$ ,  $0.09\pm0.02$ MPa) decreased and elongation at break ( $102.42\pm0.9$ ,  $128.72\pm0.7$  %) increased. The values of the tensile strength of the skin are usually in the range 2.5–16 MPa (Wang *et al.*, 2002) and the elongation is approximately 70% in the most flexible zones. Comparing these values with the mechanical properties of the developed POL-CAR and POL-SA (BLK and DL) films; POL-CAR (BLK and DL) films present adequate properties for skin application and application to the difficult areas such as knees and joints.

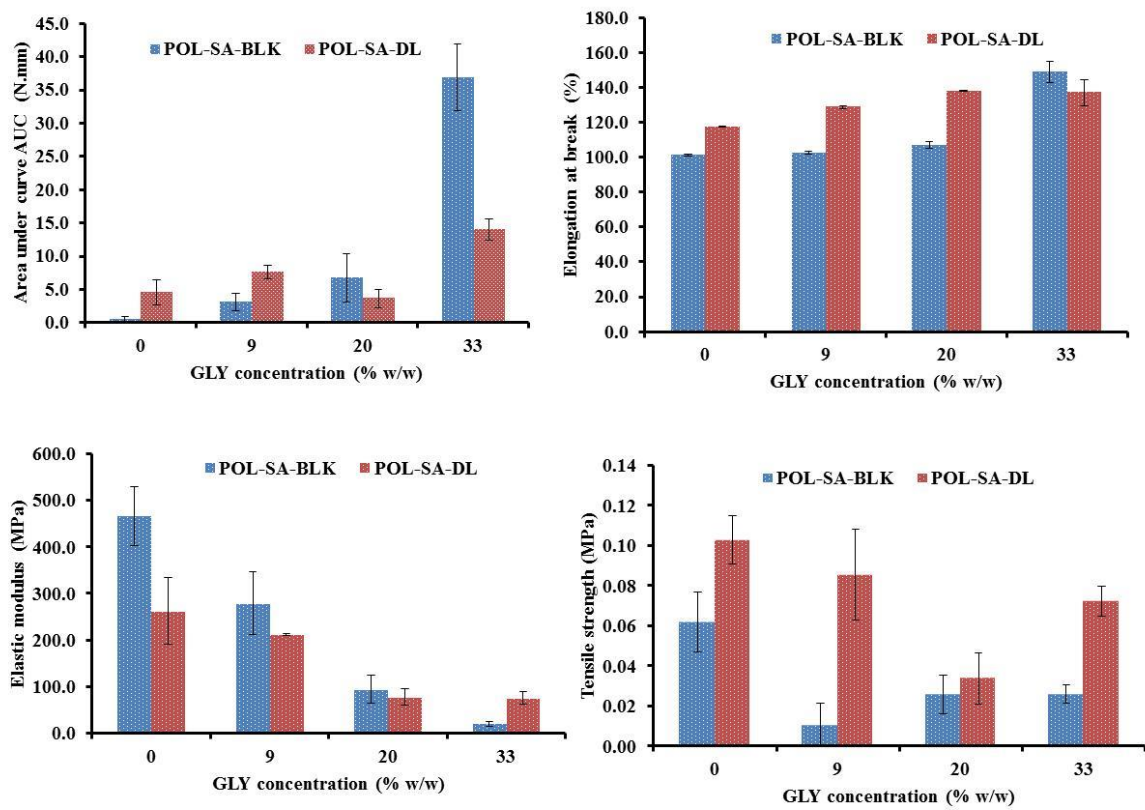


Figure 2.22: Mechanical properties (Toughness, elongation at break, elastic modulus and tensile strength) of POL-SA (BLK and DL) films (mean± SD, n=3).

However, the tensile strength of POL-SA is far from the average skin value but maintaining high elongation at break than the above specified value which make them preferable in the flexible zones of the body (Pereira *et al.*, 2013). Thus POL-CAR and POL-SA (20.00% and 9.09%) films have sufficient mechanical strength which is required in biomedical applications. Consequently, these films can be used for covering of wounds as these can

withstand some frictional stresses during day-to-day activities and absorb the energy without breaking and will thus provide a protective effect over the wound.

## 2.5 Conclusion

Films prepared from synthetic (POL) and natural biopolymer (CAR and SA) showed homogeneous surface morphology with the addition of GLY and were flexible and transparent compared to POL-CS and POL-HPMC films. FTIR analysis revealed specific intermolecular interactions between POL and CAR, CS, SA and HPMC. Drug loaded POL-CAR and POL-SA films possess properties that meet desirable characteristics of an ideal dressing. This is due to their smooth homogeneous surface morphology, elegant appearance and fair transparency which will allow observation of progression of the healing process. High elasticity provided optimum flexibility that will allow better conformation to the wound surface. The advantage of incorporating STP and DLF in the same dressing to target two different phases of the wound healing (reduce bacterial infection and also inflammation associated with wound healing) is expected to help to achieve rapid wound healing. The dressing can help to reduce bacterial infection by the antimicrobial action of STP and potentially in synergy with DLF while the latter can also help to reduce the swelling and pain associated with injury due to its the anti-inflammatory action. These will however, require further investigations in an *in vivo* study. Overall, POL-CAR-DL and POL-SA-DL films may have potential to be used as a wound healing drug delivery film dressing.

## CHAPTER 3: DEVELOPMENT, OPTIMISATION AND PHYSICO-CHEMICAL CHARACTERISATION OF MEDICATED LYOPHILISED WAFER DRESSING.

### 3.1 Introduction

Polysaccharides, being naturally occurring biomolecules, have been an obvious choice as potential wound management aids (Lloyd, 1998). It has been previously demonstrated that combining synthetic and natural polymers helps to improve the properties which makes them suitable for their application in the biomedical field (Sionkowska, 2011). Lyophilised wafers are produced by freeze-drying polymer solutions and gels to yield solid porous structures that can easily be applied to exuding wound surfaces. Their physical architecture resembles those of foam dressings which are made of porous polyurethane. Stability of drugs should be better in a lyophilised dosage form than a semi-solid hydrogel based formulation. It is anticipated that a lyophilised polymer matrix would preserve the size, shape and form of contained compounds unlike a conventional gel suspension, where crystal ripening, agglomeration and polymorphic changes may occur (Matthews *et al.*, 2008; Ayensu *et al.*, 2012). Wafers provide a potential means of delivering pharmacological agents to wound surfaces to aid healing (Matthews *et al.*, 2005). Lyophilized wafers have the ability to incorporate soluble and insoluble antimicrobial compounds greater than their minimum bactericidal concentration for antibacterial activity against pathogenic bacteria (Labovitiadi *et al.*, 2012). In addition, wafers have capacity to absorb large amount of exudate due to their porous nature and maintain moist environment without damage to newly formed tissue. Wafers also offer high drug loading capacity compared to solvent cast films (Boateng *et al.*, 2010).

In this study, we report on formulation, optimisation and characterisation of the physico-mechanical properties of lyophilised wafer dressings prepared from polymeric gels of Polyox<sup>®</sup> (POL) with carrageenan (CAR) and sodium alginate (SA) (Boateng *et al.*, 2013) for improved functional properties expected for better wound healing effect compared to previously reported solvent cast films, using model drugs of streptomycin sulphate (STP) and diclofenac sodium (DLF) which can target two different stages of wound healing. The wafers were characterised using scanning electron microscopy (SEM), texture analysis (mechanical properties), differential scanning calorimetry (DSC), attenuated total reflectance-Fourier transform infrared spectroscopy (ATR-FTIR) and X-ray diffraction (XRD).

## 3.2 Materials

(Polyox<sup>TM</sup> WSR 301  $\approx$ 4000 kDa) was obtained as a gift from Colorcon Ltd (Dartford, UK),  $\kappa$ -carrageenan (CAR) (Gelcarin GP 812 NF) was obtained from IMCD Ltd (Sutton, UK), diclofenac sodium (DLF) and streptomycin sulphate (STP) were all purchased from Sigma Aldrich, (Gillingham, UK). Sodium alginate (SA), ethanol (laboratory grade), were all purchased from Fisher Scientific (Leicestershire, UK).

## 3.3 Methods

### 3.3.1 Preparation of POL-CAR and POL-SA [blank (BLK) and drug loaded (DL)] gels

Polymeric gels of POL-CAR and POL-SA gels were prepared as previously reported. In brief, blends of POL with CAR and POL with SA (weight ratio of 75/25 and 50/50 respectively) yielding 1% w/w of total polymer weight were prepared by stirring on a magnetic stirrer at 70°C to form a uniform gel (POL-CAR-BLK and POL-SA-BLK).

The composition of the polymers, drugs used for the preparation of gels are summarised in Table 2.1 in *chapter 2*. DL gels of POL-SA and POL-CAR were prepared with 4 ml ethanolic solution of DLF containing 100 mg and 250 mg of the drug (2.50% w/v solution for POL-SA gel to achieve 10% w/w and 6.25% w/v solution for POL-CAR to achieve 25% w/w of DLF in the polymeric gel. These gels were subsequently cooled to 40°C with constant stirring. Similarly, a 4 ml aqueous solution containing 250 mg and 300 mg of STP (6.25% w/v solution for POL-SA and 7.50% w/v solution for POL-CAR) was subsequently added to achieve a final STP concentration of 25% w/w (POL-SA) and 30% w/w (POL-CAR) in the DL gels.

### 3.3.2 Freeze drying cycle development with annealing step

Preliminary DSC studies on the POL-CAR-BLK and POL-SA-BLK gels were carried out. A differential scanning calorimeter DSC-1 (Mettler Toledo, Leicester, UK), was used to analyse the thermal events in the gels to determine a more suitable lyophilisation cycle. Approximately 7-12 mg of gel was placed in 40  $\mu$ l aluminium pans (ME-00026763, Mettler Toledo) and cooled from 25°C to -60°C at a rate of 10°C/min. They were then re-heated back to 25°C at 20°C/min and the cycle repeated. Based on thermal events observed during the heating cycles, an annealing temperature of -25°C was chosen. The samples were then cooled to -60°C,

warmed to -25°C, held at that temperature for 10 min, cooled back to -60°C and then warmed through to 25°C at 20 °C/min.

Table 3.1: Composition of polymers and drugs (varying quantity) present in gels used to produce freeze dried wafers.

<b>Pure material</b>	<b>POL-CAR-BLK</b>	<b>POL-CAR-DL</b>	<b>POL-SA-BLK</b>	<b>POL-SA-DL</b>
	<b>(weight in gm)</b>			
POL	0.75	0.75	0.50	0.50
CAR	0.25	0.25	-	-
SA	-	-	0.50	0.50
STP	-	0.30	-	0.25
DLF	-	0.25	-	0.10
Total weight	1.00	1.55	1.00	1.35

### 3.3.3 Lyophilisation

10 gm of each homogeneous gel was transferred into 6 well moulds (diameter 35 mm) (Thermo-Fisher Scientific Nunc, Leicestershire UK), placed in a Virtis Advantage XL 70 freeze dryer (Biopharma Process Systems, Winchester, UK) and lyophilised using the automated lyophilisation cycle. Figure 3.1 shows a schematic diagram of the freeze drying cycle. This involved initially cooling samples from room temperature to -5°C and then -50°C over a period of 10 h (at 200 mTorr). An annealing step at -25°C for 2 h was applied based on the preliminary DSC studies and its effect on the different formulations was investigated. The frozen samples were then heated in a series of thermal steps to -25°C under vacuum (20-50 mTorr) over a 24 h period. Secondary drying of the wafers was carried out at 20°C (10 mTorr) for 7 h.

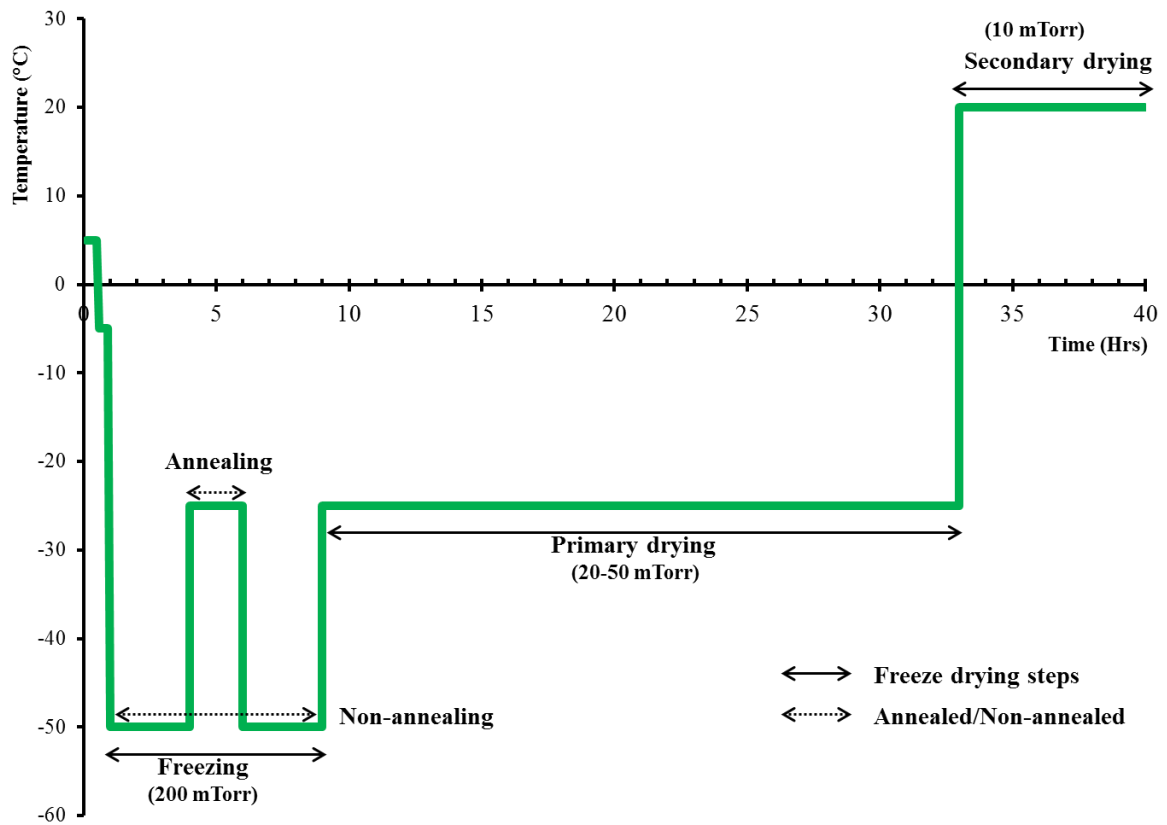


Figure 3.1: Schematic diagram of the lyophilisation cycles used for the preparation of wafers.

### 3.3.4 Scanning electron microscopy (SEM)

Surface morphology of the lyophilised wafers (as shown in table 3.2) was analysed by a Hitachi SU 8030, (Hitachi High-Technologies, Germany) scanning electron microscope at low accelerating voltage (1 kV). Wafers were cut into thin uniform slices using a sharp blade and mounted on aluminium stubs (1 inch diameter) with ‘Agar Scientific G3347N’ double sided adhesive carbon tape. Images of the wafers were acquired at a working distance of 8.0- 15.0 mm at magnifications of x500 - x1500.

Table 3.2: Lyophilised wafers used to analyse surface morphology.

Sr. no	Formulations
1	POL-CAR-BLK-Nan
2	POL-CAR-BLK-An
3	POL-CAR-DL-An
4	POL-SA-BLK-Nan
5	POL-SA-BLK-An
6	POL-SA-DL-An

Where NAn and An stands for non-annealed and annealed wafers respectively.

### 3.3.5 Mechanical properties of wafers (TA)

The mechanical properties (resistance to deformation and ease of recovery) of the freeze-dried wafers were investigated by compressing on a Texture Analyser (TA) (Stable Microsystems Ltd., Surrey, UK) equipped with 5 kg load cell and *Texture Exponent-32*<sup>®</sup> software program (Boateng *et al.*, 2010). Wafers as shown in table 3.2 were compressed using a 6 mm (P/6) cylindrical stainless steel probe (Stable Microsystems Ltd., Surrey, UK) in compression mode. The effects of compression speed (0.1 - 3.0 mm/sec) and depth (0.2 – 3.0 mm) on different wafers were evaluated. The ‘hardness’ (resistance to deformation) of the wafers were evaluated by compressing the sample at three different locations to a depth of 2 mm at a speed of 1 mm/sec using a trigger force of 0.001N and withdrawn till it lost complete contact with the wafer. Five wafers of each formulation [POL-CAR and POL-SA (NAn, An, and DL-An)] were compressed to determine the reproducibility in the response of the wafers to deformation by compression. The same settings were used to determine the effects of STP and DLF contents on the force-time profiles during deformation by compression.

### 3.3.6 X-ray diffraction (XRD)

XRD analyses of the wafers (POL-CAR-BLK-An, POL-SA-BLK-An, POL-CAR-DL-An, and POL-SA-DL-An) were performed using a D8 Advantage X-Ray diffractometer (Bruker AXS GmbH, Karlsruhe, Germany). The lyophilised wafers were compressed to a width size of 0.5

mm using a clean pair of compression glasses and mounted on the sample holder. The transmission diffractograms were acquired using DIFFRAC plus XRD commander over a start to end diffraction angle of  $2\theta$  from  $5^\circ$  to  $45^\circ$ , step size of 0.02 and a scan speed of 0.3 sec. X-ray patterns of the wafers and starting materials were obtained with DIFFRAC plus (Bruker Coventry, UK) having an XRD commander programme. A Goebbel mirror was used as monochromator which produced a focused monochromatic  $\text{CuK}_{\alpha 1\&2}$  primary beam ( $\lambda=1.54184 \text{ \AA}$ ) with the exit slit of 0.6 mm. The detector used for performing the experiment was Lynx Eye. The operating condition during the experiment was 40 kV and 40 mA.

### 3.3.7 Differential scanning calorimetry (DSC)

Differential scanning calorimetry analysis of the POL-CAR and POL-SA wafers (both BLK-An and DL-An) and starting materials (POL, CAR, SA, DLF and STP) was carried out on the DSC1 Mettler Toledo instrument (Leicester, UK) calibrated with indium (based on heating range). Wafers were cut into small pieces and 3-5 mg of sample was placed into 40 $\mu\text{l}$  aluminium pans with lids (Mettler Toledo, Leicester, UK) and sealed using crucible sealing press (Metler Toledo Leicester, UK). An empty aluminium pan sealed with lid was used as reference. *STAR<sup>e</sup>* software program was used to run the samples. This programming involved initially cooling of sample from  $25^\circ\text{C}$  to  $-50^\circ\text{C}$  and then heated from  $-50^\circ\text{C}$  to  $350^\circ\text{C}$  at the rate of  $10^\circ\text{C}/\text{min}$  under constant purge of dry nitrogen gas (100 ml/min) to evaluate the thermal behaviour of the polymers and drugs present in the wafer.

### 3.3.8 Attenuated total reflectance-Fourier transform infrared spectroscopy (ATR-FTIR)

A FTIR spectrophotometer was used in combination with (Thermo Nicolet, Thermoscientific, UK), Zinc Selenide (ZnSe) attenuated total reflectance (ATR) accessory to characterise the wafers (POL-CAR-BLK-An, POL-SA-BLK-An, POL-CAR-DL-An, POL-SA-DL-An). The FTIR was equipped with potassium bromide (KBr) beam splitter and MCT detector. The wafers were placed on ZnSe ATR crystal ( $45^\circ$ ) and maximum pressure was applied by using a pressure clamp accessory to allow for intimate contact of the wafers with the ATR crystal. Similarly, the pure starting materials (POL, CAR, SA, STP and DLF) were analysed as controls. Spectra were recorded at  $4 \text{ cm}^{-1}$  resolution within a range of  $650\text{-}4000 \text{ cm}^{-1}$  using OMNIC<sup>®</sup> software. True absorbance of each sample was obtained by background subtracting spectral information for the ATR crystals.

### 3.4 Results and discussion

#### 3.4.1 Freeze drying cycle development with annealing step

Figure 3.2 shows the DSC thermograms of gels evaluated from -60°C to 25°C which informed the freezing (annealing/non-annealing) stages during the development of the freeze drying cycle of the prepared polymeric gels. Glass-transition (T<sub>g</sub>) temperature of -54.54°C and -56.95°C was observed for the POL-CAR gel and POL-SA gels respectively. The eutectic melt for both gels were observed between -8 to -13°C and ice melts were observed between an onset of -1°C and endset of (6to11°C) which is associated with melting of ice in the interstitial spaces of the frozen cake. To avoid the formation of a metastable glass which will eventually crystallize and affect the stability of the formulations, samples were heated to -25°C above the measured glass transition temperature (but below the eutectic and/or ice melting temperature) of the mixture, allowing the glass to relax and crystallize during the freezing stage. It has previously been demonstrated that gels which are annealed between the glass transition and eutectic melt peaks improves the metastable state (Ayensu *et al.*, 2012). Annealing of the polymeric gels below its eutectic and ice melt temperature leads to transformation of its structure towards a more relaxed state and is manifested by a continuous change in all physical properties such as hydration, mucoadhesion and drug release properties of the formulations (Ayensu *et al.*, 2012). Figure 3.2 shows the thermogram of the heating stage of the POL-CAR and POL-SA-An gels, where no glass transition but rather the eutectic melt [-10.52°C (POL-CAR-An gel), -9.54°C (POL-SA-An gel)] and ice melt [2.04°C (POL-CAR-An gel), 2.65°C (POL-SA-An gel)], were observed. The effectiveness of the annealing process was evidenced by the disappearance of the glass transition in the heating cycle. Based on the thermal events observed during the heating cycle, an annealing temperature of -25°C was chosen which was within the safety margin and incorporated into the thermal treatment for the freezing step of the lyophilisation cycle. Annealing is a process which maintains the samples at a specified temperature below the equilibrium freezing point but above the glass transition temperature (-25 °C) for 2 h. This allowed formation of larger ice crystals resulting in increased sublimation rate during the primary drying stage, creating larger pores in the process. In addition, annealing facilitated the fusion of smaller ice crystals together, to form larger crystals that leave large pores following ice sublimation (Ayensu *et al.*, 2012).

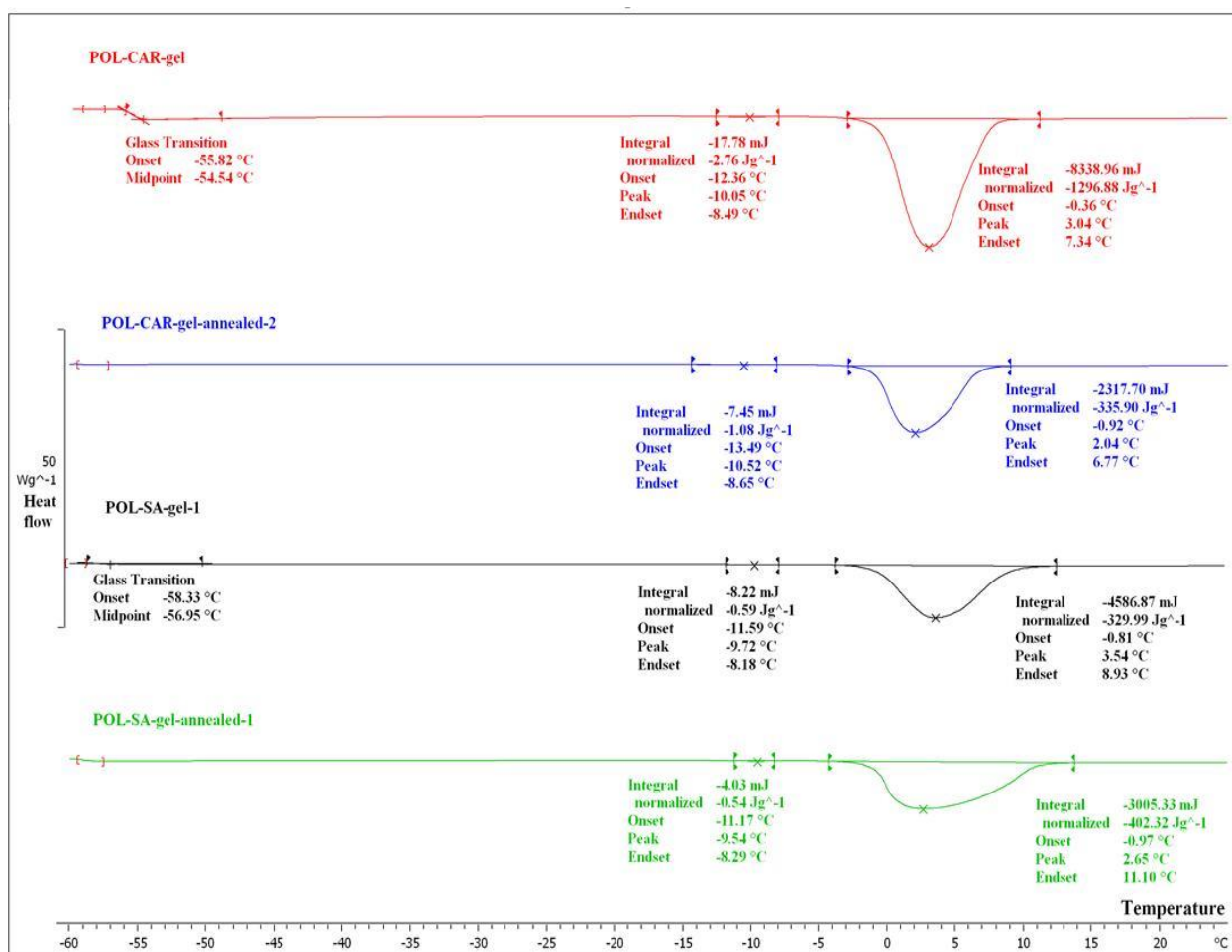


Figure 3.2: DSC thermogram of the POL-CAR and POL-SA gels (NAn and An) at -25°C.

### 3.4.2 Freeze-drying formulation development and optimisation

The temperature selection for the freezing of the sample was to improve the homogeneity of crystallisation and formation of a porous ice cake (Tang and Pikal 2004). To avoid collapse of the cake, primary drying of the sample was carried out at -25°C. Low chamber pressure allows for a high sublimation rate and homogenous heat transfer from the sample and for that purpose, chamber pressure was maintained between 20-50 mTorr. Compositions of different wafers POL-CAR-BLK, POL-CAR-DL, POL-SA-BLK, and POL-SA-DL (NAn and An) were visually examined for acceptable lyophilisation behaviour and physical elegance of the resulting product. All wafers prepared from the blending of POL-CAR and POL-SA were of uniform mass, texture and thickness, soft and flexible especially POL-SA wafers which were softer and more pliable in nature compared to POL-CAR wafers. These wafers were deemed flexible enough to allow ease of handling for their application as an effective wound dressing with a low

likelihood of causing contact irritation. Unlike the films, the addition of plasticizer may result in collapse during freeze-drying, resulting in sticky wafers which may affect the ease application (Boateng *et al.*, 2010). As a result the use of plasticizer was avoided during the development and optimisation of wafers.

### 3.4.3 Scanning electron microscopy (SEM)

SEM images of POL-CAR-BLK (NAn and An), POL-CAR-DL-An, POL-SA-BLK (NAn and An) and POL-SA-DL-An wafers are shown in figure 3.3. POL-CAR-BLK-An and POL-SA-BLK-An wafers formed a porous interconnecting network of polymeric strands having circular shaped pores after annealing. POL-CAR-BLK-NAn showed smaller pores with a leafy structure whilst POL-SA-BLK-NAn wafers showed elongated sponge like strands with a less porous nature. The SEM images show the effect of annealing on the pore distribution of the wafers. POL-CAR-BLK-An wafers formed a sponge-like network whilst POL-SA-BLK-An wafers formed a less porous structure. The annealing step allowed the formation of larger ice crystals by merging smaller ice crystals resulting in increased sublimation rate during the primary drying stage (Ayensu *et al.*, 2012). Consequently, sponge-like, porous polymeric network of uniform and large pores that are regularly distributed throughout the wafers were observed in figure 3.3 for POL-CAR-BLK-An and POL-SA-BLK-An wafers. The annealed wafers also had better elegance as compared to the non-annealed wafers. This may be because all the polymers used have a high affinity for water (water solubility) which subsequently affects the formation of ice crystals during the freezing process. As a result, the formulation of non-annealed wafers (POL-CAR-BLK-NAn and POL-SA-BLK-NAn) was discontinued.

The SEM images of POL-CAR-DL-An and POL-SA-DL-An wafers showed significant differences in surface topography. The POL-CAR-DL-An wafer at high drug loading (25% w/w DLF and 30% w/w STP based on total polymer weight) showed the least porosity as the surface texture appeared as leafy strands with irregular pores while the POL-SA-DL-An wafer (at 10% w/w DLF and 25% w/w STP based on total polymer weight) showed a more porous texture with uniform pore size distribution. The changes in the surface structure and reduced porosity of POL-CAR-DL-An wafers could be attributed to the different amounts of STP and DLF incorporated in this wafer's matrix.

In terms of applications, the differences observed in the pore size morphologies of the POL-CAR-BLK annealed and non-annealed wafers can affect functional properties such as rate of hydration, swelling, mucoadhesion and consequent drug release characteristics in the presence of wound exudate. Wafers with high porosity can absorb high exudate due to high water ingress which leads to high swelling and subsequent diffusion of drug from the swollen matrix (Boateng *et al.*, 2008, 2010). Highly exuding chronic wounds such as diabetic foot and venous ulcers limit the application of film dressings due to the high amount of exudate which causes maceration at the wound site. It also requires frequent changes in the dressing which adversely affect the patient's compliance. Further, annealed POL-SA-DL-An wafers may offer a better drug delivery system due to their more porous nature compared to POL-CAR-DL-An wafer, and can therefore absorb high exudate volumes and also keep the wound environment moist for rapid healing. However, excessive hydration may cause wafer wetting and formation of slippery mucilage which can decrease the mucoadhesion properties at the wound site (Matthews *et al.*, 2005, 2006).

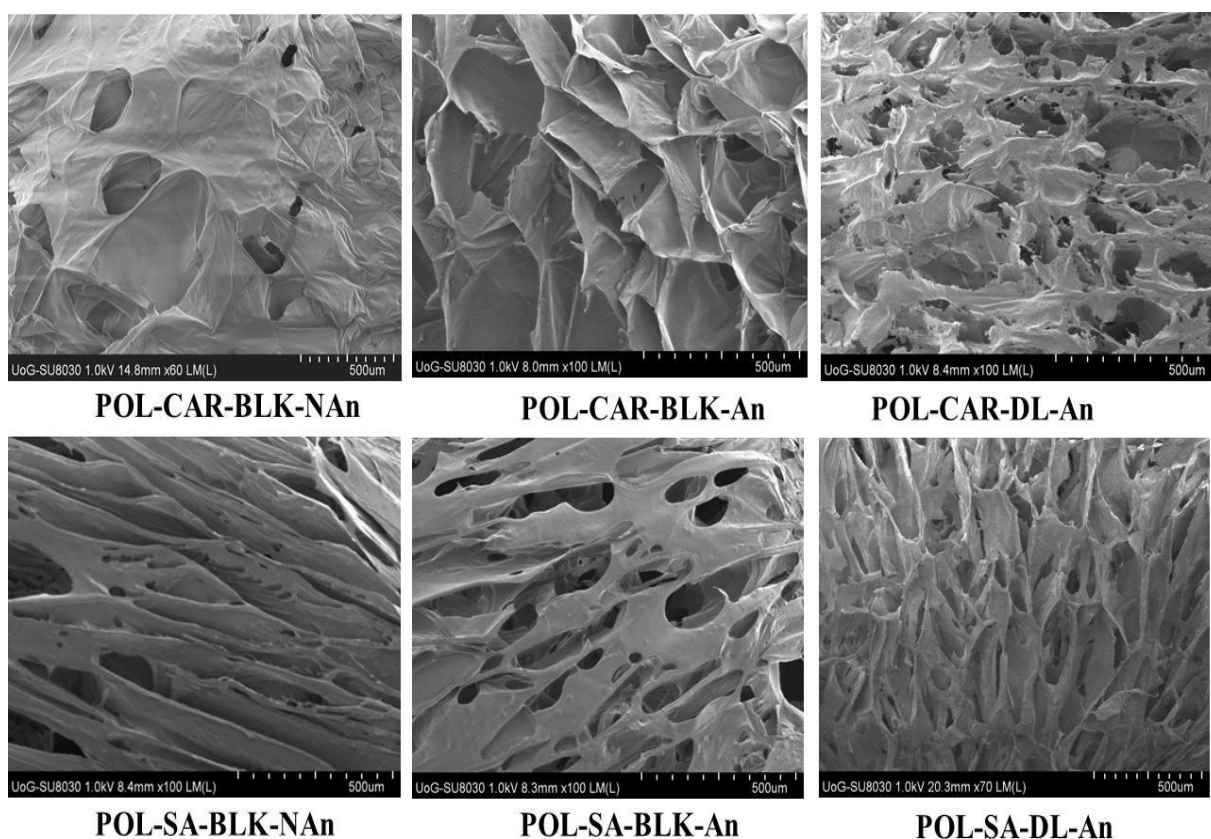


Figure 3.3: SEM images of POL-CAR-BLK-NAn, POL-CAR-BLK-An, POL-CAR-DL-An, POL-SA-BLK-NAn, POL-SA-BLK-An, POL-SA-DL-An.

#### 3.4.4 Mechanical properties of wafers (TA)

For wound healing application freeze dried wafers would undergo various stresses during its handling and application as a medicated dressing, and therefore necessitates optimum mechanical strength, so as to maintain their structural integrity during and after application (Thakur *et al.*, 2012). Figures 3.4 and 3.5 show the effect of speed and depth of compression on the hardness of wafers prepared from POL-CAR-BLK and POL-SA-BLK (NAn and An) in addition to POL-CAR-DL-An and POL-SA-DL-An. The result shows an increase in the resistance to compressive deformation with increasing test speed (Figure 3.4). POL-CAR-BLK-NAn wafers showed high resistance to compressive forces at all speeds (0.2-3.0 mm) but was decreased for the POL-CAR-BLK-An wafers. This may be due to the compact nature which resists the penetration of the probe into the polymeric network. However, after annealing, the wafers showed a porous nature due to improved interconnecting polymeric network which allowed better penetration. Hardness is the measure of the peak force required to compress the wafer to the required depth. There was significant difference in the 'hardness' between the POL-CAR-BLK-An and POL-CAR-DL-An and POL-SA-BLK-An and POL-SA-DL-An wafers ( $p < 0.001$ ). The differences in the number, size and shape of pores between POL-CAR and POL-SA wafers could account for the differences in their mechanical strength measured on the texture analyser (Boateng *et al.*, 2010).

When wafers were compressed to a greater depth peak force required to penetrate the wafers increased due to reduction in porosity of wafers at greater depth and more intimate contact of the polymer chains. It has been observed that a higher force was required to penetrate the probe (2 mm) for all the wafers with increasing speed (Figure 3.5). This may be due to the arrangement of the polymer network which resists penetration and requires a higher force with increased speed of compression. The wafers prepared from POL-CAR (An and NAn) showed significantly higher hardness ( $p < 0.001$ ) when compared with the POL-SA wafers. POL-CAR wafers showed a more rigid polymeric network than the POL-SA wafers and these results support the SEM observations.

The effect of speed and depth of compression on hardness are critical, as significant changes to wafer dimensions could affect properties such as its pore size (Boateng *et al.*, 2010). Such variations if large enough (POL-CAR-BLK-NAn and POL-CAR-BLK-An) may result in significant changes in hydration, swelling and possibly drug release characteristics which

ultimately affect its performance as a wound dressing. However, this will need to be further investigated. Based on these results and the SEM observations, only annealed wafers were used for all subsequent investigations.

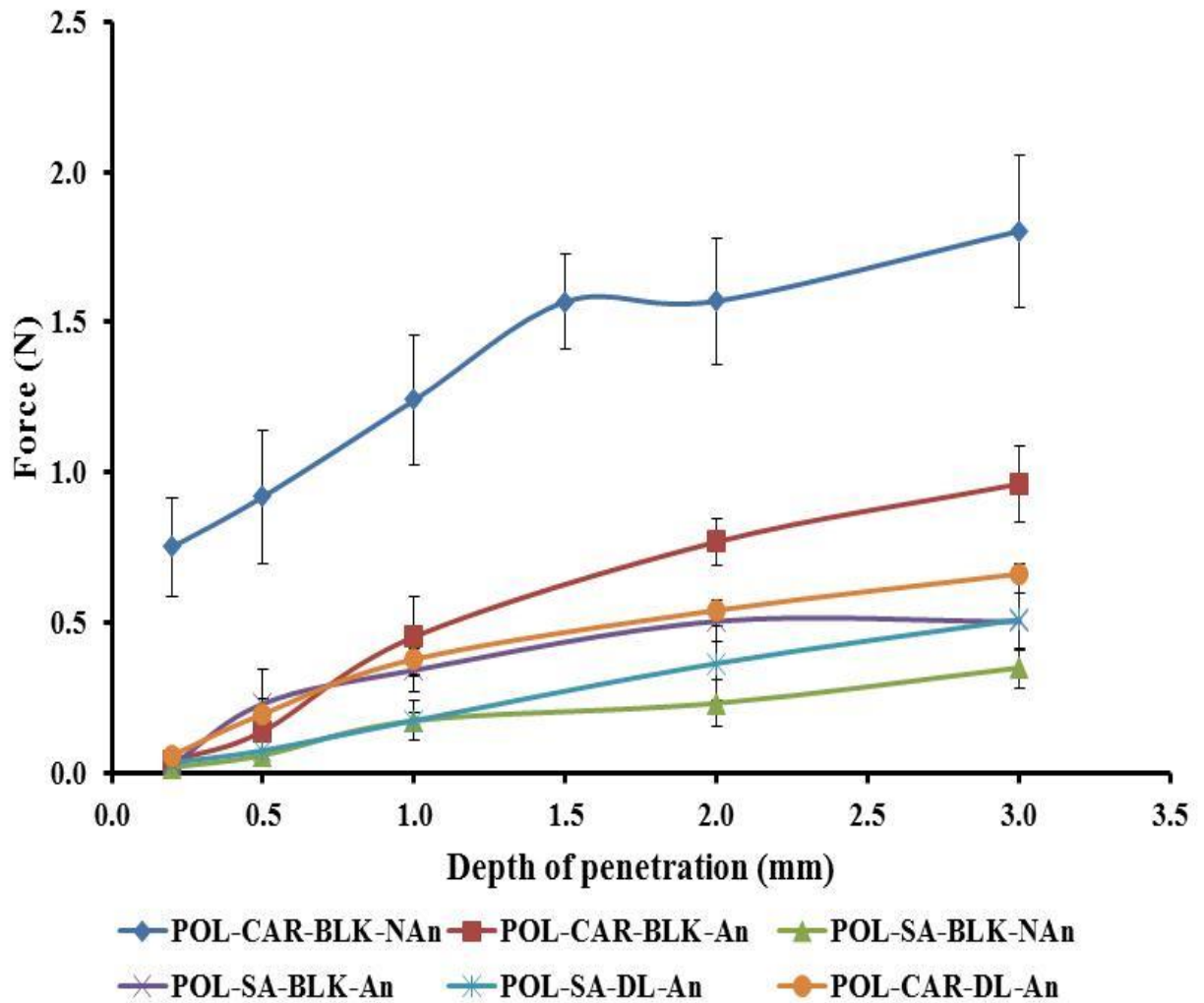


Figure 3.4: Effect of depth of the compression of POL-CAR and POL-SA BLK NAn and An wafers and DL POL-CAR and POL-SA An wafers (at a speed of 1mm/sec, mean± SD, n=5).

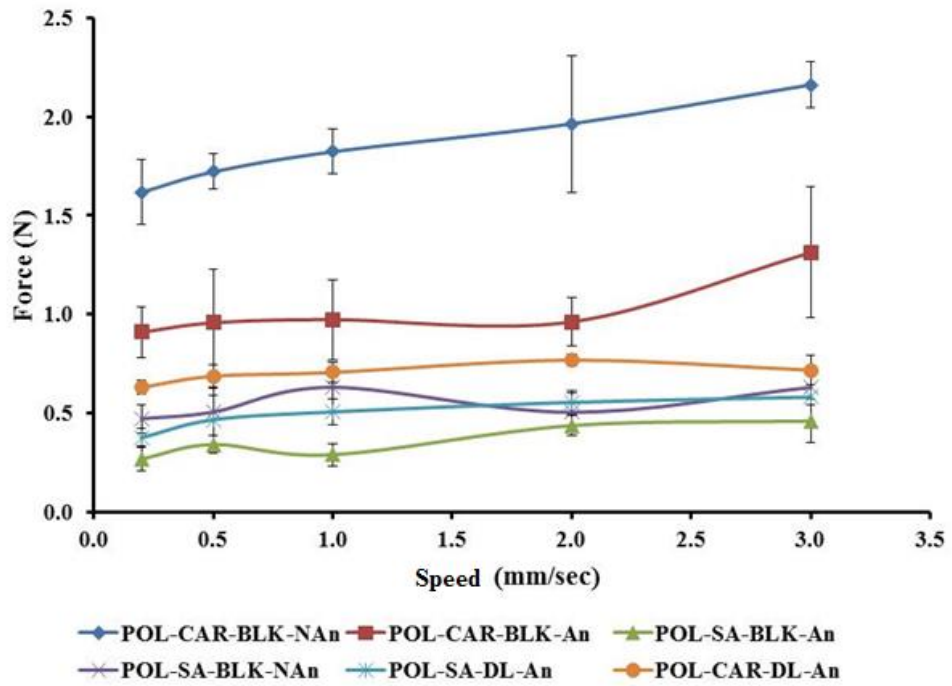


Figure 3.5: Effect of speed of compression on POL-CAR and POL-SA BLK (NAn and An) wafers and POL-CAR-DL and POL-SA-DL-An wafers (depth 2.0 mm, mean± SD, n=5).

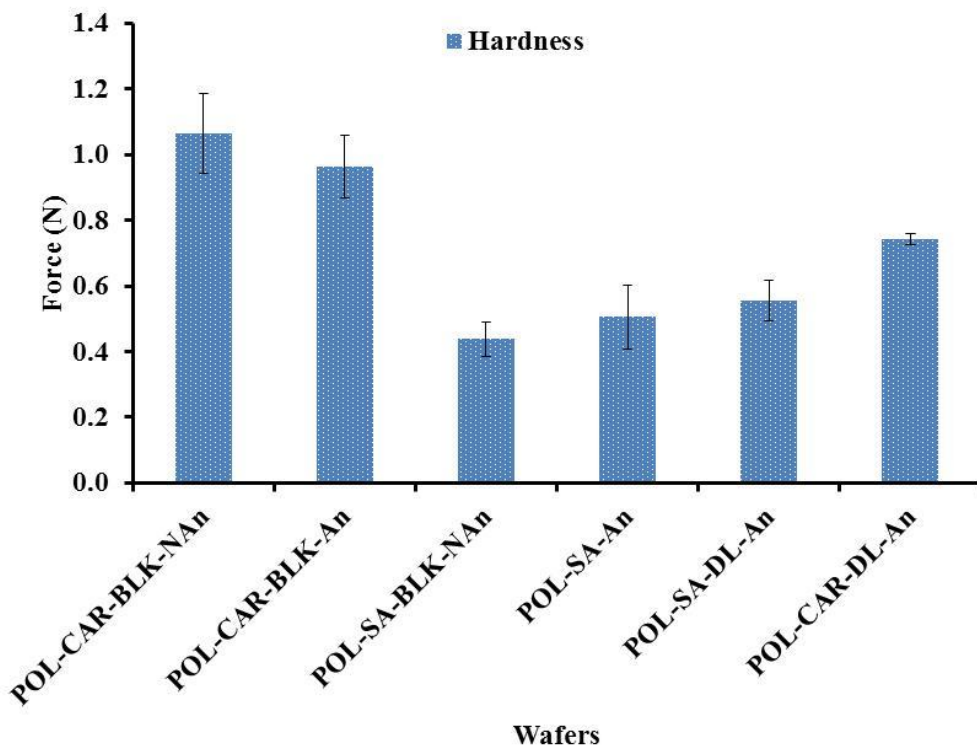


Figure 3.6: Hardness profiles of POL-CAR-BLK and POL-SA-BLK (An and NAn) and POL-CAR-DL, POL-SA-DL (An) wafers (at a speed of 1mm/sec, depth 2.0mm, mean± SD, n=5).

### 3.4.5 X-ray diffraction (XRD)

Figure 3.7 shows the XRD diffractograms of wafers (POL-CAR-BLK-An, POL-CAR-DL-An, POL-SA-BLK-An and POL-SA-DL-An). The XRD patterns of pure polymers and drugs (POL, SA, CAR, DLF and STP) have been previously discussed in *chapter 2, section 2.4.4*. XRD patterns for POL-CAR and POL-SA (BLK-An and DL-An) wafers are shown in figure 3.7. POL-CAR-BLK-An and POL-SA-BLK-An wafers showed decreased intensities at  $19.11^\circ$ ,  $23.22^\circ$  which indicates that the crystallinity of POL was reduced in the presence of CAR and SA. POL-SA wafers further decreased intensities due to the increased amount of SA. All drug loaded wafers did not show distinct peaks of DLF and STP, however there was a peak observed at  $31.73^\circ$  which may be due to the formation of sodium sulphate associated with the DLF and STP. The crystalline properties affect various characteristics such as water uptake, mucoadhesion and biodegradability of the polymers (Prabaharan and Gong, 2008). The reduction in POL crystallization by SA and CAR is probably a result of interruption of POL-POL interactions because of formation of hydrogen bonds between ether and hydroxyl groups from POL and SA or CAR respectively (Zivanovic *et al.*, 2007). This decreased crystallinity of POL-CAR and POL-SA blends and the presence of molecular dispersity of STP and DLF will have high surface energy due to less ordered amorphous structures than the semi-crystalline form. The increase in the surface energy allows greater molecular interaction between the solute and solvent hence they are more soluble and are expected to release the drugs (STP and DLF) quickly when applied to the wound site which can help to reduce bacterial infection. However, it is important to maintain the amorphous form during storage since high energy level in such form may cause a reversion back to the crystalline form of POL and DLF (which are respectively semi-crystalline and crystalline in nature) and needs further evaluation through stability studies. The decreased crystallisation of POL may help to improve its properties stated above and its performance as a dressing such as exudate absorption, prolonged retention at wound site which can increase the bioavailability of the drug and ultimately reduce the frequency of dressing application.

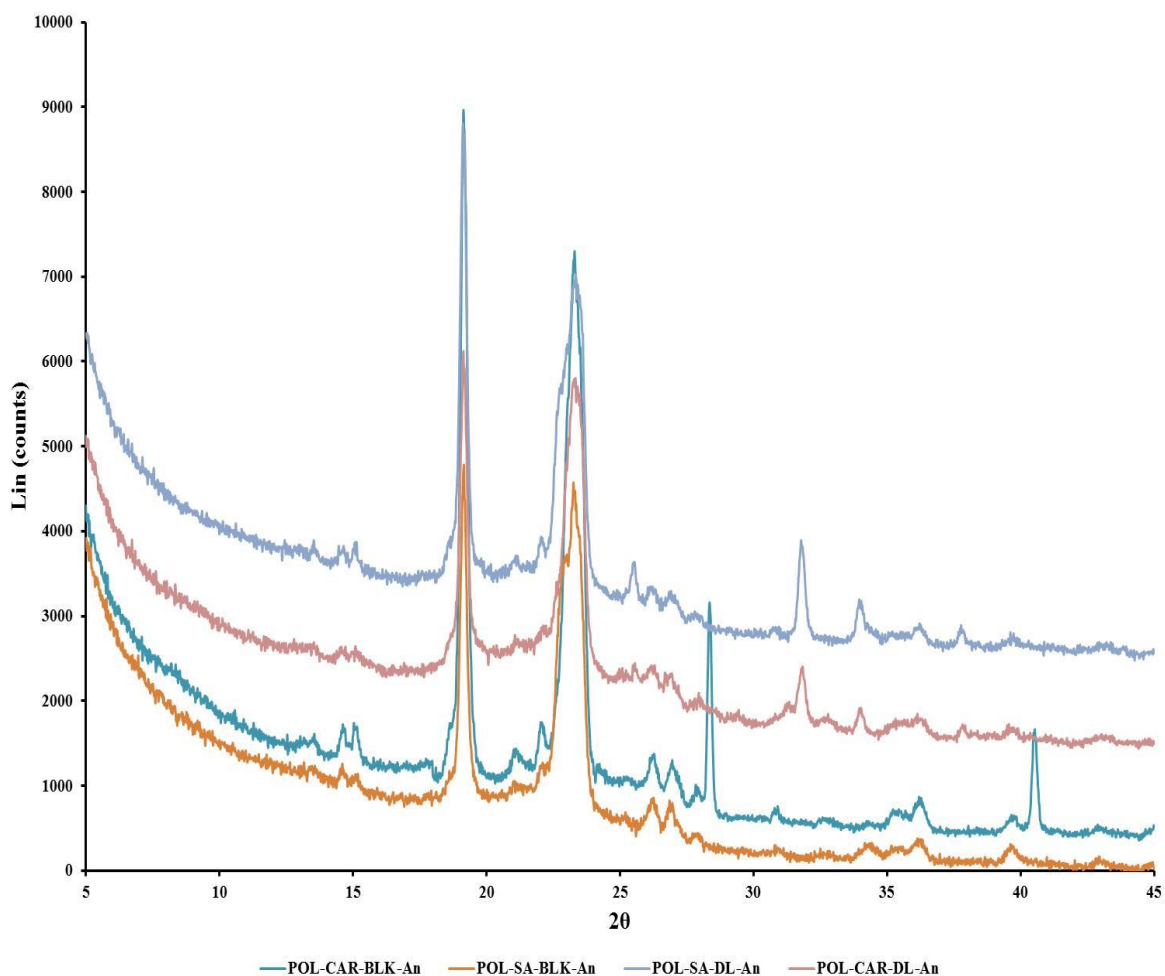


Figure 3.7: XRD patterns of POL-CAR and POL-SA (BLK-An and DL-An) wafers.

### 3.4.6 Differential scanning calorimetry (DSC)

Figure 3.9 shows the DSC thermograms for pure polymers, pure drugs and their corresponding wafers. STP showed a broad endothermic peak at 152.73°C which undergoes recrystallization and then eventually melts. This may be associated with the presence of basic guanido moieties and relatively weakly basic methylamino functional groups which are responsible for two melt peaks and needs further investigation. SA showed a glass transition peak at 60.28°C with subsequent endothermic peaks at 152.73°C, whereas CAR showed an endothermic peak at 148.76°C which consequently decomposed at 192.56°C with a sharp exothermic peak. DLF showed melting peaks at 293.96°C in addition to immediate decomposition. POL showed an endothermic peak at 70.22°C with an exothermic peak at 177.21°C which could be attributed to the recrystallization from the melt. DSC curves of all POL-CAR and POL-SA (BLK and DL) wafers showed a suppression of the POL melting peak

(59-61°C) due to the molecular chain of CAR and SA which has a significant effect on the overall chain mobility in the mixture and retards the rate of crystal growth of POL.

POL-CAR-BLK-An wafers further showed an exothermic peak at 130°C due to the POL but this was absent in the POL-CAR-DL-An wafers due to the drug-polymer interaction. POL-CAR (BLK-An and DL-An) wafers showed endothermic peaks between (162-164°C) which may be associated with CAR. POL-CAR (BLK-An and DL-An) wafers showed exothermic peaks at 212.34°C and 270.42 respectively which may be due to the interactions between the polymer and drug. POL-SA (BLK-An and DL-An) wafers showed an endothermic peak at 135.30°C and 139.90°C and exothermic peak 238.70°C and 242.23°C due to the effect of melting and recrystallization of added SA which appears to be semi-crystalline. Wafers showed hydrogen bonding interaction between the polymer blends of POL-SA and POL-CAR which confirms the compatibility of these polymers.

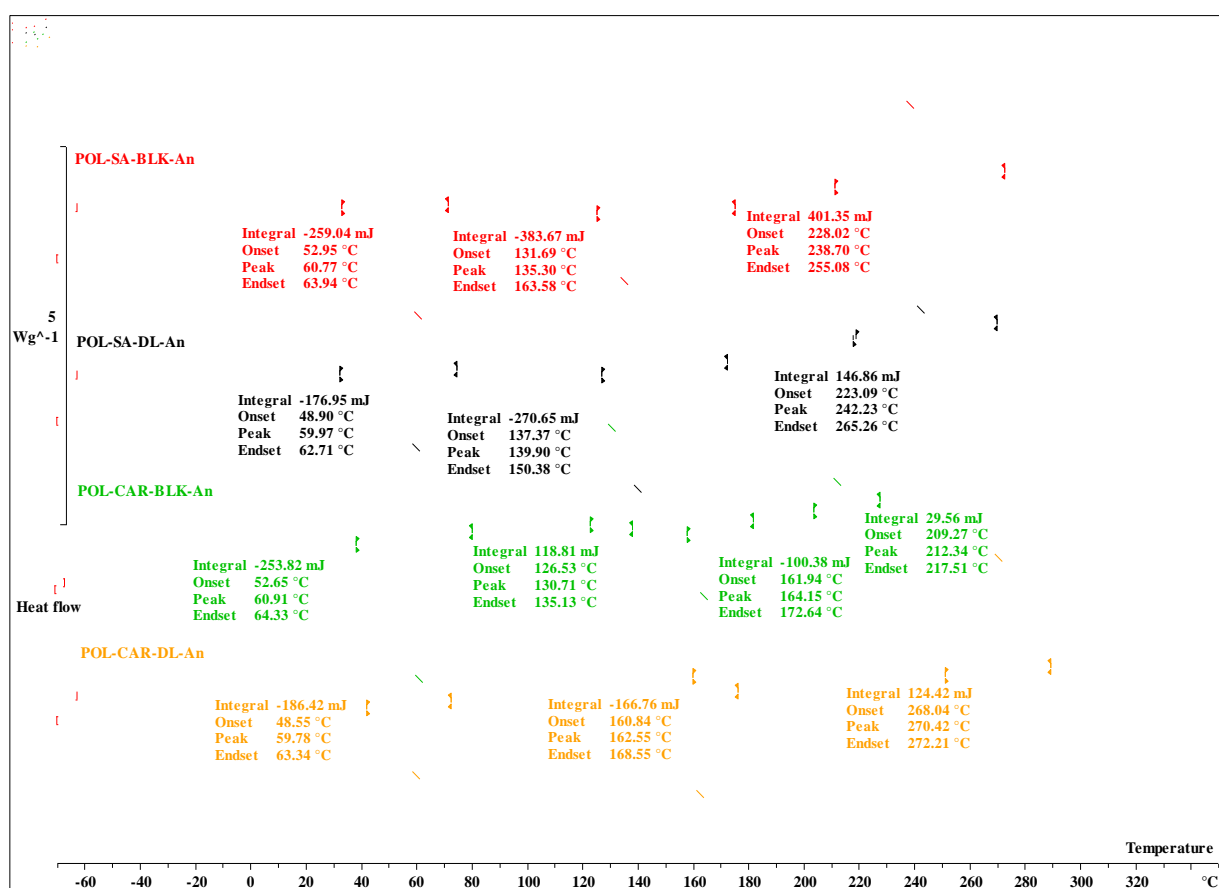


Figure 3.8: DSC profiles of the pure polymers, drugs and POL-CAR and POL-SA (BLK-An and DL-An) wafers.

Huang and co-workers reported that molecularly dispersed drug prompted by hydrogen bonding between drug and polymers had improved physical stability which did not affect release kinetics of the drug (Huang *et al.*, 2006). Both POL-CAR-DL-An and POL-SA-DL-An wafers did not show any peaks for DLF and STP which suggests the molecular dispersion of the drugs within the wafer matrix. Such molecularly dispersed drug in the polymer matrix helps to improve physical stability and drug release from the dosage forms. This can help to maintain biological as well as environmental stability of STP and DLF and their expected controlled release will help to reduce the frequent change in the dressing with improved wound healing however this needs to be evaluated by stability studies (Huang *et al.*, 2006).

### 3.4.7 Attenuated total reflection-Fourier transform infrared spectroscopy (ATR-FTIR)

Structural information of the combined wafers of POL with either CAR or SA in ratio of 75/25wt or 50/50wt respectively with or without drug (STP and DLF) was obtained through FTIR analysis. Characteristic peaks for pure polymers and drugs are shown in *chapter 2 Table 2.4 (section 2.4.5) and figure 2.18*. Figure 3.10 below shows the FTIR spectra of POL-CAR and POL-SA (BLK-An, and DL-An) wafers. The ATR-FTIR spectra show the respective absorption peaks of POL at  $1100\text{cm}^{-1}$  due to the C-O-C asymmetric stretching. An absorption band at  $2885\text{cm}^{-1}$  was also attributed to CH symmetric stretching vibration in POL, while absorption bands at  $1465\text{cm}^{-1}$ ,  $1242\text{cm}^{-1}$ ,  $1278\text{cm}^{-1}$  and  $958\text{cm}^{-1}$  were associated with  $\text{CH}_2$  scissoring, asymmetric twisting and wagging respectively. CAR showed an absorption peak at  $1232\text{cm}^{-1}$  due to the presence of sulphate ester moiety. The peaks at  $924\text{cm}^{-1}$ ,  $844\text{cm}^{-1}$ ,  $890\text{cm}^{-1}$  and  $1155\text{cm}^{-1}$  were assigned to 3, 6 anhydrogalactose residue, galactose 4-sulphate, C-H stretching of  $\beta$ -galactopyranosyl residue and C-O stretching of pyranose ring of the CAR. In the FTIR spectrum of SA, C-O stretching of uronic acid, C-C, C-O stretching and C-OH deformation vibrations were observed at  $929\text{cm}^{-1}$ ,  $1024\text{cm}^{-1}$ ,  $1084\text{cm}^{-1}$ ,  $1400\text{cm}^{-1}$  respectively. DLF showed the characteristic peak at  $1402\text{cm}^{-1}$ ,  $1573\text{cm}^{-1}$  which is due to the O-C-O symmetric and asymmetric stretching, whereas observed peaks at  $1556\text{cm}^{-1}$ ,  $1602\text{cm}^{-1}$ ,  $1585\text{cm}^{-1}$  are associated with ring stretching. Peaks at  $1469\text{cm}^{-1}$  and  $1450\text{cm}^{-1}$  were due to C-N stretching. The same stretching band of C-N at  $1458\text{cm}^{-1}$  was observed for STP. Primary  $\text{NH}_2$  group, O-H stretching and C-O-C stretching at  $3365\text{cm}^{-1}$ ,  $3201\text{cm}^{-1}$  and  $1035\text{cm}^{-1}$  was observed for STP.

All the POL blended wafers with SA and CAR with or without STP and DLF showed hydrogen bonding or complexation between the POL and/or CAR or SA by monitoring the band

shift at  $1100\text{cm}^{-1}$  C-O-C stretching. Intermolecular interaction between the POL with CAR or SA was responsible for the increased physical stability of the prepared wafers. All DL wafers did not show any characteristic peaks of DLF due to the homogeneous mixing into the POL-CAR and POL-SA. However, the presence of C=N and N-H stretching band at  $1618\text{cm}^{-1}$ - $1654\text{cm}^{-1}$  confirms the presence of STP in the all POL-CAR (DL) wafers. FTIR study of two different formulation types i.e. POL-CAR and POL-SA [films (chapter 2, section 2.4.5) and wafer] did not show much differences in their FTIR spectra which means the drying method involved to obtain the films and wafers are not the main mechanism behind changes in the starting material but rather due to the interactions between them.

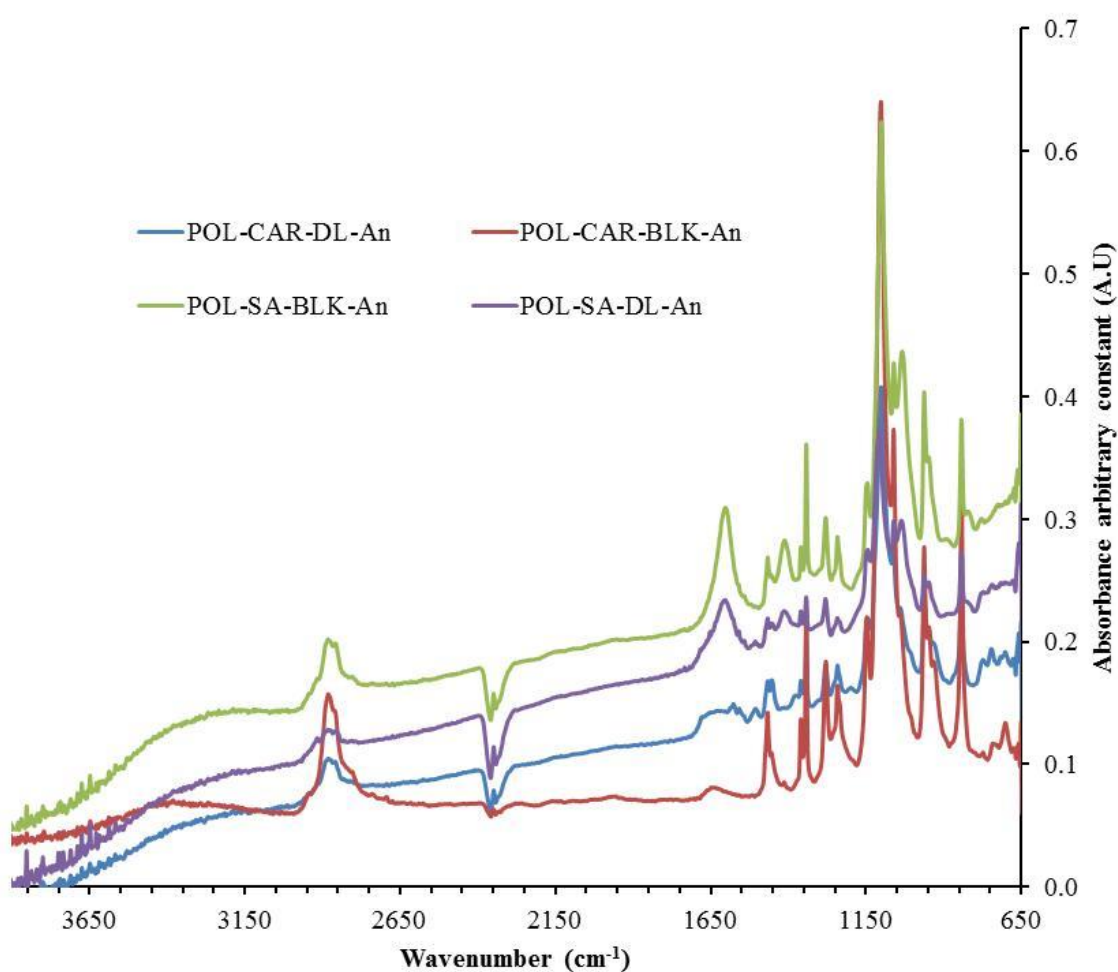


Figure 3.9: FTIR spectra showing peaks for different components within freeze dried POL-CAR and POL-SA (BLK-An and DL-An) wafers.

### 3.5 Conclusions

Characterisation of the two different wafers (POL-CAR and POL-SA) (BLK-An and DL-An) showed marked differences in their microscopic structure and physical properties which is expected to impact on their wound healing performance characteristics. The annealing step in the lyophilisation cycle helped to produce soft, flexible and desired porous structure in the formulated wafers. This helped to improve mechanical strength and expected to help improve ease of hydration, mucoadhesion and the *in vitro* drug release characteristics of the DL wafers. The mechanical properties demonstrate that the wafers prepared from annealing step reduced the hardness but were still strong enough to withstand the mechanical stresses occurring during day-to-day activities, while flexible enough to prevent potential damage to newly formed skin tissue. DSC and XRD studies showed decreased crystallinity of the POL with molecular dispersion of the drugs within the wafer polymer matrix as observed for the films. Such dispersion of both drugs can improve the physical stability of the dosage form and controlled release of both drugs which can help to improve wound healing by acting on two different stages of wound healing. The results show that the annealed wafers can be potentially used for highly exuding wounds such as chronic ulcers.

## **CHAPTER 4: IN VITRO SWELLING AND DRUG DISSOLUTION STUDIES OF SOLVENT CAST FILMS AND FREEZE DRIED WAFERS**

### **4.1 Introduction**

Polymer swelling in a controlled release matrix system mainly results in two very important consequences. Firstly, the length of the diffusion path increases, resulting in decreasing drug concentration gradients potentially decreasing drug release rates. The second effect is that the mobility of the polymer macromolecules significantly increases, resulting in increased drug mobility and potentially increasing drug release rates (Siepmann and Siepmann 2008).

Increased or decreased drug release rates potentially depend on the type of polymer and type of drug delivery system. Upon contact of a swellable matrix with dissolution medium, water diffuses into the system and polymer chain mobility increases with increasing water content. Drug delivery systems are often classified on the basis of their design or their rate-controlling release mechanism such as diffusion, erosion/chemical reactions and swelling (Frenning 2011). The timely and reproducible release of active pharmaceutical ingredients from delivery vehicles of various kinds is of paramount importance for safe and efficient treatment of disease (Frenning 2011). The study of drug release from polymeric systems usually involves the uptake of water by the glassy polymer and subsequent swelling to form a gel layer which controls drug release by viscous resistance to drug diffusion (Boateng *et al.*, 2009).

The different kinetic models commonly discussed in the literature to describe the release kinetics of drugs the pharmaceutical dosage forms based on the drug dissolution or release data have been summarised in table 4.1 below.

Table 4.1: Different drug release kinetic models with their respective equation, definition of terms and its implications (Shoeb et al., 2006).

Kinetic model	Representative equation	Definition of terms	Conditions
Zero order	$M=K_0t$	$K_0$ is zero order rate constant for drug released $M$ in time $t$	Release rate is independent of drug concentration
First order	$\text{Log } M = \text{Log } M_0 - \frac{K_1 t}{2.303}$	$M_0$ is initial amount of drug, $M$ is cumulative amount of drug remained at time $t$ and $K_1$ is the first order release constant	Release rate depends on drug concentration
Higuchi	$M = K_H t^{1/2}$	$M$ is the drug concentration; $K_H$ is a constant that relates to the design variables of the system.	Drug release from a non-degradable monolithic system whereby drug particles are dispersed uniformly throughout the matrix is depends upon the diffusion.
Korsmeyer-Peppas	$\frac{M_t}{M_\infty} = K_P t^n$	$M_t$ and $M_\infty$ are the absolute cumulative amounts of drug released at time $t$ and infinite time respectively, $K_P$ is the release constant incorporating structural and geometric characteristics of the system and $n$ is the release exponent.	Drug release through the matrix is dependent upon the Fickian diffusion or non-Fickian diffusion which is combination of both diffusion and erosion controlled rate release
Hixson-Crowell	$M_0^{1/3} - M_t^{1/3} = K_{HC}^t$	$M_0$ and $M_t$ are the initial amount and amount of drug released from formulation in time $t$ respectively. $K_{HC}$ is the rate constant for Hixson-Crowell equation	Drug released by dissolution and through the change in surface area and diameter of particles or tablets.

The present chapter aims to determine the *in vitro* swelling characteristics of films and wafers (BLK and DL) and release profiles of STP and DLF from the drug loaded films (POL-CAR-DL, POL-CAR-DL-20%GLY, POL-SA-DL and POL-SA-DL-9%GLY) and drug loaded lyophilised wafers (POL-CAR-DL-An and POL-SA-DL-An). In addition, it evaluates the dissolution properties of the DL lyophilised wafers and solvent cast films. The release characteristics of STP and DLF from the wafers and films were compared to investigate the effect of differences in their physical structure. The drug release data were fitted to zero-order, first order, Higuchi, Korsmeyer-Peppas and Hixon Cromwell equations to identify the equation that best model release of STP and DLF from the films and wafers. The effect of different variables [amount of polymer, drugs (STP and DLF) and GLY (for films)] and formulation type (wafer and film) on drug release characteristics were also investigated.

## **4.2 Materials**

(Polyox™ WSR 301  $\approx$ 4000 kDa) was obtained as a gift from Colorcon Ltd (Dartford, UK), kappa-carrageenan (Gelcarin GP 812 NF) (CAR) was obtained from IMCD Ltd (Sutton, UK), sodium hexane sulphonate, sodium phosphate tribasic, dodecahydrate (>98%), bovine serum albumin (BSA), diclofenac sodium (DLF) and streptomycin sulphate (STP) were all purchased from Sigma Aldrich, (Gillingham, UK). Sodium alginate (SA), acetonitrile (HPLC grade), glycerol (GLY), tris(hydroxymethyl)aminomethane, calcium chloride dihydrate, ethanol (laboratory grade), sodium hydroxide and orthophosphoric acid (analytical grade) were all purchased from Fisher Scientific (Leicestershire, UK). Potassium phosphate monobasic (99% extra pure) was purchased from Acros Organic Ltd (New Jersey, USA).

### **4.2.1 *In vitro* swelling studies of POL-CAR films**

#### **4.2.1.1 Swelling studies using phosphate buffer (PBS)**

A piece of the film was cut, weighed accurately and immersed into 20 ml of phosphate buffer of pH 7.3. At specific time intervals, the changes in weight of the films were recorded. The time intervals were kept at 15 min for the first 1 h and sampling time subsequently increased gradually until 5 h. Four different films POL-CAR-BLK, POL-CAR-BLK-25%GLY, POL-CAR-DL, POL-CAR-DL-25%GLY as previously formulated in *chapter 2*, were used for the study.

#### 4.2.1.2 Swelling studies using simulated wound fluid (SWF)

Furthermore all the films (POL-CAR-BLK, POL-CAR-DL, POL-CAR-BLK-20%GLY, POL-CAR-DL-20%GLY and POL-SA-BLK, POL-SA-DL, POL-SA-BLK-9%GLY, POL-SA-DL-9%GLY, POL-SA-BLK, POL-SA-DL and wafers (POL-CAR-BLK-An, POL-CAR-DL-An, POL-SA-BLK-An, POL-SA-DL-An] were cut into 2 x 2 cm<sup>2</sup> strips, weighed accurately and immersed in 20 ml of simulated wound fluid (SWF) containing (2% BSA, 0.02 M calcium chloride, 0.4 M sodium chloride, 0.08 M tris(hydroxymethyl)aminomethane in deionised water, pH 7.5) (Lindsay *et al.*, 2010). The changes in weight of the films and wafers were recorded at 15 min time intervals.

To quantify swelling behaviour, percent swelling index  $I_s$  (%) was calculated using the following equation (4.1).

$$I_s = \frac{W_s - W_d}{W_d} \times 100 \quad \text{Equation 4.1}$$

Where,  $W_d$  is dry weight of polymeric films and  $W_s$  denotes weight of film after swelling. The effects of medium, plasticizer and drugs on the swelling performance of films and wafers were evaluated.

#### 4.2.2 *In vitro* drug dissolution studies

Before drug dissolution studies, calibration graphs were plotted for both STP and DLF. The concentration of STP and DLF in mobile phase was assayed by HPLC as described in section 4.2.5 below.

##### 4.2.2.1 Drug dissolution studies for POL-CAR films using phosphate buffer

For drug loaded POL-CAR films, *in vitro* drug dissolution studies were performed with a Franz diffusion cell across a wire mesh using 8 ml of phosphate buffer (pH 7.3) as dissolution medium in the receptor compartment. POL-CAR-DL and POL-CAR-DL-20%GLY films containing STP and DLF were placed on the wire mesh. The donor and receiver compartments were kept in intimate contact by wrapping Parafilm<sup>®</sup> at the junction between both compartments as shown in figure 4.1. The temperature of the diffusion cell was maintained at  $37 \pm 0.5^\circ\text{C}$  by a circulating water jacket. The whole assembly was kept on a magnetic stirrer (600 rpm) and the dissolution medium was constantly stirred throughout each experiment using magnetic beads at

the bottom of the receiver compartment. At predetermined time intervals, 0.5 ml aliquots of dissolution media were withdrawn and analysed by HPLC, and replaced with the same amount of buffer solution to maintain a constant volume throughout. The percentage release of STP and DLF from the films was calculated taking into consideration the dilution due to the 0.5 ml aliquots that were discarded and replaced with fresh dissolution medium and plotted against time (Thakur *et al.*, 2008).

#### **4.2.2.2 In vitro drug dissolution studies of films and wafers using SWF**

*In vitro* drug dissolution studies were performed with a Franz diffusion cell as described in the previous *sub section 4.2.3.1* but using 8 ml of SWF at pH 7.5 as dissolution media in the receptor compartment as previously reported (Singh and Pal., 2011). The pH of 7.5 was chosen in order to represent the natural chronic wound environment which has been reported in the range of 7.15–8.90 (Gethin, 2007).

The SWF was prepared as described in *section 4.2.2.2* above but without BSA to avoid blocking of the HPLC column. Pure drugs (STP and DLF) were used as positive control during the drug dissolution of films and wafers. The films (POL-CAR-DL, POL-CAR-DL-20%GLY, POL-SA-DL and POL-SA-DL-9%GLY) and wafers (POL-CAR-DL-An and POL-SA-DL-An) containing STP and DLF were placed on the wire mesh. The donor and receiver compartments were kept in intimate contact by wrapping Parafilm<sup>®</sup> at the junction between both compartments. The temperature of the diffusion cell was maintained at  $37\pm 0.5^{\circ}\text{C}$  by a circulating water jacket (Figure 4.1). The dissolution medium was constantly stirred (600 rpm) throughout the experiments using magnetic beads on a magnetic stirrer. 1.0 ml aliquots of dissolution media were withdrawn at predetermined time intervals and analysed by HPLC, and replaced with the same amount of SWF to maintain a constant volume throughout. The percentage cumulative release of STP and DLF from the films and wafers was calculated, taking into consideration the dilution due to the 1.0 ml aliquots that were discarded and replaced with fresh dissolution medium. The calculated values were plotted against time (Thakur *et al.*, 2008).

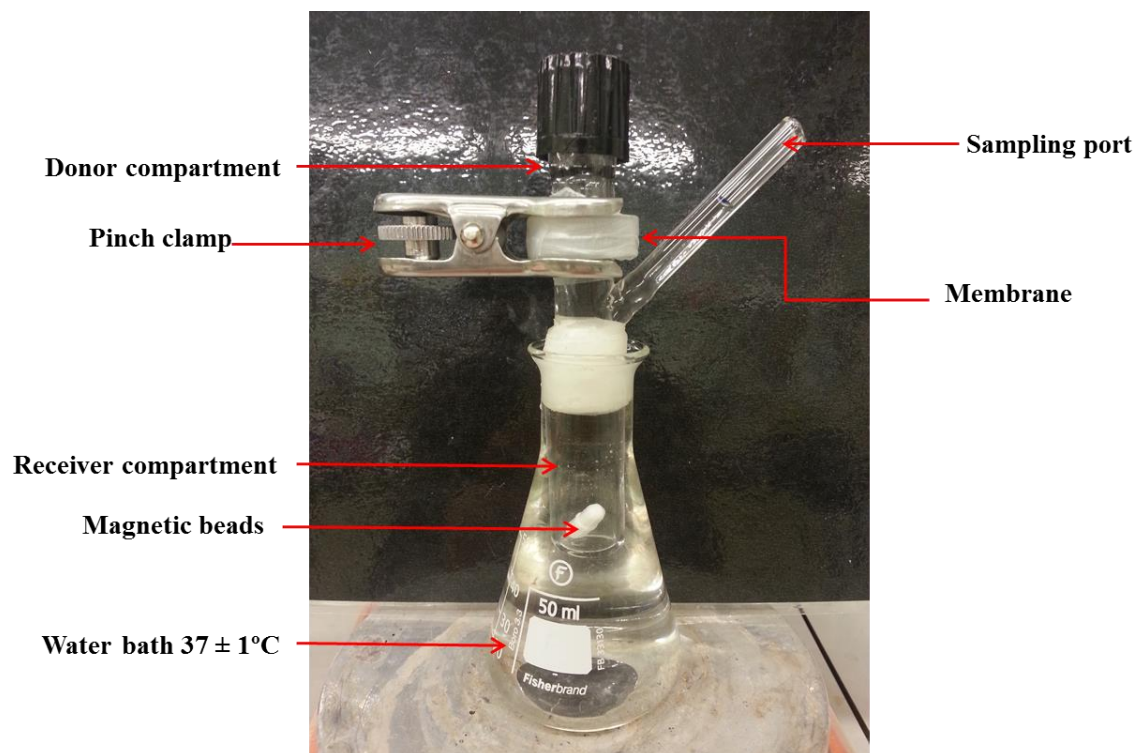


Figure 4.1: Digital photograph of modified Franz-type diffusion cell as set up for drug release experiments in the current project.

### 4.2.3 HPLC analysis

Concentration of STP and DLF in calibration solutions as well as drug release in dissolution studies were analysed using an Agilent 1200 HPLC equipped with an auto sampler (Agilent Technologies, Cheshire, UK,) with a chemstation<sup>®</sup> software program. The column used for analysis was ACE-3 C-18 HL (150 X 4.6 mm) (Advanced Chromatography Technologies; Aberdeen, UK) (for the drug release study from phosphate buffer pH 7.3) and Hichrome (150 x 4.6 mm, 5 $\mu$ m) (Hichrome ltd; Berkshire, UK) (for the drug release study from SWF pH 7.5). The mobile phase consisted of a mixture of phosphate buffer and acetonitrile in the ratio of 85:15 (v/v) and 50:50 (v/v) for the drug release study of POL-CAR films. Furthermore two different mobile phases were used to analyse the STP and DLF released from films and wafers in the presence of SWF which consisted of phosphate buffer (pH 6.0) and acetonitrile in the ratio of 85:15 (v/v) for STP and deionised water and acetonitrile in the ratio of 40:60 (v/v) for DLF. The buffer was prepared by mixing 20mM of sodium hexane sulphonate and 25mM of tribasic sodium phosphate in distilled water and pH adjusted to 6.0 using ortho-phosphoric acid. The flow rate of the mobile phase was maintained at 1.0 ml/min and detector wavelengths for STP and DLF were set at 195 nm and 284 nm respectively. 20  $\mu$ l volumes were injected during each

run. Standards from 5-500 µg/ml were used to plot calibration curves for STP and DLF ( $r^2 > 0.99$ ) (Granados and Meza, 2007; Adams *et al.*, 2000; Heda *et al.*, 2010; Giordano *et al.*, 2003)

#### 4.2.4 Drug release kinetics

Representative plots for the STP and DLF were obtained by fitting experimental release data with their corresponding kinetic models. The following profiles were plotted: cumulative % drug release vs. time (zero order kinetic model); log cumulative of % drug remaining vs. time (first order kinetic model); cumulative % drug release vs. square root of time (Higuchi model); log cumulative % drug release vs. log time (Korsmeyer model) and cube root of drug % remaining in matrix vs. time (Hixson-Crowell cube root law) (Shoaib *et al.*, 2006). To compare the dissolution profiles, a model independent approach was used by calculating the difference ( $f_1$ ) and a similarity ( $f_2$ ) factors. The difference factor calculates the percent difference between the two curves at each time point and is a measurement of the relative error between the two curves. Difference factor ( $f_1$ ) and a similarity factor ( $f_2$ ) was calculated using equation 4.2 and 4.3 as shown below (Boateng *et al.*, 2009).

$$f_1 = \frac{\sum_{j=1}^n |R_j - T_j|}{\sum_{j=1}^n R_j} \times 100 \quad \text{Equation 4.2}$$

$$f_2 = 50 \times \log \left\{ \left[ \frac{1}{N} \sum_{j=1}^n |R_j - T_j|^2 \right]^{-0.5} \times 100 \right\} \quad \text{Equation 4.3}$$

Where n is the number of time points,  $R_j$  is the dissolution value of the reference batch at time t, and  $T_j$  is the dissolution value of the test batch T at time t.

### 4.3 Results and discussion

#### 4.3.1 Swelling studies

Since drug dissolution and release properties were directly affected by hydration and swelling, swelling studies were carried out to determine the swelling capacity for each formulation in the presence of dissolution media. Preliminary studies of POL-CAR films were focused on two different media which were phosphate buffer and SWF. Subsequently the studies were carried out in SWF which can mimic actual wound exudate.

POL is a water-soluble resin and is often used as a polymeric excipient in oral dosage formulations for controlling the rate of drug release. The control of drug release involves a series of interrelated events such as polymer surface wetting, hydration, hydrogel formation and

erosion (or dissolution). For a hydrophilic drug, the swelling behaviour of hydrophilic polymers (e.g. POL, CAR, and SA) is believed to be a controlling factor because the drug molecules must diffuse through the hydrated gel layer to reach the delivery site. Ultimately, swelling studies can give information about the drug release and hydration/erosion behaviour in the presence of SWF and therefore is important to study (Fan *et al.*, 2001). A major goal in drug delivery is to develop systems that deliver therapeutic agents at a controlled rate over an extended period. This can be achieved by using systems in which polymer swelling and subsequent drug diffusion are the controlling mechanisms for drug release (Lowman *et al.*, 2004). On the other hand, adequate hydration (which occurs during the initial stages of swelling) is an essential property for uniform and prolonged release of the drug and for effective mucoadhesion (Peppas and Buri, 1985). The initial swelling rate is generally considered to be a function of the hydrophilicity of the polymer. However, the observed difference in the swelling of all formulations studied in the current project (film and wafer) cannot be explained solely by differences in hydrophilicity of just the polymers (Hagesaether and Sande 2008).

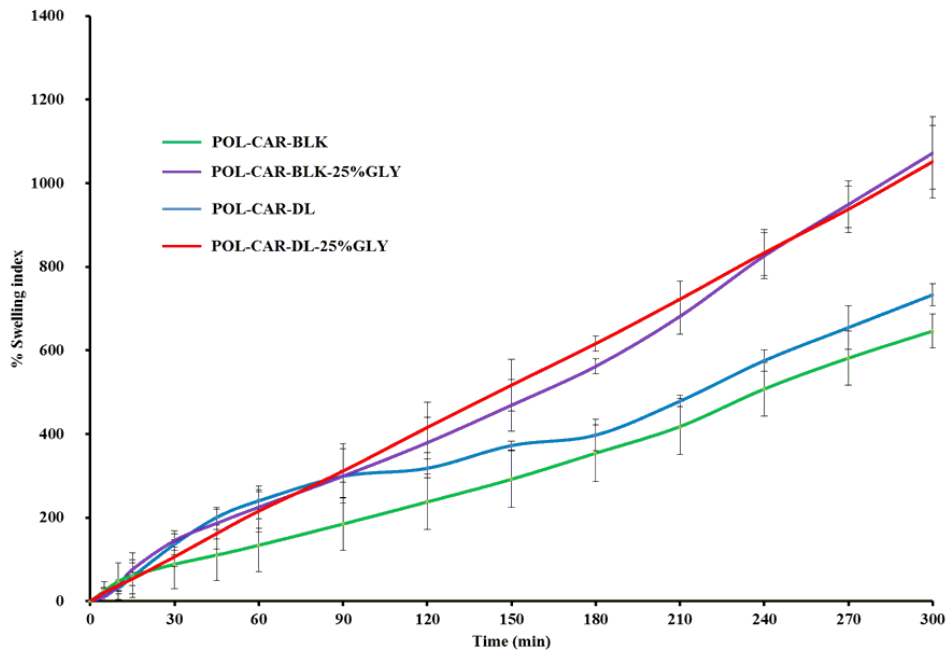


Figure 4.2: Swelling profiles of POL-CAR films in PBS of pH 7.3 showing plot of % swelling index against time (mean  $\pm$ SD, n=4)

### 4.3.1 Swelling capacity of POL-CAR films

Figures 4.2 and 4.3 show the swelling profiles with time (percentage swelling index) of the POL-CAR films (BLK and DL) prepared from gels plasticized with 20% GLY in PBS 7.3 and SWF. All the profiles obtained showed that percentage swelling increased with time. The films swelled more quickly in SWF as compared to PBS. This may be due to the difference in the ionic strength of both media (ionic strength 0.35M and 0.20M respectively). Both (POL-CAR-BLK and POL-CAR-BLK-20%GLY) films maintained their structural integrity for the first 20 min in both media but these films started to lose their integrity after 120 min in SWF possibly due to polymer erosion.

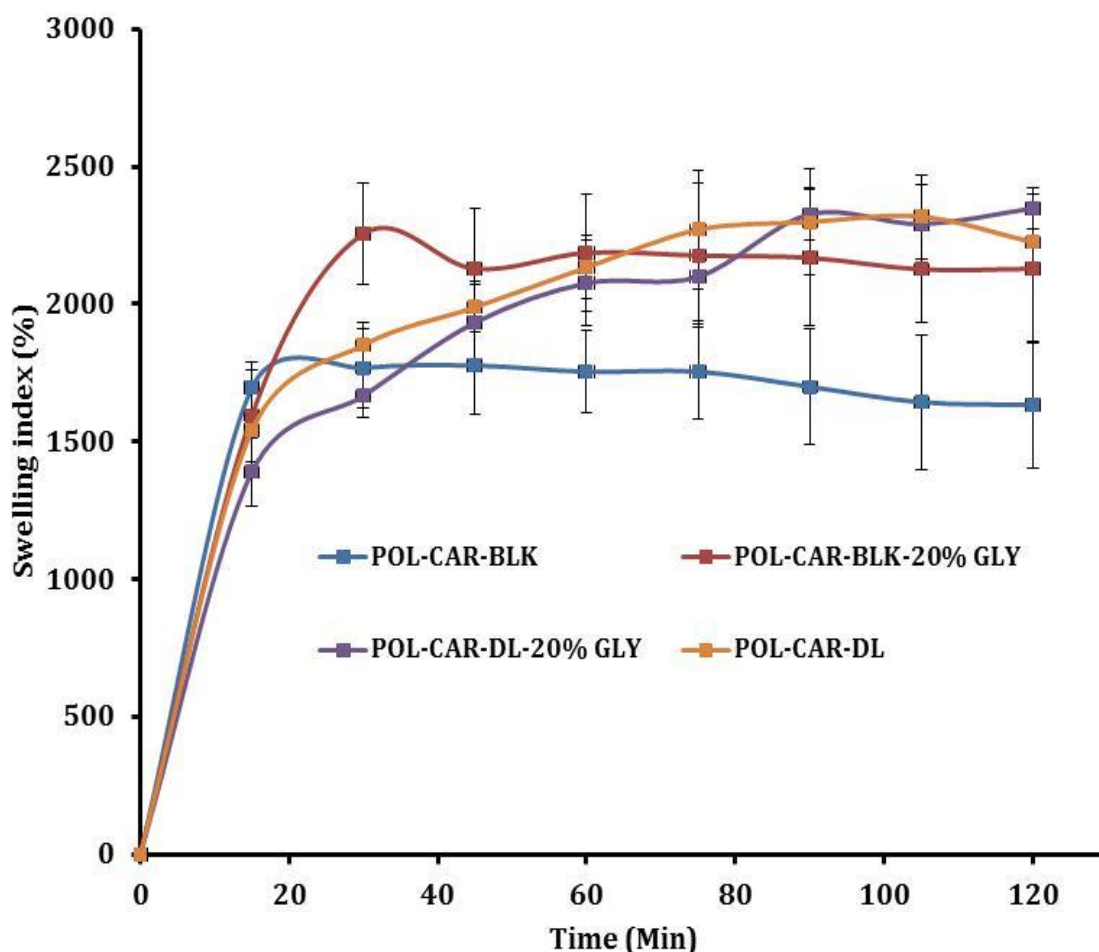


Figure 4.3: Swelling index of POL-CAR films in presence of SWF (mean  $\pm$ SD, n=4).

The swelling profiles in both media showed that the films containing plasticizer had higher swelling capacity as compared to BLK non plasticised films due to the effect of the GLY which causes flexibility by increasing the spaces between the polymer chains and therefore allowed a higher rate of water ingress and hence the enhanced water absorption capacity (Azevedo *et al.*, 2006). On the other hand, loading of drugs into the films (POL-CAR-DL and POL-CAR-DL-20% GLY) resulted in a noticeable effect on the film swelling in SWF. The more steady increase in the swelling may be attributed to the release of drug (STP and DLF) present within the films which increased the medium solute concentration and therefore less water molecules became available for absorption by the polymer. POL-CAR-DL films showed maximum swelling of  $2317 \pm 152\%$  which was increased to  $2327 \pm 93\%$  for POL-CAR-DL-20% GLY films. Both DL (POL-CAR-DL and POL-CAR-DL-20% GLY) films formed a gel initially and started to lose integrity after 105 and 135 min respectively due to the dissolution of the films. This was not the case in PBS where both DL films showed constant increase in weight and maintained the integrity of the films after 5 hrs. POL-CAR-DL films showed maximum swelling of  $733 \pm 26\%$  within 5 h which increased to  $1051 \pm 86\%$  for the POL-CAR-DL-20% GLY films. It can be concluded that the POL-CAR films are freely swellable in SWF and PBS which was increased with the addition of plasticizer and also affected by the drug which might reduced helical content in the gels in the presence of SWF and the salt forms of DLF and STP (Bajpai and Sharma, 2004; Singh *et al.*, 2009). These films eventually showed a steady weight gain in the presence of PBS without disturbing the integrity of all the POL-CAR films.

Most film dressings have the disadvantage of poor absorbency and impermeability for wound exudate which accumulates under the dressing and causes skin maceration, bacterial proliferation and the risk of infection. Thus, they require frequent changes which can result in patient non-compliance. POL-CAR DL films showed high swelling index indicating a high holding capacity for exudate while still maintaining their structural integrity for prolonged periods and therefore could help to overcome the challenge of excess exudate collecting under the dressing (Boateng *et al.*, 2008). It is reported that moderate to high exuding wounds typically produce approximately 3-5 ml of exudate per  $10 \text{ cm}^2$  in 24 h (Thomas, 2007). In this study, it was shown that  $2 \text{ cm}^2$  of POL-CAR-DL-20% GLY film absorbed 2327% of SWF within 90 min which indicates that these dressings could absorb a high volume of fluid and retain their physical dimensions and can be suitable for moderate to high exuding wounds.

### 4.3.2 Swelling capacity of POL-SA films

POL-SA-BLK-9%GLY films showed higher overall swelling capacities in all the plasticised films whilst unplasticised POL-SA films showed more rapid swelling and disintegration compared to the POL-CAR films described above. POL-SA films with a 50/50 ratio of both POL and SA swelled more quickly in SWF achieving maximum swelling capacity in 15-30 min with values of  $1608 \pm 174$  % (POL-SA-BLK) and  $2314 \pm 112$ % (POL-CAR-DL-9%GLY) after which the swelling capacity started to decrease due to disintegration of SA (Figure 4.4). Furthermore, swelling capacity of DL films was increased with the addition of plasticizer and was also affected by the drug which might have interactions with the common ions present in the SWF and the salt forms of DLF and STP. POL-SA-DL films achieved maximum swelling capacity up to  $1531 \pm 100$ % which was increased to  $1766 \pm 122$ % due to the addition of GLY.

The gelling property of alginates is attributed to the presence of  $\text{Ca}^{++}$  ions which help to form a crosslinked polymeric gel that degrades slowly (Boateng *et al.*, 2008). Bajpai and Sharma (2009) reported that the swelling mechanism of SA was affected by  $\text{Na}^+$  ions present in the external solution which undergoes ion exchange process with  $\text{Ca}^{++}$  ions present in the alginate by binding with  $-\text{COO}^-$  groups mainly present in mannuronate side chains. As a result, the electrostatic repulsion among negatively charged  $-\text{COO}^-$  groups increases which ultimately causes chain relaxation and enhances the gel swelling. It is therefore possible that in the initial phase of the swelling process, the  $\text{Ca}^{++}$  ions present in mannuronate units are exchanged with  $\text{Na}^+$  ions present in SWF thus causing the films to increase their swelling capacity. Bajpai and Sharma (2009) reported that the  $\text{Na}^+$  ions exchanging with  $\text{Ca}^{++}$  ions caused the bead structure to lose its integrity whilst phosphate ions interact with the  $\text{Ca}^{++}$  to form calcium phosphate. Here we used SWF containing  $\text{CaCl}_2 \cdot 2\text{H}_2\text{O}$  and  $\text{NaCl}$  which might be responsible for the exchange of  $\text{Na}^+$  and  $\text{Ca}^{++}$  ions to form a  $\text{CaCl}_2$  and responsible for the loss of integrity. The report of Bajpai and Sharma (2009) explained that the more rapid swelling of sodium alginate is due to the polymannuronate block where the  $\text{Ca}^{++}$  ions binds to the polygluconate units and this interaction starts to disintegrate and dissolve the swollen beads (Bajpai and Sharma 2009).

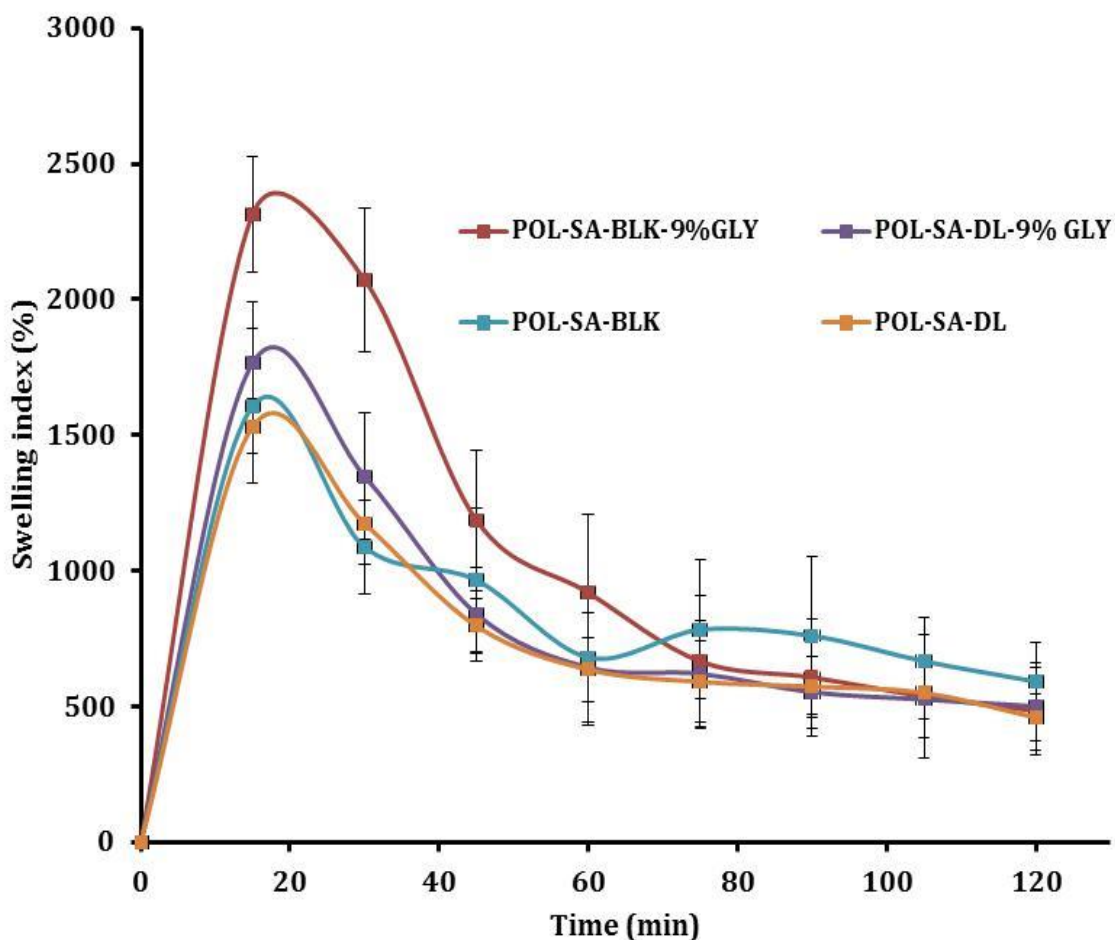


Figure 4.4: Swelling profiles showing the change in % swelling index with time of POL-SA films in the presence of SWF (mean  $\pm$ SD, n=4).

### 4.3.3 Swelling capacity of POL-CAR and POL-SA wafers

Figure 4.5 shows the change in swelling capacity (%) of wafers with time. The difference in the hydration capacity of the optimised POL-CAR-BLK wafer ( $3770 \pm 283\%$ ) and POL-SA-BLK ( $1711 \pm 46\%$ ) was statistically significant ( $p < 0.0001$ ). The water uptake of the samples reached the maximum value within 30 min of incubation, due to increased hydrophilicity of the POL, CAR and SA in presence of SWF. In addition, the annealing process enhanced ice crystal size during the freezing stage to increase wafer porosity. The highly porous structure of freeze-dried wafers allowed a more rapid ingress of water initially which affected the swelling capacity compared to the corresponding films. It is interesting to note that wafers maintained their structural integrity after 2 h of incubation at  $37^\circ\text{C}$  due possibly to the mechanically stronger

formulations obtained by annealing. The POL-CAR-BLK wafers showed high swelling capacity which was dramatically decreased in the POL-CAR-DL wafers (1449.9162.3%). This difference was also observed between the POL-SA-BLK and POL-SA-DL wafers even though the differences were only noticeable during the first 40 minutes. This may be due to the effect of added drug which decreased the porosity (SEM data in *chapter 3*) as well as the formation of sodium sulphate which decreases the swelling capacity of wafers as was the case for the films. The POL-SA-DL wafer showed maximum swelling capacity (1227±134%).

Singh and co-workers (2009) reported the effect of sodium sulphate on gels of the polysaccharide, agarose. They reported that the hydration capacity of agarose polysaccharide decreased with increasing concentration of sodium sulphate which is associated with the strong hydrophobic hydration of the highly osmotic sodium sulphate (Singh *et al.*, 2009). The presence of sodium sulphate formed in the polymeric gels (POL-CAR and POL-SA) appears to be behaving in the same manner to reduce the swelling capacity of the DL films and wafers compared with the BLK films and wafers. The presence of sodium sulphate in the DL films and wafers (POL-CAR and POL-SA) keeps the water molecules away from the polymers and prevents the formation of high-density water zone at surface of POL-CAR and POL-SA which in turn disfavours the organization of water molecules into the tetrahedral arrangement in the vicinity of POL-CAR and POL-SA polymer chains. A part of the total sodium sulphate present in the gel is used to reduce the interactions of hydrophilic OH groups of CAR and SA with the water molecules, thereby reducing the organization of water molecules into a tetrahedral arrangement in the vicinity of hydrated CAR and SA. There was marked influence of sodium sulphate on swelling index of POL-SA-DL-An and POL-CAR-DL-An which may be due to the higher loading of both drugs (STP and DLF), which may further affect the drug release through the wafers.

In both films and wafers, POL-CAR showed higher swelling capacity than the POL-SA, which may be due to the use of different polymers in different their ratios (75/25 and 50/50, respectively). In the initial 30 min, the swelling index of both DL wafers (POL-CAR-DL-An and POL-SA-DL-An) were the same which further decreased for POL-SA-DL-An but were consistently increasing for POL-CAR-DL-An.

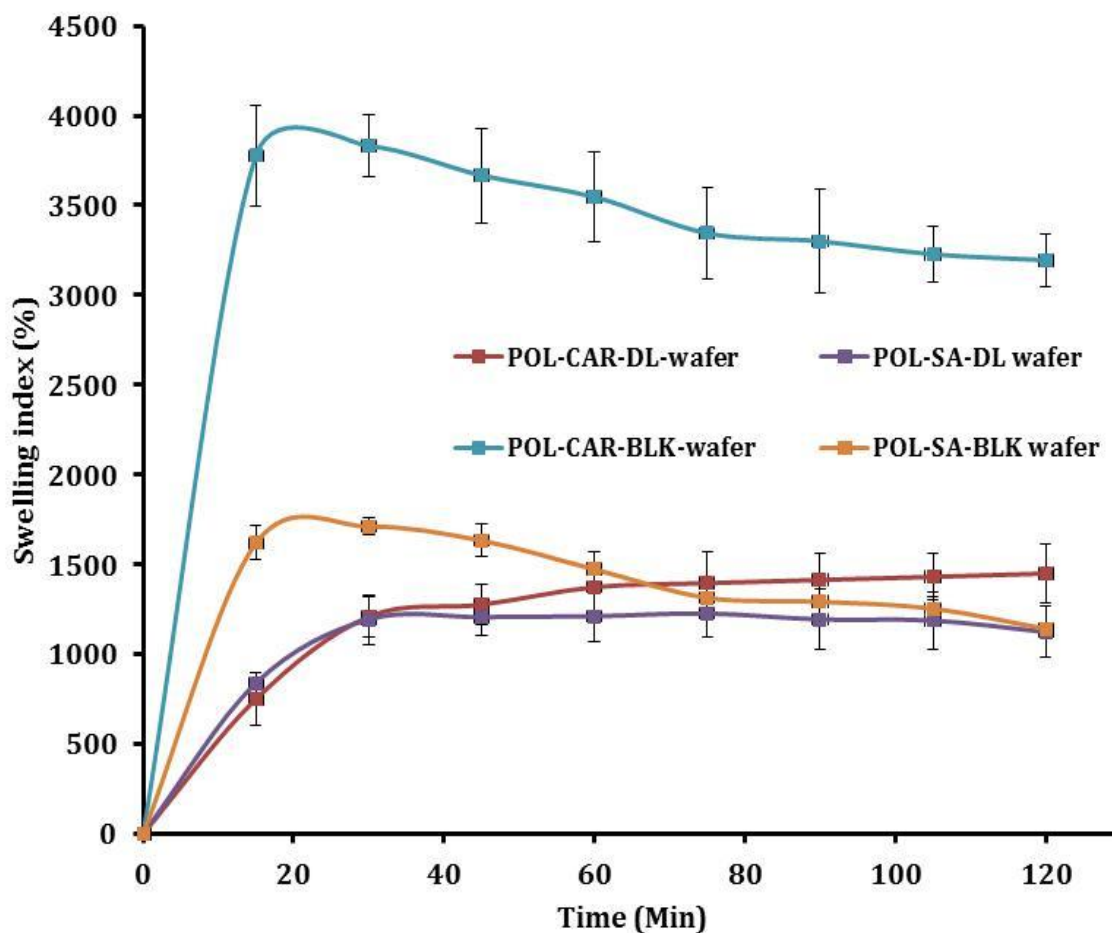


Figure 4.5: Swelling index of POL-CAR and POL-SA wafers in presence of SWF (mean  $\pm$ SD, n=4).

#### 4.3.4 *In vitro* drug dissolution studies

The standard calibration curves for the STP and DLF are shown in figure 4.6 which proves that Beer's law was maintained for both drugs at wavelengths of 195 and 284 respectively (Boateng *et al.*, 2009).

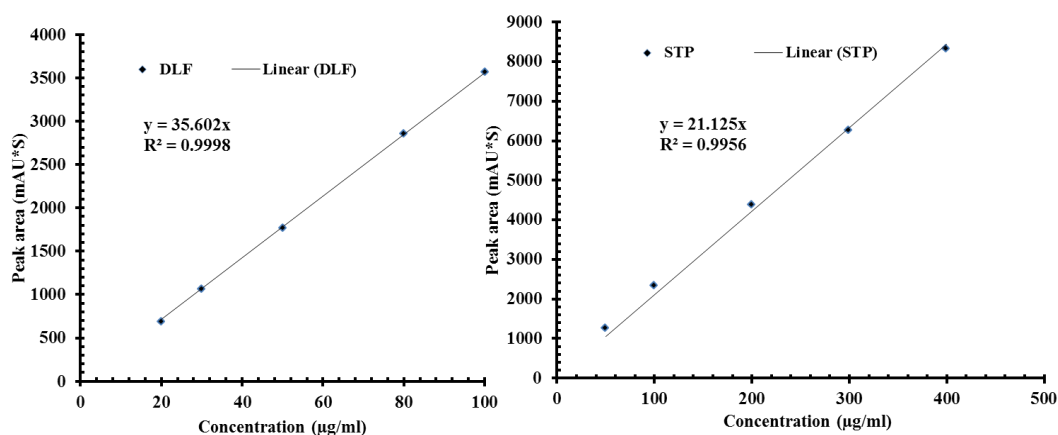


Figure 4.6: Standard HPLC calibration curves for DLF and STP for determining the release of STP and DLF during the drug dissolution study for the films and wafers.

#### 4.3.4.1 Release of STP and DLF from the POL-CAR films in PBS

Drug dissolution profiles for POL-CAR-DL and POL-CAR-DL-20% GLY films (both loaded with 30% w/w STP and 10% w/w DLF) are shown in figure 4.7A and B. POL-CAR-DL films showed lower cumulative drug release within 72 h when compared with POL-CAR-DL-20% GLY films. For the first few hours, drug release from both formulations was similar but was decelerated in the POL-CAR-DL films after 12 h with only  $52.11 \pm 2.38\%$  STP and  $55.26 \pm 4.26\%$  DLF released from POL-CAR-DL films within 72 h. This may be attributed to the possible interaction between the anionic sulphate group of CAR and the primary and secondary amino groups of STP and DLF. Such ionic interactions were absent between POL and CAR due to the neutral (non-ionic) nature of the former polymer. It is therefore possible that this ionic interaction could explain the reason for the absence of the drug related peaks in the XRD/DSC study (apart from the molecular diffusion) discussed previously, however, this will need further investigation. In addition, during drug dissolution studies, the films were hydrated and swelled to form a viscous gel which was not completely dissolved even after the dissolution period. The release from the plasticised (POL-CAR-DL-20% GLY) films was higher ( $60.03 \pm 5.56\%$  STP,  $63.39 \pm 1.92\%$  DLF). The difference between the swelling capacity of the unplasticised and plasticised films (discussed above) resulted in the differences observed between the rate and overall cumulative drug release from the two formulations with the plasticised DL films showing a higher rate of release of the STP and DLF. This may be due to the plasticisation effect of GLY as it has high miscibility with water and allows the opening of channels in the films which

facilitates solvent uptake, leading to enhancement in the drug release from plasticised POLCAR films (Azevedo *et al.*, 2006).

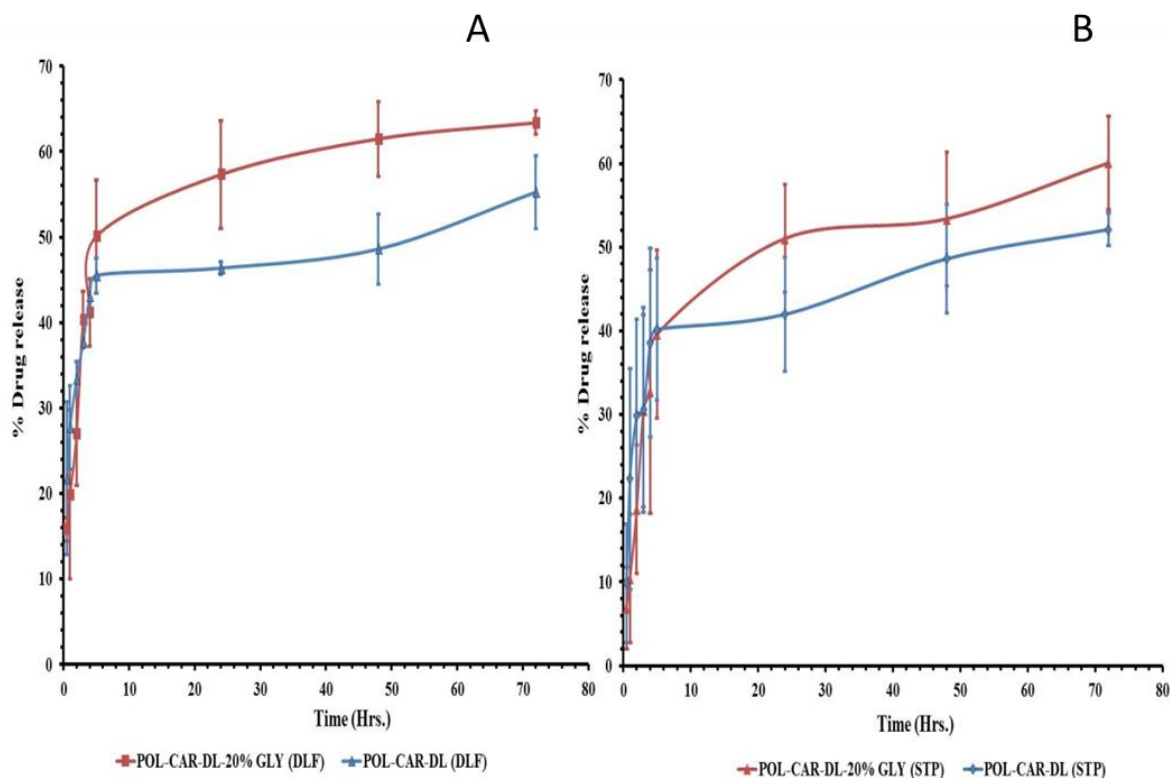


Figure 4.7: *In vitro* drug release profiles of (A) DLF and (B) STP from POL-CAR-DL and POL-CAR-DL-20% GLY films showing mean percent cumulative release (mean  $\pm$ SD, n = 3) against time in presence of phosphate buffer pH 7.3.

These drug release results over a three day period are interesting with regards to the physiology and progress of wound healing. The inflammatory phase starts within a few minutes of injury up to 24 h and lasts for about 3 days. This therefore necessitates effective analgesic delivery within this inflammatory period. The film dressings formulated in this study showed continuous delivery of the anti-inflammatory drug (DLF) for three consecutive days and is also expected to help reduce the bacterial load by the action of the antibiotic (STP) which should help to improve patient's compliance by removing the need for daily change of dressing. However, the frequency of dressing change is affected by the size, type and depth of the wound in addition to the amount and viscosity of wound exudate produced (Boateng *et al.*, 2008). For example, acute wounds produce relatively low quantities of exudate and therefore the film dressings will be able to maintain an ideal moist environment for a longer period and will therefore not need

frequent changing. On the other hand, highly exuding wounds might require more frequent changes (especially for film dressings) to avoid the collection of excessive amounts of exudate underneath the dressing which can cause skin maceration and damage to newly formed tissue.

#### 4.3.4.2 Release of STP and DLF from the POL-CAR films (SWF)

Drug dissolution profiles for POL-CAR-DL and POL-CAR-DL-20%GLY films (both loaded with 30% (w/w) STP and 10% (w/w) DLF) are shown in figure 4.8 A and B. POL-CAR-DL films showed higher cumulative drug release within 72 h when compared with POL-CAR-DL-20%GLY films. For the first few hours, drug release from both formulations was similar but was decelerated in the POL-CAR-DL-20%GLY films after 24 h. The maximum percent cumulative release of STP occurred within 24 h (69.34% for POL-CAR-DL films and 40.56% for POL-CAR-DL-20%GLY). In the case of DLF, the maximum percent cumulative release was achieved after 72 h (60.26% for POL-CAR-DL films and 52.31% for POL-CAR-DL-20%GLY films).

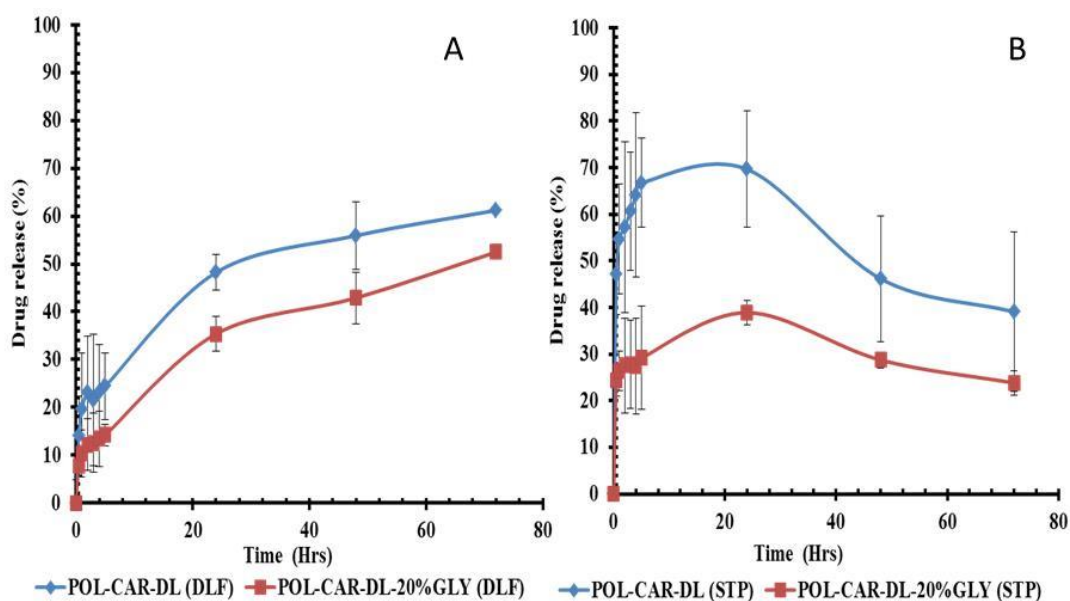


Figure 4.8: *In vitro* drug release profiles of (A) DLF and (B) STP from POL-CAR-DL and POL-CAR-DL-20% GLY films showing plot of mean percent cumulative release ( $n = 3; \pm SD$ ) against time in presence of SWF.

Both formulated film dressings appeared to show better controlled release of DLF than STP and might relate to the relative differences in drug solubilities, swelling or drug-polymer

interactions. It has been suggested that the dissolution media affects the drug release properties as the salts present in SWF has an effect on the dissolution kinetics of the STP and DLF from the films. This seems highly plausible since different drug release characteristics were observed when the dissolution medium (SWF) was replaced with phosphate buffer . The controlled release of DLF from the films may be attributed to the swelling of the polymeric network of the POL and CAR which releases the drug gradually into the dissolution medium. The STP showed burst release which is helpful initially to kill bacteria present in the wound in the first several hours of dressing application. The decrease in STP release after 24 h may be associated with the possible interaction between the primary and secondary amino groups of STP with either SWF or anionic sulphate group of CAR. However, it appears to be enough STP released after 24 h to prevent re-infection. Overall release of the drug in significant amounts is important to ensure that enough is available initially to exert the required antibacterial action and sustained (prolonged) enough to prevent re-colonisation as well as the need for frequent dressing change.

#### **4.3.4.3 Release of STP and DLF from POL-SA films (SWF)**

Drug dissolution profiles for POL-SA-DL and POL-SA-DL-9%GLY films (both loaded with 15% (w/w) STP and 5% (w/w) DLF) are shown in figure 4.9A and B. POL-SA-DL-9%GLY films showed a higher cumulative release of STP within 72 h when compared with the unplasticised POL-SA-DL films. For the first few hours, DLF release from both formulations was similar but was decelerated in the unplasticised POL-SA-DL films after 24 h. The maximum percent cumulative release of STP occurred within 48 h ( $86.25 \pm 6.22\%$  for POL-SA-DL films and  $92.59 \pm 6.10\%$  for POL-SA-DL-9%GLY). In the case of DLF, the maximum percent cumulative release was achieved after 72 h ( $56.27 \pm 1.57\%$  for POL-SA-DL films and  $38.96 \pm 4.79\%$  for POL-SA-DL-9%GLY films). These results indicate that the presence of DLF in the films does not affect the release of STP. DLF was released in a similar manner to STP from the POL-SA DL films (Figure 4.9A and B). The release of DLF was slow from both POL-SA-DL films compared to STP, with around  $56.27 \pm 1.57\%$  and  $38.96 \pm 4.79\%$  of the drug released cumulatively. The result indicated that in POL-SA-DL films and POL-SA-DL-9%GLY films STP was released rapidly in 24 h, with 71-77% of STP released. The release of STP from the films was decreased after 48 h. Release rates of STP and DLF from the POL-SA-DL and POL-SA-DL-9%GLY are found to be time-dependent and can be characterized by an initial, burst release stage in the first 5 h followed by a prolonged, slow release stage thereafter.

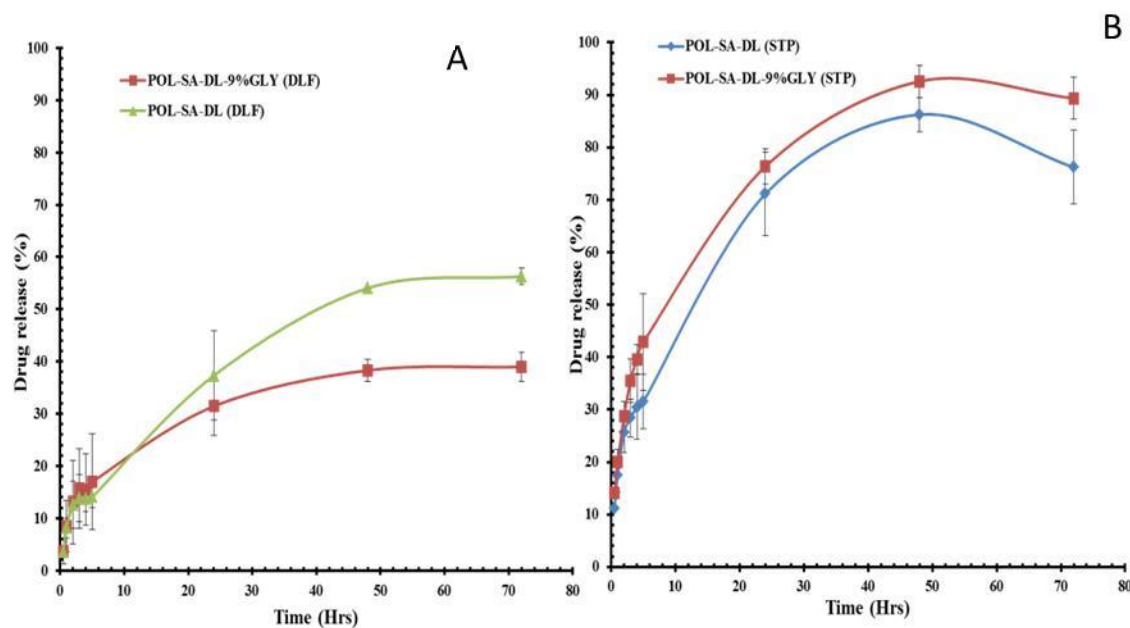


Figure 4.9: *In vitro* drug release profiles of (A) DLF and (B) STP from POL-SA-DL and POL-SA-DL-9% GLY films showing plot of mean percent cumulative release ( $n = 3; \pm SD$ ) against time in presence of SWF.

The rate and extent of drug release are affected by the proportion and grade of polymer (Samani *et al.*, 2003) and polymer hydration characteristics (Salsa *et al.*, 2003), the type and amount of polymer (Williams *et al.*, 2002). Kibria *et al.*, (2008) reported the effect of the plasticizer on the drug release of DLF. It was revealed that release of STP and DLF decreased along with presence of GLY (Figure 4.9A and 4.9B). But a reverse phenomenon was depicted in the case of POL-SA-DL films. This could be due to the different amounts of the drugs (STP and DLF) present in the films and the amount of plasticizer present in both films (POL-CAR and POL-SA). Samani and co-authors reported that the release rate of drug decreases with higher molecular weight of polymer and viscosities. Here POL is a higher molecular weight and has higher viscosity. In POL-CAR, the ratio of POL was higher compared to POL-SA which resulted in differences in the release rate. There could be another reason for the observed differences in the drug release rate between the POL-CAR and POL-SA films and might be related to the difference in the amount of drug added in the films (Samani *et al.*, 2003).

#### 4.3.4.4 Release of STP and DLF from the POL-CAR and POL-SA wafers (SWF)

Figure 4.10 shows the dissolution profiles of STP and DLF from POL-CAR and POL-SA wafers. The drug loading capacities for POL-CAR-DL wafers were  $68.20 \pm 1.07\%$  (STP) and  $90.21 \pm 1.01\%$  (DLF) whilst that for the POL-SA-DL-wafers were  $61.85 \pm 18.4\%$  (STP) and  $93.91 \pm 4.66\%$  (DLF) ( $n = 3$ ). The total cumulative percent of STP released in 72 h from the POL-CAR-DL-wafer and POL-SA-DL-wafers were  $81.37 \pm 3.81\%$  and  $79.59 \pm 4.88\%$ , respectively which was statistically significant ( $p < 0.0189$ ), though both formulations exhibited a sustained (controlled) release of STP. In addition, the rate of release was faster from the POL-CAR-DL-wafers than the POL-SA-DL wafers within the first hour of release attributed to the different ratios of POL, where POL-CAR wafer swelled more quickly and formed a gel that easily hydrated in the SWF during the initial stages of drug dissolution. Bunte *et al.*, (2010) observed that drug release is facilitated by the porous network of lyophilised wafers (Bunte *et al.* 2010). An increased surface area of the dispersed drug in the porous cake occurs, accelerating dissolution significantly. The difference in the drug released through both formulations may also be associated with the varying amount of STP and DLF present which can affect the drug release. As discussed previously in the swelling studies, POL-SA-DL wafers showed less swelling than the POL-CAR-DL-wafers which was also responsible for the slow release of STP. Both wafers showed very slow and constant release of DLF from the formulations. Only 30-33% of DLF was released from both wafers. It has been previously observed that the increase in sodium sulphate largely affected the hydration capacity of the films and this might also be the case for the corresponding wafers.

All the DL Films and wafers showed slow release. It has been previously reported that wafers have quicker hydration and faster release compared to films due to their porous nature (Boateng *et al.*, 2010). In the case of POL-CAR and POL-SA DL films/wafers, the release rates were affected by the presence of sodium sulphate which resulted in the slow release of both drugs (STP and DLF) (Sing *et al.*, 2009).

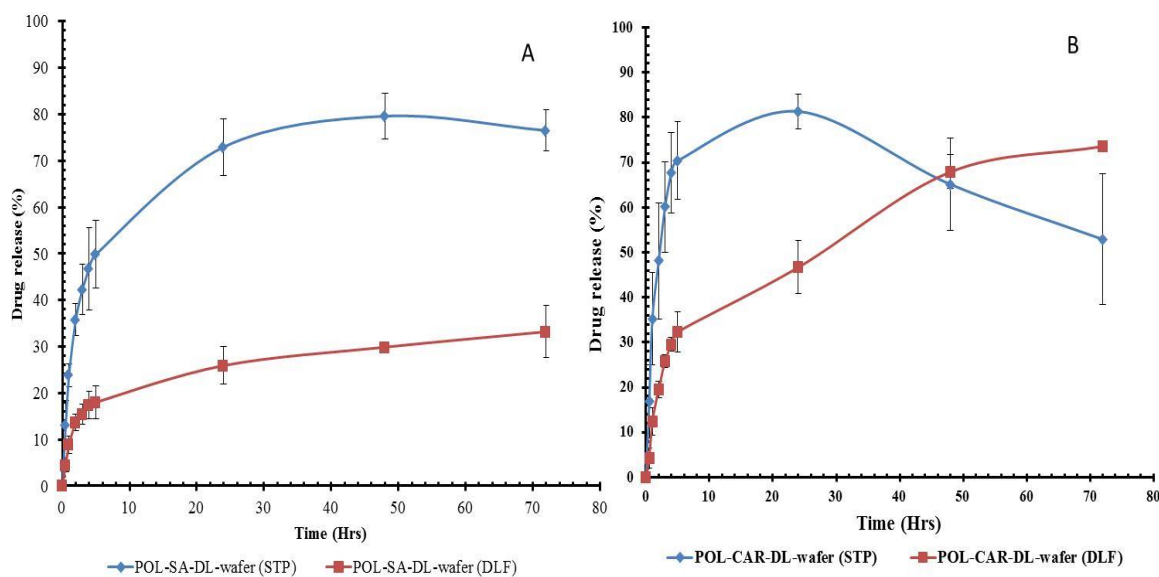


Figure 4.10: *In vitro* drug release profiles of STP and DLF from POL-SA-DL-wafer and POL-CAR-DL-wafer showing plot of mean percent cumulative release ( $n = 3$ ;  $\pm$ SD) against time in presence of SWF.

#### 4.3.5 Kinetic mechanism

Model dependent methods based on mathematical functions were used to describe the dissolution profiles of STP and DLF released from the films and wafers. These included zero order, first order, Higuchi, Hixson-Crowell and Korsmeyer-Peppas models which have been represented respectively by the plots in figure 4.11 (a-e) based on the initial linear portions of the release profiles. Release parameters obtained from fitting experimental dissolution release data to the different kinetic equations have been summarised in Tables 4.2-4.3.

The slope ( $n$ ) values from the Korsmeyer-Peppas equation which characterises the release mechanism of drugs from cylindrical matrices (for wafers) and thin film matrices as described in Table 4.1. Thus, a release exponent ( $n$ ) of 0.5 can serve as an indication for diffusion controlled drug release, assuming film geometry with negligible edge effects, time- and position-independent diffusion coefficients in a non-swellable and insoluble matrix former. In contrast, if polymer swelling is the sole release rate controlling mechanism and in the case of a delivery system with film geometry, zero order drug release kinetics are observed corresponding to a release exponent of  $n = 1$ . Release exponents that are in-between these extreme values for the respective device geometry indicate so-called anomalous or non-Fickian diffusion transport, with

an overlapping of different types of phenomena, potentially including drug diffusion and polymer swelling (Siepmann and Siepmann 2008). The slope (n) values ranged from 0.06 – 0.78 for the STP and 0.31-0.63 for DLF in the films and was in the range of 0.57-0.60 for STP and 0.60-0.84 for DLF in the case of wafers.

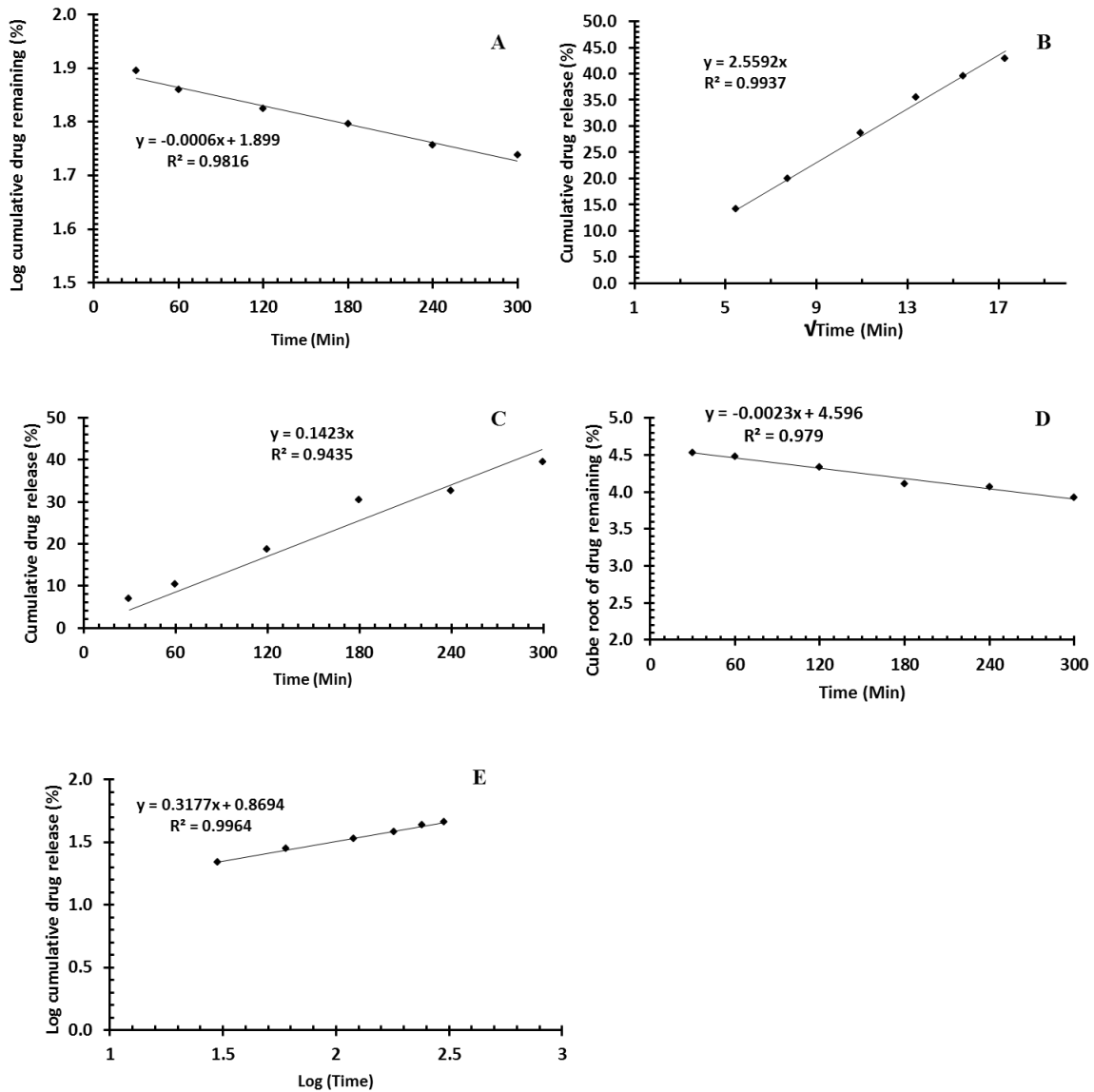


Figure 4.11: Representative plots of experimental release data of films and wafers fitted into different kinetic models, showing (a) first order (b) zero order (c) Higuchi (d) Hixon-Cromwell cube root law and (e) Korsmeyer-Peppas.

The *in-vitro* release profiles of STP from the film and wafers could best be described by Korsmeyer-Peppas equation which showed the highest linearity ( $R^2= 0.90-0.99$ ) compared to the other equations (Table 4.2). This indicates that diffusion was the major driving force for the release of STP from the films and wafers. Drug release from swellable matrices is usually complex and though some processes may be distinctly classified as either diffusion or erosion controlled, drug release is mostly governed by both mechanisms. Analysis of the experimental data using equation, and interpretation of the release exponents (n), provides a better understanding of the mechanisms controlling release. Over all, the release exponents of STP generally varied from 0.5 to 0.8 for all the formulations (except POL-CAR-DL,  $n=0.1$  and POL-CAR-DL-20%GLY films,  $n=0.07$  which is less than 0.5 and indicate that drug follow release mechanism called Fickian diffusion). Release exponents of POL-SA-DL and POL-SA-DL-9%GLY films shows Fickian diffusion process whereas POL-CAR-DL and POL-CAR-DL-20%GLY, POL-CAR-DL-An and POL-SA-DL-An films and wafers show an anomalous (non-Fickian) transport for most of the formulations, suggesting that both diffusion of STP through the hydrated polymer combined with gel erosion controlled drug release.

POL-SA-DL and POL-CAR-DL films showed low linearity ( $R^2=0.86, 0.83$ ) amongst all other formulations and kinetic equations. Both POL-SA-DL-An and POL-CAR-DL-An wafers and POL-SA-DL-9%GLY films showed (anomalous) non-Fickian diffusion process for the release of DLF, whereas all films except POL-SA-DL-9%GLY showed Fickian diffusion process for the release of DLF suggesting that both diffusion of DLF through the hydrated polymer combined with gel erosion controlled the release of DLF.

Table 4.2: Release parameters obtained from fitting experimental drug dissolution (release) data to different kinetic equations for films and wafer containing STP.

Formulation	Zero order		First order		Higuchi		Hixon Crowell		Korsmeyer-Peppas		
	$K_0$	$R^2$	$K_1$	$R^2$	$K_H$	$R^2$	$K_{HC}$	$R^2$	$K_P$	n	$R^2$
					(% min <sup>1/2</sup> )		(% min <sup>-1/3</sup> )		(% min <sup>-n</sup> )		
*POL-CAR-DL	0.16	0.42	0.001	0.90	2.43	0.93	-0.0019	0.89	0.25	0.56	0.91
*POL-CAR-DL-20%GLY	0.14	0.49	0.002	0.98	2.07	0.90	-0.0023	0.98	-0.34	0.79	0.99
POL-CAR-DL	0.29	-14.64	0.002	0.96	4.59	-3.47	-0.0018	0.95	1.47	0.14	0.97
POL-CAR-DL-20%GLY	0.13	-77.75	0.002	0.76	2.09	-26.82	-0.0003	0.76	1.30	0.07	0.88
POL-SA-DL	0.13	0.01	0.001	0.87	2.02	0.99	-0.0013	0.87	0.41	0.46	0.96
POL-SA-DL-9%GLY	0.17	0.47	0.004	0.89	2.56	0.91	-0.0021	0.97	0.43	0.49	0.99
POL-CAR-DL-wafer	0.28	0.58	0.004	0.97	4.26	0.97	-0.0046	0.95	0.40	0.60	0.95
POL-SA-DL-wafer	0.20	0.54	0.001	0.95	3.01	0.97	-0.0027	0.93	0.32	0.57	0.97

$K_0$ ,  $K_1$ ,  $K_H$ ,  $K_{HC}$  and  $K_P$  are the release rate constants for zero order, first order, Higuchi, Hixson-Crowell and Korsmeyer-Peppas models respectively,  $R^2$  is the correlation coefficient and n is the release exponent. \*Drug release parameters obtained from fitting experimental dissolution data (with phosphate buffer as dissolution medium) to different kinetic equations for the POL-CAR films.

Table 4.3: Release parameters obtained from fitting experimental drug dissolution (release) data to different kinetic equations for films and wafers containing DLF.

Formulation	Zero order		First order		Higuchi		Hixon Crowell		Korsmeyer-Peppas		
	$K_0$	$R^2$	$K_1$	$R^2$	$K_H$	$R^2$	$K_{HC}$	$R^2$	$K_P$	n	$R^2$
					(% min <sup>1/2</sup> )		(% min <sup>-1/3</sup> )		(% min <sup>-n</sup> )		
*POL-CAR-DL	0.19	-0.89	0.001	0.98	2.86	0.78	-0.0018	0.97	0.87	0.32	0.99
*POL-CAR-DL-20%GLY	0.19	0.68	0.002	0.97	2.78	0.97	-0.0026	0.98	0.41	0.51	0.97
POL-CAR-DL	0.11	-5.40	0.001	0.87	1.67	-0.64	-0.0005	0.68	0.87	0.21	0.84
POL-CAR-DL-20%GLY	0.06	-3.67	0.0002	0.68	0.95	0.038	-0.0003	0.87	0.56	0.24	0.96
POL-SA-DL	0.06	0.15	0.0004	0.73	0.93	0.83	-0.0006	0.73	0.20	0.58	0.87
POL-SA-DL-9%GLY	0.07	0.46	0.0004	0.83	1.05	0.91	-0.0007	0.83	0.27	0.63	0.91
POL-CAR-DL-wafer	0.12	0.86	0.001	0.96	1.82	0.93	-0.0018	0.95	0.51	0.84	0.95
POL-SA-DL-wafer	0.07	0.51	0.0004	0.88	1.11	0.95	-0.0008	0.88	0.18	0.60	0.95

$K_0$ ,  $K_1$ ,  $K_H$ ,  $K_{HC}$  and  $K_P$  are the release rate constants for zero order, first order, Higuchi, Hixson-Crowell and Korsmeyer-Peppas models respectively,  $R^2$  is the correlation coefficient and n is the release exponent. \*Drug release parameters obtained from fitting experimental dissolution data (with phosphate buffer as dissolution medium) to different kinetic equations for the POL-CAR films.

### 4.3.6 Comparison of release profiles

The similarity factor is a logarithmic reciprocal square root transformation of the sum of squared error and is a measurement of the similarity in the percent dissolution between the two curves. This model independent method is most suitable for dissolution profile comparison when three or more dissolution time points are available (Dash *et al.*, 2006). Release curves are considered similar when the calculated  $f_1$  value (difference factor) is close to 0 and  $f_2$  (similarity factor) is 50–100 respectively (Boateng *et al.*, 2010). The dissolution profiles of the pure drugs (STP and DLF) were used as a reference in calculating the similarity factors ( $f_2$ ) and difference factor ( $f_1$ ) for the films and wafers (as test batch) and are highlighted in parenthesis as ‘Ref’ in Table 4.4. Release of pure drug was chosen as the reference for the dissolution profile comparisons between the various formulations as it is the pre-change formulation and the others are the post-change formulations (test formulations).

Table 4.4: Model independent difference ( $f_1$ ) and similarity ( $f_2$ ) factors for release profiles of STP and DLF and pure drug (STP and DLF) are used as reference batch (Rj).

Formulation	STP		DLF	
	$f_1$	$f_2$	$f_1$	$f_2$
*POL-CAR-DL-20%GLY	56.91	12.48	24.55	35.39
*POL-CAR-DL	56.32	13.55	13.04	40.26
POL-CAR-DL-20%GLY	68.31	17.31	64.59	40.93
POL-CAR-DL	27.33	27.10	39.28	44.67
POL-SA-DL-9%GLY	31.54	12.32	38.04	37.38
POL-SA-DL	49.61	13.47	48.62	42.50
POL-CAR-DL-An	13.42	15.04	222.30	54.00
POL-SA-DL-An	22.62	16.07	18.81	72.34
STP	Ref	Ref	Ref	Ref
DLF	Ref	Ref	Ref	Ref

\*Indicate the similarity factor and difference factor of the POL-CAR-DL-20%GLY and POL-CAR-DL films in phosphate buffer solution of pH 7.3.

The difference factors for all formulations (films and wafers) ranged from 13-68 (Table 4.4) when compared with the reference STP and was far from zero signifying a difference between release profiles. The similarity factor for all the formulations (films and wafers) was less than 50 ( $f_2 = 12 - 27$ ) which confirms that there was no similarity between the reference STP dissolution and films and wafers. The reference DLF, when compared with the films and wafers, showed a difference factor ranging from 18-222 which also confirms the differences in the dissolution of DLF from the films and wafers. Based on the FDA guidelines, the dissolution profiles were found to be different with  $f_2 < 50$ . It has been observed that the films had lower  $f_2$  ( $< 50$ ) whilst the value was greater than 50 for wafers (POL-CAR-DL-An  $f_2=54$ ; POL-SA-DL-An  $f_2=72.34$ ). The result implies that factors such as swelling and hydration were involved apart from the drug solubility which resulted in the differences observed in the  $f_1$  and  $f_2$  values. The sodium sulphate formed in the films and wafers could also be a contributory factor which resulted in the differences in the  $f_1$  and  $f_2$  values as seen from the results of the films and wafer swelling study.

#### **4.4 Conclusions**

Films containing plasticizer had higher swelling capacity as compared to non-plasticised films due to the effect of the GLY which allowed a higher rate of water ingress and hence the enhanced water absorption. BLK films and wafers showed high swelling index compared to DL films and wafers due to the formation of sodium sulphate which affected their swelling capacity. These films and wafers have capacity to absorb wound exudate while still maintaining their physical integrity for a reasonable time period. This could potentially help to overcome the challenge of collection of excess exudate when applied to a moderate to highly exuding wound (Boateng *et al.*, 2008). During the first hours after wounding, a relatively high drug release is essential to eliminate infections present at acute wounds that may not have been eliminated during wound cleansing and might create a resistant biofilm whereas chronic wounds are usually associated with the presence of bacteria which is the main cause of the delayed healing and burst release of these drug will help to reduce the infection caused by resistance microorganisms such as *S. aureus*, *P. aeruginosa* and *E. coli* and the biofilms formed from these microorganisms and progress wound healing more rapidly. The subsequent sustained release can help to maintain a bacteria free wound for more than 3 days which usually depends upon the wound exudate.

Release of DLF can help to reduce the pain and swelling associated with the wound during the inflammatory phase.

## CHAPTER 5: *IN VITRO* MUCOADHESION STUDIES OF SOLVENT CAST FILMS AND FREEZE DRIED WAFERS USING TA AND ATR-FTIR

### 5.1 Introduction

The development of prolonged and/or controlled release mucosal formulations (including wound dressings) has often utilized bioadhesive polymers which can adhere to the cellular secretions, mucus, extracellular matrix, cells or tissues in the presence of water or wound exudate (Saiano *et al.*, 2002). Several approaches including the use of mucoadhesive tablets (Llabot *et al.*, 2002), films (Sigh and Pal, 2012) and wafers (Boateng *et al.*, 2010; Ayensu *et al.*, 2012) have been explored as conventional mucoadhesive dosage forms for controlled drug delivery. It has been suggested that the interaction between the mucosal surface and mucoadhesive polymers is a result of physical entanglement and secondary interactive forces, mainly due to hydrogen bonding and van der Waals attraction forces which depend upon the chemical structure of the polymer (Thirawong *et al.*, 2007). Peppas and Buri (1985) proposed certain characteristics which are necessary for effective mucoadhesion. These include polymers containing strong H-bonding groups, strong anionic charges, high molecular weight, sufficient chain flexibility, and surface energy properties which favour spreading of the polymer onto the mucosal surface (Peppas and Buri 1985). For the purpose of wound dressings, mucoadhesive properties of the polymers could be affected by degree of hydration, amount of exudate released from wounds, exudate viscosity, salts and proteins which are present in exudate, presence of microorganisms, depth and area of the wound.

There are different approaches used to evaluate the mucoadhesive performance of polymers and polymeric dosage forms. These include texture analyser, (Thirawong *et al.*, 2007; Ayensu *et al.*, 2012; Boateng *et al.*, 2013; Smart, 2005), rheometric measurements (Tamburic and Craig, 1997) and attenuated total reflection-Fourier transform infrared spectroscopy (ATR-FTIR) (Saiano *et al.*, 2002; Jabbari *et al.*, 1993) methods. The texture analyser (TA) technique measures the maximum force required to separate the polymer or dosage form from the surface of a mucosal substrate after a specified contact time and applied force. This method evaluates stickiness, work of adhesion (WOA) and cohesiveness of dosage forms. Stickiness is the maximum force required to separate the probe attached to films and wafers from the SWF or mucin equilibrated with gelatine substrate (i.e. maximum detachment force) whereas, total amount of work or energy involved in the probe withdrawal from the substrate is calculated from

the area under the forces versus distance curve and cohesiveness is the intermolecular attraction between the substrate and formulations and determined by the travel distance in mm on the force versus distance profile (Thirawong *et al.*, 2007). The rheometric method involves studying the extent of interpenetration of mucin (or moisture) with polymeric gels by measuring differences in the rheological parameters of polymeric gel and their mixture with mucin (Tamburic and Craig, 1997). The attenuated total reflection-Fourier transform infrared spectroscopy (ATR-FTIR) approach involves the study of chain interpenetration or diffusion occurring between polymers or dosage forms (e.g. films and wafers) and mucosal fluid such as mucin solution (Saiano *et al.*, 2002; Jabbari *et al.*, 1993) or SWF (Boateng *et al.*, 2013).

In this chapter, we report on the mucoadhesion studies of the different formulations (films and wafers) as shown in table 5.1 using texture analyser and ATR-FTIR. Initially, the mucoadhesive performance of the films and wafers was assessed in an *in vitro* environment using a texture analyser to measure the stickiness, WOA and cohesiveness. The effect of viscosity of SWF [SWF (2% w/w BSA or 5% w/w BSA)] on the films and wafers containing polymers, drugs [(STP) and (DLF)] and GLY (for films) was determined. Mucoadhesion properties of all formulations were further evaluated using ATR-FTIR spectroscopy with model protein mucin (2% w/w mucin solution in phosphate buffer solution (PBS) pH 7.4) and compared the diffusion of mucin through the formulations to establish proof of concept for measuring mucin interaction and its diffusion through the films and wafers.

## **5.2. Materials**

Bovine serum albumin (BSA), mucin from porcine stomach type three (bound sialic acid 0.5-1.5%), phosphate buffered saline tablet (one tablet dissolved in 200 mL of deionized water yields 0.01 M phosphate buffer, 0.0027 M potassium chloride and 0.137 M sodium chloride, pH 7.4, at 25°C) were all purchased from Sigma Aldrich, (Gillingham, UK). Glycerol (GLY), tris(hydroxymethyl)aminomethane, calcium chloride dihydrate, gelatine, were all purchased from Fisher Scientific (Leicestershire, UK).

Table 5.1: Optimised formulations used for the *in vitro* mucoadhesion study

	Formulation
1	POL-CAR-BLK-film
2	POL-CAR-DL-film
3	POL-CAR-BLK-20%GLY-film
4	POL-CAR-DL-20%GLY-film
5	POL-SA-BLK-film
6	POL-SA-DL-film
7	POL-SA-BLK-9%GLY-film
8	POL-SA-DL-9%GLY-film
9	POL-SA-BLK-wafer
10	POL-CAR-BLK-wafer
11	POL-SA-DL-wafer
12	POL-CAR-DL-wafer

### 5.3 Methods

#### 5.3.1 Mucoadhesion studies by TA [SWF (2% and 5%w/w BSA) and 2%w/w mucin]

Adhesive measurements were performed on the different films and wafers (Table 5.1) containing different polymers, drugs and/or plasticizer (films) using a TA.HD *plus* Texture Analyser (Stable Micro Systems, Surrey, UK) fitted with a 5 kg load cell. The films and wafers ( $n = 4$ ) were attached to an adhesive probe (75 mm diameter) using double sided adhesive tape. For this purpose, gelatin was used as the mucosal substrate. Gelatin solution at a concentration of 6.67% w/v was prepared by heating distilled water to 60°C in a beaker and adding the powdered gelatin with mechanical stirring until completely dissolved (Matthew *et al.*, 2006). The gelatin solutions were poured into Petri plates and kept in a fridge to solidify. The surface of the gelatin gel in a Petri dish (86 mm diameter), was equilibrated with 0.5 ml of SWF containing 2% BSA or 5% BSA, 0.02 M calcium chloride, 0.4 M sodium chloride, 0.08 M tris(hydroxymethyl)aminomethane in deionised water, pH 7.5, (Lindsay *et al.*, 2010) to mimic a wound surface and also with 2% mucin (model protein) in PBS of pH 7.4. The probe, lined with film or wafer was set to approach the model wound surface with the following pre-set conditions: pre-test speed 0.5 mm/s; test speed 0.5 mm/s; post-test speed 1.0 mm/s; applied force

1 N; contact time 60.0 s; trigger type auto; trigger force 0.05 N and return distance of 10.0 mm. The adhesive strength (stickiness), total work of adhesion (WOA) and cohesiveness were calculated using the *Texture Exponent 32*<sup>®</sup> software.

### 5.3.2 Mucoadhesion studies by ATR-FTIR (2% w/w mucin).

FTIR spectrometer (Thermonicolet, USA) with an ATR accessory (Smart arc), with a cover to prevent spillage of mucin solution, was used for the diffusion studies in the settings shown in table 5.2. As shown in figure 5.1, the IR beam enters into the film or wafer to a small fixed depth and be specifically attenuated according to the molecules present in this region. The ATR crystal was ZnSe 50 mm long, 10 mm wide and 2 mm thick. All formulations shown in table 5.1 were placed on the crystal and were monitored with 500  $\mu$ l of 2% mucin solution (PBS 7.4). The wavenumber range was 4000-650 $\text{cm}^{-1}$  and the spectra were collected every 9 sec with an average of 16 scans and resolution of 4  $\text{cm}^{-1}$ . The spectrometer was linked to a computer equipped with *Omnic*<sup>®</sup> software which allows continuous automated collection of full spectra kinetically as a function of time. Data collected was analysed using *InSight*<sup>®</sup> software (InSight 2009, DiKnow Ltd UK) based on chemometric multivariate data deconvolution to monitor the diffusion of mucin solution through the films and wafers. This experimental set up is similar to that published previously (Saiano *et al.*, 2002).

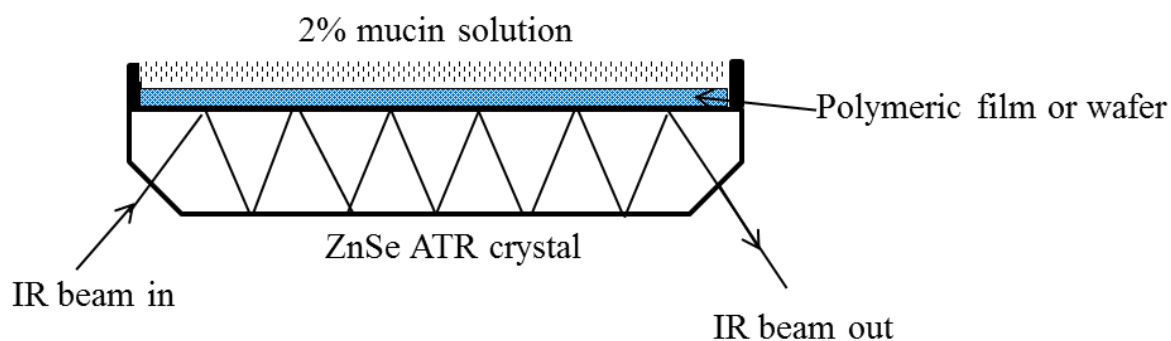


Figure 5.1: ATR assembly for in situ measurement of inter-diffusion of mucin solution through the films and wafers.

### 5.3.3 Chemometric analysis

Chemometric data analysis was used to deconvolute the possible overlapping spectral profiles of the optimised formulations (films and wafers) using 2% mucin solution. Chemometrics may be defined as the science of extracting information from chemical systems by data-driven means using methods frequently employed in core data-analytic disciplines such

as multivariate statistics, applied mathematics, and computer science, in order to address problems in chemistry, biochemistry, medicine, biology and chemical engineering. One chemometric analytical technique, amongst a host of others used in this study, is multivariate target factor analysis (TFA).

Table 5.2: Settings used for mucin diffusion through films and wafers.

<b>Spectrometer description</b>		<b>Data collection information</b>	
Spectrometer:	Nexus	Number of sample scans	16
Source:	IR	Sampling interval	6.33
Detector:	MCT/A	Resolution	4
Beamsplitter:	KBr	Levels of zero filling	0
Sample spacing:	2	Number of scan points	8480
Digitizer bits:	20	Number of FFT points	8192
Mirror velocity:	1.8988	Laser frequency	15798.3 cm <sup>-1</sup>
Aperture:	12	Interferogram peak position	4096
Sample gain:	8	Apodization	Happ-Genzel
High pass filter:	200	Number of background scans	16
Low pass filter:	20000	Background gain:	8
<b>Data description</b>		<b>Series description</b>	
Number of points:	1738	Minimum value:	0.11
X-axis:	Wavenumbers (cm <sup>-1</sup> )	Maximum value:	12.11
Y-axis:	Absorbance	Step size:	0.17
First X value	649.904	Number of spectra:	71
Last X value:	3999.7058	Gram-Schmidt offset:	10
Data spacing:	1.928498	Gram-Schmidt interferogram points:	100
<b>Data processing history</b>			
Data collection type:	Kinetics		
Total collection time:	12.11		
Final format:	Absorbance		
Resolution:	4.000 from 650 to 4000		

Multivariate TFA approach was used to deconvolute the spectral profiles of the mucin solution together with the wafer (or film) formulations in the wavenumber range 1400-1700 cm<sup>-1</sup>. This method is based on the numerical decomposition of a data matrix using the technique of principal component analysis (or factor analysis). TFA is a multivariate curve resolution (MCR) technique. This technique enables the deconvolution of diffusion profiles of a targeted factor (mucin) in a complex data matrix without prior information on other overlapping unknown factors. This technique has been previously applied for the diffusion of solvents through membranes such as skin has been published (McAuley *et al.*, 2009 and Dias *et al.*, 2004). Using a similar ATR-FTIR spectroscopic setup, the diffusion of 2% w/w mucin in PBS was kinetically monitored through the films and wafers listed in Table 5.1. The relative rate of diffusion was then deduced from the data generated after subjecting the data to the TFA process in the *InSight*<sup>®</sup> software (InSight 2009, DiKnow Ltd UK). An overview of the target factor analysis (TFA) technique is presented below

### 5.3.3.1 Overview of target factor analysis (TFA)

The chemometric TFA process involved; (1) subjecting the multivariate data generated to factor analysis, (2) determining the number of significant factors suitable for modelling the data (3) using known spectral targets in combination with the identified significant factors in both spectral and time domain to aid the target component identification and deconvolution of its diffusion profiles. A schematic representation of the data analysis process is shown in figure 5.2 and a summary of the theory is also provided below.

Figure 5.2 shows the systematic steps involved in the TFA. Figure 5.2 (1) is the complex data matrix (**D**) of an ATR-FTIR spectral profile of the diffusion of mucin through the different formulations consisting of the rows (**R**) and columns (**C**) and can be represented by the equation 5.1 below.

$$D = RC \qquad \text{Equation 5.1}$$

Where **D** is the data matrix generated in box 1 [see Figure 5.2 (1)]. **R** contains all the factors in the row dimension of **D** and **C** contains all the factors in the column dimension of **D**. As shown in figure 5.2 (2), chemometric factor analysis decomposes the data matrix into the product of an abstract row matrix **R** and an abstract column matrix **C** to obtain the significant factors which are mainly involved in the data matrix. Each **R** and **C** yield the number of factors

which can be further divided into primary sets of the true factors which account for the real, measurable features of the data and secondary sets also called as null set which is associated entirely with the experimental error or noise. The row and column abstract factors are not recognised as physical or chemical parameters, therefore target reference spectra ( $R_t$ ) was used to confirm the presence of the expected components [see figure 5.2 (4)]. Target transformation is a process that allows searching for basic factors individually in complex data space. Equation 5.2 shows a target transformation process in spectral space.

$$\underline{R}^+ \cdot R_t = T \quad \text{Equation 5.2}$$

T is the so called target transformation matrix (coefficients) obtained by a least squares process in equation 5.2.  $\underline{R}^+$  is the generalised inverse of  $\underline{R}$  and  $R_t$  is target reference spectra spanning the rows of D. A least squares procedure is employed to generate a transformation factor that will yield predicted spectrum  $R_p$  most closely matching to target reference spectra (see figure 5.2 box 6). Equations 5.3 and 5.4 show the transformations to  $R_p$  and  $C_p$  respectively.

$$\underline{R} \cdot T = R_p \quad \text{Equation 5.3}$$

$$T^+ \cdot \underline{C} = C_p \quad \text{Equation 5.4}$$

Where  $\underline{R}$  and  $\underline{C}$  are the significant factors in the row and column dimensions of D;  $T^+$  is the generalised inverse of T;  $R_p$  is the newly predicted spectra and  $C_p$  is the predicted intensity or concentration (diffusion) of  $R_p$ . The least square process minimises the deviation between the test vector and predicted vector producing the best possible transformation for the individual target test being considered.

A typical data analysis using 2% mucin on POL-CAR-BLK in the wavenumber window 1400-1700 $\text{cm}^{-1}$ , with a spectral correlation minimum limit of 0.8, is shown below. Figures 5.3a and 5.3b show a typical data set obtained from the ATR-FTIR setup equivalent to data matrix D in the schematic figure 5.2 (1). The data is subjected to chemometric factor analysis to obtain the significant factors in row domain  $\underline{R}$  and corresponding column domain  $\underline{C}$  as shown in 5.2 (2). These significant factors for the diffusion of 2% mucin through POL-CAR-BLK film are shown in figure 5.3 c, d and e. The significant factors were estimated using various methods such as factor indicator function (IND, Figure 5.3c), the percentage significant level (%SL, Figure 5.3d) and the cumulative percentage variance (CPV, Figure 5.3e) to determine true factor space. Detailed background on the determination of the significant factors is described elsewhere (Malinowski, 1991).

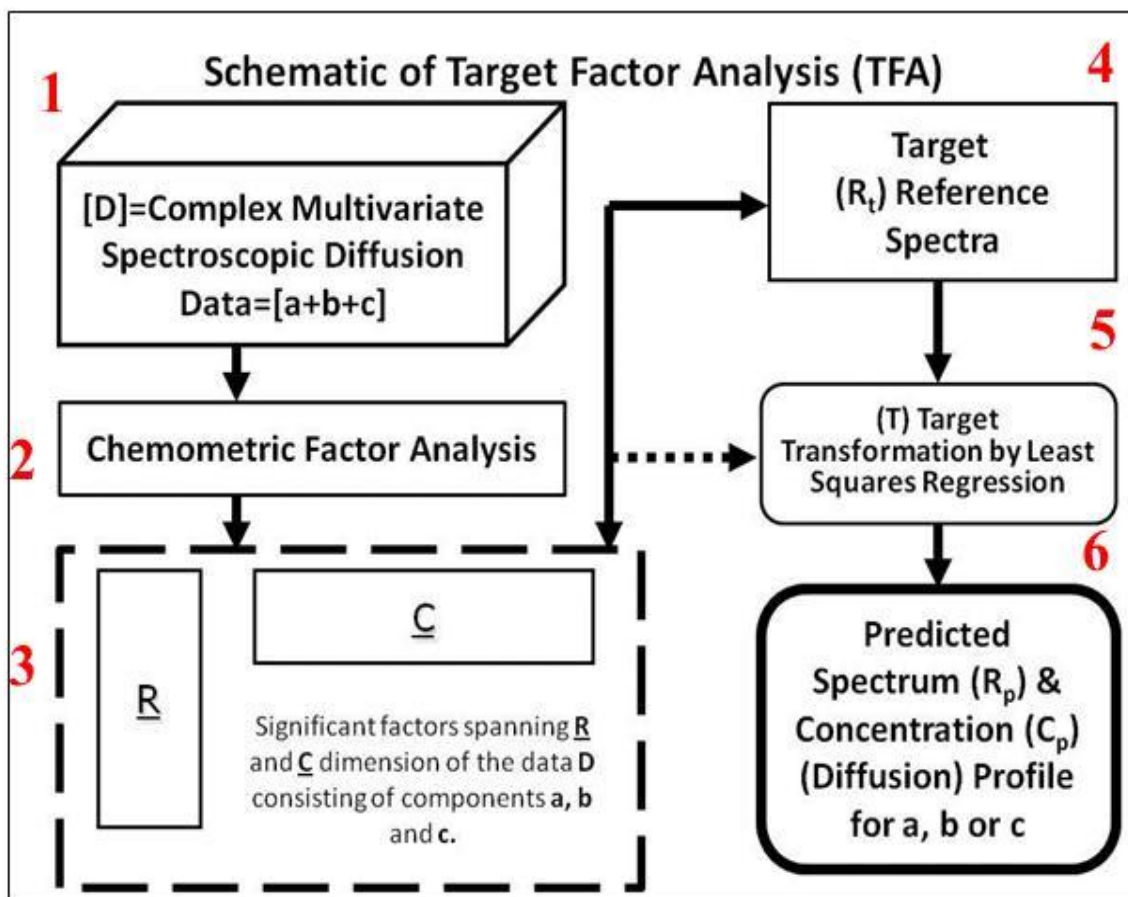


Figure 5.2: Schematic layout of the target factor analysis process: (1) complex data matrix ( $D$ ); (2) chemometric factor analysis; (3) significant factors affecting data matrix; (4) target reference spectra ( $R_t$ ) used in combination with the  $\underline{R}$  and  $\underline{C}$ ; (5) target transformation through least square regression; (6) predicted spectrum ( $R_p$ ) and concentration profile ( $C_p$ ).

A typical output of this data for row domain  $\underline{R}$  is shown in Figure 5.4 and the corresponding column domain  $\underline{C}$  is also shown in Figure 5.5 where only three factors (marked 1, 2 and 3) were identified as significant. The rest of the factors were non-significant as they have no structure in both spectral and concentration domains. An example of the target reference spectra in figure 5.2 (4) ( $R_t$ ) is shown in figure 5.6 where dotted line is  $R_t$  and solid line is predicted spectrum ( $R_p$ ) after least square fitting based on the generalised inverse operation after obtaining the transformation matrix  $T$  in figure 5.2 (6) (see equation 5.2). Figure 5.7 shows the deconvoluted diffusion output of the 2% mucin through the POL-CAR-BLK film and other factors within the same spectra window used for the analysis. It is clear that besides mucin (e.g a in figure 5.2 box 6), two other factors (e.g. b and c in figure 5.2 box 6) also contributed to the diffusion process. These hidden profiles would be very difficult to know without the use of

multivariate target factor analysis. The diffusion profile obtained in figure 5.7 (b) enabled the relative diffusion coefficient to be calculated by determining the slope of the curve before the film or wafer was saturated (i.e. before the plateau of the curve).

The process described above was used to analyse all other formulations to deduce the diffusion profiles for the mucin and thus enable direct comparison of the relative rate of diffusion between the different formulations by normalisation of data.

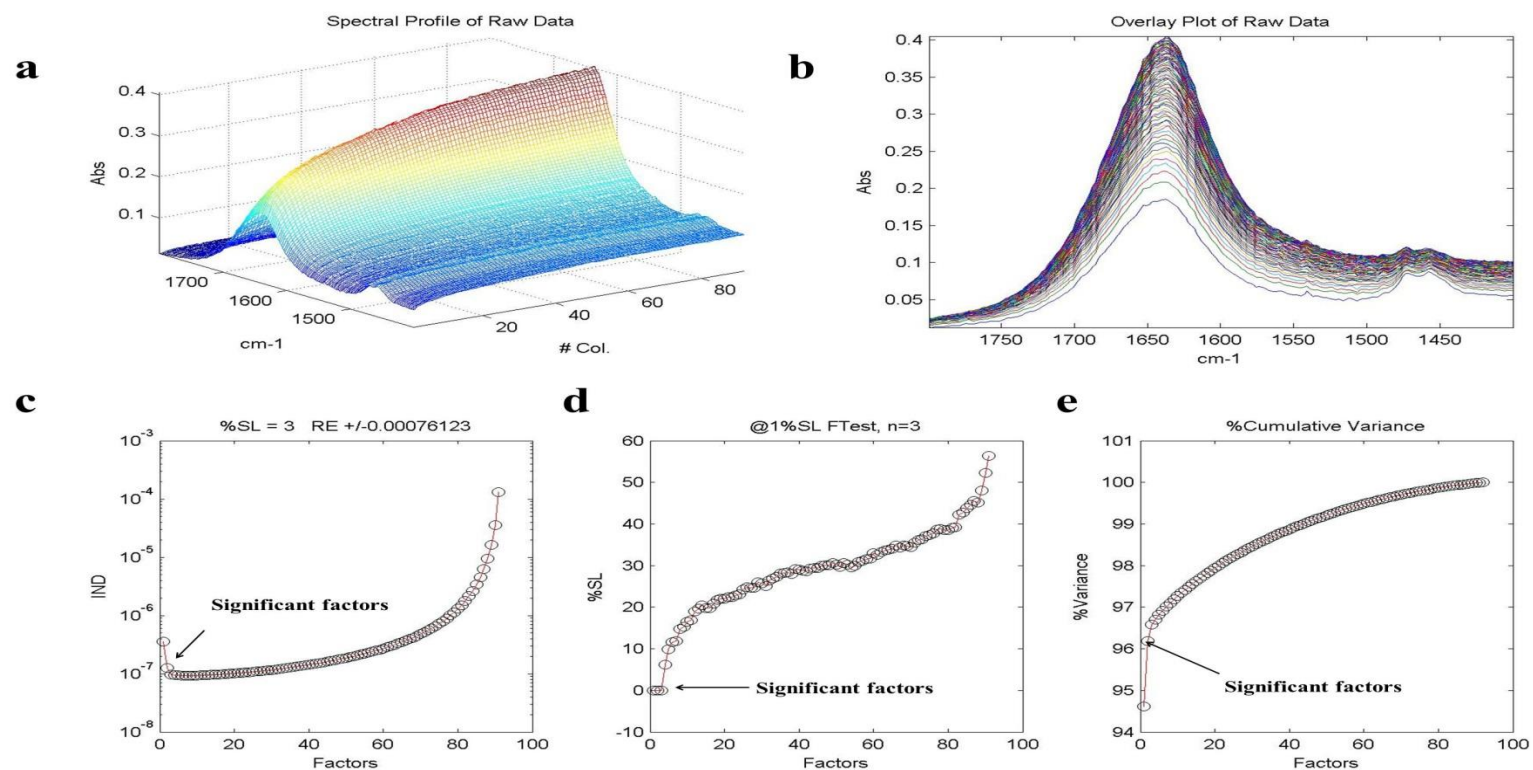


Figure 5.3: (a) shows a typical ATR-FTIR 3D spectral profile for the selected window 1400-1700  $\text{cm}^{-1}$  (b) overlay plot of raw ATR-FTIR spectral profile (c) significant factor calculated using factor indicator function (IND) (d) percentage significant level (%SL) plotted against the number of factors (e) cumulative percentage variance (CPV) accounted for the abstract factor reproduction. The arrow indicates the cutoff point for the selection of number of significant factors.

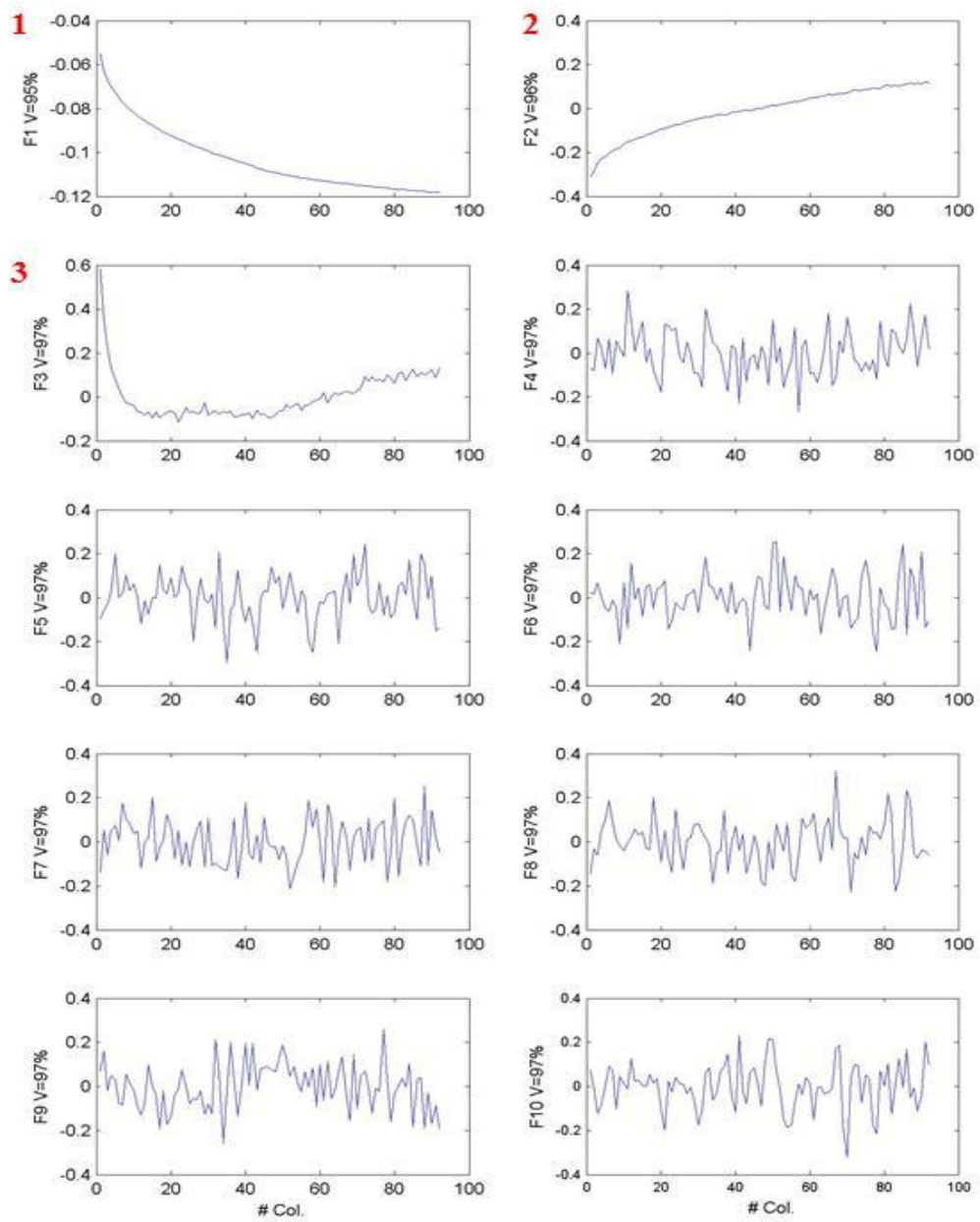


Figure 5.4: Ten abstract factors of the row domain  $\underline{R}$  (spectral profiles) from that only 1, 2 and 3 are significant whereas rest of the factors are experimental noise.

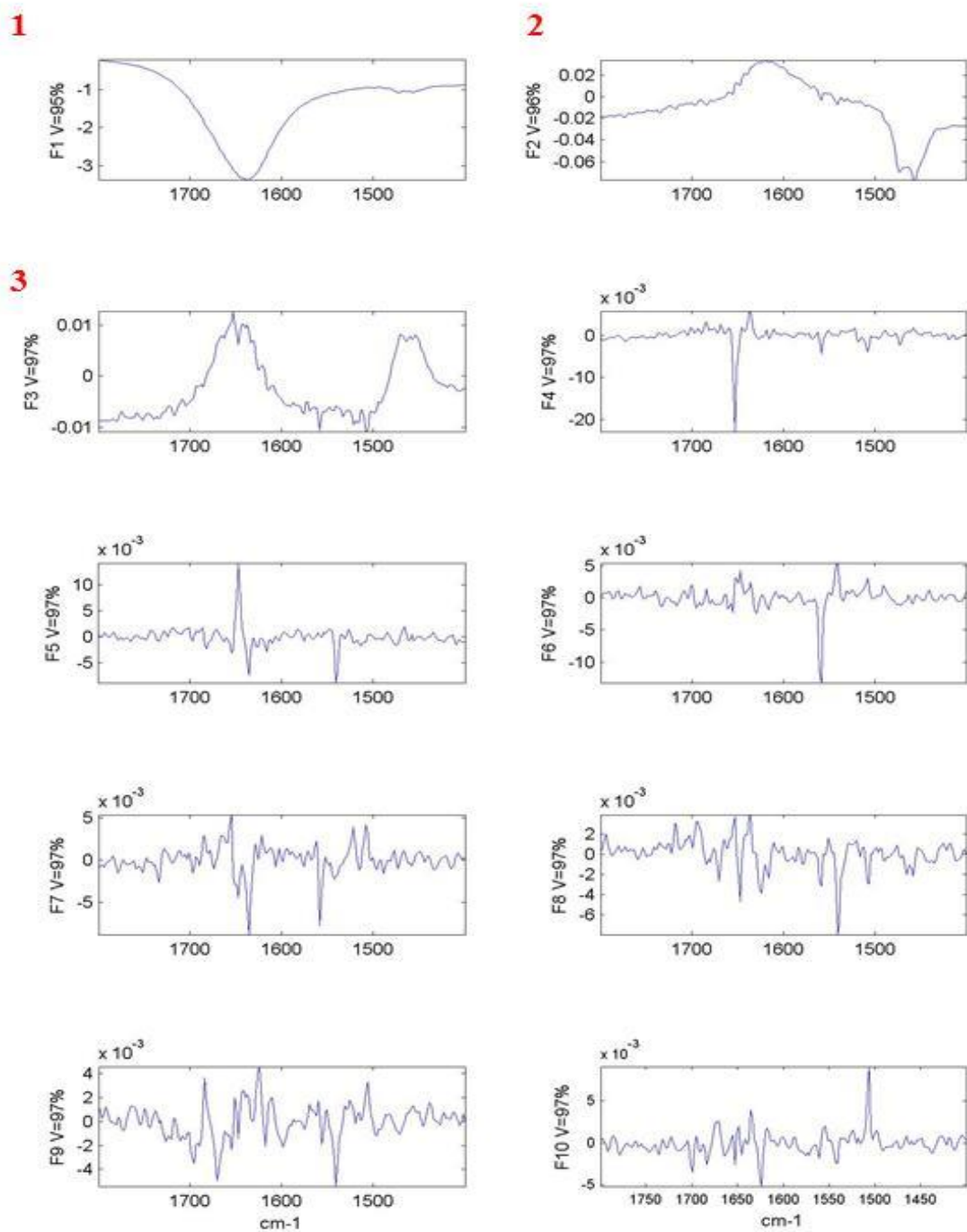


Figure 5.5: Visual inspection of ten abstract factors corresponding column domain  $\underline{C}$  from that only 1, 2 and 3 are significant whereas rest of the factors are experimental noise.

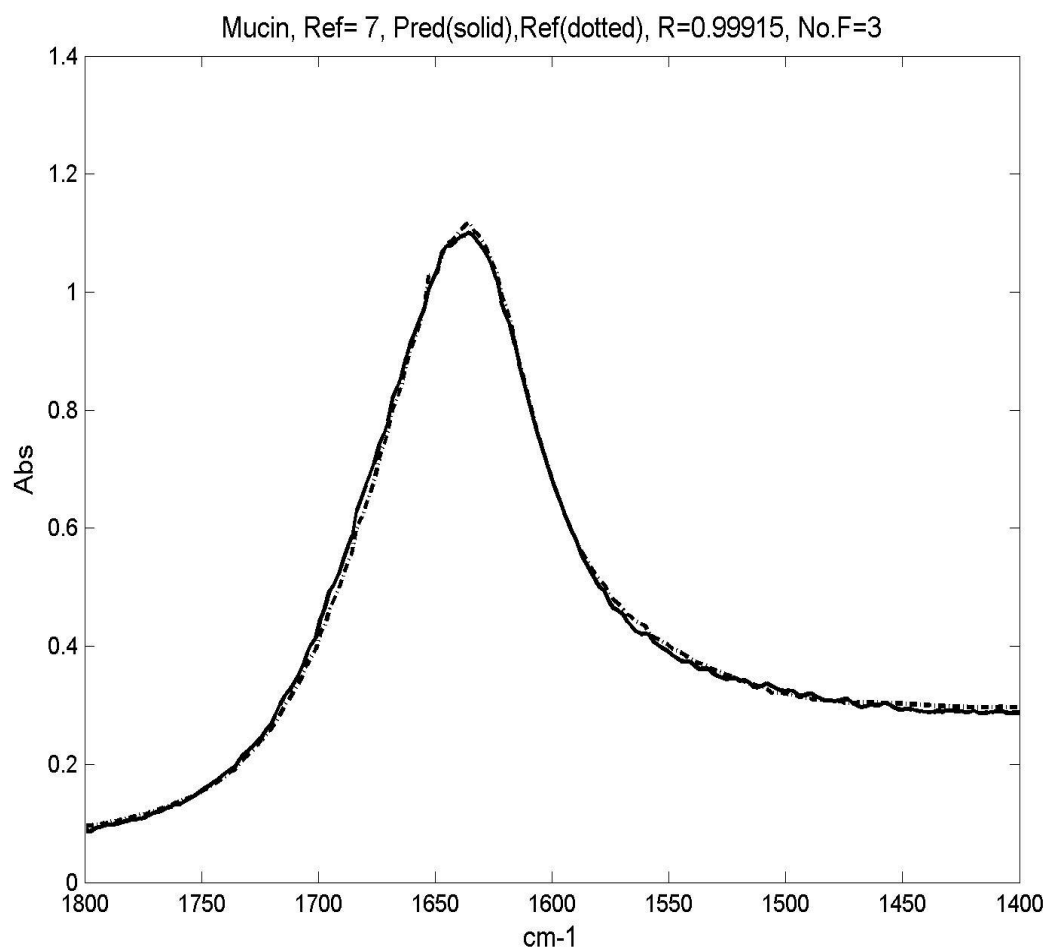


Figure 5.6: An example of a match between the reference spectra of mucin (black dotted line) and the predicted spectral profiles of the targets (black solid line) with correlation coefficient of  $R=0.99915$  of diffusion of mucin across the formulation.

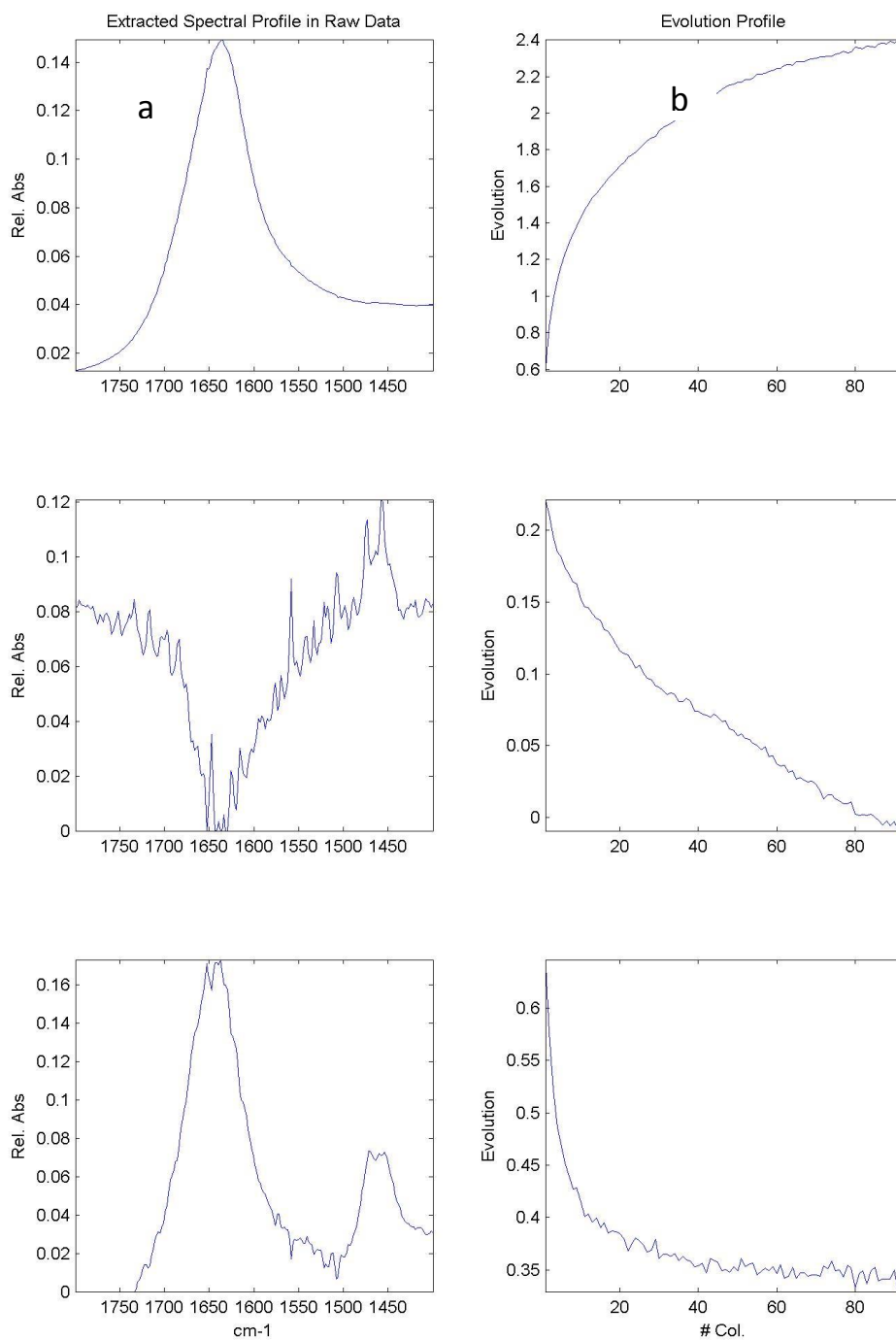


Figure 5.7: The deconvoluted diffusion output of the 2% mucin and other factors within the spectrum window 1400-1700cm<sup>-1</sup> used for the analysis.

## 5.4 Results and discussion

### 5.4.1 Mucoadhesion studies by TA [SWF (2% and 5%w/w BSA)]

Gelatin is a biopolymer that is readily obtained by controlled hydrolysis of collagens, which are the most abundant structural fibrous insoluble proteins found in skin, tendons, cartilages, bones, and connective tissues. Its composition and biological properties are almost identical to its precursors and can mimic a wound surface in the presence of SWF (Rattanuengsrikul *et al.*, 2009). A force of 1 N was applied due to the concern of newly formed tissue which may be interrupted or damaged if high forces were applied.

#### 5.4.1.1 Unplasticised films

Figure 5.8 and 5.9 shows the effect of viscosity of SWF (2% w/w and 5% w/w BSA) on the mucoadhesive performance of the films. Both POL and CAR have strong hydrogen bonding groups while POL has sufficient chain flexibility and high molecular weight and viscosity which helps to improve the mucoadhesive performance of the prepared formulation (Boyapally *et al.*, 2010).

Figure 5.8 shows the stickiness, WOA and cohesiveness of POL-CAR and POL-SA films upon being detached from the model wound surface (gelatin equilibrated with SWF containing 2% BSA). When there is an intimate contact between the formulation and SWF, polymers diffuse across the interface as a function of time. Mucoadhesion is mainly dependent upon the extent of diffusion and interfacial thickness between the two surfaces. POL-SA-BLK films showed a high force of detachment ( $1.9 \pm 0.4\text{N}$ ) and WOA ( $1.1 \pm 0.7\text{N}\cdot\text{mm}$ ) compared to POL-CAR-BLK ( $0.6 \pm 0.1\text{N}$ ), ( $0.4 \pm 0.1\text{N}\cdot\text{mm}$ ) films. The observed cohesiveness for both films was similar (POL-CAR-BLK  $1.2 \pm 0.1\text{mm}$ , POL-SA-BLK  $1.3 \pm 0.2\text{mm}$ ). With reference to mucoadhesion theories, various polymeric structures and functional groupings could have an effect on the degree of polymer-mucosal membrane interactions (Smart, 2005). It is well accepted that mucoadhesive polymers such as POL, SA and CAR possess hydrophilic functional groups which are responsible for increased mucoadhesive performance of their formulations (Lefnaoui and Moulai-Mostefa, 2011).

In the presence of viscous SWF (5%w/w BSA), POL-CAR-BLK films showed higher values for stickiness ( $2.5 \pm 0.7\text{N}$ ), WOA ( $1.5 \pm 0.5\text{N}\cdot\text{mm}$ ) which were decreased for POL-SA-BLK

films ( $1.7\pm 0.7\text{N}$  and  $1.1\pm 0.5\text{N}\cdot\text{mm}$  respectively). This may be associated with the fact that the increased viscosity of BSA forms a gel like structure and helps more intimate contact with the substrate and therefore requires a stronger force to detach the POL-CAR-BLK films. In the presence of SWF (5%w/w BSA) CAR gets hydrated to form a gel and is responsible for increased mucoadhesive performance. The increased intra-molecular attraction of the concentrated SWF (5%w/w BSA) solution and the formation of internal cross-linkages on the gelatin surface might limit solvent diffusion into the polymeric matrix which results in decreased mucoadhesion for the POL-SA-BLK film. There was no significant difference ( $p=0.75$ ) in the cohesiveness of POL-CAR-BLK ( $2.6\pm 0.5\text{mm}$ ) and POL-SA-BLK films ( $2.5\pm 1.1\text{mm}$ ).

The structural polymeric components significantly influence the extent of diffusion, entanglement and ultimately bioadhesion. Using polyelectrolyte polymers such as CAR and SA which possess anionic charges and when used alone showed higher mucoadhesion as reported by (Roy *et al.*, 2009). The presence of such charged groups are important in controlling the degree of hydration of both the polymer and the mucous network (Gu *et al.*, 1988). Gu and co-authors (1988) also reported that the expanded nature of the swollen polymer and mucus enhances the inter-diffusion process and permits both mechanical entanglement and an increase in surface contact for hydrogen bonding and/or electrostatic interaction between the polymer and the mucous network which was true for the BLK films in the presence of SWF in the current project (Gu *et al.*, 1988).

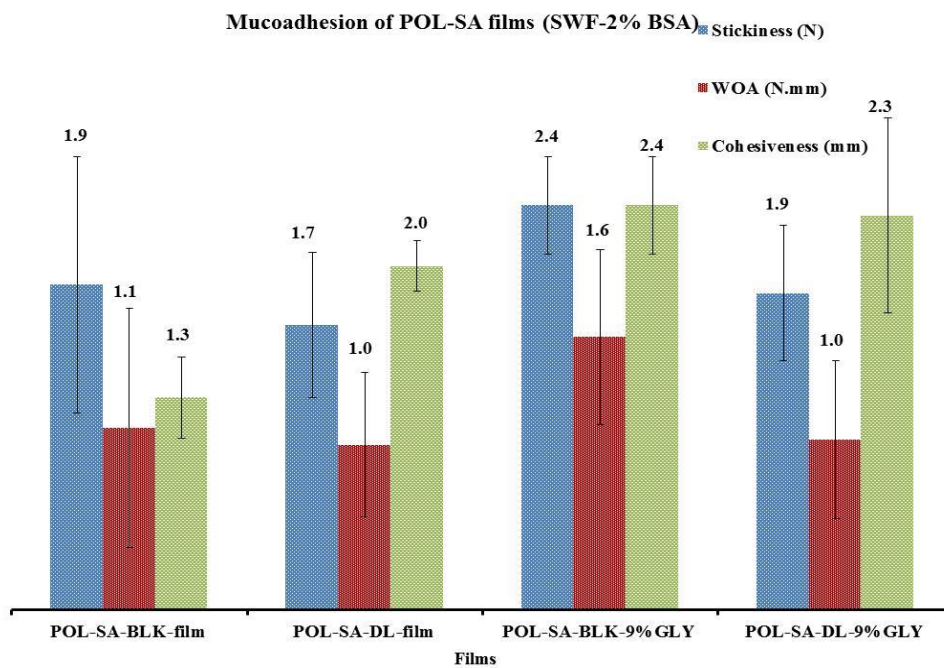
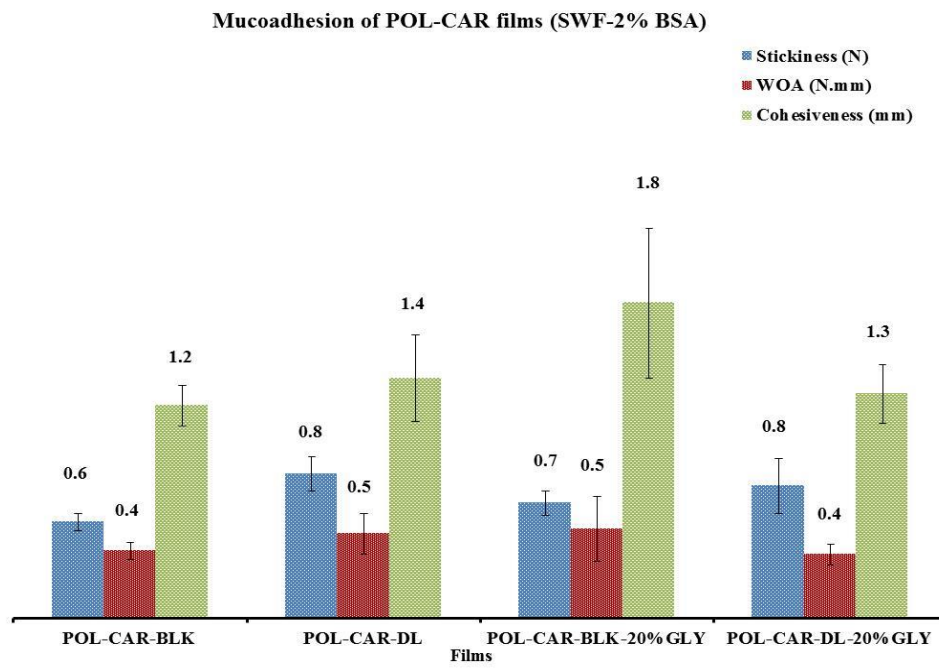


Figure 5.8: Mucoadhesion profiles of unplasticised POL-CAR and POL-SA films with SWF containing 2% w/w BSA.

### 5.3.1.2 Plasticised films

Figures 5.8 and 5.9 also illustrate the effect of concentration of plasticiser on the mucoadhesive performance of the films. In the presence of GLY, mucoadhesive performance of the POL-SA-BLK films increased from  $1.9\pm 0.7$  N to  $2.4\pm 0.3$  N ( $P = 0.1315$ ) and increased from  $(0.6\pm 0.1$  N to  $0.7\pm 0.1$  N) ( $P < 0.0233$ ) for POL-CAR-BLK films. GLY acts as an adhesion promoter by enhancing hydrogen bonding between the polymeric chains and SWF which is an important contributor to favourable adhesion properties. Another possible mechanism is that the plasticised films hydrate relatively more quickly in the presence of SWF which consequently imparts the increased stickiness to films.

Artificial exudate (SWF) contains large amounts of proteins and salts which may interfere with the polymer-drug interactions and may affect the mucoadhesive and drug release characteristics. Films plasticized with GLY (POL-CAR-DL-20%GLY and POL-CAR-BLK-20%GLY) demonstrated high detachment force indicating the strong interactions between the polymeric chains of both polymers (POL-CAR) and the model wound surface (Morales and McConville, 2011). In the presence of viscous SWF (5%BSA) the stickiness [POL-CAR-BLK-20%GLY ( $2.1\pm 0.5$ N) and POL-SA-BLK-9%GLY ( $1.7\pm 0.8$ N)] was decreased whilst WOA [POL-CAR-BLK-20%GLY ( $2.1\pm 0.9$ N) and POL-SA-BLK-9%GLY- $1.1\pm 0.5$ N)] and cohesiveness [POL-CAR-BLK-20%GLY ( $3.4\pm 0.4$ N) and POL-SA-BLK-9%GLY ( $2.8\pm 1.0$ N)] was increased. This may be due to the fact that in the presence of GLY, SWF in higher concentration behaves as a slippery mucilage which results in reduced net mucoadhesive performance.

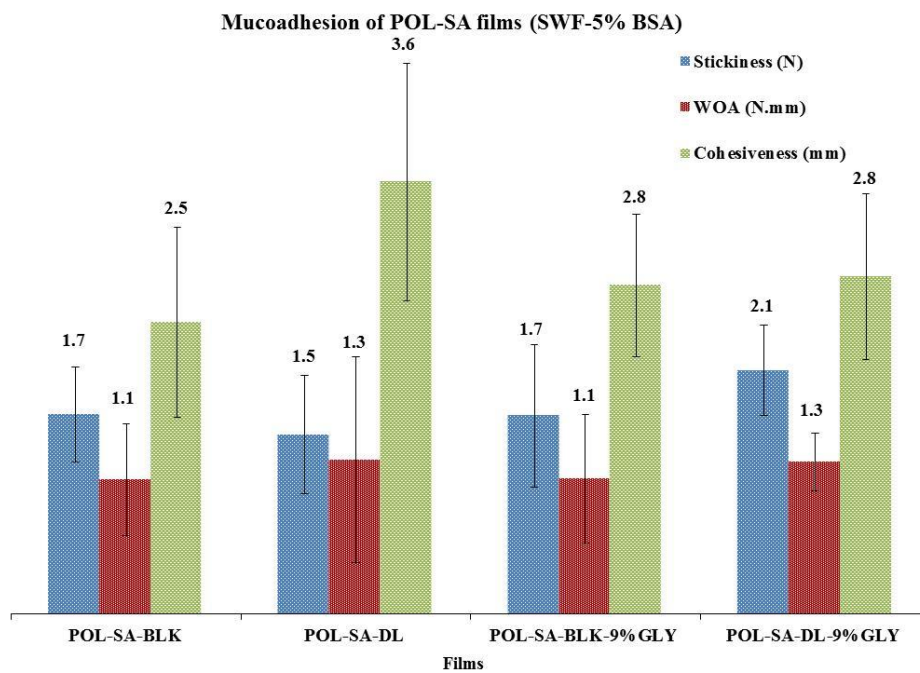
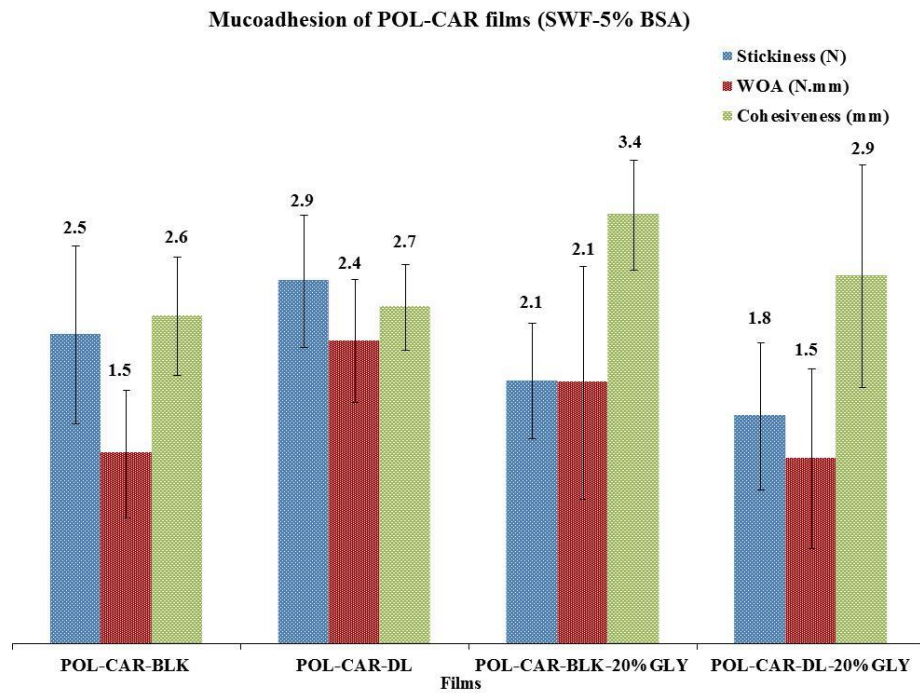


Figure 5.9: Mucoadhesion characteristics of POL-CAR and POL-SA films with SWF containing 5% w/w BSA.

### 5.3.1.3 Drug loaded (DL) films

Figures 5.8 and 5.9 also depict the mucoadhesive performance of DL films at different viscosities of SWF (2%BSA and 5%BSA). POL-CAR-DL films showed higher stickiness ( $0.8\pm 0.1\text{N}$ ) than the corresponding plasticized films ( $0.8\pm 0.2\text{N}$ ). A higher force was required to detach the POL-SA-DL films (POL-SA-DL,  $1.7\pm 0.4\text{N}$ ; POL-SA-DL-9%GLY,  $1.9\pm 0.4\text{N}$ ) when compared with POL-CAR DL films. There were no significant differences observed between the stickiness of the plasticized BLK and non-plasticized DL films. Presence of drugs decreased the WOA and cohesiveness for POL-SA and POL-CAR films with and without plasticizer. The observed work of adhesion for the POL-CAR-DL and POL-CAR-DL-20%GLY films were ( $0.5\pm 0.1\text{N}\cdot\text{mm}$ ) and ( $0.4\pm 0.1\text{N}\cdot\text{mm}$ ) while it increased for POL-SA-DL and POL-SA-DL-9%GLY films ( $1.0\pm 0.4$  and  $1.0\pm 0.5\text{N}\cdot\text{mm}$ ) but decreased when compared with the BLK films. Interestingly, in the presence of SWF with 5% w/w BSA, stickiness increased for POL-CAR-DL films ( $2.9\pm 0.5\text{N}$ ) and POL-SA-DL-9%GLY films ( $2.1\pm 0.4\text{N}$ ) but decreased for the DL [(POL-CAR-DL-20%GLY,  $1.82\pm 0.6\text{N}$ ) and (POL-SA-DL,  $1.51\pm 0.7\text{N}$ )] films with or without plasticizer. WOA of the POL-CAR-DL films and POL-SA-DL films decreased in the presence of added drug. There are two main reasons behind the decreased adhesion. Firstly, ionic interactions occurred between the anionic polymers (CAR and SA) and cationic STP which had an effect on the hydrogen bonding mechanism between the polymers and SWF which contains salts and proteins. Secondly, Tobyn and co-workers reported that increased ionic strength of the media and the presence of sodium and potassium ions resulted in decreased adhesion WOA (Tobyn *et al.*, 1997) in the current study. The sodium sulphate which is present in the films increased the ionic strength of the SWF resulting in decreased adhesion. In the case of the DL films (POL-CAR and POL-SA), the presence of sodium sulphate may have interfered with the physical properties of the delivery matrix and reduced the extent of adhesion to the gelatin substrate equilibrated with SWF (2%w/w and 5%w/w BSA).

### 5.3.1.4 Freeze-dried wafers (BLK and DL)

Figures 5.10 and 5.11 show the effect of two different concentration of BSA (2% w/w and 5% w/w) representing thin watery and viscous thick exudate respectively, on mucoadhesion properties of POL-CAR and POL-SA (BLK-An and DL-An) wafers. POL-CAR-BLK-An and POL-SA-BLK-An wafers showed similar ( $4.9\pm 1.3\text{N}$  and  $4.7\pm 1.1\text{N}$  respectively) stickiness

values in the presence of thin SWF (2% w/w BSA) whereas the stickiness was decreased in POL-CAR-DL-An and POL-SA-DL-An wafers. This again may be because of the presence of sodium sulphate which has marked effect on the hydration of the wafers resulting in decreased stickiness. WOA and cohesiveness were higher in the POL-SA (BLK-An and DL-An) wafers which decreased for POL-CAR (BLK-An and DL-An) wafers. Both POL-CAR-BLK-An and POL-SA-BLK-An wafers showed high stickiness in the presence of viscous SWF (5% w/w BSA) which decreased for the POL-SA-DL-An and POL-CAR-DL-An wafers. It was observed that WOA was decreased in descending order for POL-CAR-BLK-An, >POL-SA-BLK-An, >POL-SA-DL-An wafers. There was a significant difference ( $p=0.001$ ) in stickiness and WOA between BLK-An and DL-An of both POL-CAR and POL-SA wafers. Overall, the POL-CAR-BLK-An wafers showed higher stickiness and WOA in the presence of viscous SWF (5% w/w BSA) whereas POL-CAR-DL-An wafers had higher stickiness and WOA in the presence of normal or thin SWF (2% w/w BSA). However, POL-SA-BLK-An and POL-SA-DL-An wafers showed higher stickiness and WOA in the presence of SWF (2% w/w BSA) compared to SWF (5% w/w BSA).

Cohesiveness is the intermolecular attraction which holds wafer and the wound substrate together. It has been observed that in the presence of SWF (2% w/w BSA) POL-CAR (BLK-An and DL-An) had similar values while POL-SA (BLK-An and DL-An) showed significant differences in the cohesiveness ( $p=0.02$ ).

Usually thin watery serous type exudate (represented by 2% BSA SWF) in a wound signifies possible bacterial infection. *S. aureus* produce staphylokinase which has fibrinolytic activity and degrades fibrin clots resulting in thin watery exudate (White and Cutting, 2006; Braff *et al.*, 2007). The POL-CAR-DL-An and POL-SA-DL-An wafers can help to manage such exudate due to their porous nature. Haemorrhagic and haemopurulent (viscous, sticky and thick) exudate signifies infection and trauma and POL-CAR (BLK-An and DL-An) wafers can provide prolonged retention of wafers at the site of injury.

Overall, mucoadhesion results from both BLK-An and DL-An wafers confirmed that the porosity plays a critical role due to the ability to absorb SWF and hydration of the polymeric network (POL, SA and CAR). The decreased stickiness in the DL wafers was associated with the decreased porosity of these wafers due to the added drugs and subsequent salt formation which inhibit rapid hydration of the wafers. From the results obtained and the overall discussion it can

be concluded that the wafers generally possessed good adhesive strength with the wound substrate containing two different types of exudate compared to the films. Therefore these wafers can adhere to the wound site and protect the wound from the external environment with the absorption of large amounts of exudate which is a primary requirement for a formulation to function as an ideal wound dressing.

**Mucoadhesion of POL-CAR and POL-SA-wafers (SWF-2% BSA)**

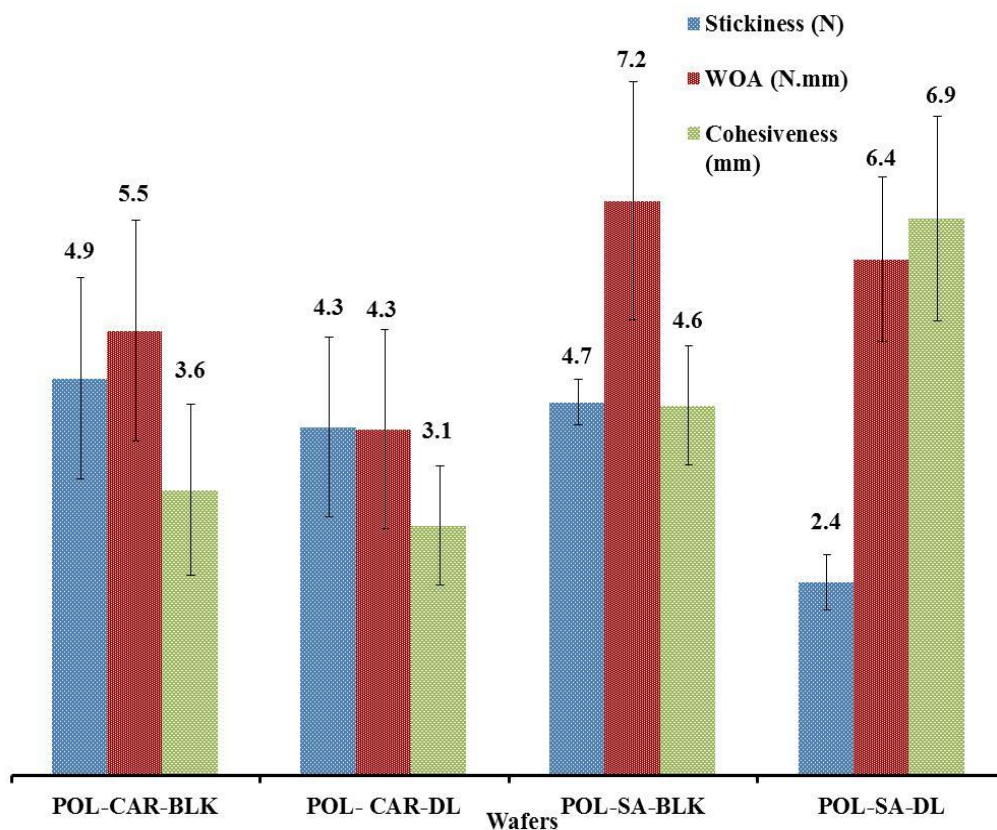


Figure 5.10: Mucoadhesion studies of POL-CAR and POL-SA wafers with SWF containing 2% w/w BSA.

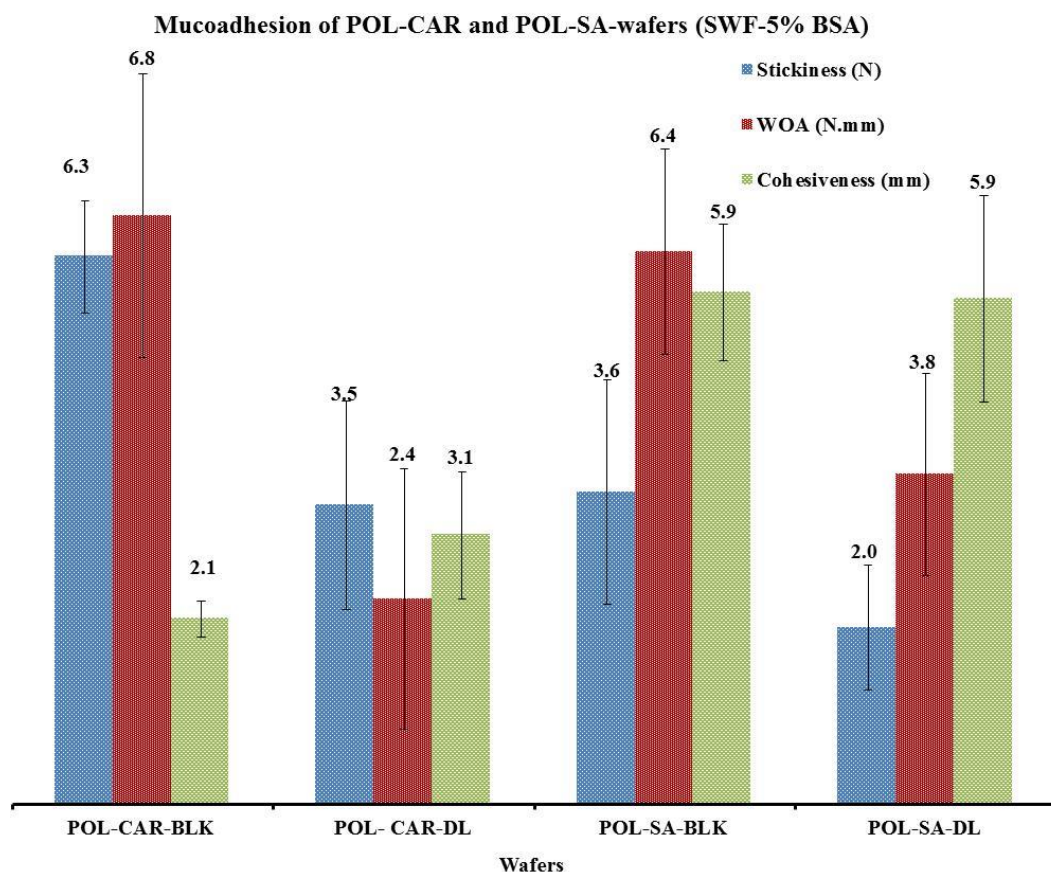


Figure 5.11: Mucoadhesion characteristics of POL-CAR and POL-SA wafers with SWF containing 5% w/w BSA.

#### 5.4.2 Mucoadhesion studies by TA (2%w/w mucin)

There are different theories proposed to explain the mucoadhesion process (Smart, 2005). Mucoadhesive bond formation involves wetting and swelling of the polymer network to intimate contact between the substrate (mucin, SWF, biological tissues) and polymer and interpenetration, entanglement of polymer chains and substrate (Sriamornsak *et al.*, 2008). For such mucoadhesion process, diffusion and swelling behaviour of the films and wafers with mucoadhesive polymers (POL, CAR and SA) has great impact on their adhesive performance. Sufficient amounts of water is necessary to hydrate and expand the mucoadhesive network which exhibits available adhesive sites for bond formation and creates pores for diffusion of polymer chains to enhance the interpenetration (Leung & Robinson, 1990 cited in Sriamornsak *et al.*, 2008).

The mucoadhesive performance of the films and wafers using 2% mucin solution by TA are shown in figure 5.12. It was observed that the wafers had a higher mucoadhesion capacity compared to the films. As wafers are porous in nature, they rehydrate more quickly in the presence of mucin solution and form strong hydrogen bonding with the protein. POL-CAR-BLK wafers showed the highest mucoadhesive forces ( $3.12\pm 0.4\text{N}$ ) and lowest cohesiveness ( $2.48\pm 0.3\text{mm}$ ). The total energy (WOA) involved in the mucoadhesion was decreased for the DL wafers but was higher for the POL-SA films. The formation of sodium sulphate due to added drugs resisted the hydration of films which ultimately decreased the WOA and also supports the swelling studies previously reported (Boateng *et al.*, 2013). Increased WOA of SA films was responsible for the strong hydrogen bonding and quick hydration compared with POL-CAR films and ultimately increased the cohesiveness of the wafers (POL-SA-BLK,  $8.38\pm 1.2\text{mm}$ ; POL-SA-DL  $4.93\pm 1.6\text{mm}$ ). Addition of GLY had a marked effect on the mucoadhesion performance of the films. Stickiness for POL-CAR-BLK-20%GLY and POL-CAR-DL-20%GLY ranged from 2.05-2.21N and from 1.91-2.37N for POL-SA-BLK-9%GLY and POL-SA-DL-9%GLY films. The stickiness, WOA and cohesiveness for POL-SA films was found in the descending order of POL-SA-BLK-9%GLY > POL-SA-DL > POL-SA-DL-9%GLY > POL-SA-BLK. The stickiness, WOA and cohesiveness for POL-CAR films was found in the decreasing order of POL-CAR-BLK-20%GLY > POL-CAR-BLK-20%GLY > POL-CAR-BLK > POL-CAR-DL.

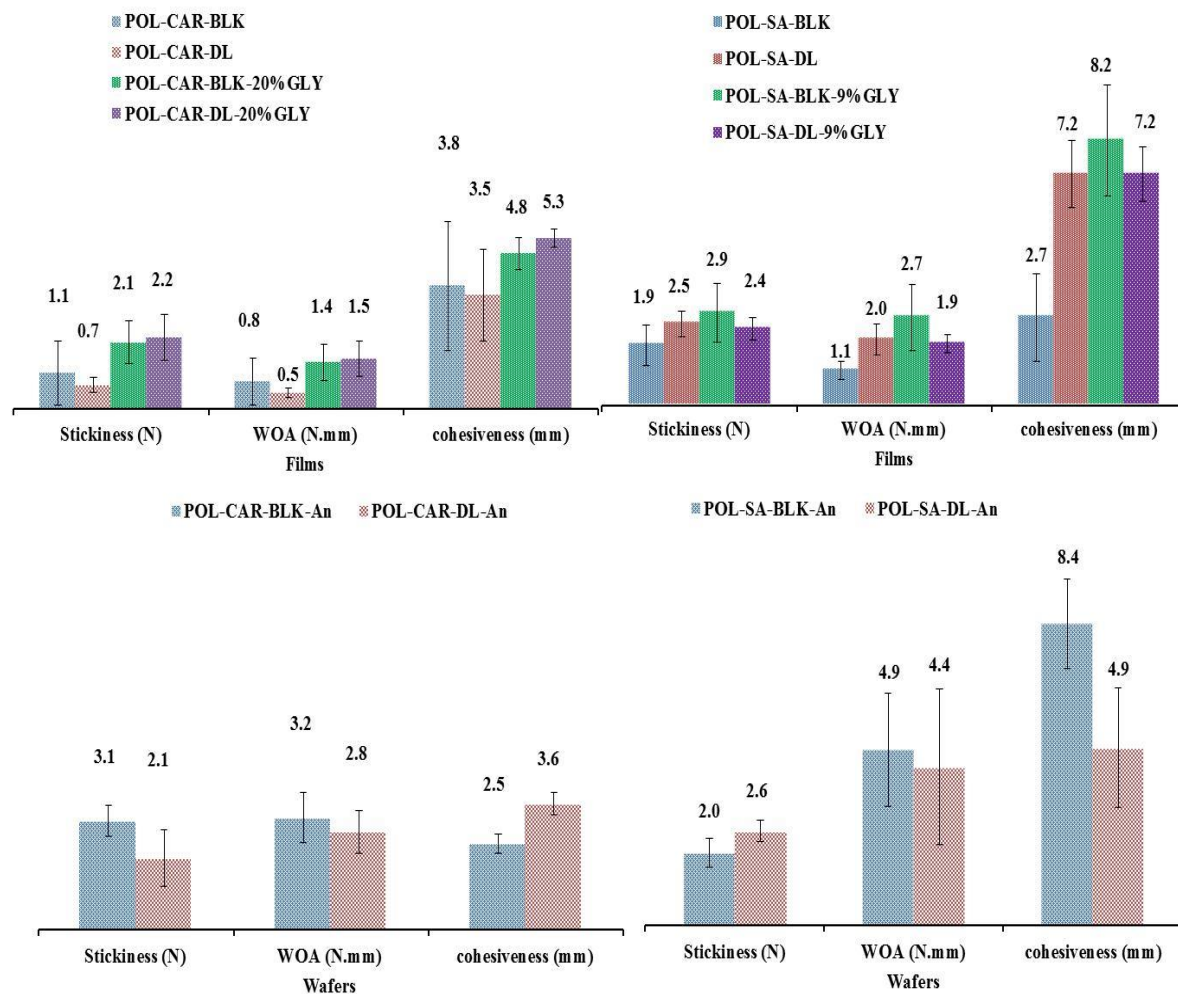


Figure 5.12: Mucoadhesion performance of POL-CAR and POL-SA films and wafers showing stickiness, WOA and cohesiveness.

### 5.4.3 ATR-FTIR analysis of mucin diffusion into films and wafers

In ATR-FTIR spectroscopy, wavelength of the incident radiation affects the depth of penetration of IR radiation into the films and wafers. Time dependent spectral data from ATR-FTIR enabled detailed characterisation of films and wafers. There were however, some challenging factors related to ATR-FTIR set-up that required careful consideration when analysing diffusion of mucin through polymeric films and wafers. These included among others, quality of contact of the formulations with the ATR crystal across the focal plane of the detector. This is important because absence of proper contact with the ATR crystal will produce inaccurate spectral profiles and can affect the diffusion results. Poor contact can be a function of

the smoothness, porous nature (in case of wafers) and thin nature (films) of the formulations (Tetteh *et al.*, 2009).

Figure 5.13 shows the ATR-FTIR spectra of mucin powder, mucin solution (2% w/v in PBS pH 7.4) and PBS only. There was a considerable difference between the IR spectra of mucin powder and mucin PBS solution. Saino *et al.*, (2002) reported a band at  $1550\text{ cm}^{-1}$  assigned to C=O stretching vibration of sialic acid of mucin type I-S from bovine submaxillary gland and also observed a C=O stretching vibration at  $1542\text{ cm}^{-1}$  for the mucin from porcine stomach type two, which has bound sialic acid from 0.5-1.5%. The IR spectrum of the mucin in PBS showed a strong peak at  $1650\text{ cm}^{-1}$  whilst mucin powder showed amide I and amide II bands at  $1650\text{ cm}^{-1}$  and  $1550\text{ cm}^{-1}$  attributed to amino acids and oligosaccharides (Khajehpour *et al.*, 2006). To measure the diffusion of mucin through the films and wafers, changes in the absorbance at a wavenumber window of  $1400\text{-}1700\text{ cm}^{-1}$  was selected which corresponds to the absorbance of the respective mucin. Figure 5.13 shows the raw spectral profiles of all the formulations for the diffusion of 2%w/w mucin.

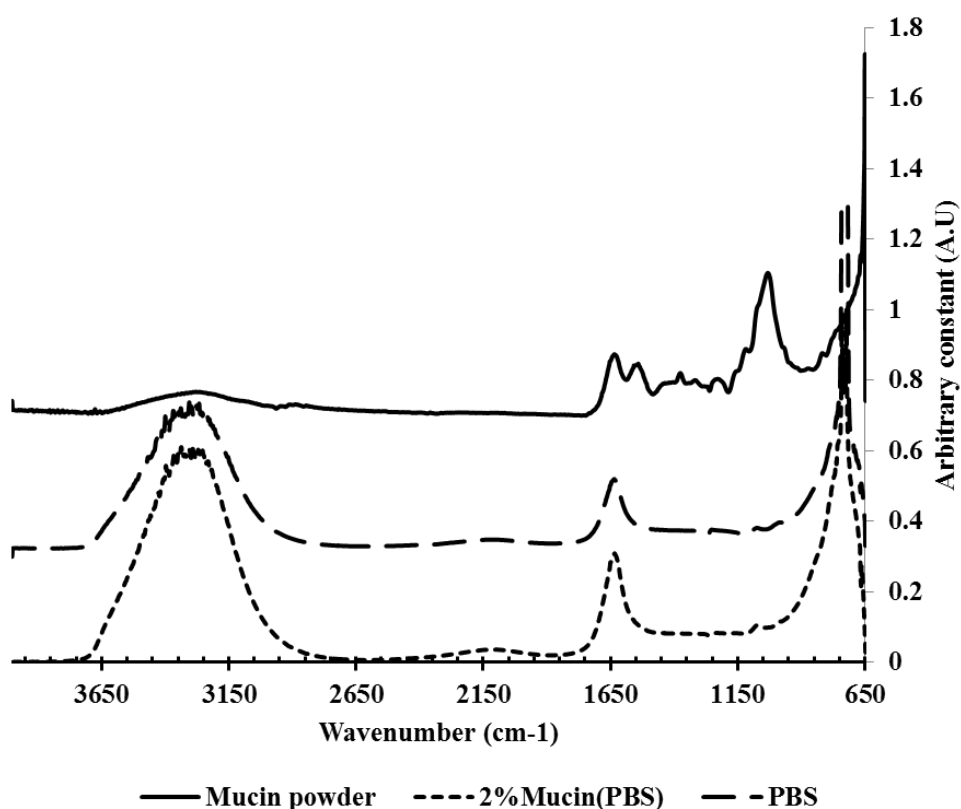


Figure 5.13: FTIR spectra of mucin powder, 2% mucin (PBS) and PBS solution.

Table 5.3: Relative absorption values of the diffusion of mucin for the POL-CAR and POL-SA BLK and DL films and wafers.

Formulations	Time (Sec)							
	50	100	200	300	400	500	600	700
POL-CAR-BLK-20%GLY	0.57±0.05	0.68±0.09	0.80±0.20	0.84±0.28	0.86±0.39	0.89±0.50	0.89±0.59	0.93±0.67
POL-CAR-BLK	0.24±0.05	0.28±0.06	0.47±0.07	0.75±0.08	0.84±0.12	0.94±0.20	0.92±0.28	0.94±0.35
POL-CAR-DL	0.05±0.05	0.20±0.07	0.39±0.14	0.62±0.24	0.72±0.37	0.82±0.49	0.91±0.90	0.98±1.03
POL-CAR-DL-20%GLY	0.66±0.14	0.28±0.35	0.09±0.55	0.18±0.52	0.32±0.65	0.42±0.76	0.57±0.84	0.75±0.99
POL-CAR-DL-An	0.34±0.09	0.21±0.17	0.16±0.28	0.42±0.31	0.68±0.33	0.81±0.35	0.72±0.43	0.87±0.51
POL-CAR-BLK-An	0.40±0.16	0.58±0.25	0.62±0.32	0.77±0.33	0.76±0.37	0.79±0.42	0.86±0.51	0.80±0.64
POL-SA-BLK-9%GLY	0.42±0.02	0.62±0.04	0.76±0.05	0.87±0.06	0.91±0.08	0.93±0.11	0.92±0.14	0.94±0.24
POL-SA-BLK	0.37±0.05	0.54±0.07	0.77±0.11	0.81±0.14	0.91±0.16	0.90±0.19	0.93±0.22	0.97±0.30
POL-SA-DL-An	0.05±0.04	0.25±0.07	0.65±0.12	0.72±0.15	0.86±0.19	0.75±0.23	0.80±0.31	0.86±0.43
POL-SA-DL-9%GLY	0.36±0.03	0.49±0.04	0.71±0.06	0.80±0.08	0.87±0.10	0.91±0.11	0.92±0.13	0.93±0.16
POL-SA-DL	0.35±0.03	0.50±0.04	0.70±0.07	0.79±0.09	0.88±0.11	0.91±0.13	0.95±0.15	0.97±0.19
POL-SA-BLK-An	0.30±0.10	0.50±0.12	0.68±0.17	0.64±0.25	0.81±0.32	0.70±0.40	0.86±0.46	0.82±0.66

McAuley (2009) reported that the wavelength influences the depth of penetration of IR radiation into the membrane. This raises the possibility of different diffusion coefficients when different spectrum window were used. This could therefore affect the interpretation of relative diffusion rates of the mucin dissolved in PBS when different windows of IR spectrum are used for the films and wafers. For that purpose, the spectrum window of 1400-1700  $\text{cm}^{-1}$  was selected to evaluate the diffusion of mucin where peak of mucin is prominent. There could be other factors that can interfere with the diffusion of mucin which could be avoided by using multivariate data analysis by selecting a particular reference spectral window of mucin. The profiles were normalised by setting the time frame of 780 sec and a representative profile of three replicates are shown in the figure 5.14. The average of three profiles is shown on the same scale for comparison. The figure plotted for the diffusion of mucin across the representative formulation error bars were added for only plus values for the clarity and comparison purpose and same process has been used in previous literature (Jabbari *et al.*, 1993; Saiano *et al.*, 2002). Table 5.3 represents the data of the diffusion (relative intensity) of mucin across the various formulations used for the study. This data was used to study the effect of polymer, drug, and GLY (for only films) on the diffusion of mucin simultaneously monitoring the changes in the IR spectrum (1400-1700  $\text{cm}^{-1}$ ).

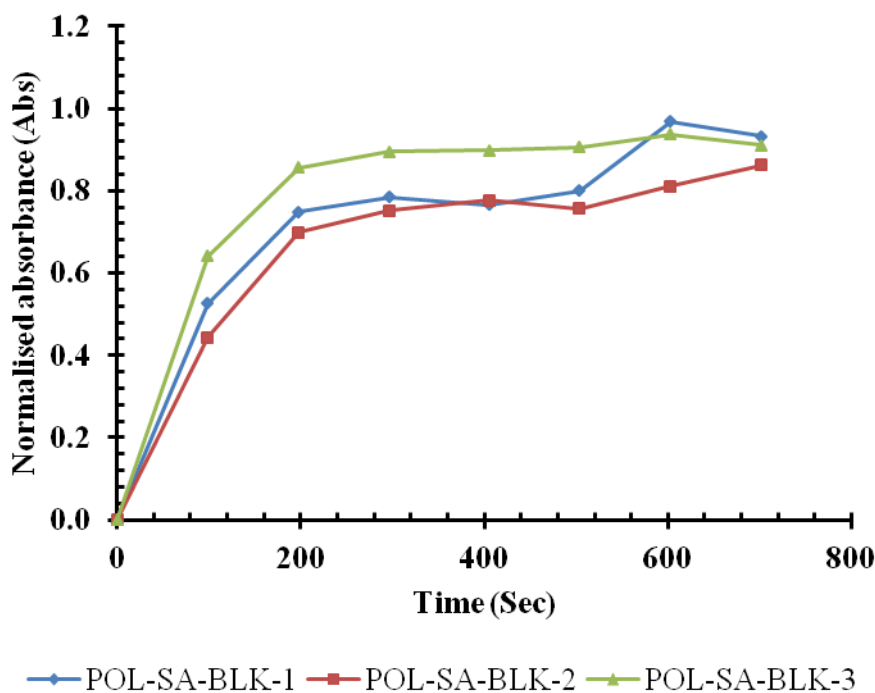


Figure 5.14: Representative plots of the POL-SA-BLK films showing reproducibility.

### 5.4.3.1 Diffusion profiles for POL-CAR and POL-SA films

The observed diffusion coefficient of mucin through the films and wafer are presented in table 5.4 below.

Table 5.4: Diffusion coefficient values for mucin through the optimised films and wafers.

<b>POL-CAR films /wafers</b>	Diffusion coefficient		Diffusion
	“D” (cm <sup>2</sup> /s)	<b>POL-SA films/wafers</b>	coefficient “D” (cm <sup>2</sup> /s)
POL-CAR-BLK	4.0×10 <sup>-3</sup>	POL-SA-BLK	6.2×10 <sup>-3</sup>
POL-CAR-DL	2.8×10 <sup>-3</sup>	POL-SA-DL	6.5×10 <sup>-3</sup>
POL-CAR-BLK-20%GLY	9.7×10 <sup>-3</sup>	POL-SA-BLK-9%GLY	7.4×10 <sup>-3</sup>
POL-CAR-DL-20%GLY	0.7×10 <sup>-3</sup>	POL-SA-DL-9%GLY	6.9×10 <sup>-3</sup>
POL-CAR-BLK-An	7.8×10 <sup>-3</sup>	POL-SA-BLK-An	6.1×10 <sup>-3</sup>
POL-CAR-DL-An	0.8×10 <sup>-3</sup>	POL-SA-DL-An	0.8×10 <sup>-3</sup>

Figures 5.15 and 5.16 show the normalised diffusion profiles for POL-CAR and POL-SA (BLK and DL) films obtained using the wavelength 1400-1700 cm<sup>-1</sup>. The profiles were normalised by setting the time frame of 780 sec and was performed to allow the average of three profiles to be shown on the same scale. Both POL-CAR-DL and POL-CAR-DL-20%GLY showed initial higher absorbance before 100sec possibly due to poor contact with the crystal and this profile was reproducible for the all three replicates. POL-CAR BLK films showed slower diffusion of mucin through the films when compared to the POL-CAR BLK-20%GLY films (Figure 5.15). The observed absorbance initially for POL-CAR-BLK film was 0.24±0.05 which increased to 0.57±0.05 in initial 50 sec due to quicker diffusion of mucin solution through POL-CAR-BLK-20%GLY. This may be due to the plasticizing effect of GLY which has a higher affinity for water. Such a high water transfer inside the matrix containing GLY has already been reported for GLY plasticised CAR films (Karbowski *et al.*, 2006). GLY as plasticizer increases the mobility and elasticity of the films. POL-CAR-BLK films showed a steady increase in relative concentration and this can support the swelling studies reported by Pawar *et al.*, (2013). POL-CAR-BLK films showed steady diffusion of mucin which is due to the slow hydration of the POL and CAR to form a gel (). After 400 sec both films showed constant diffusion of mucin

which may be associated with the saturation of mucin solution within the films and ranged from 0.84-0.94.

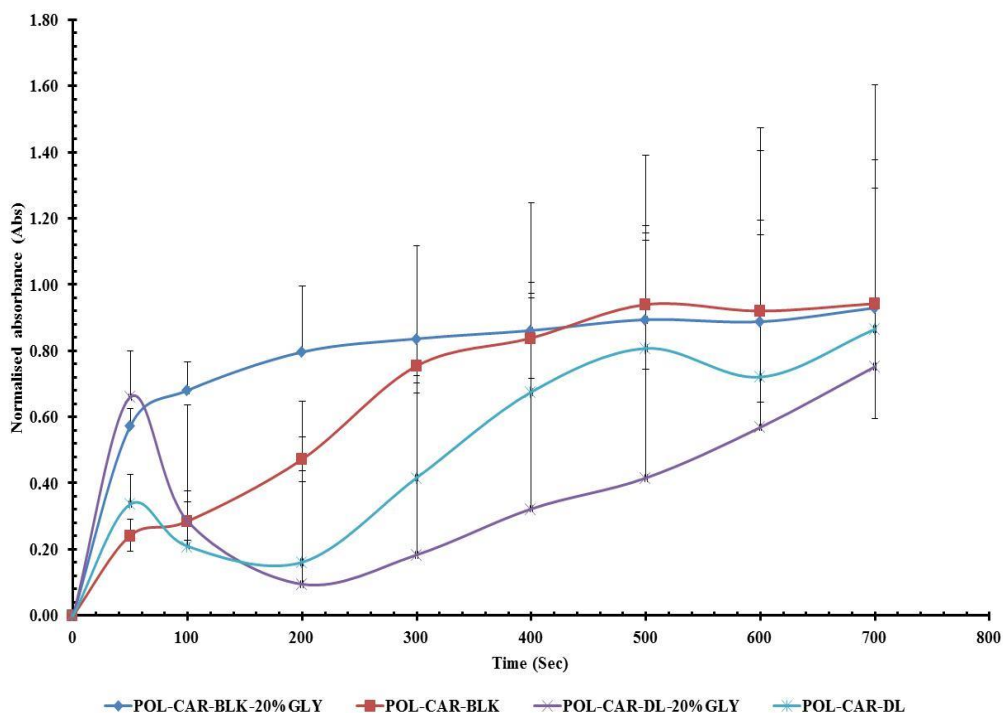


Figure 5.15: Normalised diffusion of mucin across POL-CAR films (mean±SD, n=3)

All POL-SA films (POL-SA-BLK and POL-SA-BLK-9%GLY) showed relatively faster swelling which ultimately increased diffusion of mucin through the films when compared with the POL-SA-DL and POL-SA-DL-9%GLY films. The individual profiles of mucin diffusion through the POL-SA films are shown in figure 5.16.

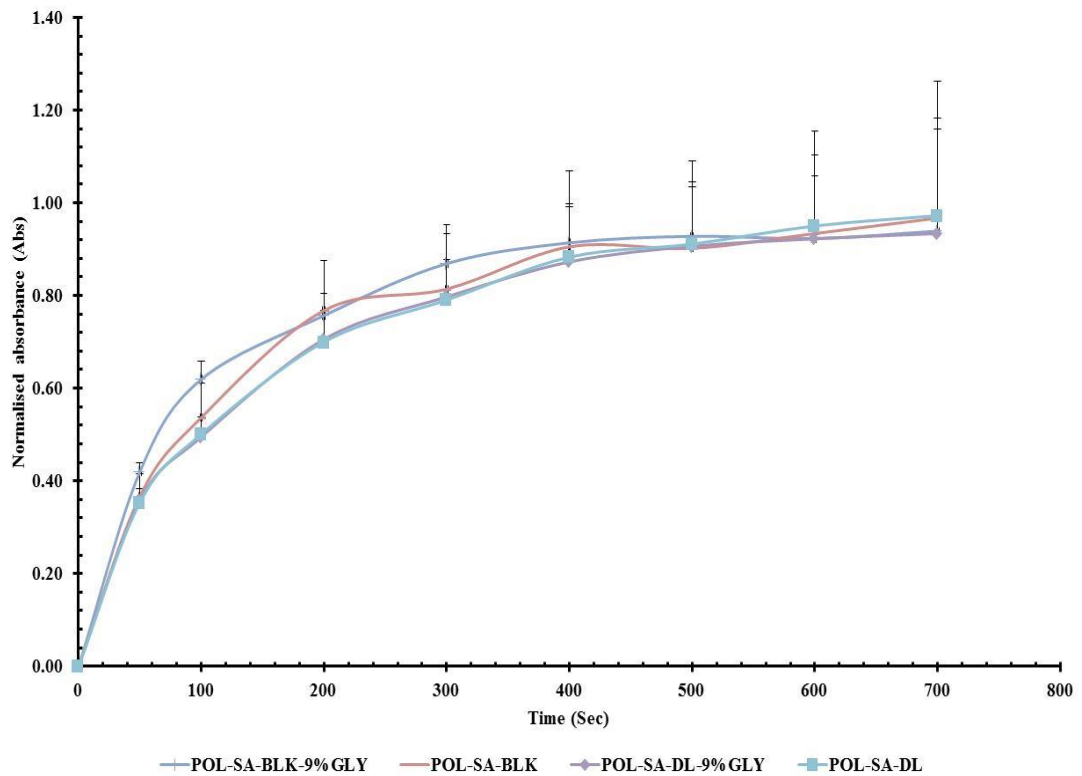


Figure 5.16: Normalised diffusion of mucin across POL-SA (BLK and DL) films (mean±SD, n=3).

#### 5.4.3.2 POL-CAR and POL-SA wafers

Figure 5.17 shows the individual profiles of mucin diffusion through the POL-CAR and POL-SA (BLK-An and DL-An) wafers. POL-CAR-BLK-An wafers showed a steady diffusion of mucin through the wafers which was the same for the initial 100 sec for the POL-SA-BLK-An wafers. The diffusion of mucin was increased for the POL-SA-BLK-An wafers after 100 sec when compared with the POL-CAR-BLK-An wafers. This is associated with the swelling mechanism of the different polymers which supports the swelling studies previously.

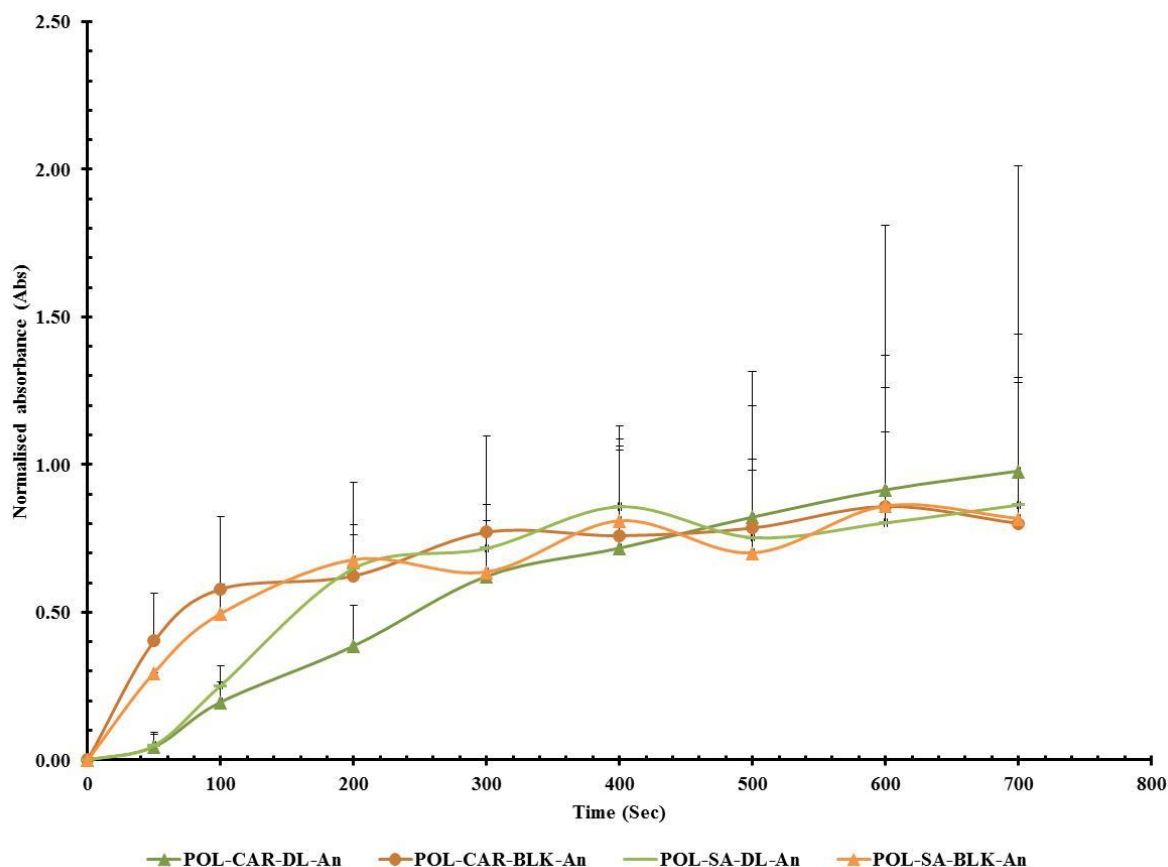


Figure 5.17: Normalised diffusion of mucin across POL-SA (BLK and DL) films (mean $\pm$ SD, n=3).

#### 5.4.3.3 Comparison of BLK films and wafers

The diffusion profiles of the mucin for the BLK films and wafers are shown in figure 5.18. In all the BLK formulations, POL-CAR-BLK film showed slower diffusion of the mucin. The BLK POL-CAR wafer showed a wavy profile of the diffusion which may be associated with the porous nature of the wafers which caused unequal distribution of mucin through these pore channels. Previously, Boateng and co-worker reported that wafers have the capacity to hydrate more quickly than their corresponding films (Boateng *et al.*, 2009). The same trend was observed when comparing POL-CAR BLK film and wafer. The diffusion of POL-CAR BLK-An wafer was higher than the POL-CAR-BLK film and consequently diffusion of mucin was increased for both POL-SA-BLK films and wafers respectively. The quicker diffusion of the mucin through the POL-SA formulations is associated with the immediate swelling of the films and wafers and reported by Bajpai, and Sharma, (2004). Such swelling in the matrix results in decreased

absorbance which shows a plateau after 400 sec. As seen above, both films showed marked effect of GLY which resulted in higher diffusion of mucin through these films. The overall trend observed for the diffusion of mucin through all BLK formulation is associated with the GLY and swelling behaviour of individual polymer (POL, CAR and SA).

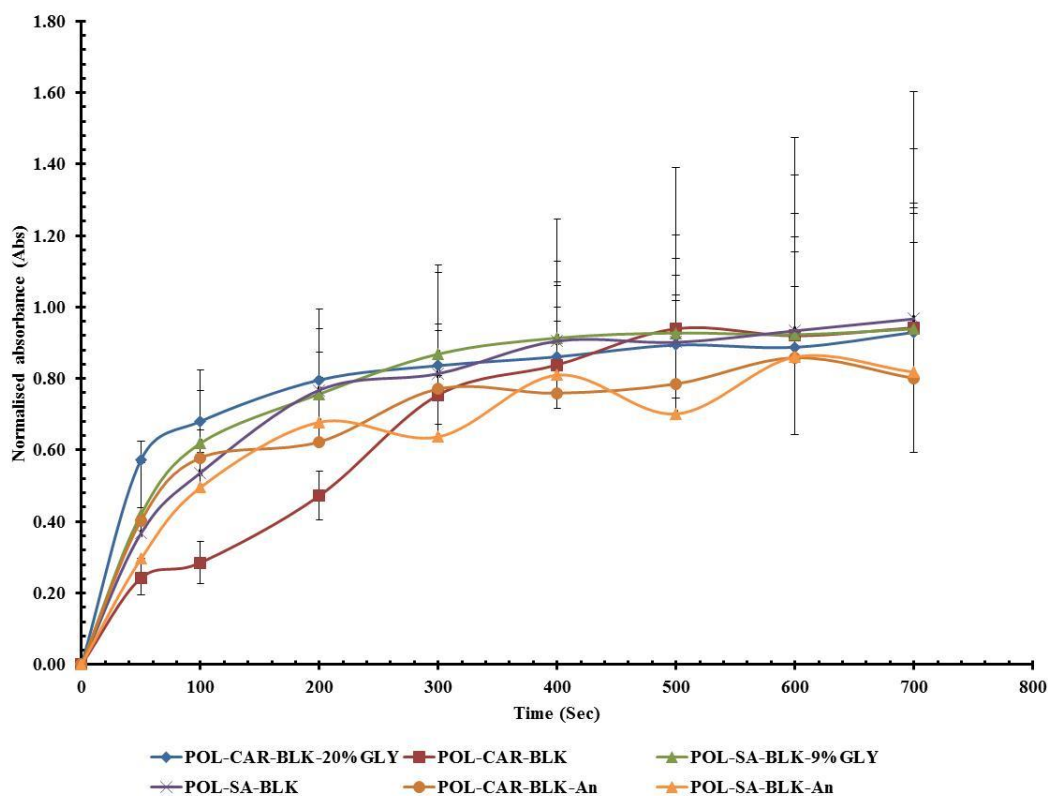


Figure 5.18: Normalised diffusion of mucin across BLK films and wafers (mean $\pm$ SD, n=3).

#### 5.4.3.4 Comparison of DL films and wafers

The overall diffusion of mucin through the POL-SA DL films and wafers was higher compared to POL-CAR films and wafers and is shown in figure 5.19. Previous swelling studies (*Chapter 4*) showed that the added drug resulted in a decreased hydration capacity and had overall impact on mucoadhesion properties. The same effect was observed for all DL films and wafers which resulted in decreased diffusion of mucin through the DL films and wafers and supports the mucoadhesion studies carried out by TA. The overall trend for the diffusion of mucin through the films and wafers is summarised in table 5.5 below. This shows that generally, diffusion was faster through the POL-SA films than the corresponding POL-CAR films with the exception of BLK plasticised films where the POL-CAR-BLK-20%GLY showed a higher

diffusion than the POL-SA-BLK-9%GLY. This is due to the higher amounts of GLY present in the POL-CAR films (20%GLY) compared to the POL-SA films (9%GLY).

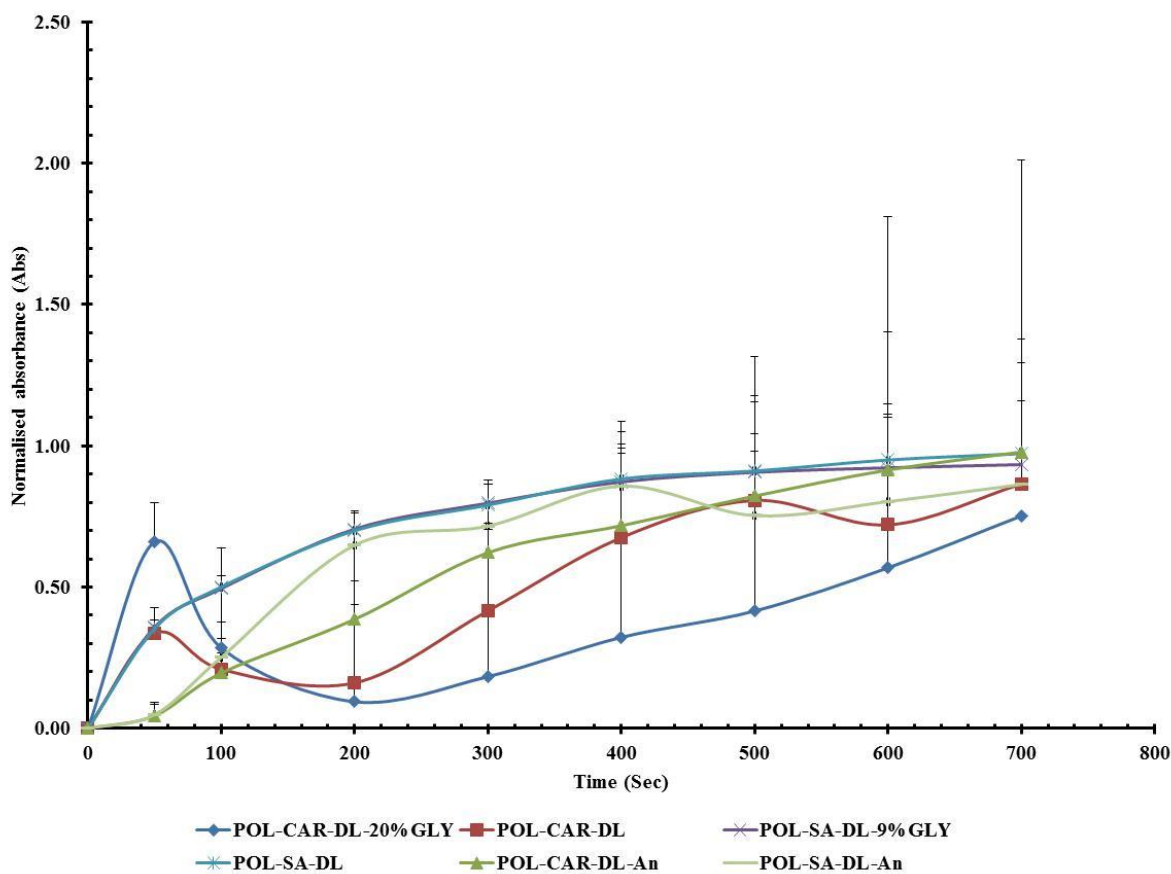


Figure 5.19: Normalised diffusion of mucin across DL films and wafers (mean±SD, n=3).

Table 5.5: Descending order of diffusion of mucin through films and wafers

1. POL-CAR-BLK-20%GLY > POL-CAR-BLK > POL-CAR-DL > POL-CAR-DL-20%GLY (films)
2. POL-SA-BLK-9%GLY > POL-SA-DL-9%GLY > POL-SA-DL > POL-SA-BLK (films)
3. POL-CAR-BLK-An > POL-SA-BLK-An > POL-SA-DL-An = POL-CAR-DL-An (wafers)

This study has shown two different techniques for the evaluation of the mucoadhesion properties of films and wafer which are TA and ATR-FTIR spectroscopy.

The former technique corresponds to the fracture theory and relates the adhesive strength to the forces required for detachment of two involved surfaces such as mucin and film or wafer after adhesion. Adamson (1990) reported that the failure of adhesive bonds normally occurs at the weakest component which is typically cohesive failure within one of the adhering surfaces and can be complicated to determine the weakest component due to blend of polymer, plasticizer (in films) and two different drugs. Also it is necessary to consider that the adhesive strength depends upon the wetting phenomena of the polymer and relates to hydrophilicity of the polymer and excipients. If the formulation has higher adhesional wetting it results in higher mucoadhesion (Adamson 1990). This trend was observed in the BLK films and wafers which showed higher mucoadhesion compared to DL films and wafers where wettability or hydration of the formulation was reduced due to the added drug (sodium sulphate formed).

The ATR-FTIR diffusion of mucin is based on the diffusion theory which represents inter-diffusion of polymers chains across an adhesive interface. It is driven by concentration gradients and affected by the available molecular chain lengths and their mobilities. The diffusion of mucin is dependent upon the diffusion coefficient and the time of contact. Smart reported that if the depth of penetration is sufficient, it creates a semi-permanent adhesive bond (Smart 2005). The mucoadhesion data generated from these two techniques were not comparable due to the different theories associated with these techniques, however it gives an overview and proof of principle of precise parameters (such as effect of polymer, plasticizer and added drug) affecting the mucoadhesion of films and wafers.

#### **5.4 Conclusion**

Mucoadhesive performance is critical as it determines the residence time of dressings at the wound site to allow for sustained drug release and eventual bioavailability. Though significant differences were observed in the mucoadhesive performances of the films and wafers, the differences were not considerable. There was also a marked effect of the different concentrations of SWF, GLY and drugs (STP and DLF) on the mucoadhesive performance. Based on the limited number (4) of replicates the following general observation can be made. POL-SA films showed higher mucoadhesion in the presence of SWF containing 2% BSA whereas POL-CAR showed high mucoadhesive performance in the presence of SWF containing 5% BSA. It appears that the POL-SA films and wafers can be used in the presence of normal exudate where concentration of protein is less to achieve prolonged retention time and

bioavailability. POL-CAR films and wafers on the other hand can be used for wounds which produce viscous exudate to achieve better bioavailability and mucoadhesive performance. Artificial exudate (SWF) contains large amounts of proteins and salts which may interfere with the polymer-drug interactions and may affect the mucoadhesive characteristics. Plasticized films (POL-CAR-DL-25%GLY, POL-CAR-BLK-25%GLY, POL-SA-BLK-9%GLY and POL-SA-BLK-9%GLY) and blank (POL-SA-BLK and POL-CAR-BLK) wafers demonstrated high detachment force indicating strong interactions between the polymeric chains of polymers (POL, SA and CAR) and the model wound surface. This will help to prolong the residence time and bioavailability of the drugs (STP and DLF) at the wound site and also help to overcome the problem of frequent dressing change. It can also control the bacterial load associated with chronic wound infection and ultimately improves wound healing.

ATR-FTIR spectroscopy has been used to follow the diffusion of mucin across the films and wafers and showed that mucin diffused independently through the solvent and across the films and wafers. POL-CAR films ( $BLK = 4.0 - 9.7 \times 10^{-3} \text{ cm}^2/\text{s}$ ;  $DL = 0.7 - 2.8 \times 10^{-3} \text{ cm}^2/\text{s}$ ) generally showed slower diffusion when compared with POL-SA films ( $BLK = 6.2 - 7.4 \times 10^{-3} \text{ cm}^2/\text{s}$ ;  $DL = 6.5 - 6.9 \times 10^{-3} \text{ cm}^2/\text{s}$ ). The diffusion through POL-CAR wafers ( $BLK = 7.8 \times 10^{-3} \text{ cm}^2/\text{s}$ ;  $DL = 0.8 \times 10^{-3} \text{ cm}^2/\text{s}$ ) and POL-SA wafers ( $BLK = 6.1 \times 10^{-3} \text{ cm}^2/\text{s}$ ;  $DL = 0.8 \times 10^{-3} \text{ cm}^2/\text{s}$ ) was the opposite. POL-CAR wafers showed higher mucoadhesion than the POL-SA wafers which decreased in the presence of drug. Plasticized films (POL-CAR and POL-SA) showed higher mucoadhesion than the BLK and DL films.

## CHAPTER 6: EVALUATION AND COMPARISON OF *IN VITRO* ANTIBACTERIAL EFFICACY OF FILM, WAFER AND COMMERCIAL WOUND DRESSINGS

### 6.1 Introduction

Effective management of wound infection necessitates reduced exogenous microbial contamination (bio-burden), debridement of devitalized tissue, use of appropriate dressing as well as topical and systemic broad-spectrum antimicrobial agents, maximization of immune resistance and provision of adequate nutrition (Bowler *et al.*, 2001). Antimicrobial agents such as antiseptics have high specificity to treat wound infection and ultimately improve wound healing (Forbes, 1961). However, the emergence of microbial resistance has resulted in the need to find alternative treatments for wound infections. In addition, systemic antibiotic treatment can be difficult in certain wounds such as diabetic ulcers due to poor blood circulation at the extremities of diabetic patients (Bowler *et al.*, 2001). In modern wound care practice, antibiotics such as neomycin, bacitracin, streptomycin (STP), gentamycin and polymixin and/or combinations of these are used to treat chronic wounds (Bowler *et al.*, 2001; Howes, 1947; Pieleesz *et al.*, 2011).

Wounds with critical colonization and bacterial infection result in possible delays in the healing process. Patients with chronic wound infection experience additional consequences such as pain and discomfort. Additionally, colonized and infected wounds are a major source for cross-infection particularly antibiotic-resistant species. For example, wounds such as burns provide a protein-rich environment containing avascular necrotic tissue which is favourable for microbial colonization and proliferation (Church *et al.*, 2006). Majority of infected wounds involve *Staphylococcus aureus*, *Pseudomonas aeruginosa*, *beta-haemolytic streptococci* and *Escherichia coli* and are responsible for delayed wound healing. *S. aureus* is considered a challenging microorganism in traumatic, surgical and burn wound infections (Bowler *et al.*, 2001). This necessitates medicated dressings with broad spectrum antimicrobials, which can decrease the resistance and multiplication of these microorganisms. Based on this observation, three different microorganisms (*S. aureus*, *E. coli* and *P. aeruginosa*) were selected to evaluate the antimicrobial activity of the DL films and wafers and their comparison with selected marketed medicated dressings.

Dutta and co-workers (2007) reported that diclofenac sodium (DLF) has notable antibacterial activity and when used in combination with the STP, it increases activity

synergistically against *Mycobacterium tuberculosis* (Dutta *et al.*, 2007). STP has been previously used to treat wound infection in combination with penicillin (Edward and Howes, 1947). It has also been reported that DLF possesses low to moderate antibacterial activity against Gram positive and Gram negative bacteria and systemic STP in combination with DLF demonstrated synergistic antimicrobial activity (Duta *et al.*, 2004; Mazumdar *et al.*, 2009). Combination of STP and DLF within a single dressing is expected to act on two phases of wound healing, i.e. STP preventing as well as treating wound infections whilst DLF can target the inflammatory phase to relieve pain and swelling associated with injury.

In this study, we report on evaluation of minimum inhibitory concentration (MIC) of STP and DLF present in films and wafers using *S. aureus*, *E. coli* and *P. aeruginosa*. *In vitro* antibacterial efficacy of the films and wafers were evaluated using disk diffusion assay and their potency compared with marketed dressings using the three different microorganisms.

## 6.2 Materials

Marketed dressings Aquacel<sup>®</sup> Ag (ConvaTech, Ltd.), Melgisorb<sup>®</sup> Ag (Mölnlycke Health Care, Ltd.) were obtained as a gift from the manufacturer and Allevyn<sup>®</sup> Ag (Smith and Nephew, Ltd.) were obtained from a local pharmacy. Nutrient agar (lab lemco powder 1.0gm/L, yeast extract 2.0gm/L, peptone 5.0gm/L, sodium chloride 5.0gm/L, agar 15.0gm/L) and nutrient broth (lab lemco powder 1.0gm/L, yeast extract 2.0gm/L, peptone 5.0gm/L, sodium chloride 5.0 gm/L) were purchased from Oxoid, UK. Phosphate buffer tablets (PBS) (one tablet dissolved in 200 mL of deionized water yields 0.01 M phosphate buffer, 0.0027 M potassium chloride and 0.137 M sodium chloride, pH 7.4, at 25°C) were purchased from Sigma-Aldrich, Gillingham, UK. Sodium chloride (NaCl), calcium chloride dihydrate (CaCl<sub>2</sub>.2H<sub>2</sub>O), tris(hydroxymethyl)aminomethane, Petri dishes of 90 mm diameter were purchased from Fisher Scientific. National Collection of Type Culture (NCTC) *S. aureus* (A 29213), *E. coli* (DTCC 25922) and *P. aeruginosa* (A 10145) strains, were used for microbiological assays.

### 6.3 Formulations

The DL films and wafers were prepared as described in *Chapter 2 (2.3.3)* and *chapter 3 (3.2.2)* respectively, and used for antibacterial study. Formulations used for this study are summarised in table 6.1.

Table 6.1: Formulations used to evaluate antimicrobial efficacy against *S. aureus*, *P. aeruginosa* and *E. coli*.

<b>Formulation</b>	<b>CODE</b>
POL-CAR-BLK	A
POL-CAR-DL	B
POL-CAR-DL-20%GLY	C
POL-SA-BLK	D
POL-SA-DL	E
POL-SA-DL-9%GLY	F
POL-CAR-BLK-An	G
POL-CAR-DL-An	H
POL-SA-BLK-An	I
POL-SA-DL-An	J
Aquacel <sup>®</sup> Ag	K
Melgisorb <sup>®</sup> Ag	L
Allevyn <sup>®</sup> Ag	M
STP	N
DLF	O

## 6.3 Methods

### 6.3.1 Bacterial storage and preparation

Bacterial stock cultures of *S. aureus*, *E. coli* and *P. aeruginosa* were stored at  $-80^{\circ}\text{C}$ . Fresh bacterial cultures were prepared at  $37^{\circ}\text{C}$  by transferring a single bead unit to 10 ml of nutrient broth and incubating for 24 hours. A loop full of bacterial culture was streaked onto a nutrient agar plate and incubated at  $37^{\circ}\text{C}$  for 24 h to yield separate colonies. Broth cultures were prepared as reported by Labovitiadi *et al.*, (2012). In brief, 100 ml of nutrient broth in a 100 ml of reagent media graduated bottle was inoculated with one discrete colony and incubated with orbital agitation (100 rpm) at  $37^{\circ}\text{C}$  for 18 h. Overnight bacterial cultures were centrifuged at 4000 rpm for 10 min in a centrifuge (Accuspin 1 centrifuge, Fisher Scientific, UK). The supernatant was discarded and bacterial pellets suspended in 20 ml of SWF. This process was repeated twice and the pellets suspended in 5 ml of SWF, followed by suitable two fold dilutions in SWF. Bacterial density was determined spectrophotometrically by measurement of the dilute suspension at a wavelength of 500 nm to yield the required density of  $10^5$  CFU/ml (Labovitiadi *et al.*, 2012).

### 6.3.2 Minimum inhibitory concentration (MIC) of STP and DLF

The MIC for STP and DLF was evaluated as reported by Andrews (2001). In brief, three different stock solutions for each drug (STP and DLF) were prepared. The potency of STP given by the manufacturer is  $785\mu\text{g}/\text{mg}$ . The amount of STP required to obtain 10000mg/L was calculated using equation 6.1. Further, two different stock solutions were prepared as shown in table 6.2. STP 254.8 mg (potency  $785\mu\text{g}/\text{mg}$ ) and DLF 200.2 mg were weighed and dissolved separately in an appropriate volume of distilled water to obtain 10000 mg/L stock solutions. Antimicrobial susceptibilities of *S. aureus*, *E. coli* and *P. aeruginosa* were determined by establishing the MIC using a standard agar dilution method. Further, 0.25-512 mg/L calibration solutions of DLF and STP dilutions were prepared. The specified amount of stock solutions and two other dilutions (10000 mg/L, 1000 mg/L and 100 mg/L respectively) were transferred into a Petri plate with the addition of 20 ml of nutrient agar ( $50^{\circ}\text{C}$ ) and mixed. The agar was allowed to set at room temperature after which 0.1ml of  $2\times 10^5$  CFU/ml of *S. aureus*, *E. coli* and *P. aeruginosa* were spread separately on the individual Petri plates. These plates were incubated at  $37^{\circ}\text{C}$  for 24h and after the incubation period, it was ensured that all microorganisms had grown

on the drug free control plate. MIC is the lowest concentration of antibiotic at which there is no visible growth of the organisms. Growth of one or two colonies or a fine film of growth was disregarded (Andrews, 2001).

$$W = \frac{1000}{P} \times V \times C \quad \text{Equation 6.1}$$

Where,  $W$  is a weight of antibiotic (mg) dissolved in volume  $V$  (ml),  $C$  is final concentration of solution (multiples of 1000 mg/L),  $P$  is the potency given by the manufacturer ( $\mu\text{g}/\text{mg}$ ), and  $V$  is the volume required in ml.

$$W = \frac{1000}{785} \times 20 \times 10$$

$$W = 254.8\text{mg}$$

Table 6.2: Stock solutions of STP and DLF used to evaluate MIC of *S. aureus*, *E. coli* and *P. aeruginosa* (mean  $\pm$  SD, n=3).

	Stock solution 1	Stock solution 2	Stock solution 3
STP	10000 mg/L (254 mg of STP + 20 ml of distilled water)	1000 mg/L (1 ml of stock solution 1 + 9 ml of distilled water)	100 mg/L (1 ml of stock solution 2 + 9 ml of distilled water)
DLF	10000 mg/L (200 mg of DLF + 20 ml of distilled water)	1000 mg/L (1 ml of stock solution 1 + 9 ml of distilled water)	100 mg/L (1 ml of stock solution 2 + 9 ml of distilled water)

### 6.3.3 *In vitro* antibacterial study

#### 6.3.3.1 Disk diffusion assay of POL-CAR-DL films using $10^9$ CFU/ml

Disk diffusion assay was used for the assessment of antibacterial activity of POL-CAR-DL and POL-CAR-DL-20%GLY films. Strains were diluted from nutrient broth into  $10^{-6}$  dilution (representing highly infected chronic wounds). For the individual strains of  $10^{-6}$  dilution, bacterial count (n=3) was determined through the plate count method (*S. aureus* (A29213) -  $1 \times 10^9$  CFU/ml; *E. coli* (DTCC25922) -  $2 \times 10^9$  CFU/ml; *P. aeruginosa* (A10145) -  $2 \times 10^9$  CFU/ml

respectively). A 0.1ml volume of a 24-h incubated nutrient broth of clinical strains of *S. aureus*, *E. coli* and *P. aeruginosa* were spread separately on nutrient agar media. Films were cut into 6 mm disc shapes and placed on the colonised agar plate. Whatmann paper discs (6 mm), each wetted with reference solutions of STP and DLF at concentrations of 3 mg/ml and 1 mg/ml respectively, were placed on the agar medium containing the bacterial strains as a positive control. Negative control was represented by using the POL-CAR-BLK film (6 mm circular disc) (data not shown). Plates were then incubated at 37°C±1°C for 24 h, after which the end zones of inhibition (ZOI) in millimetres, formed on the medium (n=3) were evaluated. The percentage zone inhibition was calculated using equation 6.2.

$$Z = \frac{B-A}{A} \times 100 \quad \text{Equation 62}$$

Where Z is the % ZOI, B is the ZOI due to combined effect of both drugs in the film and A is the ZOI due to the effect of each individual drug.

#### **6.3.3.2 Disk diffusion assay of films and wafers and marketed dressing using 10<sup>5</sup>**

##### **CFU/ml**

The disk diffusion method was used for the assessment of the antibacterial activity of the films, wafers and marketed dressings (as shown in table 6.1). 2×10<sup>5</sup> CFU/ml of each bacterial strain (*S. aureus*, *E. coli* and *P. aeruginosa*) was prepared as specified in (section 6.3.1) and then 0.1ml of clinical strains of *S. aureus*, *E. coli* and *P. aeruginosa* having 10<sup>5</sup> CFU/ml were spread separately on nutrient agar media. The inoculated microorganisms were incubated at 37°C±1°C for 4 h initially before placing the DL formulations (films, wafers and marketed dressings) to initiate growth of microorganism on the inoculated culture medium. Films were cut into 2 cm diameter disc shapes before they were placed on the colonised agar plate. For the wafers, 2 g of drug loaded gels of POL-CAR-DL-An and POL-SA-DL-An were placed in 2 cm diameter containers and freeze-dried to obtain the same size of films and placed on prepared agar plates. Circular Whatmann<sup>®</sup> paper discs (2 cm diameter), each wetted with (80 µl) reference solutions of STP and DLF at concentrations of 6 mg/ml and 5 mg/ml respectively, were placed on the agar medium containing the bacterial strains as a positive control. Negative control was represented by using the BLK film and wafers (2 cm diameter discs). Plates were then incubated at 37°C±1°C for 24 h after which the end zones of inhibition (ZOI) in millimetres formed on the

medium (n=3) were evaluated. Graphical representation of the disk diffusion assay is shown in figure 6.1.

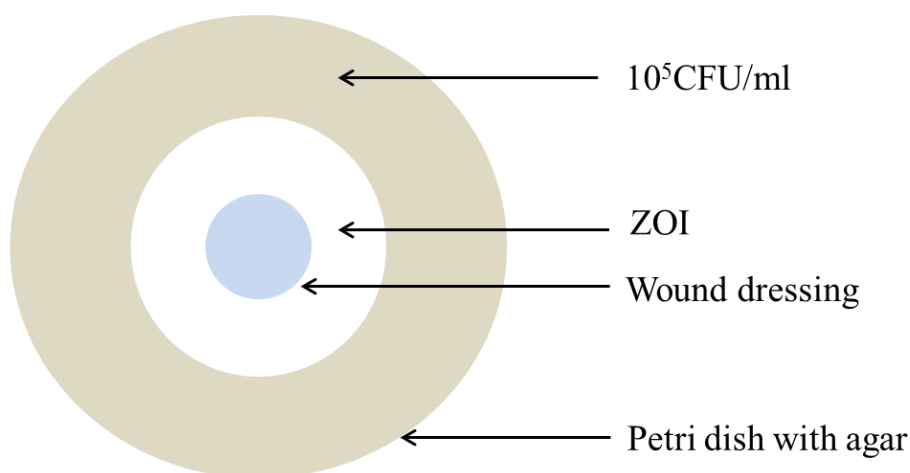


Figure 6.1: Graphical representation of disk diffusion assay

#### 6.3.4 Statistical analysis

Statistical data evaluation was performed using two tailed student t-test with 95 % confidence interval (p value < 0.05) as the minimal level of significance. Statistical analysis of data obtained from the ZOI was performed using Graph Pad Prism 4 software.

### 6.4 Results and discussion

#### 6.4.1 Minimum inhibitory concentration (MIC) of STP and DLF

To kill the bacteria, STP and DLF must interact with the binding site to occupy critical number of sites of the bacteria and remain there for a time period to inhibit normal biochemical reactions. The concentration required to occupy the number of binding sites necessary to terminate biochemical process of bacteria STP is relatively low compared to DLF. However, this proportional concentration can easily be measured in terms of MIC. The MIC for DLF is reported in the literature for *S. aureus*, *E. coli* and *P. aeruginosa* as 5-100 mg/L, 25-200 mg/L and 200-500 mg/L respectively whereas MIC for STP was found to be  $\geq 20$  mg/L for *E. coli*, and 16-64 mg/L for *P. aeruginosa* (Martindale, 1993; Harrel and Evans, 1978). The concentrations of the reference solutions used were higher [1 mg/ml (DLF) and 3 mg/ml (STP)] than their respective MICs. The MIC of antimicrobial compounds (STP and DLF) was determined for known densities ( $10^5$  CFU/ml) of common bacterial strains (*S. aureus* *P. aeruginosa* *E. coli*)

associated with infected, non-healing chronic wounds. Table 6.3 shows the measured values of MIC for STP and DLF tested against a bacterial density of  $10^5$  CFU/ml. As can be seen from the figures, the MIC of DLF was much higher than that of the conventional antibacterial drug (STP). A MIC value of STP for *S. aureus* and *E. coli* ranged from 4-8 mg/L but increased two fold for the *P. aeruginosa* ranging from 8-16 mg/L. Both *S. aureus* and *E. coli* are Gram negative microorganisms whilst *P. aeruginosa* is Gram positive and requires a higher MIC compared to the *S. aureus* and *E. coli*. This means STP is more effective against the Gram positive microorganism *P. aeruginosa* than the Gram negative *E. coli* and *S. aureus*. In previous studies, it has been demonstrated that the time required to kill the *S. aureus* is higher than the *P. aeruginosa* which is time dependent. In contrast to STP, DLF required higher concentrations to kill the bacteria that are beyond those clinically achievable with antibiotics such as STP. It was observed that to kill the *P. aeruginosa*, DLF required higher concentrations compared to that for *E. coli* and *S. aureus*. The experiential MIC values of DLF for the *P. aeruginosa* was greater than 512 mg/L but ranged from 256 - 512 mg/L for *E. coli* and *S. aureus* respectively. Dutta *et al.*, (2004) previously demonstrated that when DLF is used *in vitro*, it showed higher MIC but *in vivo*, the amount of DLF required to protect an animal from *Mycobacterium spp* was much lower than that of STP. This suggests that such drugs might be used as adjuvants to current antimicrobials used for the management of bacterial infections (Dutta *et al.*, 2004; 2007; Mazumdar *et al.*, 2006). DLF also consists of a secondary amino group and a phenyl ring, both ortho positions of which are occupied by chlorine atoms, causing an angle of torsion between the two aromatic rings, which mimic the structural similarities with phenothiazine and responsible for the antibacterial activity against the microorganisms such as *E. coli*, *S. aureus* and *P. aeruginosa* (Mazumdar *et al.*, 2009, Dutta *et al.*, 2004; 2007; 2008).

Table 6.3: MIC values for STP and DLF for *S. aureus*, *P. aeruginosa* and *E. coli* (mean  $\pm$  SD, n = 3).

Bacterial strains	MIC	
	STP	DLF
<i>S. aureus</i>	4 – 8 mg/L	512 mg/L
<i>P. aeruginosa</i>	8 – 16 mg/L	$\geq$ 512 mg/L
<i>E. coli</i>	4 – 8 mg/L	256 mg/L

#### 6.4.2 Antimicrobial efficacy of control pure STP and DLF

The ZOI of the STP and DLF positive control for *S. aureus*, *P. aeruginosa* and *E. coli* are shown in figure 6.2. The positive control of STP and DLF was selected based on the maximum amount of the STP and DLF present in the films and wafers. STP showed significantly ( $P = 0.0004$ ) low ZOI ( $3.2 \pm 0.1 \text{mm}$ ) for the *S. aureus* compared to *P. aeruginosa* and *E. coli*. The maximum ZOI of *P. aeruginosa* was  $4.1 \pm 0.1 \text{mm}$  which was lower compared to *E. coli* ( $4.6 \pm 0.1 \text{mm}$ ) and was statistically significant ( $P = 0.0036$ ).

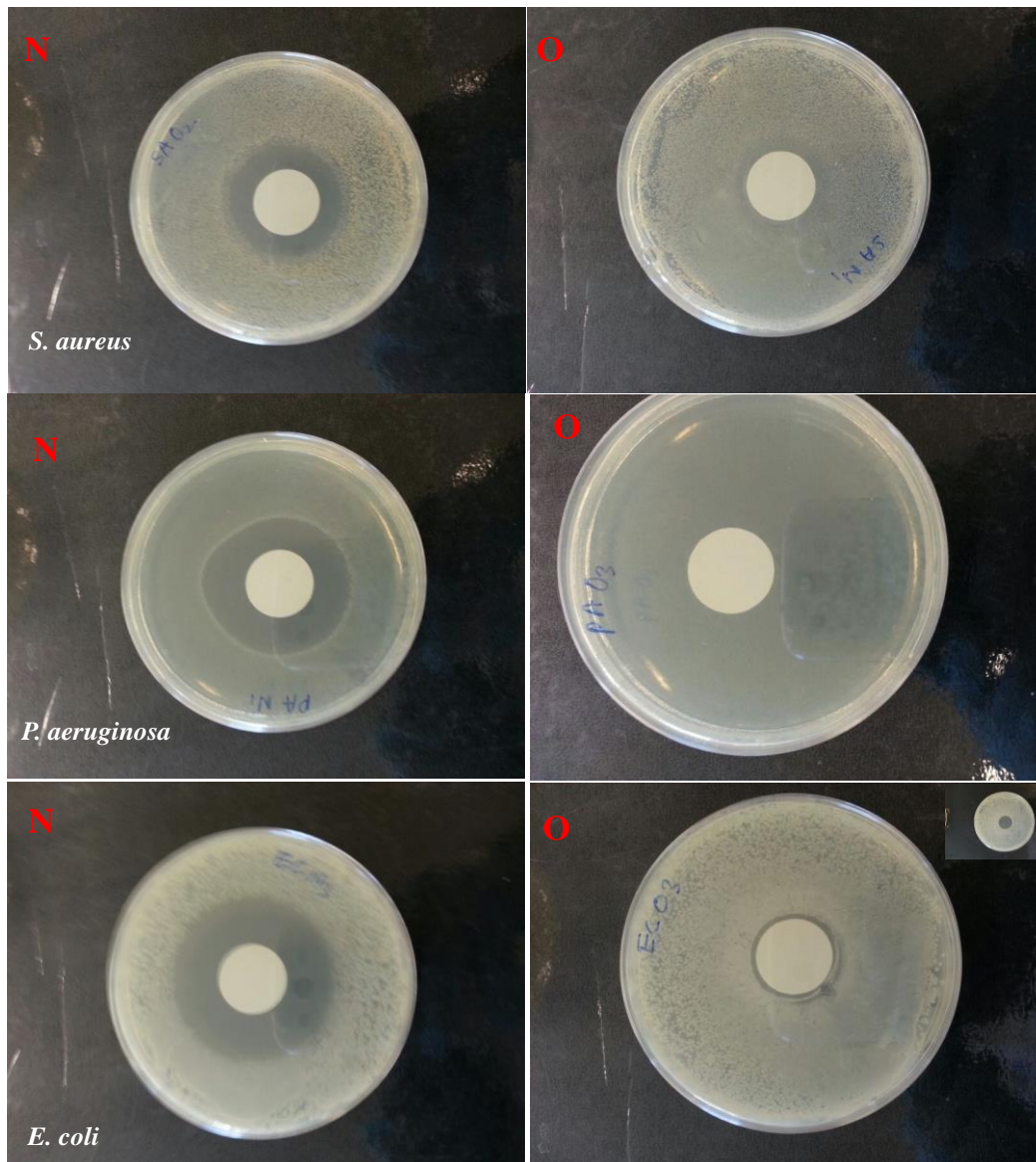


Figure 6.2: ZOI of (N) control STP (O) control DLF for *S. aureus*, *P. aeruginosa* and *E. coli*. The inset of control DLF shows the absence of bacteria around the applied area of the disk (mean  $\pm$  SD,  $n = 3$ ).

The observed ZOI of STP, DLF and all the formulations (films, wafers and marketed dressing) are shown in table 6.4. DLF did not show ZOI for *S. aureus*, *P. aeruginosa* and *E. coli* but there was no bacteria growing under the DLF disc rather than around the disc as shown in inset (Figure 6.2) which showed that their effectiveness is limited with their application.

Table 6.4: ZOI of film, wafer and marketed dressings with the positive control of STP and DLF for *S. aureus*, *P. aeruginosa* and *E. coli* (mean  $\pm$  SD, n = 3).

Formulation	ZOI $\pm$ SD (mm)		
	<i>S. aureus</i>	<i>P. aeruginosa</i>	<i>E. coli</i>
POL-CAR-BLK	-	-	-
POL-CAR-DL	3.6 $\pm$ 0.1	4.3 $\pm$ 0.1	4.8 $\pm$ 0.2
POL-CAR-DL-20% GLY	3.5 $\pm$ 0.1	4.3 $\pm$ 0.1	4.7 $\pm$ 0.1
POL-SA-BLK	-	-	-
POL-SA-DL	4.6 $\pm$ 0.2	4.8 $\pm$ 0.2	5.0 $\pm$ 0.2
POL-SA-DL-9% GLY	4.1 $\pm$ 0.2	5.2 $\pm$ 0.2	5.5 $\pm$ 0.2
POL-CAR-BLK-An	-	-	-
POL-CAR-DL-An	3.1 $\pm$ 0.1	3.9 $\pm$ 0.1	4.5 $\pm$ 0.1
POL-SA-BLK-An	-	-	-
POL-SA-DL-An	3.3 $\pm$ 0.1	4.1 $\pm$ 0.2	4.6 $\pm$ 0.3
Aquacel <sup>®</sup> Ag	2.0 $\pm$ 0.1	2.0 $\pm$ 0.0	2.0 $\pm$ 0.0
Melgisorb <sup>®</sup> Ag	2.2 $\pm$ 0.1	2.0 $\pm$ 0.0	2.0 $\pm$ 0.0
Allevyn <sup>®</sup> Ag	2.3 $\pm$ 0.1	2.0 $\pm$ 0.0	2.9 $\pm$ 0.0
Control STP	3.2 $\pm$ 0.1	4.1 $\pm$ 0.1	4.6 $\pm$ 0.2
Control DLF	2.0 $\pm$ 0.0	2.0 $\pm$ 0.0	2.1 $\pm$ 0.0

#### 6.4.3 Antibacterial efficacy of POL-CAR films ( $10^9$ CFU/ml)

Table 6.5 shows diameters and percentage ZOIs of the individual drugs as well as combined drugs present within POL-CAR films when placed on agar cultures containing  $1 \times 10^9$ ,  $2 \times 10^9$ ,  $2 \times 10^9$  CFU/ml of *S. aureus*, *E. coli* and *P. aeruginosa* strains respectively. The ZOI with regards to DLF and STP, DL loaded films were larger in size compared to those for the

individual drugs (Figure 6.3). These differences were determined statistically using a student's t-test which showed significant ( $P < 0.01$ ) differences in ZOI's with respect to all the bacterial strains. At a lower concentration, there was a 60-70% increase in ZOI of *S. aureus*, 30-50% for *E. coli* and 80-90% for *P. aeruginosa* when compared with the individual ZOIs of DLF. Films containing both drugs showed 10-16% increase in ZOI for *P. aeruginosa* and *S. aureus* and 8-15% for *E. coli* when compared with percent increase in individual ZOIs of STP.

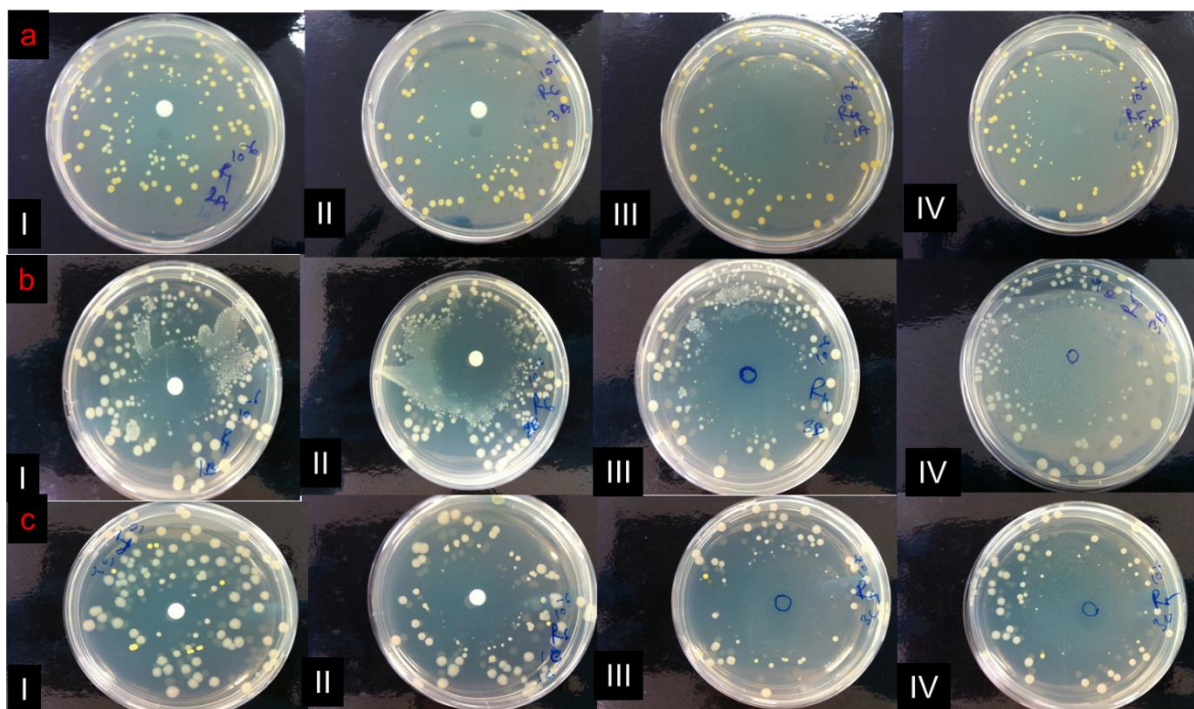


Figure 6.3: Antibacterial activity of STP, DLF and combined (STP + DLF) within film at bacterial load of  $10^9$  CFU/ml for (a) *S. aureus* (b) *E. coli* (c) *P. aeruginosa*. (I-DLF reference, II-STP reference, III- POL-CAR-DL films, IV-POL-CAR-DL-20% GLY).

The study confirmed that the DL films were effective against the main causative microorganisms found in infected chronic wounds and can inhibit both Gram positive and Gram negative bacteria. It has been shown previously that the combination of both drugs in systemic administration provides a synergistic effect in antimicrobial activity of STP (Mazumdar *et al.*, 2009) and this was confirmed *in vitro* when both drugs (STP and DLF) were incorporated into a single polymeric film.

Table 6.5: The diameter and percentage increase in the ZOI of *S. aureus*, *E. coli* and *P. aeruginosa* using bacterial load of  $10^9$  CFU/ml (mean  $\pm$  SD, n = 3).

10 <sup>9</sup> (CFU/ml) bacterial solution	Diameter of ZOI (mm)				% Increase in ZOI for each drug in films			
	Reference drug		DL film		DLF		STP	
	DLF	STP	POL-CAR-DL	POL-CAR-DL- 20%GLY	POL-CAR- DL	POL-CAR-DL- 20%GLY	POL-CAR-DL	POL-CAR-DL- 20%GLY
<i>S. aureus</i> (A29213) 1x10 <sup>9</sup>	2.4 ( $\pm$ 0.2)	3.4 ( $\pm$ 0.1)	4.0 ( $\pm$ 0.1)	3.9 ( $\pm$ 0.1)	67.6	62.7	15.9	12.6
<i>E. coli</i> (DTCC25922) 2x10 <sup>9</sup>	2.7 ( $\pm$ 0.2)	3.3 ( $\pm$ 0.2)	3.8 ( $\pm$ 0.1)	3.5 ( $\pm$ 0.2)	45.6	32.1	14.22	7.7
<i>P. aeruginosa</i> (A10145) 2x10 <sup>9</sup>	2.2 ( $\pm$ 0.1)	3.6 ( $\pm$ 0.1)	4.1 ( $\pm$ 0.2)	4.0 ( $\pm$ 0.2)	86.8	80.9	13.9	10.2

#### 6.4.4 Antibacterial activity of POL-CAR films ( $10^5$ CFU/ml)

Figures 6.4 and 6.5 show the ZOI of (POL-CAR-DL and POL-CAR-DL-20% GLY) films for *S. aureus*, *P. aeruginosa* and *E. coli* bacterial strains. POL-CAR-BLK films did not show any zone for all three different microorganisms (Figure 6.5).

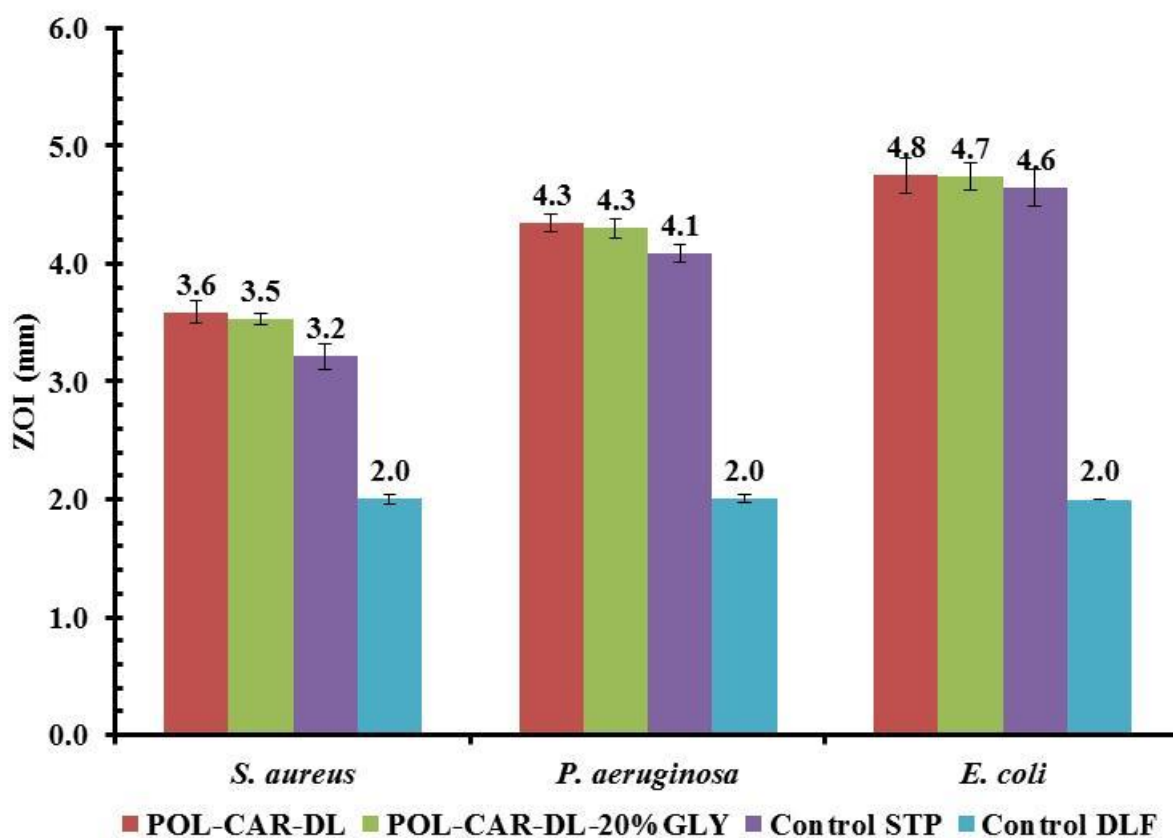


Figure 6.4: ZOI of *S. aureus*, *P. aeruginosa* and *E. coli* for the POL-CAR (DL and DL-20%GLY) films and STP and DLF (mean  $\pm$  SD, n = 3).

There was a significant difference observed for ZOI of all POL-CAR films for the individual strains of bacteria. Both DL films (POL-CAR-DL and POL-CAR-DL-20% GLY) showed a smaller ZOI for *S. aureus* but was increased for *P. aeruginosa* and *E. coli*. For all strains of bacteria both DL films showed higher ZOI compared to control STP and DLF. For *S. aureus* the observed ZOI for POL-CAR-DL and POL-CAR-DL-20%GLY films was  $3.6 \pm 0.1$  mm and  $3.5 \pm 0.1$  mm respectively whereas STP was  $3.2 \pm 0.1$  mm and the difference was statistically significant ( $P < 0.0213$ ). For *P. Aeruginosa*, the observed ZOI was higher than *S. aureus* but less than *E. coli*. POL-CAR-DL and POL-CAR-DL-20%GLY films showed similar ZOI  $4.3 \pm 0.1$  mm which was higher than the control STP  $4.1 \pm 0.1$  mm and the difference was not statistically

significant ( $P < 0.0705$ ). The maximum ZOI of POL-CAR-DL and POL-CAR-DL-20%GLY films was  $4.8 \pm 0.2$  mm,  $4.7 \pm 0.1$  mm for *E. coli* and  $4.6 \pm 0.2$  mm for the control STP and the differences were not statistically significant ( $P = 0.4818$ ).

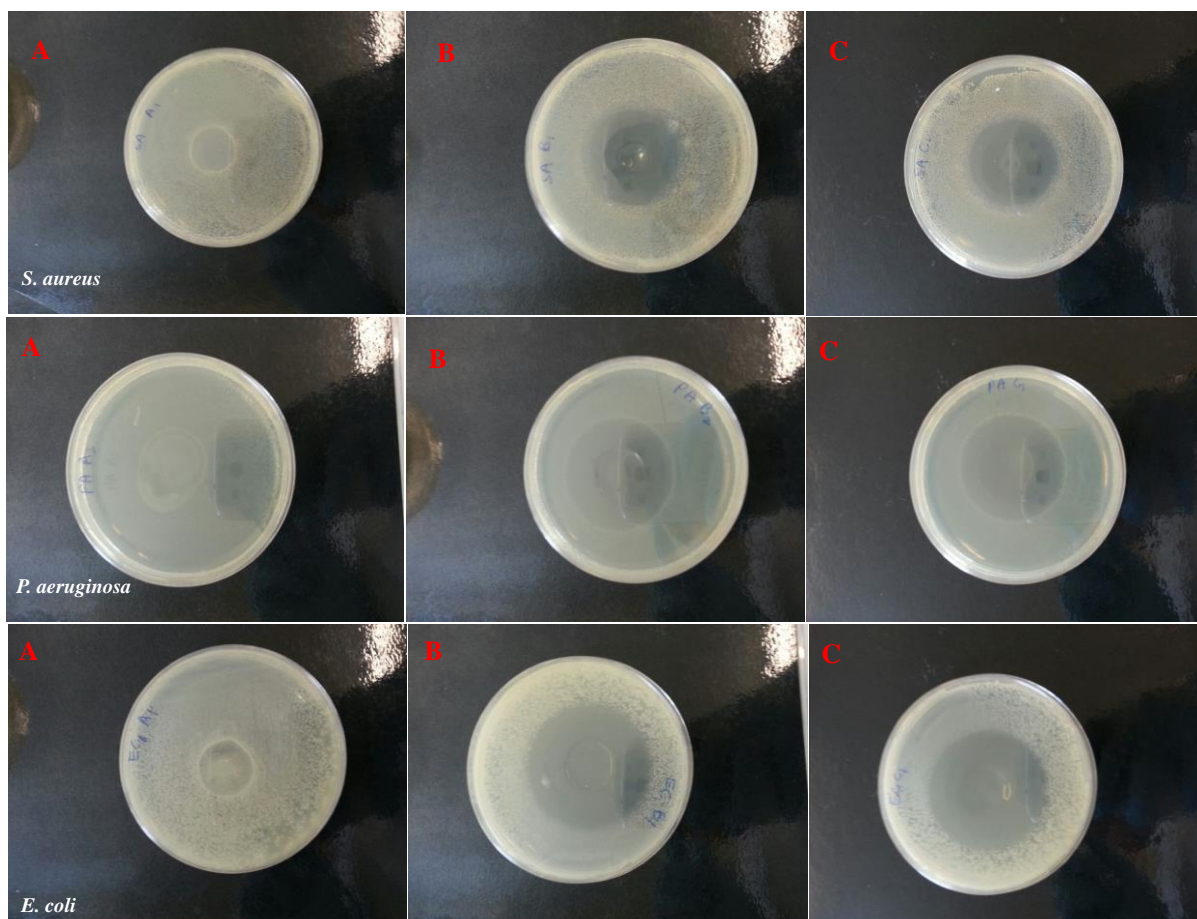


Figure 6.5: The digital images of ZOI of (A) POL-CAR-BLK, (B) POL-CAR-DL, (C) POL-CAR-DL-20%GLY observed for *S. aureus*, *P. aeruginosa* and *E. coli* (mean  $\pm$  SD,  $n=3$ ).

#### 6.4.5 Antibacterial activity of POL-SA films ( $10^5$ CFU/ml)

Figures 6.6 and 6.7 show the ZOI of POL-SA-DL and POL-SA-DL-9% GLY) films for *S. aureus*, *P. aeruginosa* and *E. coli* bacterial strains. POL-SA-BLK films did not show any zone for all three different microorganisms (Figure 6.7). There were significant differences observed for the ZOIs of all POL-SA films for the individual strains of bacteria. Both DL films (POL-SA-DL and POL-SA-DL-9% GLY) showed a smaller ZOI for *S. aureus* but were increased for *P. aeruginosa* and *E. coli*.

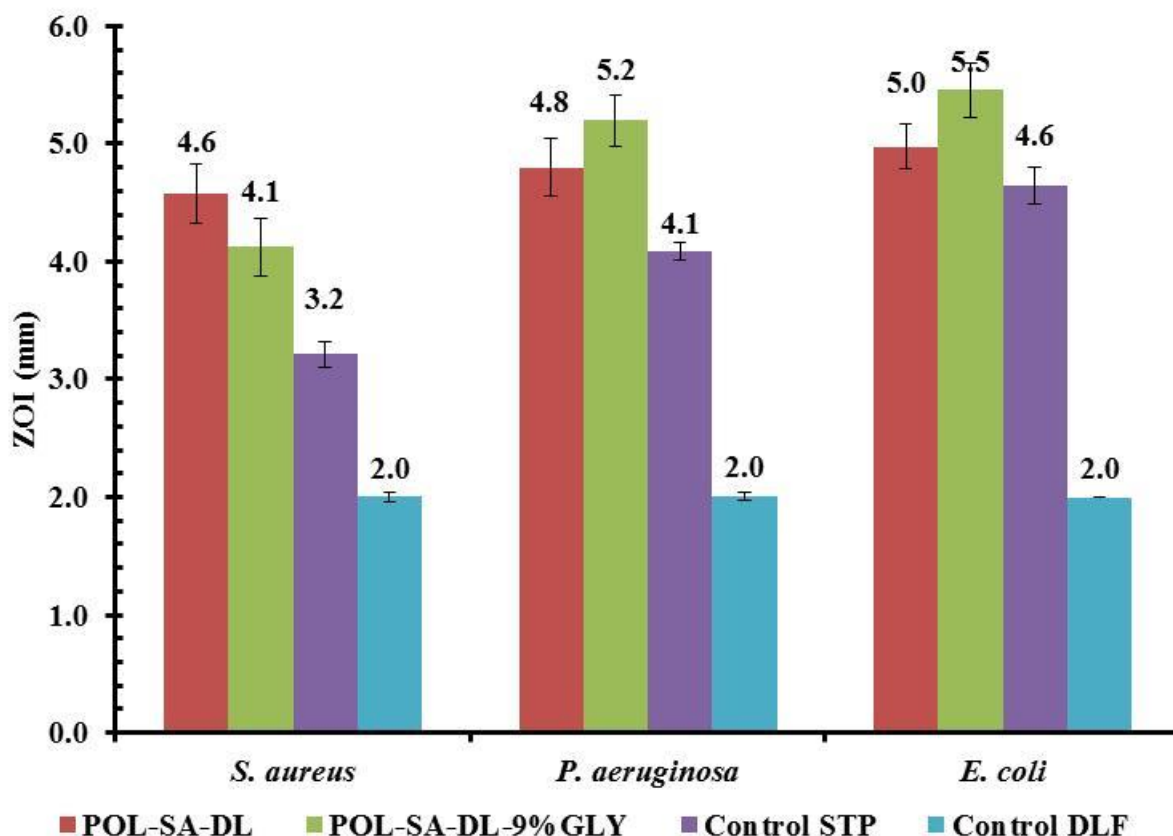


Figure 6.6: ZOI of *S. aureus*, *P. aeruginosa* and *E. coli* for the POL-SA-DL and POL-SA-DL-9%GLY films and control STP and DLF (mean  $\pm$  SD, n = 3).

For all strains of bacteria both DL-SA films showed higher ZOI compared to control STP and DLF. For *S. aureus*, the observed ZOI for POL-SA-DL and POL-SA-DL-9%GLY films was  $4.6 \pm 0.2$ mm and  $4.1 \pm 0.2$ mm respectively which was very high compared to the STP  $3.2 \pm 0.1$ mm and it was statistically significant ( $P = 0.0022$ ). POL-SA-DL films showed higher ZOI than the POL-SA-9%GLY films for *S. aureus* whereas the reverse was true for *P. aeruginosa* and *E. coli*. The ZOI was increased from  $4.6 \pm 0.2$ mm (*S. aureus*) to  $4.8 \pm 0.2$ mm (*P. aeruginosa*) and  $5.0 \pm 0.2$ mm (*E. coli*) for POL-SA-DL films while for POL-SA-9%GLY films it was increased from  $4.1 \pm 0.2$ mm (*S. aureus*) to  $5.1 \pm 0.2$ mm (*P. aeruginosa*) and  $5.5 \pm 0.2$ mm (*E. coli*) respectively. For *P. aeruginosa*, the observed ZOI was higher than *S. aureus* but less than *E. coli*. POL-SA-DL and POL-SA-DL-9%GLY films showed  $4.8 \pm 0.2$ mm and  $5.2 \pm 0.2$ mm ZOI which was higher than the control STP  $4.1 \pm 0.1$ mm and the difference was statistically significant ( $P = 0.0128$ ). The maximum ZOI of POL-CAR-DL and POL-CAR-DL-20%GLY films were respectively  $5.0 \pm 0.2$ mm,  $5.5 \pm 0.2$ mm for *E. coli* and  $4.6 \pm 0.2$ mm for the control STP. It can easily be observed that both films had significantly higher ZOI suggesting a synergistic effect when

both drugs were combined together compared to the ZOI for each individual drug. ZOI was ellipsoidal due to the quick swelling of the polymer matrix and rapid diffusion of the drugs (STP and DLF) through POL-SA DL films.

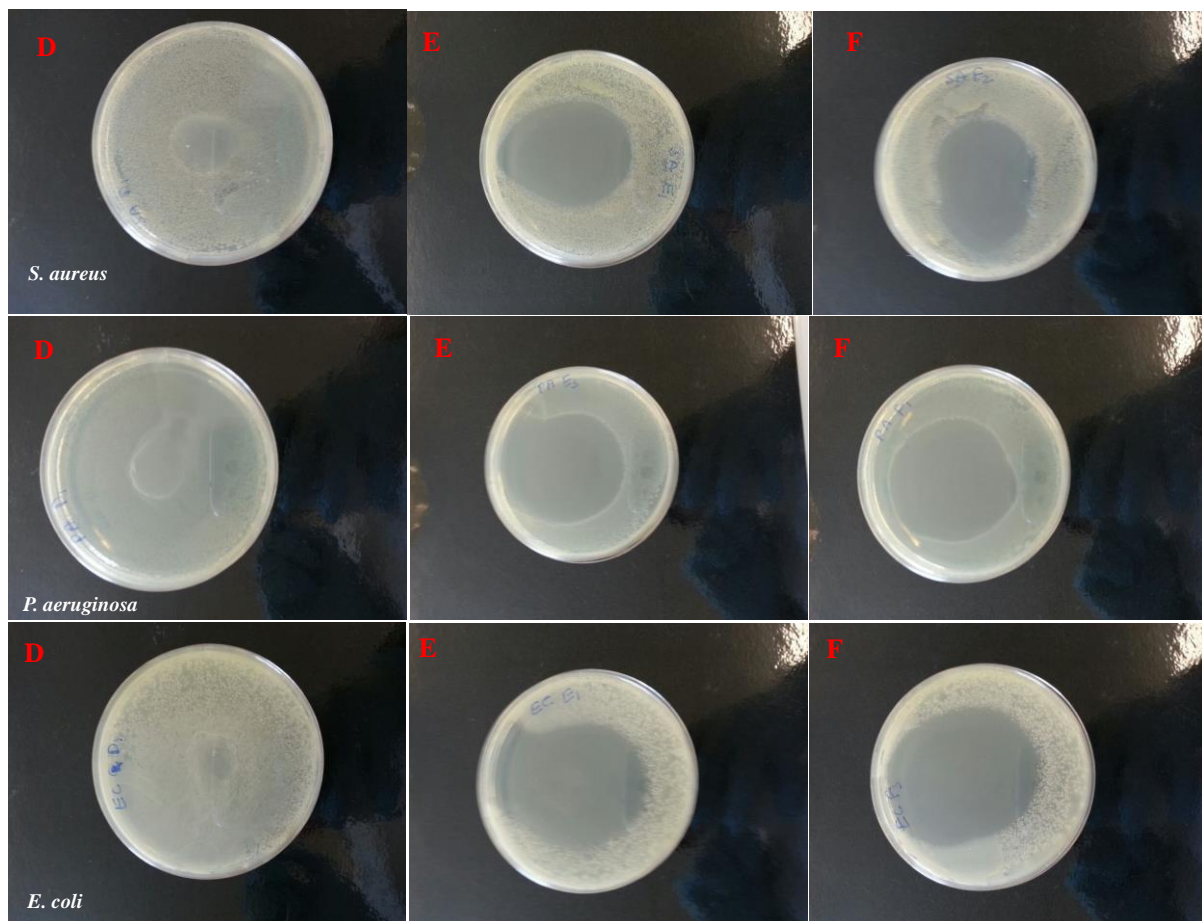


Figure 6.7: The digital images of ZOI of (D) POL-SA-BLK, (B) POL-SA-DL, (C) POL-SA-DL-9%GLY observed for *S. aureus*, *P. aeruginosa* and *E. coli* (mean  $\pm$  SD, n = 3).

#### 6.4.6 Antibacterial activity of POL-CAR and POL-SA wafers ( $10^5$ CFU/ml)

Figures 6.8 and 6.9 show the ZOI of POL-CAR and POL-SA (BLK-An and DL-An) wafers for *S. aureus*, *P. aeruginosa* and *E. coli* bacterial strains. As was observed for the corresponding films, POL-CAR-BLK-An and POL-SA-BLK-An wafers did not show any inhibition zone for all three different microorganisms (Figure 6.9, G and I).

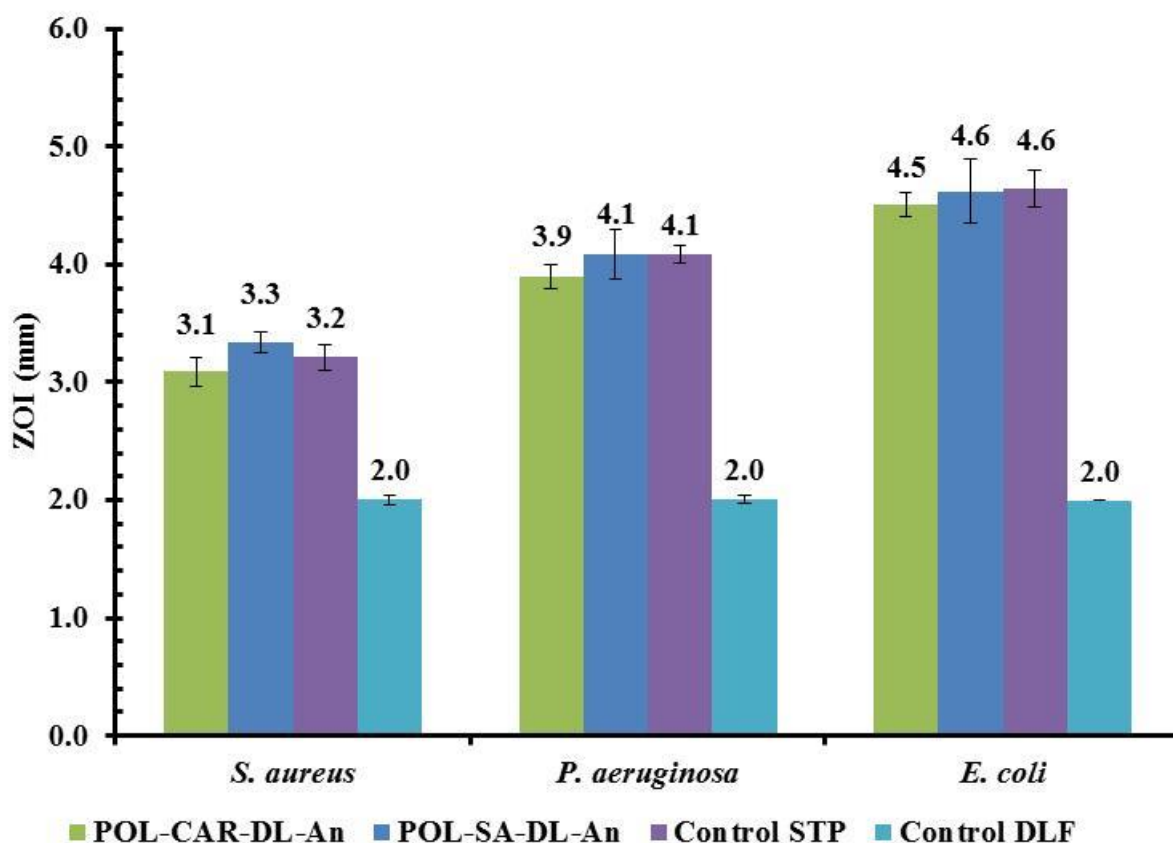


Figure 6.8: ZOI of *S. aureus*, *P. aeruginosa* and *E. coli* for POL-CAR-DL-An and POL-SA-DL-An wafers and control STP and DLF (mean  $\pm$  SD, n = 3).

There were significant differences observed for all POL-CAR-DL-An and POL-SA-DL-An wafers ZOI for *S. aureus*. Both DL wafers showed a smaller ZOI for *S. aureus* but was increased for *P. aeruginosa* and *E. coli*. For all strains of bacteria, both DL wafers showed similar ZOI compared to control STP. For *S. aureus*, the observed ZOI for POL-CAR-DL-An was smaller compared to the POL-SA-DL-An wafers. The ZOI of POL-CAR-An for *S. aureus* was  $3.1 \pm 0.1$  mm which increased to  $3.3 \pm 0.1$  mm whereas STP had a value of  $3.2 \pm 0.1$  mm which was not statistically significant. For *P. aeruginosa*, the observed ZOI was higher than *S. aureus* but less than *E. coli*. POL-SA-DL-An and STP showed similar ZOI of  $4.1 \pm 0.2$  mm which subsequently decreased for POL-CAR-DL-An ( $3.9 \pm 0.1$  mm). The maximum ZOI of POL-CAR-DL-An and POL-SA-DL-An wafers was respectively  $4.5 \pm 0.1$  mm and  $4.6 \pm 0.3$  mm for *E. coli* and  $4.6 \pm 0.2$  mm for the control STP. Differences in the ZOI of POL-CAR-DL-An and POL-SA-DL-An could be associated with two different polymers and their percentage ratios used for the formulation of wafers and their different swelling mechanisms which subsequently affects the diffusion of drug through the matrix.

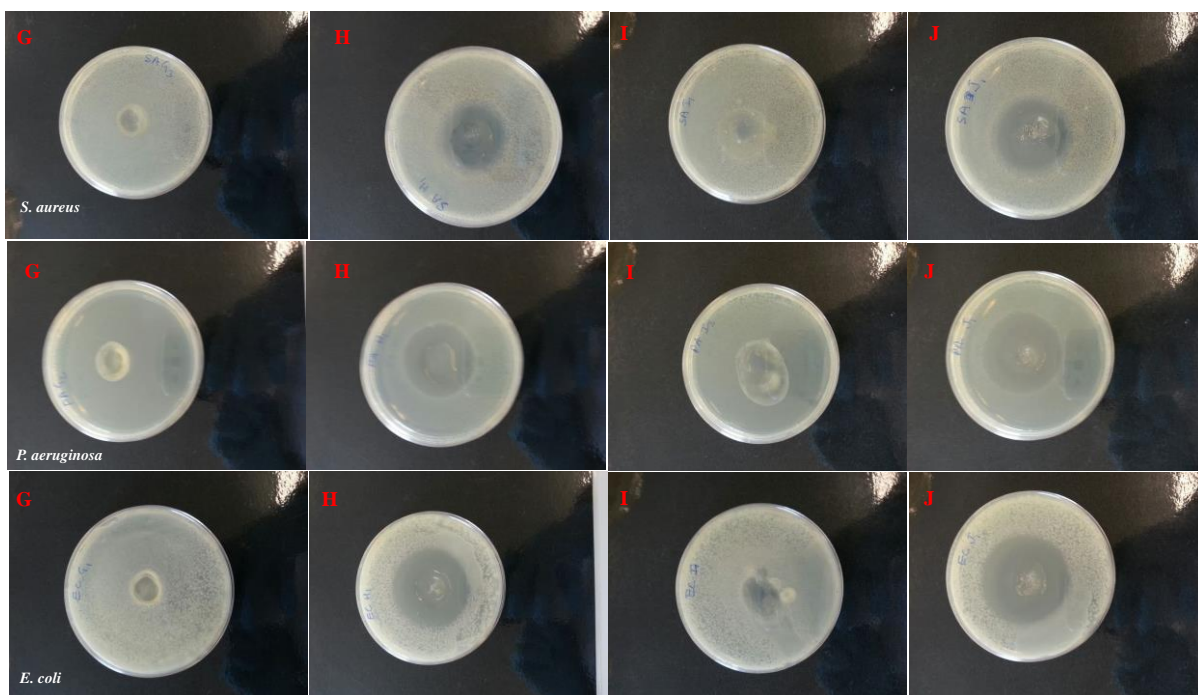


Figure 6.9: Digital images of ZOI of (G) POL-CAR-BLK-An, (H) POL-CAR-DL-An, (I) POL-SA-BLK-An, (J) POL-SA-DL-An, observed for *S. aureus*, *P. aeruginosa* and *E. coli* (mean  $\pm$  SD, n = 3).

#### 6.4.7 Antimicrobial efficacy of marketed wound dressings ( $10^5$ CFU/ml)

Silver is a broad spectrum antimicrobial agent and has wide spread use to treat infected chronic wounds. Figure 6.10 and figure 6.11 show the ZOI of marketed dressings (Aquacel<sup>®</sup> Ag, Melgisorb<sup>®</sup> Ag and Allevyn<sup>®</sup> Ag) for *S. aureus*, *P. aeruginosa* and *E. coli* bacterial strains.

To compare the performance in terms of antibacterial activity of the formulated films, wafers and marketed medicated dressings, against *S. aureus*, *P. aeruginosa* and *E. coli* Aquacel<sup>®</sup> Ag, Melgisorb<sup>®</sup> Ag and Allevyn<sup>®</sup> Ag were selected. Their manufacturer and description are given in the table 6.6.

Table 6.6: Description of the silver containing dressings used for antimicrobial study (Hamberg *et al.*, 2012).

Product	Manufacturer	Formulation details	Silver content (mg/cm <sup>2</sup> )
Aquacel <sup>®</sup> Ag	ConvaTec	Sodium carboxymethylcellulose with ionic silver	0.08-0.09
Melgisorb <sup>®</sup> Ag	Mölnlycke Health Care	Alginate dressing with silver sodium hydrogen zirconium phosphate	0.08
Allevyn <sup>®</sup> Ag	Smith & Nephew	Polyurethane foam dressing with soft gel adhesive and silver sulphadiazine	0.90

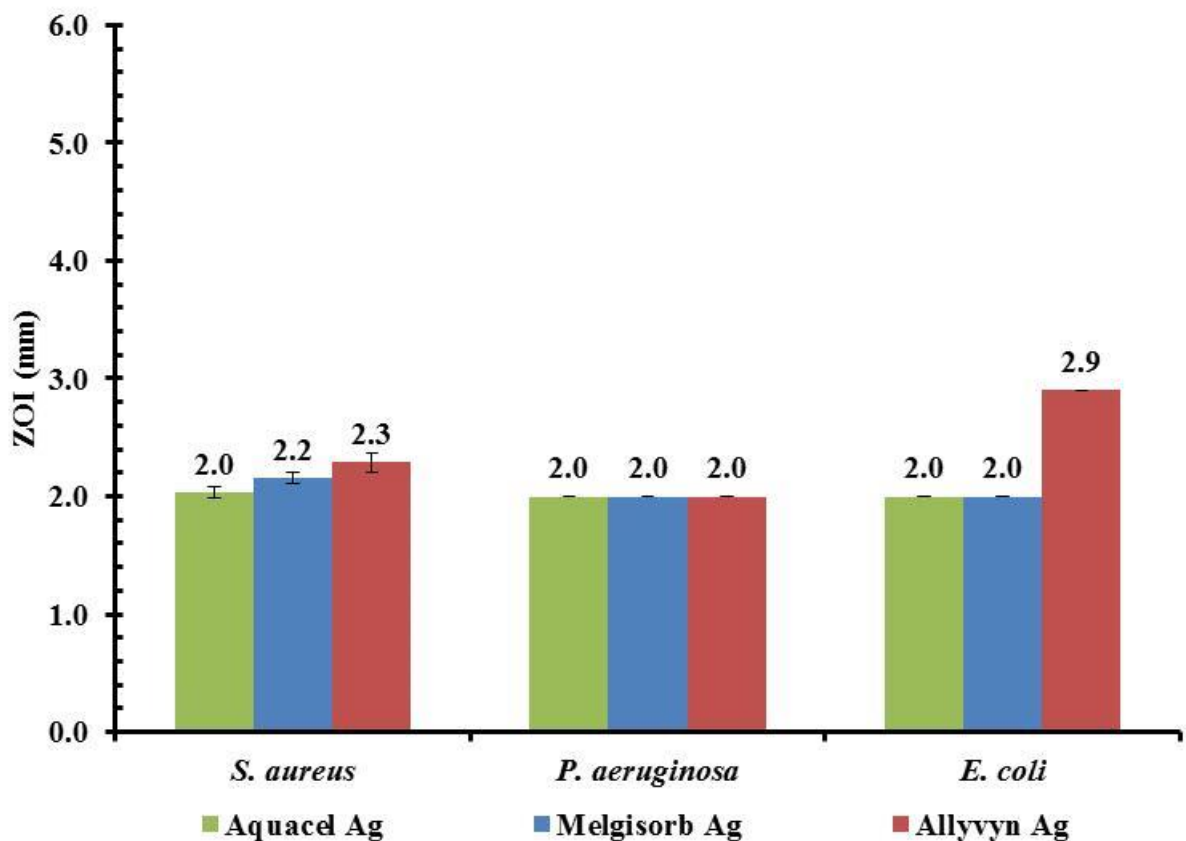


Figure 6.10: ZOI of *S. aureus*, *P. aeruginosa* and *E. coli* for the marketed dressings (Aquacel<sup>®</sup> Ag, Melgisorb<sup>®</sup> Ag, Allevyn<sup>®</sup> Ag (mean  $\pm$  SD, n=3).

There was very small ZOI observed for all three different strains of microorganisms but there was absence of these bacteria in the area directly underneath the dressing as shown in figure 6.11 inset (M). The ZOI for *S. aureus* was increased for Allevyn Ag while all three marketed dressings showed a ZOI of  $2.0 \pm 0.1$  mm for *P. aeruginosa*. The ZOI for *E. coli* was higher for Allevyn<sup>®</sup> Ag foam dressing ( $2.9 \pm 0.0$  mm) compared to Aquacel<sup>®</sup> Ag, Melgisorb<sup>®</sup> Ag ( $2.0 \pm 0.0$  mm).

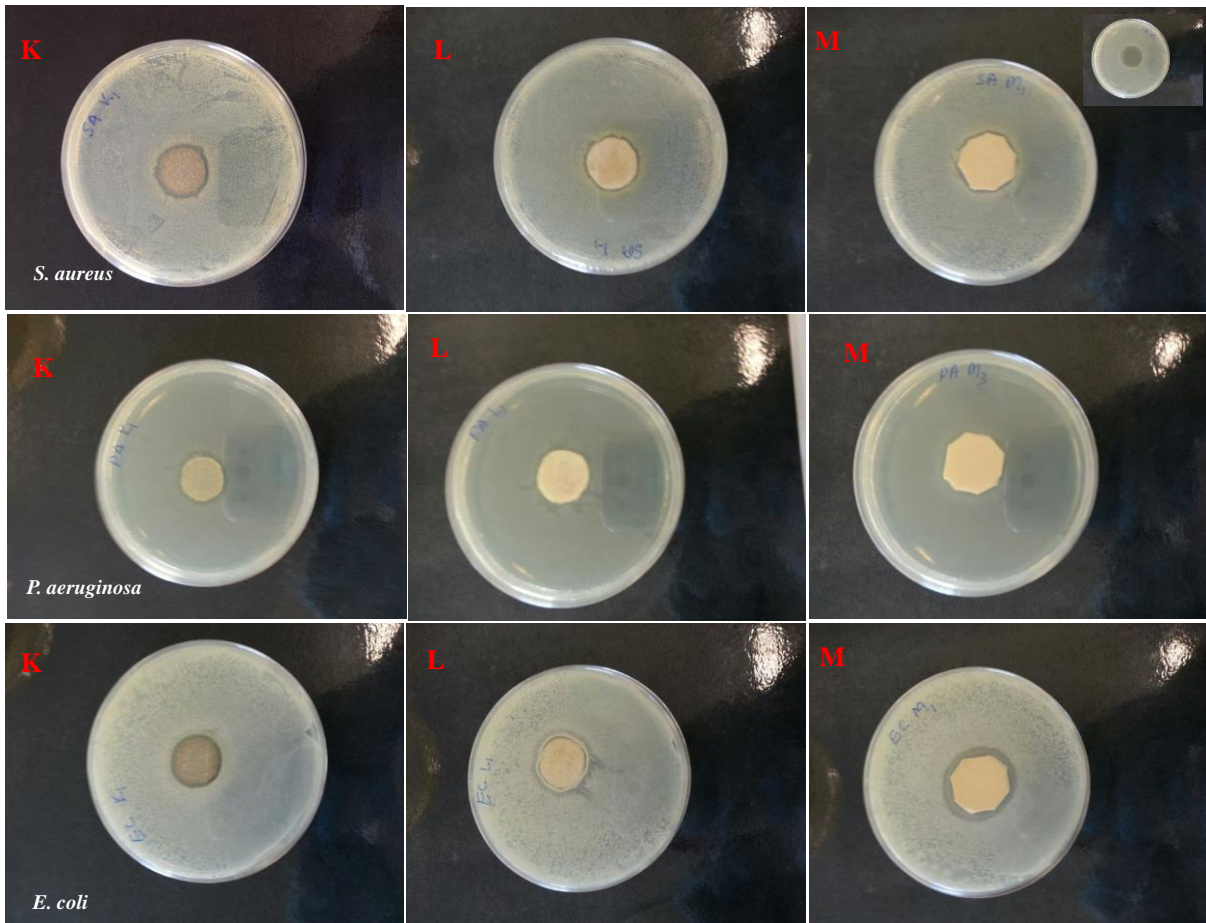


Figure 6.11: Digital images of ZOI observed for *S. aureus*, *P. aeruginosa* and *E. coli* of (K) Aquacel<sup>®</sup> Ag; (L) Melgisorb<sup>®</sup> Ag; and (M) Allevyn<sup>®</sup> Ag. Inset shows the absence of bacteria at the applied area of dressing (mean  $\pm$  SD, n = 3).

#### 6.4.8 Comparison of antibacterial activity of the film, wafer and marketed wound dressings

Many texts refer to bacterial bio-burden greater than  $10^5$  CFU/ml organisms per gram of tissue or  $10^6$  CFU/ml of wound fluid as a criterion for infection (Bowler *et al.*, 2001; White *et al.*, 2001). In this study we used  $2 \times 10^5$  CFU/ml of *S. aureus*, *P. aeruginosa* and *E. coli* to

evaluate antimicrobial efficacy of DL film and wafer dressings and compared their performance against the marketed low adherent dressings containing silver. For *S. aureus*, different ZOIs were observed for the films, wafers and marketed dressings. This can correlate with the swelling studies and diffusion of STP and DLF from the films and wafers. Maximum ZOI was observed for POL-SA-DL and POL-SA-DL-9%GLY films. When these films were applied on the inoculated agar they swelled very rapidly and subsequently allowed the diffusion of both drugs (STP and DLF) from the swollen films. The increased ZOI is associated with the quick swelling and disintegration of SA which supports the swelling and drug release studies (*chapter 4*). This rapid disintegration of POL-SA films allowed the formation of less viscous and free flowing liquid gel which passed through the incubated *S. aureus*, *P. aeruginosa* and *E. coli*, resulting in the ellipsoidal shaped ZOI (Figure 6.7). POL-CAR-DL and POL-CAR-DL-20% GLY films showed less ZOI compared to POL-SA films with the ZOI for POL-CAR-DL and POL-CAR-DL-20%GLY films for *S. aureus* being  $3.6\pm 0.1\text{mm}$  and  $3.5\pm 0.1\text{mm}$  and  $4.3\pm 0.1\text{mm}$  for *P. aeruginosa*,  $4.8\pm 0.1\text{mm}$  and  $4.7\pm 0.1\text{mm}$  for *E. coli* respectively. The presence of sodium sulphate formed from the salt forms of the drugs reduced the hydration capacity of both films and wafers. This salt induced reduction in hydration capacity decreased the diffusion rate of drugs (STP and DLF) from POL-CAR DL films when compared with POL-SA-DL films.

Wafers generally have a higher loading capacity, faster hydration and cumulative percent drug release compared to films due to their porous nature (Boateng *et al.*, 2009). However, it was observed that higher drug loading in the wafers resulted in the formation of greater amounts of sodium sulphate compared to the films which decreased the hydration capacity (as seen in *chapter 4*) of DL wafers subsequently affecting diffusion of STP and DLF with a consequent decrease in ZOI compared to films but greater than the marketed dressings. The observed ZOI for POL-CAR-DL-An and POL-SA-DL-An wafers for *S. aureus* was  $3.1\pm 0.1\text{mm}$  and  $3.3\pm 0.1\text{mm}$ ,  $3.9\pm 0.1\text{mm}$  and  $4.1\pm 0.2\text{mm}$  respectively for *P. aeruginosa* and  $4.5\pm 0.1\text{mm}$  and  $4.6\pm 0.3\text{mm}$  respectively for *E. coli*. All the marketed dressing showed either lower or absence of ZOI for all three different microorganisms which may be due to the presence of lower amounts of silver present in these dressings (Table 6.6) relative to the concentration of STP and DLF present in the films and wafers. Silver is a widely used anti-microbial agent effective against causative wound pathogens which are responsible for delayed wound healing and can be added to a range of composite dressings (Vermeulen, *et al.*, 2009). Silver containing wound dressings liberate silver ions which vary due to the different forms (silver sulfadiazine, ionic silver etc.)

and the amount of the silver present in wound dressing (Dowsett, 2004). Silver in the presence of moisture such as wound exudate readily ionises to release silver ions ( $\text{Ag}^+$ ) or other biologically active ions, which binds to the nucleophilic amino acids and proteins within cell membranes, resulting in protein denaturation and enzyme inhibition (Jung *et al.*, 2008). Although there are important questions raised by some authors in regards to the use of silver in infected wounds and formation of biofilms by the microorganisms, the versatile effect of silver carries a low risk of resistance even though some studies in burn wounds have shown bacterial resistance to silver sulfadiazine and silver nitrate by *Pseudomonas spp* (Modak, 1981). Moreover, the antimicrobial effect of silver incorporated in a number of dressings depends on the release rate of silver ions which influences the resulting antimicrobial effect (Ovington, 2004). Furthermore, *in vivo* silver binds to proteins present in biofilms which is an extracellular protein matrix instead of binding to the bacterial cell walls resulting in reduced antimicrobial effect against the bacteria (Mertz 2003). Another potential concern is that silver does not act specifically against bacteria but also acts on any host proteins. Hence, if very few bacteria counts are present at the wound site, then the effect on host tissue is greater which could slow down healing (Innes *et al.*, 2001). Concentrations above 1mg/L (1 parts per million) of silver reacts with wound exudate and may cause transient skin staining which was observed *in vitro* testing (Percival *et al.*, 2005). Therefore, there is the need to consider possible toxic effects of silver. Li and co-authors suggested that bacterial resistance could be induced when low concentrations of silver were used (Li *et al.*, 1997). There is therefore the possibility of these silver containing dressings to induce resistance from *S. aureus* and *P. aeruginosa* which are capable to form biofilm in a chronic wound infection (Braff *et al.*, 2007).

DLF's antibacterial activity was due to its inhibition of bacterial DNA synthesis whereas STP acts by binding to 30S ribosomal subunits in the microorganisms and disrupting the initiation and elongation steps in protein synthesis. There was absence of bacteria at the application area of the marketed dressings which means these dressing are effective to kill the bacteria at only the applied area of the wound. However, dressings containing STP and DLF (i.e. POL-CAR and POL-SA films and wafers) appear to show synergistic action of the two drugs with consequent increase in the ZOI and could potentially resist the formation of biofilms within the wounds. All the DL films showed greater antibacterial activity compared to wafers whilst POL-SA films and wafers were more effective to kill bacteria than POL-CAR films and wafers due to the rapid swelling of the polymeric network and subsequent diffusion of STP and

DLF from the resulting swollen gel. Similarly, wafers showed lower ZOI due to reduced hydration which limited diffusion of the STP and DLF. Both films showed synergetic effect of combined addition of STP and DLF in film matrix but did not show any synergetic effect in wafers due to their limited hydration and subsequent slower diffusion of STP and DLF. From a formulation perspective, film and wafer dressings were different in their weight which ranged from 22.1 mg and 30.3 mg for POL-CAR DL films and wafers respectively. These could be associated with the different loading capacity and the total amounts of polymer present in films and wafers which resulted in the different hydration rate of films and wafer and eventually different ZOIs. This was also true for the POL-SA DL films and wafers where their weights ranged from 17.9 mg and 24.6 mg with different types and ratios of polymer used for the preparation of films and wafers.

The formulated films and wafers with varying degrees of hydration can be advantageous for the variety of chronic infected wounds from low to moderate exuding wounds as wound exudate production varies from 3-5 ml/10cm<sup>2</sup>/24 hours. In other words, slow hydration of films and wafers will allow the absorbance of the exudate and maintaining a moist environment with the diffusion of STP and DLF. However, it must be remembered that a wound typically has non-uniform surfaces which can affect the release of STP and DLF from the dressing but in such case, the dressing may align well with the wound edges to prevent further bacterial contamination. This sustained release of STP and DLF will minimise bacterial load which will ultimately decrease the wound healing time.

## 6.5 Conclusion

The future threat of ineffectual control of wound infections caused by antibacterial-resistant strains of pathogens is sufficient reason to consider modifying present approaches towards finding a modified dressing which can avoid resistance and reduce the formation of biofilm formed by bacteria. The formulated films, wafers and marketed dressing showed antibacterial efficacy against bacterial bio-burden greater than 10<sup>5</sup> CFU/ml of *S. aureus*, *P. aeruginosa* and *E. coli* which is a criterion for infection. Films and wafers were highly effective against *E. coli*, *P. aeruginosa* and *S. aureus*. POL-SA films were more effective to kill the bacteria compared to the POL-CAR films. Furthermore, POL-SA wafers showed greater antibacterial effect than POL-CAR wafers. In all the formulations, the formulated film dressings, showed greater antibacterial efficacy than wafers and marketed dressing. STP and DLF present

in both films and wafers can act synergistically not only to kill the bacteria but also avoid the resistance and biofilm formation of the bacteria compared to marketed dressings. STP can help to reduce bacterial infection by its antimicrobial action and potentially in synergy with DLF while the latter can also help to reduce the swelling and pain associated with injury due to its anti-inflammatory action. These will however, require further investigations in an *in vivo* study.

## CHAPTER 7: SUMMARY CONCLUSIONS AND FUTURE WORK

### 7.1 Summary conclusions

This project aimed to develop, formulate, characterise and optimise solvent cast films and freeze-dried wafers to deliver antimicrobial and anti-inflammatory drugs (STP and DLF) to act on two different phases of wound healing with low toxicity to improve chronic wound healing. In this section, a summary of conclusions on the formulation, optimisation and analytical characterisation of the films and wafers using various techniques (SEM, XRD, DSC, TA and FTIR) and determination of functional characteristics including swelling capacity, mucoadhesion, *in vitro* release profiles and release kinetics in addition to antibacterial activity of films, wafers and marketed dressing as a medicated wound dressing for chronic wound healing is presented.

Solvent cast film dressing from synthetic POL and combination of natural and semi-synthetic polymer CAR, SA, CS and HPMC were prepared from an optimum 1% polymer gel. Combination of POL with two different natural polymers (CAR and SA) in different ratios (75/25 and 50/50 respectively) showed homogeneous surface morphology and transparency compared to POL combined with either HPMC or CS. Improved flexibility was obtained by incorporating GLY in POL-SA and POL-CAR films while XRD studies showed a reduction in spherulitic crystallisation of POL by addition of the hydrophilic natural (CAR, SA, CS) and semi-synthetic (HPMC) polymers. FTIR analysis revealed specific intermolecular interactions between POL and these four hydrophilic polymers (CAR, CS, SA and HPMC). This was confirmed by DSC studies which revealed suppression of melting peak of POL due to the molecular chain of CAR and SA which had a significant effect on overall chain mobility within the film matrix and retarded spherulitic crystallisation. Films with 20%GLY (POL-CAR) and 9%GLY (POL-SA) were tough and flexible and easy to handle. The optimised films present ideal characteristics for wound healing application to difficult areas such as knees and joints and also can withstand some frictional stresses during day-to-day activities. This implies that these films have the potential to absorb energy without breaking in the event of accidental frictional stress and thus provide a protective effect over the wound. However, the films showed relatively low drug loading capacities. Films loaded with 5-10% DLF and 15-30% of STP resulted in the formation of sodium sulphate which reduced transparency in the films.

DSC was used to determine an appropriate lyophilisation cycle by evaluating thermal events before lyophilisation to select a suitable annealing temperature. The annealing step in lyophilisation cycle helped to obtain the desired porous structure for POL-CAR and POL-SA wafers. Wafers showed higher drug loading capacities with 15-25% DLF and 25-30% DLF without affecting the physical structure and appearance of the wafers. Wafers were soft, flexible and porous in nature, showed adequate mechanical strength which is enough to withstand mechanical stresses occurring during day-to-day activities and also flexible enough to prevent potential damage to newly formed tissue.

As was the case in films, XRD showed the presence of sodium sulphate whereas DSC showed molecular dispersion of both drugs within both films and wafers.

POL-CAR-DL and POL-SA-DL films possessed properties that meet desirable characteristics of an ideal dressing. This was due to their smooth homogeneous surface morphology, elegant appearance and fair transparency which can allow observation of progression of the wound healing process. High elasticity provided optimum flexibility that can allow better conformation to wound surface especially around joints such as knees and elbows. However, their application is not suited for highly suppurating wounds unlike POL-SA and POL-CAR DL-An wafers which is an advantage for the latter two formulations, due to their soft, flexible and in particular porous nature which improves ease of hydration, mucoadhesion and *in vitro* drug release characteristics. Therefore, DL films and wafers can be potentially used respectively for medium and highly exuding chronic wound ulcers.

The findings of the swelling study helped to evaluate the capacity of the formulated film and wafer dressings to withstand exudate (3-5ml/10cm<sup>2</sup>/24h) produced by suppurating chronic wounds whilst ensuring a moist environment as well as maintaining the structural integrity of the applied dressing. BLK wafers showed higher swelling capacity due to their porous nature followed by GLY containing BLK films, DL films (plasticised and unplasticised) and DL-An wafers. Increased swelling capacity of BLK films and wafers was associated with the hydrophilicity of the polymers and the added GLY (films) which allowed a higher rate of water ingress. The reduced hydration and swelling of DL films and wafers was attributed to the formation of sodium sulphate due to the salt forms of the two model drugs (STP and DLF). POL-SA films showed more rapid swelling and disintegration compared POL-CAR films, whereas POL-CAR wafers showed higher swelling capacity compared POL-SA wafers. However,

between the two, POL-CAR films and wafers were better at maintaining their physical structure than POL-SA films and wafers. These films and wafers (POL-CAR) have the capacity to hold wound exudate for a reasonable time period. This could potentially help to overcome challenge of collection of excess exudate when applied to a moderate to highly exuding wound as well prevent the need for frequent dressing changes which can result in patient non-compliance.

*In vitro* dissolution studies showed sustained release of STP and DLF from both the films and wafers. Reduced hydration resulted in a slower release of DLF whereas STP was released in a more rapid but controlled manner for 3 days. During the first hours after wounding, a relatively high amount of antimicrobial drug release is essential to eliminate infections present in acute wounds that may not have been eliminated during wound cleansing and might create a resistant biofilm whereas chronic wounds are usually associated with the presence of bacteria which is the main cause of delayed healing. The initial burst release of these drugs can reduce infection which can progress wound healing quicker. Subsequently, a continuous sustained release can help to maintain a bacteria free wound for more than three days which usually depends upon wound exudate.

Mucoadhesive performance is critical in determination of residence time of films and wafers at a wound site to allow for sustained drug release and eventual bioavailability. Artificial exudate (SWF) contains large amounts of proteins and salts which may interfere with polymer-drug interactions and may affect mucoadhesive characteristics. Though significant differences were recorded in mucoadhesive performances of films and wafers, the differences were not by several folds. There was also a marked effect of different concentrations of SWF, GLY and drugs (STP and DLF) on mucoadhesive performance. Wafers showed higher mucoadhesive strength compared to the films due to their porous nature which allowed faster initial hydration which is important for mucoadhesion. DL films and wafers showed optimum mucoadhesive strength which was greater in BLK POL-SA and POL-CAR films and wafers. It appears that POL-SA films and wafers can be used in the presence of less viscous exudate to achieve prolonged retention time and bioavailability. POL-CAR films and wafers on the other hand can be used for wounds having viscous exudate to achieve better bioavailability and mucoadhesive performance. This can prolong residence times and bioavailability of drugs (STP and DLF) at the wound site and further help to overcome the problem of frequent dressing change. It can also control bacterial load associated with chronic wound infection and ultimately improve wound healing. ATR-FTIR spectroscopy has been used to follow diffusion of mucin as a model protein

across the films and wafers. Mucin diffused independently through the solvent and then across the films and wafers. POL-CAR films and wafers showed slow diffusion when compared with POL-SA films and wafers. POL-CAR wafers showed higher mucoadhesion in the presence of model protein mucin solution than POL-SA wafers which decreased in the presence of drug while plasticized films (POL-CAR and POL-SA) showed higher mucoadhesion than BLK and DL films.

The DL films and wafers were highly effective against *E. coli*, *P. aeruginosa* and *S. aureus*. POL-SA films were more effective to kill these bacteria compared to POL-CAR films. Furthermore POL-SA wafers showed greater antibacterial effect than POL-CAR wafers. In all formulations, films showed greater antibacterial efficacy than the wafers and both films and wafers had a greater efficacy to kill the bacteria compared to marketed silver based dressings. It was postulated that STP and DLF present in both films and wafers acted synergistically not only to kill the bacteria but also to avoid resistance and biofilm formation of bacteria compared to the marketed dressings. The advantage of incorporating both drugs in a single entity is that STP can help to reduce bacterial infection by its antimicrobial action and potentially in synergy with DLF while the latter can also help to reduce inflammation and pain associated with injury due to its anti-inflammatory action. Thus, it is expected to help speed the healing of wounds and thereby improve patients' compliance and comfort.

## **7.2 Future work**

1. Films and wafers prepared from the combination of synthetic and natural polymer were evaluated for intermolecular hydrogen bonding through FTIR analysis. This can be further evaluated through molecular and computer modelling.
2. *In vitro* mucoadhesion studies using the ATR-FTIR technique helped to monitor the entrapment of mucin into films and wafers which determined rate of diffusion of mucin solution through films and wafers. The same model can be used to further evaluate interaction and diffusion rate of the prepared formulations and chronic wound exudate (either artificial or from clinical surroundings). Further, porcine skin can be used with artificial wound exudate to evaluate the performance of the formulated wound dressing *ex vivo*.

3. Possible studies to determine antimicrobial potential and extent of synergism of STP and DLF can be designed to evaluate these further for films and wafers. Further, synergism of STP and DLF in the inhibition of bacterial infection as well as reduction of pain and inflammation can be further evaluated *in vivo* animal models particularly considering wound-healing parameters (e.g., complete wound healing, healing rate, and wound size reduction).
4. POL can undergo chain cleavage via auto-oxidation. Therefore, storage stability is an important issue for POL. The rate of auto-oxidation can be minimized through the addition of antioxidants since POL water-soluble resins contain some level of butylated hydroxytoluene (BHT) antioxidant. Further, stability studies for the DL films and wafers based on the International conference on harmonization (ICH) guidelines will need to be carried out to fully establish the stability of the formulated DL films and wafers. This will include possible instability due to the interactions of both drugs within the film and / or wafer matrix.
5. Quantify the porosity of the prepared BLK and DL POL-SA and POL-CAR annealed and non annealed wafers and water content of the BLK and DL films and annealed wafers.
6. Investigate the *in vivo* effect of DLF in wounds.

## CHAPTER 8: REFERENCES

1. Abdekhodaie, M. J. and Wu, X. Y. (2008) 'Drug release from ion-exchange microspheres: Mathematical modeling and experimental verification', *Biomaterials*, 29(11), 1654-1663.
2. Abruzzo, A., Bigucci, F., Cerchiara, T., Cruciani, F., Vitali, B. and Luppi, B. (2012) 'Mucoadhesive chitosan/gelatin films for buccal delivery of propranolol hydrochloride', *Carbohydrate Polymers*, 87(1), 581-588.
3. Adamson, A. W. (1990) *Physical chemistry of surfaces*, Wiley-Interscience, New York, 110–113.
4. Adams, E., Rafiee, M., Roets, E. and Hoogmartens, J. (2000) 'Liquid chromatographic analysis of streptomycin sulphate', *Journal of Pharmaceutical and Biomedical Analysis*, 24(2), 219-226.
5. Adderley, U. J. (2010) 'Managing wound exudate and promoting healing', *British journal of community nursing*, 15(3), S15-20.
6. Adekogbe, I. and Ghanem, A. (2005) 'Fabrication and characterization of DTBP-crosslinked chitosan scaffolds for skin tissue engineering', *Biomaterials*, 26(35), 7241-50.
7. Adeodato Vieira, M. G., da Silva, M. A., dos Santos, L. O. and Beppu, M. M. (2011) 'Natural-based plasticizers and biopolymer films: A review', *European Polymer Journal*, 47(3), 254-263.
8. Albritton, J., (1991) 'Complications of wound repair', *Clinics in Podiatric Medicine and Surgery*, 8(4), 773-785.
9. Alves, V., Costa, N., Hilliou, L., Larotonda, F., Goncalves, M., Sereno, A. and Coelho, I. (2006) 'Design of biodegradable composite films for food packaging', *Desalination*, 199(1-3), 331-333.
10. American Society of Testing and Materials, (D882-02). 2002. Annual book of ASTM standards. American Society for Testing and Materials. Philadelphia, PA, USA: pp 156–167, 324–332.
11. Andrews, J. M. (2001). Determination of minimum inhibitory concentrations. *Journal of antimicrobial Chemotherapy*, 48(suppl 1), 5-16.
12. Audic, J. L. and Chaufer, B. (2005) 'Influence of plasticizers and crosslinking on the properties of biodegradable films made from sodium caseinate', *European Polymer Journal*, 41(8), 1934-1942.

13. Ayensu, I., Mitchell, J. C. and Boateng, J. S. (2012) 'In vitro characterisation of chitosan based xerogels for potential buccal delivery of proteins', *Carbohydrate Polymers*, 89(3), 935–941.
14. Ayensu, I., Mitchell, J. C. and Boateng, J. S. (2012a) 'Development and physico-mechanical characterisation of lyophilised chitosan wafers as potential protein drug delivery systems via the buccal mucosa', *Colloids and Surfaces B: Biointerfaces*, 91(1), 258-265.
15. Ayensu, I., Mitchell, J. C. and Boateng, J. S. (2012b) 'Effect of membrane dialysis on characteristics of lyophilised chitosan wafers for potential buccal delivery of proteins', *International Journal of Biological Macromolecules*, 50(4), 905-909.
16. Azevedo, E. P., Saldanha, T. D. P., Navarro, M. V. M., Medeiros, A. C., Ginani, M. F. and Raffin, F. N. (2006) 'Mechanical properties and release studies of chitosan films impregnated with silver sulfadiazine', *Journal of Applied Polymer Science*, 102(4), 3462-3470.
17. Barresi, A. A., Pisano, R., Fissore, D., Rasetto, V., Velardi, S. A., Vallan, A., Parvis, M. and Galan, M. (2009) 'Monitoring of the primary drying of a lyophilization process in vials', *Chemical Engineering and Processing: Process Intensification*, 48(1), 408-423.
18. Beanes, R. S., Dang, C., Soo, C. and Ting, K. (2003). 'Skin repair and scar formation: the central role of TGF-[beta]'. *Expert Reviews in Molecular Medicine*, 5, 1-22.
19. Beldon, P. (2001) 'Recognising wound infection', *Nursing times*, 97(3), 3-4.
20. Beldon, P. (2010) 'Basic science of wound healing', *Surgery (Oxford)*, 28(9), 409-412.
21. Bendy, R. H., Jr., Nuccio, P. A., Wolfe, E., Collins, B., Tamburro, C., Glass, W. and Martin, C. M. (1964) 'Relationship of quantitative wound bacterial counts to healing of decubiti: effect of topical gentamicin', *Antimicrobial agents and chemotherapy*, 10, 147-55.
22. Berchane, N. S., Carson, K. H., Rice-Ficht, A. C. and Andrews, M. J. (2007) 'Effect of mean diameter and polydispersity of PLG microspheres on drug release: Experiment and theory', *International Journal of Pharmaceutics*, 337(1-2), 118-126.
23. Berger, J., Reist, M., Mayer, J. M., Felt, O. and Gurny, R. (2004a) 'Structure and interactions in chitosan hydrogels formed by complexation or aggregation for biomedical applications', *European Journal of Pharmaceutics and Biopharmaceutics*, 57(1), 35-52.
24. Bertrand, N., Leclair, G. and Hildgen, P. (2007) 'Modeling drug release from bioerodible microspheres using a cellular automaton', *International Journal of Pharmaceutics*, 343(1-

- 2), 196-207.
25. Bjarnsholt, T., Kirketerp-Møller, K., Jensen, P. Ø., Madsen, K. G., Phipps, R., Krogfelt, K., Høiby, N. and Givskov, M. (2008) 'Why chronic wounds will not heal: a novel hypothesis', *Wound Repair and Regeneration*, 16(1), 2-10.
  26. Boateng, J. S., Auffret, A. D., Matthews, K. H., Humphrey, M. J., Stevens, H. N. E. and Eccleston, G. M. (2010) 'Characterisation of freeze-dried wafers and solvent evaporated films as potential drug delivery systems to mucosal surfaces', *International Journal of Pharmaceutics*, 389(1-2), 24-31.
  27. Boateng, J. S., Matthews, K. H., Auffret, A. D., Humphrey, M. J., Stevens, H. N. and Eccleston, G. M. (2009a) 'In vitro drug release studies of polymeric freeze-dried wafers and solvent-cast films using paracetamol as a model soluble drug', *International Journal of Pharmaceutics*, 378(1-2).
  28. Boateng, J. S., Matthews, K. H., Stevens, H. N. E. and Eccleston, G. M. (2008) 'Wound healing dressings and drug delivery systems: A review', *Journal of Pharmaceutical Sciences*, 97(8), 2892-2923.
  29. Boateng, J. S., Pawar, H. V. and Tetteh, J. (2013) 'Polyox and carrageenan based composite film dressing containing anti-microbial and anti-inflammatory drugs for effective wound healing', *International Journal of Pharmaceutics*, 441(1-2), 181-191.
  30. Boateng, J. S., Stevens, H. N. E., Eccleston, G. M., Auffret, A. D., Humphrey, M. J. and Matthews, K. H. (2009b) 'Development and mechanical characterization of solvent-cast polymeric films as potential drug delivery systems to mucosal surfaces', *Drug Development and Industrial Pharmacy*, 35(8), 986-996.
  31. Boddupalli, B. M., Mohammed, Z. N. K., Nath, R. A. and Banji, D. (2010) 'Mucoadhesive drug delivery system: An overview', *Journal of advanced pharmaceutical technology & research*, 1(4), 381-387.
  32. Bornhoft, M., Thommes, M. and Kleinebudde, P. (2005) 'Preliminary assessment of carrageenan as excipient for extrusion/spheronisation', *European Journal of Pharmaceutics and Biopharmaceutics*, 59(1), 127-131.
  33. Bowler, P. G., Duerden, B. I. and Armstrong, D. G. (2001) 'Wound microbiology and associated approaches to wound management', *Clinical Microbiology Reviews*, 14(2), 244-269.

34. Bowler, P. (2003) 'Progression toward healing: wound infection and the role of an advanced silver-containing Hydrofiber dressing'. *Ostomy Wound Management.*, 49(suppl8A): 2-5
35. Boyapally, H., Nukala, R. K., Bhujbal, P. and Douroumis, D. (2010) 'Controlled release from directly compressible theophylline buccal tablets', *Colloids and Surfaces B-Biointerfaces*, 77(2), 227-233.
36. Braff, M. H., Jones, A. L., Skerrett, S. J. and Rubens, C. E. (2007) 'Staphylococcus aureus exploits cathelicidin antimicrobial peptides produced during early pneumonia to promote staphylokinase-dependent fibrinolysis', *Journal of Infectious Diseases*, 195(9), 1365-1372.
37. Breidenbach, W. C. and Trager, S. (1995) 'Quantitative culture technique and infection in complex wounds of the extremities closed with free flaps', *Plastic and Reconstructive Surgery*, 95(5), 860-865.
38. Breitenbach, A., Pistel, K. F. and Kissel, T. (2000) 'Biodegradable comb polyesters Part II. Erosion and release properties of poly (vinyl alcohol)-g-poly (lactic-co-glycolic acid)', *Polymer*, 41(13), 4781-4792.
39. Brook, I. (1996) 'Aerobic and anaerobic microbiology of necrotizing fasciitis in children', *Pediatric Dermatology*, 13(4), 281-284.
40. Brook, I. and Frazier, E. H. (1998) 'Aerobic and anaerobic microbiology of infection after trauma', *American Journal of Emergency Medicine*, 16(6), 585-591.
41. Bryan, J. (2004) 'Moist wound healing: a concept that changed our practice', *Journal of wound care*, 13(6), 227-228.
42. Bunte, H., Drooge, D. J., Ottjes, G., Roukema, R., Verrijck, R. and Yessine, M. (2010). 'Key considerations when developing freeze-dried formulation and current trends', *Pharmaceutical Technology Europe Digital*, 22: 2-4.
43. Burke, S. E. and Barrett, C. J. (2004) 'pH-Dependent Loading and Release Behavior of Small Hydrophilic Molecules in Weak Polyelectrolyte Multilayer Films', *Macromolecules*, 37(14), 5375-5384.
44. Burke, S. E. and Barrett, C. J. (2005) 'Swelling Behavior of Hyaluronic Acid/Polyallylamine Hydrochloride Multilayer Films', *Biomacromolecules*, 6(3), 1419-1428.
45. Campo, V. L., Kawano, D. F., da Silva, D. B., Jr. and Carvalho, I. (2009) 'Carrageenans:

- Biological properties, chemical modifications and structural analysis - A review', *Carbohydrate Polymers*, 77(2), 167-180.
46. Campos, M., Cordi, L., Durán, N. and Mei, L. (2006) 'Antibacterial Activity of Chitosan Solutions for Wound Dressing', *Macromolecular Symposia*, 245-246(1), 515-518.
  47. Cao, N., Yang, X. and Fu, Y. (2009) 'Effects of various plasticizers on mechanical and water vapour barrier properties of gelatine films', *Food Hydrocolloids*, 23(3), 729-735.
  48. Carter, M. J., Tingley-Kelley, K. and Warriner, R. A., III (2010) 'Silver treatments and silver-impregnated dressings for the healing of leg wounds and ulcers: A systematic review and meta-analysis', *Journal of the American Academy of Dermatology*, 63(4), 668-679.
  49. Caykara, T., Demirci, S., Eroglu, M. S. and Guven, O. (2005) 'Poly (ethylene oxide) and its blends with sodium alginate', *Polymer*, 46(24), 10750-10757.
  50. Cheng, L. H., Karim, A. A. and Seow, C. C. (2006) 'Effects of Water-Glycerol and Water-Sorbitol Interactions on the Physical Properties of Konjac Glucomannan Films', *Journal of Food Science*, 71(2), E62-E67.
  51. Chirico, S., Dalmoro, A., Lamberti, G., Russo, G. and Titomanlio, G. (2007) 'Analysis and modeling of swelling and erosion behavior for pure HPMC tablet', *Journal of Controlled Release*, 122(2), 181-188.
  52. Choi, J. S. and Park, W. H. (2004) 'Effect of biodegradable plasticizers on thermal and mechanical properties of poly (3-hydroxybutyrate)', *Polymer Testing*, 23(4), 455-460.
  53. Chung, A. J. and Rubner, M. F. (2002) 'Methods of Loading and Releasing Low Molecular Weight Cationic Molecules in Weak Polyelectrolyte Multilayer Films', *Langmuir*, 18(4), 1176-1183.
  54. Church, D., Elsayed, S., Reid, O., Winston, B. and Lindsay, R. (2006) 'Burn wound infections', *Clinical Microbiology Reviews*, 19(2), 403-434.
  55. Colombo, P., Bettini, R. and Peppas, N. A. (1999) 'Observation of swelling process and diffusion front position during swelling in hydroxypropyl methyl cellulose (HPMC) matrices containing a soluble drug', *Journal of Controlled Release*, 61(1-2), 83-91.
  56. Coulthard, P., Esposito, M., Worthington, H. V., van der Elst, M., van Waes, O. J. F. and Darcey, J. (2010) 'Tissue adhesives for closure of surgical incisions', *Cochrane Database of Systematic Reviews*, (5) 1-48.
  57. Crowley, M. M., Fredersdorf, A., Schroeder, B., Kucera, S., Prodduturi, S., Repka, M. A. and McGinity, J. W. (2004) 'The influence of guaifenesin and ketoprofen on the

- properties of hot-melt extruded polyethylene oxide films', *European Journal of Pharmaceutical Sciences*, 22(5), 409-418.
58. Cruse, P. J. E. and Foord, R. (1980) 'The epidemiology of wound-infection - a 10-year prospective-study of 62,939 wounds', *Surgical Clinics of North America*, 60(1), 27-40.
  59. Cutting, K. F. and White, R. J. (2005) 'Criteria for identifying wound infection - Revisited', *Ostomy Wound Management*, 51(1), 28-34.
  60. Cutting, K. F. (2004) Exudate: Composition and functions. In: White, R (ed). *Trends in Wound Care: Volume III*. Salisbury: Quay Books, MA Healthcare Ltd, 41-49.
  61. Çaykara, T., Demirci, S., Eroglu, M. S. and Guven, O. (2005) 'Poly(ethylene oxide) and its blends with sodium alginate', *Polymer*, 46(24), 10750-10757.
  62. Da Silva, M. A., Krause Bierhalz, A. C. and Kieckbusch, T. G. (2009a) 'Alginate and pectin composite films crosslinked with  $\text{Ca}^{2+}$  ions: Effect of the plasticizer concentration', *Carbohydrate Polymers*, 77(4), 736-742.
  63. Dalafu, H., Chua, M. T. and Chakraborty, S. (2010) 'Development of kappa-Carrageenan Poly (acrylic acid) Interpenetrating Network Hydrogel as Wound Dressing Patch', *Biomaterials*, 1054, 125-135.
  64. Daltrey, D. C., Rhodes, B. and Chattwood, J. G. (1981) 'Investigation into the microbial-flora of healing and non-healing decubitus ulcers', *Journal of Clinical Pathology*, 34(7), 701-705.
  65. Dash, M., Chiellini, F., Ottenbrite, R. M. and Chiellini, E. (2011) 'Chitosan-A versatile semi-synthetic polymer in biomedical applications', *Progress in Polymer Science*, 36(8), 981-1014.
  66. Dastidar, S. G., Ganguly, K., Chaudhuri, K. and Chakrabarty, A. N. (2000) 'The anti-bacterial action of diclofenac shown by inhibition of DNA synthesis', *International Journal of Antimicrobial Agents*, 14(3), 249-251.
  67. David, H. (1981) 'A new technique of skin grafting using steri-greffe and a self-adhering foam pad', *British Journal of Plastic Surgery*, 34(2), 181-185.
  68. De Ascentiis, A., deGrazia, J. L., Bowman, C. N., Colombo, P. and Peppas, N. A. (1995) 'Mucoadhesion of poly(2-hydroxyethyl methacrylate) is improved when linear poly(ethylene oxide) chains are added to the polymer network', *Journal of Controlled Release*, 33(1), 197-201.
  69. Di Gioia, L. and Guilbert, S. (1999) 'Corn protein-based thermoplastic resins: Effect of some polar and amphiphilic plasticizers', *Journal of Agricultural and Food Chemistry*,

- 47(3), 1254-1261.
70. Dias, M., Hadgraft, J., Raghavan, S. L. and Tetteh, J. (2004) 'The effect of solvent on permeant diffusion through membranes studied using ATR-FTIR and chemometric data analysis', *Journal of Pharmaceutical Sciences*, 93(1), 186-196.
  71. Dobaria, N., Badhan, A. and Mashru, R. (2009) 'A Novel Itraconazole Bioadhesive Film for Vaginal Delivery: Design, Optimization, and Physicodynamic Characterization', *AAPS PharmSciTech*, 10(3), 951-959.
  72. Dodane, V., Khan, M. A. and Merwin, J. R. (1999) 'Effect of chitosan on epithelial permeability and structure', *International Journal of Pharmaceutics*, 182(1).
  73. Dowsett, C. (2004) 'The use of silver-based dressings in wound care', *Nursing standard (Royal College of Nursing (Great Britain):1987)*, 19(7), 56-60.
  74. Duerden, B. I. (1994) 'Virulence Factors in Anaerobes', *Clinical Infectious Diseases*, 18 (ArticleType: research-article / Issue Title: Supplement 4. Centennial Symposium on Anaerobes: A Memorial to André Veillon: The Secret Pathogens / Full publication date: May, 1994 / Copyright © 1994 Oxford University Press), S253-S259.
  75. Dutta, N., Mazumdar, K., Baek, M., Kim, D., Na, Y., Park, S., Lee, H., Lee, B. and Park, J. (2008) 'In vitro efficacy of diclofenac against *Listeria monocytogenes*', *European Journal of Clinical Microbiology & Infectious Diseases*, 27(4), 315-319.
  76. Dutta, N. K., Annadurai, S., Mazumdar, K., Dastidar, S. G., Kristiansen, J. E., Molnar, J., Martins, M. and Amaral, L. (2007a) 'Potential management of resistant microbial infections with a novel non-antibiotic: the anti-inflammatory drug diclofenac sodium', *International Journal of Antimicrobial Agents*, 30(3), 242-249.
  77. Dutta, N. K., Dastidar, S. G., Kumar, A., Mazumdar, K., Ray, R. and Chakrabarty, A. N. (2004) 'Antimycobacterial activity of the antiinflammatory agent diclofenac sodium, and its synergism with streptomycin', *Brazilian Journal of Microbiology*, 35, 316-323.
  78. Dutta, N. K., Mazumdar, K., Dastidar, S. G. and Park, J.-H. (2007b) 'Activity of diclofenac used alone and in combination with streptomycin against *Mycobacterium tuberculosis* in mice', *International Journal of Antimicrobial Agents*, 30(4), 336-340.
  79. Dutta, N. K., Mazumdar, K. and Park, J. H. (2009) 'In vitro synergistic effect of gentamicin with the anti-inflammatory agent diclofenac against *Listeria monocytogenes*', *Letters in Applied Microbiology*, 48(6), 783-785.
  80. Dutta, N. K., Mazumdar, K., Seok, S. H. and Park, J. H. (2008) 'The anti-inflammatory drug Diclofenac retains anti-listerial activity in vivo', *Letters in Applied Microbiology*,

- 47(2), 106-111.
81. Dyson, M., Young, S. and Pendle, C. L. (1988) 'Comparison of the effects of moist and dry conditions on dermal repair', *Journal of investigative dermatology*, 91(5), 434-9.
  82. Elgindy, N. and Samy, W. (2009) 'Evaluation of the mechanical properties and drug release of cross-linked Eudragit films containing metronidazole', *International Journal of Pharmaceutics*, 376(1-2), 1-6.
  83. Enoch, S. and Leaper, D. J. (2008) 'Basic science of wound healing', *Surgery (Oxford)*, 26(2), 31-37.
  84. Enoch, S. and Leaper, D. J. (2005) 'Basic science of wound healing', *Surgery (Oxford)*, 23(2), 37-42.
  85. Fahs, A., Brogly, M., Bistac, S. and Schmitt, M. (2010) 'Hydroxypropyl methylcellulose (HPMC) formulated films: Relevance to adhesion and friction surface properties', *Carbohydrate Polymers*, 80(1), 105-114.
  86. Falanga, V. (2000) 'Classifications for wound bed preparation and stimulation of chronic wounds', *Wound Repair and Regeneration*, 8(5), 347-352.
  87. Fan, L., Wang, L., Gao, S., Wu, P., Li, M., Xie, W., Liu, S. and Wang, W. (2011) 'Synthesis, characterization and properties of carboxymethyl kappa carrageenan', *Carbohydrate Polymers*, 86(3), 1167-1174.
  88. Ferreira, M. C., Tuma, P., Jr., Carvalho, V. F. and Kamamoto, F. (2006) 'Complex wounds', *Clinics (Sao Paulo, Brazil)*, 61(6), 571-578.
  89. Field, F. K. and Kerstein, M. D., (1994) 'Overview of wound healing in a moist environment.' *American journal of surgery*, 167(1A), 2S-6S.
  90. Fletcher, J. (2003) 'The application of foam dressings', *Nursing times*, 99(31), 59-59.
  91. Fonder, M. A., Lazarus, G. S., Cowan, D. A., Aronson-Cook, B., Kohli, A. R. and Mamelak, A. J. (2008) 'Treating the chronic wound: A practical approach to the care of non-healing wounds and wound care dressings', *Journal of the American Academy of Dermatology*, 58(2), 185-206.
  92. Forbes, G. B. (1961) 'Staphylococcal infection of operation wounds with special reference to topical antibiotic prophylaxis', *Lancet*, 2(7201), 505-509.
  93. Ford, J. L. (1999) 'Thermal analysis of hydroxypropylmethylcellulose and methylcellulose: powders, gels and matrix tablets', *International Journal of Pharmaceutics*, 179(2), 209-228.
  94. Franz, M. G., Steed, D. L. and Robson, M. C. (2007) 'Optimizing healing of the acute

- wound by minimizing complications', *Current Problems in Surgery*, 44(11), 691-763.
95. Frenning, G. (2011) 'Modelling drug release from inert matrix systems: From moving-boundary to continuous-field descriptions', *International Journal of Pharmaceutics*, 418(1), 88-99.
  96. Fuller, C. S., MacRae, R. J., Walther, M. and Cameron, R. E. (2001) 'Interactions in poly(ethylene oxide)-hydroxypropyl methylcellulose blends', *Polymer*, 42(23), 9583-9592.
  97. Gabrielsson, J., Lindberg, N. O. and Lundstedt, T. (2002) 'Multivariate methods in pharmaceutical applications', *Journal of Chemometrics*, 16(3), 141-160.
  98. Gallagher, K. M. and Corrigan, O. I. (2000) 'Mechanistic aspects of the release of levamisole hydrochloride from biodegradable polymers', *Journal of Controlled Release*, 69(2), 261-272.
  99. Galvan, L. (1996) 'Effects of heparin on wound healing', *Journal of wound, ostomy, and continence nursing: official publication of The Wound, Ostomy and Continence Nurses Society / WOCN*, 23(4), 224-6.
  100. Gemperline, P. J. (2006) Practical guide to chemometrics, second Eds. Taylor and Francis Group, LLC.
  101. Gethin, G. (2007). The significance of surface pH in chronic wounds. *Wounds UK*, 3(3), 52.
  102. George, M. and Abraham, T. E. (2006) 'Polyionic hydrocolloids for the intestinal delivery of protein drugs: Alginate and chitosan — a review', *Journal of Controlled Release*, 114(1), 1-14.
  103. Gilchrist, T. and Martin, A. M. (1983) 'Wound treatment with Sorbsan — an alginate fibre dressing', *Biomaterials*, 4(4), 317-320.
  104. Gilliland, E. L., Nathwani, N., Dore, C. J. and Lewis, J. D. (1988) 'Bacterial-colonization of leg ulcers and its effect on the success rate of skin-grafting', *Annals of the Royal College of Surgeons of England*, 70(2), 105-108.
  105. Giordano, F., Rossi, A., Pasquali, I., Bettini, R., Frigo, E., Gazzaniga, A., Sangalli, M. E., Mileo, V. and Catinella, S. (2003) 'Thermal degradation and melting point determination of diclofenac', *Journal of Thermal Analysis and Calorimetry*, 73(2), 509-518.
  106. Giovino, C., Ayensu, I., Tetteh, J. and Boateng, J. S. (2012) 'Development and characterisation of chitosan films impregnated with insulin loaded PEG-b-PLA nanoparticles (NPs): A potential approach for buccal delivery of macromolecules',

- International Journal of Pharmaceutics*, 428(1-2).
107. Goepferich, A. (1996) 'Polymer degradation and erosion: Mechanisms and applications', *European Journal of Pharmaceutics and Biopharmaceutics*, 42(1), 1-11.
  108. Gombotz, W. R. and Wee, S. F. (2012) 'Protein release from alginate matrices', *Advanced Drug Delivery Reviews*, 64, 194-205.
  109. Gottrup, F., Melling, A., Hollander, D. A. (2005) An overview of surgical site infections: aetiology, incidence and risk factors. *EWMA Journal*. 2 (1), 11-15.
  110. Gourgiotis, S., Villias, C., Germanos, S., Foukas, A. and Ridolfini, M. P. (2007) 'Acute limb compartment syndrome: A Review', *Journal of Surgical Education*, 64(3), 178-186.
  111. Granados, O. and Meza, G. (2007) 'A direct HPLC method to estimate streptomycin and its putative ototoxic derivative, streptidine, in blood serum: Application to streptomycin-treated humans', *Journal of Pharmaceutical and Biomedical Analysis*, 43(2), 625-630.
  112. Grassi, M., Voinovich, D., Franceschinis, E., Perissutti, B. and Filipovic-Grcic, J. (2003) 'Theoretical and experimental study on theophylline release from stearic acid cylindrical delivery systems', *Journal of Controlled Release*, 92(3), 275-289.
  113. Greiderer, A., Steeneken, L., Aalbers, T., Vivo-Truyols, G. and Schoenmakers, P. (2011) 'Characterization of hydroxypropylmethylcellulose (HPMC) using comprehensive two-dimensional liquid chromatography', *Journal of Chromatography A*, 1218(34), 5787-5793.
  114. Gu, J. M., Robinson, J. R. and Leung, S. H. S. (1988) 'Binding of acrylic polymers to mucin epithelial surfaces - structure-property relationships', *Crc Critical Reviews in Therapeutic Drug Carrier Systems*, 5(1), 21-67.
  115. Guo, S. and DiPietro, L. A. (2010) 'Factors Affecting Wound Healing', *Journal of Dental Research*, 89(3), 219-229.
  116. Hagesaether, E. and Sande, S. A. (2008) 'Effect of pectin type and plasticizer on in vitro mucoadhesion of free films', *Pharmaceutical Development and Technology*, 13(2), 105-114.
  117. Halbert, A. R., Stacey, M. C., Rohr, J. B. and Jopp-McKay, A. (1992) 'The effect of bacterial colonization on venous ulcer healing', *The Australasian journal of dermatology*, 33(2), 75-80.
  118. Hamberg, K., Jakobsen, C., Taherinejad, F. and Kaszony, G. (2012) 'Correlation of silver release and antimicrobial effect of silver containing wound dressing in vitro'. *European tissue repair society*, Greece (poster).

119. Hamilton, R., J., and Sewell, P., A. (1982) Introduction to high performance liquid chromatography, Second edition, Bristol, UK: J. W. Arrow-smith Ltd.
120. Hanna, J. R. and Giacobelli, J. A. (1997) 'A review of wound healing and wound dressing products', *The Journal of Foot and Ankle Surgery*, 36(1), 2-14.
121. Hantash, B. M., Zhao, L. M., Knowles, J. A. and Lorenz, H. P. (2008) 'Adult and fetal wound healing', *Frontiers in Bioscience*, 13, 51-61.
122. Harding, K. G., Morris, H. L. and Patel, G. K. (2002) 'Science, medicine, and the future - Healing chronic wounds', *British Medical Journal*, 324(7330), 160-163.
123. Harrell, L. J. and Evans, J. B. (1978) 'Anaerobic resistance of clinical isolates of staphylococcus-aureus to aminoglycosides', *Antimicrobial Agents and Chemotherapy*, 14(6), 927-929.
124. Heda, A. A., Gadade, D. D., Kathiriya, J. M. and Puranik, P. K. (2010) 'HPLC method development and validation for simultaneous analysis of diclofenac sodium and Rabeprazole Sodium', *E-Journal of Chemistry*, 7, S386-S390.
125. Heenan, A. (1998) 'Hydrocolloids: Frequently asked questions. ', *World Wide Wounds*, 1, 1-17.
126. Heinzelmann, M., Scott, M. and Lam, T. (2002) 'Factors predisposing to bacterial invasion and infection', *American Journal of Surgery*, 183(2), 179-190.
127. Hickey, J., Panicucci, R., Duan, Y. J., Dinehart, K., Murphy, J., Kessler, J. and Gottardi, W. (1997) 'Control of the amount of free molecular iodine in iodine germicides', *Journal of Pharmacy and Pharmacology*, 49(12), 1195-1199.
128. Hinman, C. D. and Maibach, H. (1963) 'Effects of air exposure and occlusion on experimental human skin wounds', *Nature*, 200, 377-378.
129. Howes, E. L. (1947) 'Topical use of streptomycin in wounds', *The American journal of medicine*, 2(5), 449-56.
130. Huang, J., Wigent, R. J. and Schwartz, J. B. (2006) 'Nifedipine molecular dispersion in microparticles of ammonio methacrylate copolymer and ethylcellulose binary blends for controlled drug delivery: Effect of matrix composition', *Drug Development and Industrial Pharmacy*, 32(10), 1185-1197.
131. Hunt, T. K. (1981) 'Surgical wound infections - an overview', *American Journal of Medicine*, 70(3), 712-718.
132. Hwang, M.-R., Kim, J. O., Lee, J. H., Il Kim, Y., Kim, J. H., Chang, S. W., Jin, S. G., Kim, J. A., Lyoo, W. S., Han, S. S., Ku, S. K., Yong, C. S. and Choi, H.G. (2010)

- 'Gentamicin-Loaded Wound Dressing With Polyvinyl Alcohol/Dextran Hydrogel: Gel Characterization and In Vivo Healing Evaluation', *AAPS Pharmscitech*, 11(3), 1092-1103.
133. Innes, M. E., Umraw, N., Fish, J. S., Gomez, M. and Cartotto, R. C. (2001) 'The use of silver coated dressings on donor site wounds: a prospective, controlled matched pair study', *Burns*, 27(6), 621-627.
  134. Jackson, S and Stevens, J. (2006) The Future of Wound Care, Available: <http://www.lek.com/sites/default/files/MX-The-Future-of-Wound-Care.pdf>. Last accessed 20 Jun 2012.
  135. Jabbari, E., Wisniewski, N. and Peppas, N. A. (1993) 'Evidence of mucoadhesion by chain interpenetration at a poly(acrylic acid)/mucin interface using ATR-FTIR spectroscopy', *Journal of Controlled Release*, 27(1), 89-89.
  136. Jagadish, R. S., Raj, B., Parameswara, P. and Somashekar, R. (2010) 'Effect of glycerol on structure–property relations in chitosan/poly(ethylene oxide) blended films investigated using wide-angle X-ray diffraction', *Polymer International*, 59(7), 931-936.
  137. Jagannath, J. H., Nanjappa, C., Das Gupta, D. K. and Bawa, A. S. (2003) 'Mechanical and barrier properties of edible starch–protein-based films', *Journal of Applied Polymer Science*, 88(1), 64-71.
  138. Japoni, A., Farshad, S. and Alborzi, A. (2009) 'Pseudomonas aeruginosa: Burn Infection, Treatment and Antibacterial Resistance', *Iranian Red Crescent Medical Journal*, 11(3), 244-253.
  139. Jayakumar, R., Prabakaran, M., Sudheesh Kumar, P. T., Nair, S. V. and Tamura, H. (2011) 'Biomaterials based on chitin and chitosan in wound dressing applications', *Biotechnology Advances*, 29(3), 322-337.
  140. Jones, A. and Vaughan, D. (2005) 'Hydrogel dressings in the management of a variety of wound types: A review', 9, S1-S11.
  141. Jones, D. S., Lawlor, M. S. and Woolfson, A. D. (2003) 'Rheological and mucoadhesive characterization of polymeric systems composed of poly(methylvinylether-co-maleic anhydride) and poly(vinylpyrrolidone), designed as platforms for topical drug delivery', *Journal of Pharmaceutical Sciences*, 92(5).
  142. Jung, W. K., Koo, H. C., Kim, K. W., Shin, S., Kim, S. H. and Park, Y. H. (2008) 'Antibacterial activity and mechanism of action of the silver ion in Staphylococcus aureus and Escherichia coli', *Applied and Environmental Microbiology*, 74(7), 2171-2178.

143. Karbowski, T., Hervet, H., Léger, L., Champion, D., Debeaufort, F. and Voilley, A. (2006) 'Effect of Plasticizers (Water and Glycerol) on the Diffusion of a Small Molecule in Iota-Carrageenan Biopolymer Films for Edible Coating Application', *Biomacromolecules*, 7(6), 2011-2019.
144. Keppeler, S., Ellis, A. and Jacquier, J. C. (2009) 'Cross-linked carrageenan beads for controlled release delivery systems', *Carbohydrate Polymers*, 78(4), 973-977.
145. Khan, T. A., Peh, K. K. and Ch'ng H. (2000) 'Mechanical, bioadhesive and biological evaluations of chitosan films for wound dressing', *Journal of pharmacy and pharmaceutical science*, 3(3), 303-311.
146. Khanna, O., Moya, M. L., Opara, E. C. and Brey, E. M. (2010) 'Synthesis of multilayered alginate microcapsules for the sustained release of fibroblast growth factor-1', *Journal of Biomedical Materials Research Part A*, 95A(2), 632-640.
147. Kianfar, F., Chowdhry, B. Z., Antonijevic, M. D., Boateng, J. S. (2012). 'Novel films for drug delivery via the buccal mucosa using model soluble and insoluble drugs'. *Drug Development and Industrial Pharmacy*. 38(10), 1207-20.
148. Kianfar, F., Antonijevic, M. D., Chowdhry, B. Z., Boateng, J. S. (2013). 'Lyophilized wafers comprising  $\kappa$ -carrageenan & pluronic acid for buccal drug delivery using model soluble and insoluble drugs'. *Colloids and Surfaces B: Biointerfaces* 103, 99-106.
149. Kibria, G., Roni, M. A., Absar, M. S. and Jalil, R.U. (2008) 'Effect of Plasticizer on Release Kinetics of Diclofenac Sodium Pellets Coated with Eudragit RS 30 D', *AAPS Pharmscitech*, 9(4), 1240-1246.
150. Kim, I. Y., Seo, S. J., Moon, H. S., Yoo, M. K., Park, I. Y., Kim, B. C. and Cho, C. S. (2008) 'Chitosan and its derivatives for tissue engineering applications', *Biotechnology Advances*, 26(1), 1-21.
151. Kim, J. O., Park, J. K., Kim, J. H., Jin, S. G., Yong, C. S., Li, D. X., Choi, J. Y., Woo, J. S., Yoo, B. K., Lyoo, W. S., Kim, J. A. and Choi, H. G. (2008) 'Development of polyvinyl alcohol–sodium alginate gel-matrix-based wound dressing system containing nitrofurazone', *International Journal of Pharmaceutics*, 359(1-2), 79-86.
152. Kirketerp-Moller, K., Zulkowski, K. and James, G. (2011) 'Chronic Wound Colonization, Infection, and Biofilms', *Biofilm Infections*, Springer New York, 11-24.
153. Kondo, T. and Sawatari, C. (1994) 'Intermolecular hydrogen bonding in cellulose/poly(ethylene oxide) blends: thermodynamic examination using 2,3-di-O- and 6-O-methylcelluloses as cellulose model compounds', *Polymer*, 35(20), 4423-4428.

154. Kong, M., Chen, X. G., Xing, K. and Park, H. J. (2010) 'Antimicrobial properties of chitosan and mode of action: A state of the art review', *International Journal of Food Microbiology*, 144(1), 51-63.
155. Kornder, J. D. (2002) 'Streptomycin revisited: molecular action in the microbial cell', *Medical Hypotheses*, 58(1), 34-46.
156. Korsmeyer, R. W., Lustig, S. R. and Peppas, N. A. (1986a) 'Solute and penetrant diffusion in swellable polymers .1. mathematical-modeling', *Journal of Polymer Science Part B-Polymer Physics*, 24(2), 395-408.
157. Korsmeyer, R. W., Vonmeerwall, E. and Peppas, N. A. (1986b) 'Solute and penetrant diffusion in swellable polymers .2. verification of theoretical-models', *Journal of Polymer Science Part B-Polymer Physics*, 24(2), 409-434.
158. Kramer, A. and Maassen, A. (2009) 'Wound dressings from a hygienic point of view using the example of sorbion sachet S.', *GMS Krankenhhyg Interdiszip*, 4(2), 1-7.
159. Krischak, G. D., Augat, P., Claes, L., Kinzl, L. and Beck, A. (2007) 'The effects of non-steroidal anti-inflammatory drug application on incisional wound healing in rats', *Journal of wound care*, 16(2), 76-78.
160. Krischak, G. D., Augat, P., Sorg, T., Blakytyn, R., Kinzl, L., Claes, L. and Beck, A. (2007) 'Effects of diclofenac on periosteal callus maturation in osteotomy healing in an animal model', *Archives of Orthopaedic and Trauma Surgery*, 127(1), 3-9.
161. Kristo, E. and Biliaderis, C. G. (2006) 'Water sorption and thermo-mechanical properties of water/sorbitol-plasticized composite biopolymer films: Caseinate–pullulan bilayers and blends', *Food Hydrocolloids*, 20(7), 1057-1071.
162. Kumar, S. and Leaper, D. J. (2005) 'Classification and management of acute wounds', *Surgery (Oxford)*, 23(2), 47-51.
163. Kurita, K. (1998) 'Chemistry and application of chitin and chitosan', *Polymer Degradation and Stability*, 59(1–3), 117-120.
164. Labovitiadi, O., Lamb, A. J. and Matthews, K. H. (2012) 'In vitro efficacy of antimicrobial wafers against methicillin-resistant *Staphylococcus aureus*', *Therapeutic delivery*, 3(4), 443-55.
165. Langer, R. and Peppas, N. (1983) 'Chemical and physical structure of polymers as carriers for controlled release of bioactive agents - a review', *Journal of Macromolecular Science-Reviews in Macromolecular Chemistry and Physics*, C23(1), 61-126.
166. Lansdown, A. B. G. (2002) 'Silver. I: Its antibacterial properties and mechanism of

- action', *Journal of wound care*, 11(4), 125-30.
167. Laohakunjit, N. and Noomhorm, A. (2004) 'Effect of Plasticizers on Mechanical and Barrier Properties of Rice Starch Film', *Starch - Stärke*, 56(8), 348-356.
  168. Leaper, D. J. (2006) 'Silver dressings: their role in wound management', *International wound journal*, 3(4), 282-94.
  169. Lee, K. Y. and Mooney, D. J. (2012) 'Alginate: Properties and biomedical applications', *Progress in Polymer Science*, 37(1), 106-126.
  170. Lefnaoui, S. and Moulai-Mostefa, N. (2011) 'Formulation and in vitro evaluation of kappa-carrageenan-pregelatinized starch-based mucoadhesive gels containing miconazole', *Starch-Starke*, 63(8), 512-521.
  171. Lehnert, B. and Jhala, G. (2005) 'The use of foam as a postoperative compression dressing', *The Journal of Foot and Ankle Surgery*, 44(1), 68-69.
  172. Leung, S. H. S. and Robinson, J. R. (1990). Polymer structure features contributing to mucoadhesion. II. *Journal of controlled release*, 12(3), 187-194.
  173. Levine, N. S., Lindberg, R. B., Mason, A. D. and Pruitt, B. A. (1976) 'Quantitative swab culture and smear - quick, simple method for determining number of viable aerobic bacteria on open wounds', *Journal of Trauma-Injury Infection and Critical Care*, 16(2), 89-94.
  174. Li, J., Zivanovic, S., Davidson, P. M. and Kit, K. (2010) 'Characterization and comparison of chitosan/PVP and chitosan/PEO blend films', *Carbohydrate Polymers*, 79(3), 786-791.
  175. Li, J., Zivanovic, S., Davidson, P. M. and Kit, K. (2011) 'Production and characterization of thick, thin and ultra-thin chitosan/PEO films', *Carbohydrate Polymers*, 83(2), 375-382.
  176. Li, X., Xie, H., Lin, J., Xie, W. and Ma, X. (2009) 'Characterization and biodegradation of chitosan-alginate polyelectrolyte complexes', *Polymer Degradation and Stability*, 94(1), 1-6.
  177. Li, X., Z., Nikaido, H., Williams, K., E.(1997) Silver-resistant mutants of Escherichia coli display active efflux Ag<sup>+</sup> and are deficient in porins. *Journal of Bacteriology*, 19, 6127-6132.
  178. Lindsay, S., Del-Bono, M., Stevenson, R., Stephens, S. and Breda, C. (2010) 'The silver release profile of antimicrobial wound dressings: standardizing in vitro evaluations', Symposium on Advanced Wound Care (SAWC), Florida, USA (poster).
  179. Lipsky, B. A. and Hoey, C. (2009) 'Topical Antimicrobial Therapy for Treating Chronic

- Wounds', *Clinical Infectious Diseases*, 49(10), 1541-1549.
180. Llabot, J. M., Manzo, R. H. and Allemandi, D. A. (2002) 'Double-layered mucoadhesive tablets containing nystatin', *AAPS PharmSciTech*, 3(3), E22-E22.
  181. Lloyd, L. L., Kennedy, J. F., Methacanon, P., Paterson, M. and Knill, C. J. (1998) 'Carbohydrate polymers as wound management aids', *Carbohydrate Polymers*, 37(3), 315-322.
  182. Loke, W. K., Lau, S. K., Yong, L. L., Khor, E. and Sum, C. K. (2000) 'Wound dressing with sustained anti-microbial capability', *Journal of Biomedical Materials Research*, 53(1), 8-17.
  183. Lowman, A. M., Dziubla, T. D., Bures, P. and Peppas, N. A. (2004) 'Structural and dynamic response of neutral and intelligent networks in biomedical environments' in Sefton, A. P. a. M. V., ed. *Advances in Chemical Engineering*, Academic Press, 75-130.
  184. López, O. V., García, M. A. and Zaritzky, N. E. (2008) 'Film forming capacity of chemically modified corn starches', *Carbohydrate Polymers*, 73(4), 573-581.
  185. Lrotonda, F. D.S. (2007) biodegradable films and coatings obtained from carrageenan from *mastocarpus stellatus* and starch from *querus sober*, (thesis) university da porto.
  186. Macfarlane, D. E., Baum, K. F. and Serjeant, G. R. (1986) 'Bacteriology of sickle-cell leg ulcers', *Transactions of the Royal Society of Tropical Medicine and Hygiene*, 80(4), 553-556.
  187. Maclaine, J. Q. G. and Booth, C. (1975) 'Effect of molecular-weight on crystallization isotherms of high molecular-weight poly (ethylene oxide) fractions', *Polymer*, 16(9), 680-684.
  188. Macmillan, B. G. (1980) 'Infections following burn injury', *Surgical Clinics of North America*, 60(1), 185-196.
  189. Madden, M. R., Nolan, E., Finkelstein, J. L., Yurt, R. W., Smeland, J., Goodwin, C. W., Hefton, J. and Staianocoico, L. (1989) 'Comparison of an occlusive and a semi-occlusive dressing and the effect of the wound exudate upon keratinocyte proliferation', *Journal of Trauma-Injury Infection and Critical Care*, 29(7), 924-931.
  190. Malinowski, E. K., (1991) Factor analysis in chemistry. Second eds., Wiley-interscience publication, John Wiley and sons. Inc, New Jersey.
  191. Mangione, M. R., Giacomazza, D., Cavallaro, G., Bulone, D., Martorana, V. and Biagio, P. L. S. (2007) 'Relation between structural and release properties in a polysaccharide gel system', *Biophysical Chemistry*, 129(1), 18-22.

192. Martindale, (1982) *The Extra Pharmacopoeia*, twentieth edition (Pharmaceutical Press), p.1213
193. Matthews, K. H., Stevens, H. N. E., Auffret, A. D., Humphrey, M. J. and Eccleston, G. M. (2005) 'Lyophilised wafers as a drug delivery system for wound healing containing methylcellulose as a viscosity modifier', *International Journal of Pharmaceutics*, 289(1-2), 51-62.
194. Matthews, K. H., Stevens, H. N. E., Auffret, A. D., Humphrey, M. J. and Eccleston, G. M. (2006) 'Gamma-irradiation of lyophilised wound healing wafers', *International Journal of Pharmaceutics*, 313(1-2), 78-86.
195. Matthews, K. H., Stevens, H. N. E., Auffret, A. D., Humphrey, M. J. and Eccleston, G. M. (2008) 'Formulation, stability and thermal analysis of lyophilised wound healing wafers containing an insoluble MMP-3 inhibitor and a non-ionic surfactant', *International Journal of Pharmaceutics*, 356(1-2), 110-120.
196. Matthews, K. H., Stevens, H.N.E., Auffret, A.D., Humphrey, M.J., Eccleston, G.M., (2005) 'Wafers for wound healing', *International journal of pharmaceutics*, 289, 51-62.
197. Mazumdar, K., Dastidar, S., Park, J. and Dutta, N. (2009) 'The anti-inflammatory non-antibiotic helper compound diclofenac: an antibacterial drug target', *European Journal of Clinical Microbiology & Infectious Diseases*, 28(8), 881-891.
198. Robson, M. C, Stenberg, B.D., Hegggers, J.P., (1990) 'Wound healing alterations caused by infection', *Clinics in Plastic Surgery*, 17(3), 485-492.
199. McAuley, W. J., Mader, K. T., Tetteh, J., Lane, M. E. and Hadgraft, J. (2009) 'Simultaneous monitoring of drug and solvent diffusion across a model membrane using ATR-FTIR spectroscopy', *European Journal of Pharmaceutical Sciences*, 38(4), 378-383.
200. McHugh, S. M., Collins, C. J., Corrigan, M. A., Hill, A. D. K. and Humphreys, H. (2011) 'The role of topical antibiotics used as prophylaxis in surgical site infection prevention', *Journal of Antimicrobial Chemotherapy*, 66(4), 693-701.
201. Mertz, P. M. (2003) 'Cutaneous biofilms: Friend or foe?' *Wounds*, 15(5), 129-132.
202. Modak, S. M. and Fox, C. L. (1981) 'Sulfadiazine silver-resistant pseudomonas in burns - new topical agents', *Archives of Surgery*, 116(7), 854-857.
203. Moon, C. H. and Crabtree, T. G. (2003) 'New Wound Dressing Techniques to Accelerate Healing', *Current treatment options in infectious diseases*, 5, 251-260.
204. Mooney, E. K., Lippitt, C., Friedman, J. (2006) 'Silver dressings', *Plastic and*

- Reconstructive Surgery*, 117(2), 666-669.
205. Morales, J. O. and McConville, J. T. (2011) 'Manufacture and characterization of mucoadhesive buccal films', *European Journal of Pharmaceutics and Biopharmaceutics*, 77(2), 187-199.
  206. Mourão, P. A. (2004) 'Use of sulfated fucans as anticoagulant and antithrombotic agents: Future perspectives', *Current Pharmaceutical Design*, 10(9), 967-981.
  207. Nichols, R. L. (1998) 'Postoperative infections in the age of drug-resistant gram-positive bacteria', *American Journal of Medicine*, 104(5 part A), 11S-16S.
  208. O'Brien, M., (2007). Medicated Dressing Policy. Available: <http://www.nscchealth.nsw.gov.au/services/wound.care/MedicatedDressingPolicy.pdf>. Last accessed 10 Jan 2011.
  209. O'Meara, S., Cullum, N., Majid, M. and Sheldon, T. (2000) 'Systematic reviews of wound care management: (3) antimicrobial agents for chronic wounds; (4) diabetic foot ulceration', *Health technology assessment (Winchester, England)*, 4(21), 1-237.
  210. Oncul, O., Yildiz, S., Gurer, U. S., Yeniiz, E., Qyrdedi, T., Top, C., Gocer, P., Akarsu, B., Cevikbas, A. and Cavuslu, S. (2007) 'Effect of the function of polymorphonuclear leukocytes and interleukin-1 beta on wound healing in patients with diabetic foot infections', *Journal of Infection*, 54(3), 250-256.
  211. Ousey K, Gillibrand W and Stephenson, J. (2011) 'Understanding and preventing wound blistering', *Wounds UK*, 7(4), 4.
  212. Ovington, L. G. (2004) 'The truth about silver', *Ostomy wound management*, 50(9A Suppl), 1S-10S.
  213. Ovington, L. G. (2007) 'Advances in wound dressings', *Clinics in Dermatology*, 25(1), 33-38.
  214. Park, H., Copeland, C., Henry, S. and Barbul, A. (2010) 'Complex Wounds and Their Management', *Surgical Clinics of North America*, 90(6), 1181-1194.
  215. Paul, W. and Sharma, P.C. (2004) 'Chitosan and Alginate Wound Dressings: A Short Review', *Trends. Biomater. Artif. Organs.*, 18(1), 6.
  216. Pawar, H., Douroumis, D. and Boateng, J. S. (2012) 'Preparation and optimization of PMAA–chitosan–PEG nanoparticles for oral drug delivery', *Colloids and Surfaces B: Biointerfaces*, 90(0), 102-108.
  217. Pawar, H. V., Tetteh, J. and Boateng, J. S. (2013) 'Preparation, optimisation and characterisation of novel wound healing film dressings loaded with streptomycin and

- diclofenac', *Colloids and Surfaces B: Biointerfaces*, 102, 102-110.
218. Paşcalău, V., Popescu, V., Popescu, G. L., Dudescu, M. C., Borodi, G., Dinescu, A., Perhaița, I. and Paul, M. (2011) 'The alginate/k-carrageenan ratio's influence on the properties of the cross-linked composite films', *Journal of Alloys and Compounds*, (536) sup., S418-S423.
  219. Peles, Z. and Zilberman, M. (2012) 'Novel soy protein wound dressings with controlled antibiotic release: Mechanical and physical properties', *Acta Biomaterialia*, 8(1), 209-217.
  220. Peppas, N. A. and Buri, P. A. (1985) 'Surface interfacial and molecular aspects of polymer bioadhesion on soft tissues', *Journal of Controlled Release*, 2, 257-276.
  221. Peppas, N. A. and Sahlin, J. J. (1989) 'A simple equation for the description of solute release .3. coupling of diffusion and relaxation', *International Journal of Pharmaceutics*, 57(2), 169-172.
  222. Peppas, N. A. and Sahlin, J. J. (1996) 'Hydrogels as mucoadhesive and bioadhesive materials: a review', *Biomaterials*, 17(16), 1553-1561.
  223. Percival, N. J. (2002) 'Classification of Wounds and their Management', *Surgery (Oxford)*, 20(5), 114-117.
  224. Percival, S. L., Bowler, P. G. and Russell, D. (2005) 'Bacterial resistance to silver in wound care', *Journal of Hospital Infection*, 60(1), 1-7.
  225. Pereira, A. G. B., Gouveia, R. F., de Carvalho, G. M., Rubira, A. F. and Muniz, E. C. (2009) 'Polymer blends based on PEO and starch: Miscibility and spherulite growth rate evaluated through DSC and optical microscopy', *Materials Science and Engineering: C*, 29(2), 499-504.
  226. Pereira, R., Carvalho, A., Vaz, D. C., Gil, M. H., Mendes, A. and Bartolo, P. (2013) 'Development of novel alginate based hydrogel films for wound healing applications', *International Journal of Biological Macromolecules*, 52, 221-230.
  227. Periti, P., Tonelli, F. and Mini, E. (1998) 'Selecting antibacterial agents for the control of surgical infection: Mini-review', *Journal of Chemotherapy*, 10(2), 83-90.
  228. Perumal, V. A., Lutchman, D., Mackraj, I. and Govender, T. (2008) 'Formulation of monolayered films with drug and polymers of opposing solubilities', *International Journal of Pharmaceutics*, 358(1-2), 184-191.
  229. Phillips, D. and Davey, C. (1997) 'Wound cleaning versus wound disinfection: a challenging dilemma', *Perspectives (Canada)*, 21(4), 15-6.

230. Pielesz, A., Machnicka, A. and Sarna, E. (2011) 'Antibacterial activity and scanning electron microscopy (SEM) examination of alginate-based films and wound dressings', *Ecological Chemistry and Engineering S-Chemia I Inzynieria Ekologiczna S*, 18(2), 197-210.
231. Prabakaran, M. and Gong, S. (2008) 'Novel thiolated carboxymethyl chitosan-g-beta-cyclodextrin as mucoadhesive hydrophobic drug delivery carriers', *Carbohydrate Polymers*, 73(1), 117-125.
232. Prudencioferreira, S. H. and Areas, J. A. G. (1993) 'Protein-protein interactions in the extrusion of soya at various temperatures and moisture contents', *Journal of Food Science*, 58(2), 378-381.
233. Rai, M., Yadav, A. and Gade, A. (2009) 'Silver nanoparticles as a new generation of antimicrobials', *Biotechnology Advances*, 27(1), 76-83.
234. Rattanuengsrikul, V., Pimpha, N. and Supaphol, P. (2009) 'Development of Gelatin Hydrogel Pads as Antibacterial Wound Dressings', *Macromolecular Bioscience*, 9(10), 1004-1015.
235. Rees, D. A. and Welsh, E. J. (1977) 'Secondary and Tertiary Structure of Polysaccharides in Solutions and Gels', *Angewandte Chemie International Edition in English*, 16(4), 214-224.
236. Revathi, G., Puri, J. and Jain, B. K. (1998) 'Bacteriology of burns', *Burns*, 24(4), 347-349.
237. Rinaudo, M. (2006) 'Chitin and chitosan: Properties and applications', *Progress in Polymer Science*, 31(7), 603-632.
238. Romanelli, M. Vowden, K and Weir, D. (2011) 'Exudate management made easy', *Wounds International*, Volume 1(2), 1-6.
239. Ross, R. (1971) 'Wound healing - recent progress - future directions', *Journal of Dental Research*, 50(2), 312-314.
240. Rothen-Weinhold, A. and Gurny, R. (1997) 'Controlled and/or prolonged parental delivery of peptides from the hypothalamic pituitary axis', *European Journal of Pharmaceutics and Biopharmaceutics*, 43 (2), 115-131.
241. Roy, S., Pal, K., Anis, A., Pramanik, K. and Prabhakar, B. (2009) 'Polymers in Mucoadhesive Drug-Delivery Systems: A Brief Note', *Designed Monomers and Polymers*, 12(6), 483-495.
242. Schatzker, J. and Tile, M. (2005). *The rationale of operative fracture care*, Third edition, New York: Springer Berlin Heidelberg.

243. Sussman, G. (2010) 'Technology update: Understanding film dressings', *Wound international*, 1(4), 1-24.
244. Sai K, P. and Babu, M. (2000) 'Collagen based dressings — a review', *Burns*, 26(1), 54-62.
245. Saiano, F., Pitarresi, G., Cavallaro, G., Licciardi, M. and Giammona, G. (2002) 'Evaluation of mucoadhesive properties of alpha,beta-poly(N-hydroxyethyl)-DL-aspartamide and alpha,beta-poly(aspartylhydrazide) using ATR-FTIR spectroscopy', *Polymer*, 43(23), 6281-6286.
246. Salamat-Miller, N., Chittchang, M. and Johnston, T. P. (2005) 'The use of mucoadhesive polymers in buccal drug delivery', *Advanced Drug Delivery Reviews*, 57(11), 1666-1691.
247. Salsa, T., Veiga, F., Teixeira-Dias, J. J. C. and Pina, M. E. (2003) 'Effect of polymer hydration on the kinetic release of drugs: A study of ibuprofen and ketoprofen in HPMC matrices', *Drug Development and Industrial Pharmacy*, 29(3), 289-297.
248. Samani, S. M., Montaseri, H. and Kazemi, A. (2003) 'The effect of polymer blends on release profiles of diclofenac sodium from matrices', *European Journal of Pharmaceutics and Biopharmaceutics*, 55(3), 351-355.
249. Scott, D. B. (2008) 'Thin Film Oral Dosage Forms' in *Modified-Release Drug Delivery Technology*, Informa Healthcare, 209-216.
250. Sedlarik KM, Vacik J, Wichterle O and M., H. (1995) 'Modern dressing hydrogels.', *Rozhl Chir.*, 74(1), 3-7.
251. Seeley, S. F. (1964) 'INfluence of ultraviolet light on postoperative infection', *JAMA: The Journal of the American Medical Association*, 189(7), 574-575.
252. Sehgal, S. C. and Arunkumar, B. K. (1992) 'Microbial-flora and its significance in pathology of sickle-cell disease leg ulcers', *Infection*, 20(2), 86-88.
253. Şenel, S. and McClure, S. J. (2004) 'Potential applications of chitosan in veterinary medicine', *Advanced Drug Delivery Reviews*, 56(10), 1467-1480.
254. Siemann, U. (2005) 'Solvent cast technology – a versatile tool for thin film production', *Progress in Colloid and Polymer Science*, 130; 1-14
255. Siepmann, F., Le Brun, V. and Siepmann, J. (2006) 'Drugs acting as plasticizers in polymeric systems: A quantitative treatment', *Journal of Controlled Release*, 115(3), 298-306.
256. Siepmann, J. and Gopferich, A. (2001) 'Mathematical modeling of bioerodible, polymeric drug delivery systems', *Advanced Drug Delivery Reviews*, 48(2-3), 229-247.

257. Siepmann, F., Siepmann, J., Walther, M., MacRae, R. J. and Bodmeier, R. (2008) 'Polymer blends for controlled release coatings', *Journal of Controlled Release*, 125(1), 1-15.
258. Siepmann, J. and Peppas, N. A. (2001) 'Modeling of drug release from delivery systems based on hydroxypropyl methylcellulose (HPMC)', *Advanced Drug Delivery Reviews*, 48(2-3), 139-157.
259. Siepmann, J. and Siepmann, F. (2008) 'Mathematical modeling of drug delivery', *International Journal of Pharmaceutics*, 364(2), 328-343.
260. Silva, C. L., Pereira, J. C., Ramalho, A., Pais, A. A. C. C. and Sousa, J. J. S. (2008) 'Films based on chitosan polyelectrolyte complexes for skin drug delivery: Development and characterization', *Journal of Membrane Science*, 320(1-2), 268-279.
261. Silva, F. R. F., Dore, C. M. P. G., Marques, C. T., Nascimento, M. S., Benevides, N. M. B., Rocha, H. A. O., Chavante, S. F. and Leite, E. L. (2010) 'Anticoagulant activity, paw edema and pleurisy induced carrageenan: Action of major types of commercial carrageenans', *Carbohydrate Polymers*, 79(1), 26-33.
262. Silva, M. A. d., Bierhalz, A. C. K. and Kieckbusch, T. G. (2009) 'Alginate and pectin composite films crosslinked with Ca<sup>2+</sup> ions: Effect of the plasticizer concentration', *Carbohydrate Polymers*, 77(4), 736-742.
263. Silva, S. S., Oliveira, J. M., Sá-Lima, H., Sousa, R. A., Mano, J. F. and Reis, R. L. (2011) '2.211 - Polymers of Biological Origin' in Editor-in-Chief: Paul, D., ed. *Comprehensive Biomaterials*, Oxford: Elsevier, 187-205.
264. Singh, B. and Pal, L. (2012) 'Sterculia crosslinked PVA and PVA-poly(AAm) hydrogel wound dressings for slow drug delivery: Mechanical, mucoadhesive, biocompatible and permeability properties', *Journal of the Mechanical Behavior of Biomedical Materials*, 9, 9-21.
265. Singh, T., Meena, R. and Kumar, A. (2009) 'Effect of Sodium Sulfate on the Gelling Behavior of Agarose and Water Structure Inside the Gel Networks', *Journal of Physical Chemistry B*, 113(8), 2519-2525.
266. Sionkowska, A. (2011) 'Current research on the blends of natural and synthetic polymers as new biomaterials: Review', *Progress in Polymer Science*, 36(9), 1254-1276.
267. Squier, C. A. and Wertz, P. W. (1996) 'Structure and Function of the Oral Mucosa and Implications for Drug Delivery'. Edited by Rathbone M. J. and Swarbrick J. *Oral Mucosal Drug Delivery, (Drugs and the Pharmaceutical Sciences)*, 1-26. Marcel Dekker,

- Inc.
268. Shoaib, M. H., Tazeen, J., Merchant, H. A. and Yousuf, R. I. (2006) 'Evaluation of drug release kinetics from ibuprofen matrix tablets using HPMC', *Pakistan journal of pharmaceutical sciences*, 19(2), 119-24.
  269. Skurtys O., Acevedo C., Pedreschi F., Enrione J., Osorio F., Aguilera J.M., (2010) 'Food hydrocolloid edible films and coatings', *Food science and technology series*. Nova Science Publishers, New York.
  270. Smith, T. L. and Jarvis, W. R. (1999) 'Antimicrobial resistance in *Staphylococcus aureus*', *Microbes and Infection*, 1(10), 795-805.
  271. Spann, C. T., Taylor, S. C. and Weinberg, J. M. (2003) 'Topical antimicrobial agents in dermatology', *Clinics in Dermatology*, 21(1), 70-77.
  272. Sriamornsak, P. and Kennedy, R. A. (2008) 'Swelling and diffusion studies of calcium polysaccharide gels intended for film coating', *International Journal of Pharmaceutics*, 358(1-2), 205-213.
  273. Sriamornsak, P., Wattanakorn, N., Nunthanid, J. and Puttipipatkachorn, S. (2008) 'Mucoadhesion of pectin as evidence by wettability and chain interpenetration', *Carbohydrate Polymers*, 74(3), 458-467.
  274. Stashak, T. S., Farstvedt, E. and Othic, A. (2004) 'Update on wound dressings: Indications and best use', *Clinical Techniques in Equine Practice*, 3(2), 148-163.
  275. Sweeney, I. R., Miraftab, M. and Collyer, G. (2012) 'A critical review of modern and emerging absorbent dressings used to treat exuding wounds', *International Wound Journal*, 9(6), 601-612.
  276. Szycher, M. and Lee, S. J. (1992) 'Modern Wound Dressings: A Systematic Approach to Wound Healing', *Journal of Biomaterials Applications*, 7(2), 142-213.
  277. Takahashi, Y., Sumita, I. and Tadokoro, H. (1973) 'Structural studies of polyethers. IX. Planar zigzag modification of poly(ethylene oxide)', *Journal of Polymer Science: Polymer Physics Edition*, 11(11), 2113-2122.
  278. Takahashi, Y. and Tadokoro, H. (1973) 'Structural Studies of Polyethers,  $(-(CH_2)_m-O-)_n$ . X. Crystal Structure of Poly(ethylene oxide)', *Macromolecules*, 6(5), 672-675.
  279. Tamburic, S. and Craig, D. Q. M. (1997) 'A comparison of different in vitro methods for measuring mucoadhesive performance', *European Journal of Pharmaceutics and Biopharmaceutics*, 44(2), 159-167.
  280. Tang, X. and Pikal, M. (2004) 'Design of Freeze-Drying Processes for Pharmaceuticals:

- Practical Advice', *Pharmaceutical Research*, 21(2), 191-200.
281. Tetteh, J., Mader, K. T., Andanson, J. M., McAuley, W. J., Lane, M. E., Hadgraft, J., Kazarian, S. G. and Mitchell, J. C. (2009) 'Local examination of skin diffusion using FTIR spectroscopic imaging and multivariate target factor analysis', *Analytica Chimica Acta*, 642(1-2), 246-256.
  282. Thakur, R. A., Florek, C. A., Kohn, J. and Michniak, B. B. (2008) 'Electrospun nanofibrous polymeric scaffold with targeted drug release profiles for potential application as wound dressing', *International Journal of Pharmaceutics*, 364(1), 87-93.
  283. Thirawong, N., Nunthanid, J., Puttipipatkachorn, S. and Sriamornsak, P. (2007) 'Mucoadhesive properties of various pectins on gastrointestinal mucosa: An in vitro evaluation using texture analyzer', *European Journal of Pharmaceutics and Biopharmaceutics*, 67(1), 132-140.
  284. Thomas, S. (2007) 'Fluid handling properties of alveyn dressing', *Wound Management Communication*, 1-8.
  285. Thomas, S. (1997) Assessment and management of wound exudate. *Journal of Wound Care*; 6(7): 327-330.
  286. Thomas, S. and Loveless, P. A. (1997) 'A comparative study of twelve hydrocolloid dressings', *World Wide Wounds* 1, 1-12.
  287. Thomas, S. S., Lawrence, J. C. and Thomas, A. (1995) 'Evaluation of hydrocolloids and topical medication in minor burns', *Journal of wound care*, 4(5), 218-20.
  288. Thu, H.E., Zulfakar, M. H. and Ng, S.F. (2012) 'Alginate based bilayer hydrocolloid films as potential slow-release modern wound dressing', *International Journal of Pharmaceutics*, 434(1-2), 375-383.
  289. Tobbyn, M. J., Johnson, J. R. and Dettmar, P. W. (1997) 'Factors affecting in vitro gastric mucoadhesion .4. Influence of tablet excipients, surfactants and salts on the observed mucoadhesion of polymers', *European Journal of Pharmaceutics and Biopharmaceutics*, 43(1), 65-71.
  290. Tonnesen, H. H. and Karlsen, J. (2002) 'Alginate in drug delivery systems', *Drug Development and Industrial Pharmacy*, 28(6), 621-630.
  291. Tudja, P., Khan, M. Z. I., Me, Scaron, Trovic, E., Horvat, M. and Golja, P. (2001) 'Thermal Behaviour of Diclofenac Sodium: Decomposition and Melting Characteristics', *Chemical and Pharmaceutical Bulletin*, 49(10), 1245-1250.
  292. Twumdanso, K., Grant, C., Alsuleiman, S. A., Abdelkader, S., Alawami, M. S.,

- Albreiki, H., Taha, S., Ashoor, A. A. and Wosornu, L. (1992) 'Microbiology of postoperative wound-infection - a prospective-study of 1770 wounds', *Journal of Hospital Infection*, 21(1), 29-37.
293. Varshney, L. (2007) 'Role of natural polysaccharides in radiation formation of PVA-hydrogel wound dressing', *Nuclear Instruments & Methods in Physics Research Section B-Beam Interactions with Materials and Atoms*, 255(2), 343-349.
294. Vermeulen, H., Van Hattem, J. M., Storm-Versloot, M. N. and Ubbink, D. T. (2007) 'Topical silver for treating infected wounds', *Cochrane Database of Systematic Reviews*, (1).
295. Vindenes, H. and Bjerknes, R. (1995) 'MICROBIAL COLONIZATION OF LARGE WOUNDS', *Burns*, 21(8), 575-579.
296. Vowden, K, Vowden P. (2004) The role of exudate in the healing process: understanding exudate management. In: White, R (ed). Trends in Wound Care: Volume III. Salisbury: Quay Books, MA Healthcare Ltd; 3-22.
297. Wang, L., Khor, E., Wee, A. and Lim, L. Y. (2002) 'Chitosan-alginate PEC membrane as a wound dressing: Assessment of incisional wound healing', *Journal of Biomedical Materials Research*, 63(5), 610-618.
298. Watson, N. F. S. and Hodgkin, W. (2005) 'Wound dressings', *Surgery (Oxford)*, 23(2), 52-55.
299. White, R. J., Cooper, R. and Kingsley, A. (2001) 'Wound colonization and infection: the role of topical antimicrobials', *British journal of nursing (Mark Allen Publishing)*, 10(9), 563-578.
300. White, R. and Cutting, K. F. (2006). Modern exudate management: a review of wound treatments. *World Wide Wounds*, 1, 1-5.
301. White, R. J., Cutting, K. and Kingsley, A. (2006) 'Topical antimicrobials in the control of wound bioburden', *Ostomy Wound Management*, 52(8), 26-58.
302. Wiechula, R. (2003) 'The use of moist wound-healing dressings in the management of split-thickness skin graft donor sites: a systematic review', *International Journal of Nursing Practice*, 9(2), S9-S17.
303. Wild, T., Rahbarnia, A., Kellner, M., Sobotka, L. and Eberlein, T. (2010) 'Basics in nutrition and wound healing', *Nutrition*, 26(9), 862-866.
304. Williams, R. O. Reynolds, T. D., Cabelka, T. D., Sykora, M. A. and Mahaguna, V. (2002) 'Investigation of excipient type and level on drug release from controlled release

- tablets containing HPMC', *Pharmaceutical Development and Technology*, 7(2), 181-193.
305. Wilson, A. P. R. (1995) 'Surveillance of wound infections', *Journal of Hospital Infection*, 29(2), 81-86.
  306. Winter, G. D. (1962) 'Formation of the scab and the rate of epithelialization of superficial wounds in the young domestic pig', *Nature*, 193, 293-4.
  307. Wittaya-areekul, S. and Prahsarn, C. (2006) 'Development and in vitro evaluation of chitosan-polysaccharides composite wound dressings', *International Journal of Pharmaceutics*, 313(1-2), 123-128.
  308. Wold, S., Sjostrom, M. and Eriksson, L. (2001) 'PLS-regression: a basic tool of chemometrics', *Chemometrics and Intelligent Laboratory Systems*, 58(2), 109-130.
  309. Wong, C. F., Yuen, K. H. and Peh, K. K. (1999) 'An in-vitro method for buccal adhesion studies: importance of instrument variables', *International Journal of Pharmaceutics*, 180(1), 47-57.
  310. Young, A. and McNaught, C. E. (2011) 'The physiology of wound healing', *Surgery (Oxford)*, 29(10), 475-479.
  311. Zaman, H. U., Islam, J. M., Khan, M. A. and Khan, R. A. (2011) 'Physico-mechanical properties of wound dressing material and its biomedical application', *Journal of the Mechanical Behavior of Biomedical Materials*, 4(7), 1369-1375.
  312. Zhai, M., Zhang, Y., Ren, J., Yi, M., Ha, H. and Kennedy, J. F. (2004) 'Intelligent hydrogels based on radiation induced copolymerization of N-isopropylacrylamide and Kappa carrageenan', *Carbohydrate Polymers*, 58(1), 35-39.
  313. Zhou, Y., Chu, J. S., Zhou, T. and Wu, X. Y. (2005) 'Modeling of dispersed-drug release from two-dimensional matrix tablets', *Biomaterials*, 26(8), 945-952.
  314. Zivanovic, S., Li, J., Davidson, P. M. and Kit, K. (2007) 'Physical, Mechanical, and Antibacterial Properties of Chitosan/PEO Blend Films', *Biomacromolecules*, 8(5), 1505-1510.
  315. Zurdo Schroeder, I., Franke, P., Schaefer, U. F. and Lehr, C.M. (2007) 'Development and characterization of film forming polymeric solutions for skin drug delivery', *European journal of pharmaceutics and biopharmaceutics:official journal of Arbeitsgemeinschaft fur Pharmazeutische Verfahrenstechnik e.V*, 65(1), 111-21.

## **Appendix**

### Appendix A: Manuscript in preparation

1. Development and characterisation of lyophilised wafers containing anti-microbial and anti-inflammatory drugs for effective wound healing.
2. Preparation and characterisation of alginate based antimicrobial film and wafer wound dressing for chronic wound healing.

1<sup>st</sup> UK Hydrocolloids Symposium, Yorkshire, UK (2013): Abstract#

## **Sodium alginate based antimicrobial wound dressings for chronic wound healing**

Harshavardhan V. Pawar<sup>1</sup>, Isaac Ayensu<sup>1</sup>, John Tetteh<sup>1</sup>, Joshua Boateng<sup>1</sup>,

<sup>1</sup>*Department of Pharmaceutical, Chemical & Environmental Sciences, School of Science, University of Greenwich at Medway, Central Avenue, Chatham Maritime, ME4 4TB, Kent UK.*

**Purpose:** This project involves preparation and physico-chemical characterisation of lyophilised antimicrobial wafers of Polyox<sup>™</sup> (POL) and sodium alginate (SA) containing streptomycin sulphate (STP) and diclofenac sodium (DLF) for chronic wounds to improve the wound healing process.

**Methods:** Gels were prepared by blending of POL and SA in a 50/50wt. ratio as described by (Boateng *et al.*, 2013) and loaded with 25%w/w STP and 10%w/w DLF. Gels were freeze dried with annealing at -25°C. Wafers were [(POL-SA-BLK and POL-SA-DL) BLK and DL stands for blank and drug loaded.] characterised by scanning electron microscopy (SEM), mechanical testing, mucoadhesion, swelling and *in vitro* drug release studies subsequently evaluated for antimicrobial efficacy against *Staphylococcus aureus*, *pseudomonas aeruginosa* and *Escherichia coli*.

**Results and discussion:** POL-SA (BLK and DL) wafers were soft, flexible and non-brittle in nature. Both wafers showed a porous texture with uniform pore size distribution. Wafers showed reduced hardness due to annealing however strong enough to cope with mechanical stresses while flexible enough to prevent potential damage to newly formed skin tissue. POL-SA (BLK and DL) wafers showed high work of adhesion and stickiness in presence of normal artificial exudate but decreased in presence of viscous artificial exudate. Cohesiveness was not

significantly changed with type of exudate. POL-SA-BLK wafers showed high swelling which decreased for POL-SA-DL wafers due to the added drug. 79.6±4.9% of STP and 33.2±5.6% of DLF was released in 72h from the POL-SA-DL wafers. These wafers showed higher zone of inhibition against 10<sup>5</sup> CFU/ml of *E. coli* (4.6±0.3mm) subsequently *P. aeruginosa* (4.1±0.2mm) and then *S. aureus* (3.3±0.1mm).

**Conclusion:** Prepared antimicrobial wafers have capacity to reduce bacterial infection by the action of STP and potentially in synergy with DLF while the latter can also help to reduce the swelling and pain associated with injury due to its the anti-inflammatory action.

**Reference:** Boateng, J. S., Pawar, H. V. and Tetteh, J. (2013) 'Polyox and carrageenan based composite film dressing containing anti-microbial and anti-inflammatory drugs for effective wound healing', *International Journal of Pharmaceutics*, 441(1-2), 181-191.

## Preparation and characterisation of novel medicated dressings for chronic wound healing



H. Pawar, J. Tetteh, J.S. Boateng.

Department of Pharmaceutical, Chemical & Environmental Sciences, School of Science, University of Greenwich at Medway, Central Avenue, Chatham Maritime, ME4 4TB, Kent UK.

ph26@gre.ac.uk

### INTRODUCTION

Chronic (non healing) wounds are a clinical challenge due to various complicating factors connected with wound. This project involves the development and characterisation of lyophilised Polyox™ (POL) and carrageenan (CAR) wafer dressings for supporting chronic wounds loaded with streptomycin (STP) and diclofenac (DLF) to target two phases of wound healing to achieve for effective healing.

### MATERIALS AND METHODS

Wafers were prepared from gels containing POL and CAR in a 75/25 ratio (1% total polymer weight) and loaded with 30% w/w STP and 25% w/w DLF. Gels were freeze-dried using a cycle incorporating an annealing step (determined by differential scanning calorimetry) as shown in figure 1. Wafers were characterised for morphology (SEM), mechanical strength and mucoadhesion (Texture analysis), swelling and *in vitro* drug release properties.

### RESULTS AND DISCUSSION

Annealing helped to improve the porosity resulting in POL-CAR wafers that were adequately flexible, elegant in appearance and non-brittle in nature. Surface morphology of the blank (BLK) wafers showed a homogeneous, sponge-like circular and interconnecting network, whereas the drug loaded (DL) wafers showed porous polymeric strands with decreased porosity due to the entrapment of drug within the polymer network (figure 2).

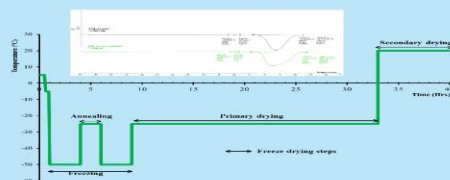


Figure 1: Steps involved in the freeze drying with annealing, (inset) DSC studies of the annealed and non-annealed gels.

Table 1: Swelling, mechanical strength and mucoadhesion (Texture analysis) properties of POL-CAR (BLK and DL) wafers.

Mucoadhesion (n=5)	POL-CAR-BLK		POL-CAR-DL	
	SWF-2% BSA	SWF-5% BSA	SWF-2% BSA	SWF-5% BSA
AVG (SD)	4.94±1.25	6.34±0.65	4.34±1.12	3.46±1.21
Stickiness (N)	4.94±1.25	6.34±0.65	4.34±1.12	3.46±1.21
Work of Adhesion (N.mm)	5.53±1.37	6.81±1.64	4.31±1.24	2.37±1.51
Cohesiveness (mm)	3.56±1.06	2.14±0.21	3.11±0.74	2.19±1.37
% Swelling index (n=5)				
POL-CAR-BLK		POL-CAR-DL		
3830.63±274.40		1449.96±362.34		
Hardness (N) (n=6)				
0.554±0.062		0.962±0.125		

Pore size morphologies affect functional properties such as rate of hydration, swelling, mucoadhesion and consequent drug release characteristics in the presence of wound exudate. Wafers with high porosity can absorb the high exudate due to high water ingress which leads to high swelling and subsequent diffusion of drug from the swollen matrix. Differences in swelling, mucoadhesion and *in vitro* drug release characteristics, could be

attributed to differences in pore size and drug present in the wafers.

DL wafers showed less swelling capacity compared to BLK though the DL wafers showed constant increase in swelling capacity. BLK wafers exhibited high stickiness, work of adhesion and cohesiveness in the presence of normal (2%BSA) and viscous (5% BSA) simulated wound fluid (SWF) (Table 1). A maximum of 81.37±3.81% of STP was released within 24 hours whilst a maximum of 73.58±3.77% DLF was released within 72 hours (figure 2).

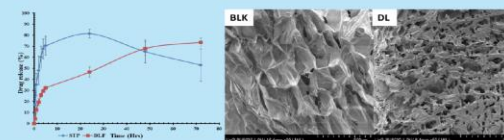


Figure 2: *In vitro* drug release profiles of POL-CAR-DL and SEM micrographs of POL-CAR (BLK and DL) wafers.

### CONCLUSIONS

The result of this study demonstrates that POL – CAR wafers were successfully prepared by freeze-drying, incorporating an annealing step. STP can prevent as well as treat bacterial infection within a wound whilst DLF can target the inflammatory phase of wound healing to relieve pain associated with injury. These wafers have the potential as dressings for drug delivery to wounds and will be tested for anti-microbial action in future.

### ACKNOWLEDGMENTS

The authors will like to thank Colorcon, UK for providing POL and to Dr Ian Slipper for his help with the SEM experiments and Devyani Amin for her help in HPLC experiments.

## Multi-targeted alginate based medicated wafers for chronic wound healing

H.V. Pawar, John Tetteh, Joshua Boateng,

Department of Pharmaceutical, Chemical & Environmental Sciences, Faculty of Engineering and Science, University of Greenwich at Medway, Central Avenue, Chatham Maritime, ME4 4TB, Kent UK.

Email: J.S.Boateng@gre.ac.uk

**Purpose:** Preparation and physico-chemical characterisation of lyophilised wafers of Polyox™ (POL)-sodium alginate (SA) loaded with diclofenac sodium (DLF) and streptomycin sulphate (STP) for application to chronic suppurating wounds to target inflammation and infection for improving the wound healing process.

**Methods:** The gels were prepared by combining POL and SA in a 50/50 weight ratio as described by (Boateng *et al.*, 2013) and loaded with 25%w/w STP and 10%w/w DLF. The gels were freeze dried as shown in Table 1. The wafers [(POL-SA-BLK and POL-SA-DL) (BLK = blank; DL = drug loaded)] were characterised by scanning electron microscopy (SEM), X-ray diffraction (XRD), Fourier transform infra-red (FTIR) spectroscopy, swelling studies and texture analysis (mechanical 'hardness' and mucoadhesion).

**Results and discussion:** Both BLK and DL wafers were soft, flexible and elegant in appearance and non-brittle in nature. POL-SA-BLK wafers showed elongated pores with sponge-like strands while POL-SA-DL wafers showed a less porous texture but uniform pore size distribution (Figure 1). The force required to penetrate (deform) the wafer increased with increasing depth (0.5-3.0 mm) and speed (0.2-3.0 mm/sec) of compression for all the wafers due to the arrangement of the polymer network which resists deformation (Table 2). POL-SA-DL wafers were mechanically stronger ('harder') compared to POL-SA-BLK. The wafers showed decreased crystallinity of POL (XRD) and a band shift at  $1105\text{cm}^{-1}$  C-O-C stretching due to hydrogen bonding between the POL and SA (FTIR). POL-SA-BLK wafers showed high swelling which decreased for POL-SA-DL wafers (Table 2) and could be attributed to the reduced porosity. POL-SA (BLK and DL) showed high work of adhesion and stickiness in the presence of normal (2% BSA) simulated wound exudate but decreased in the presence of viscous (5% BSA) simulated wound exudate whilst cohesiveness was not significantly changed ( $P < 0.9068$ ).

**Conclusion:** POL-SA wafers showed high absorption and adhesion which are necessary for formulations used as wound dressings. The optimised dressing has the potential to reduce bacterial infection by the action of STP and potentially in synergy with DLF while the latter can also help to reduce the swelling and pain associated with injury due to its the anti-inflammatory action. Work is ongoing with *in vitro* drug release and anti-bacterial studies.

**Reference:** Boateng, J.S., Pawar, H.V., Tetteh, J. (2013) 'Polyox and carrageenan based composite film dressing containing anti-microbial and anti-inflammatory drugs for effective wound healing', *International Journal of Pharmaceutics*, 441(1-2), 181-191.

**Preparation and evaluation of solvent cast film dressings containing streptomycin and diclofenac for wound healing**

H. V. Pawar, J. Tetteh, J. S. Boateng  
University of Greenwich

**Purpose**

Formulation and evaluation of Polyox® WSR301 (POL) and carrageenan (CAR) films loaded with streptomycin (STP) and diclofenac (DLF) to target different phases of wound healing. Evaluation involved *in vitro* characterisation (swelling, muco-adhesion and bacterial inhibition) performed to predict the functional performance of the dressings *in vivo*.

**Methods**

Films were prepared from gels containing POL and CAR in a 75/25 ratio (1% total weight of polymer) and loaded with 30% w/w STP and 10% w/w DLF. Glycerol (GLY) (25% w/w) was added as plasticizer and the gels dried in an oven at 40°C for 18 hrs. The blank (BLK) and drug loaded (DL) films [(POL-CAR-BLK, POL-CAR-BLK-25%GLY, POL-CAR-DL, POL-CAR-DL-25%GLY)] were evaluated for % swelling capacity in phosphate buffer solution (pH 7.3), muco-adhesion using simulated wound fluid (SWF), antibacterial activity by disk diffusion method and *in vitro* drug release with Franz cell at 37°C.

**Results**

Table 1 summarises results from swelling, adhesion, antibacterial, drug loading and release studies. Films obtained were homogeneous and of uniform thickness (0.09±0.01 mm), flexible and transparent in appearance. Plasticized films (POL-CAR-DL-25%GLY and POL-CAR-BLK-25%GLY) showed higher % swelling capacity compared to unplasticized films (POL-CAR-BLK and POL-CAR-DL). This was due to penetration of GLY into the polymer cross-linking. Antibacterial studies showed that films containing DLF and STP significantly increased zone of inhibition (ZOI) in bacterial strains of *Escherichia coli*, *Staphylococcus aureus* and *Pseudomonas aeruginosa* compared to the ZOI for each individual drug. Plasticized films showed higher peak adhesive force-*Fmax*, work of adhesion-WOA and cohesiveness, in contrast to unplasticized films. Plasticized films also showed higher drug loading [(89.78 ± 4.73%) STP], [87.85 (± 9.05) % DLF] and % drug release (60.03 ± 5.56% STP; 63.39 ± 1.92% DLF respectively) compared to unplasticized films (52.11 ± 2.38% STP and 55.26 ± 4.26% DLF) within 72 hrs.

**Conclusion**

Plasticized film dressings (POL-CAR-25%GLY-DL) containing both STP and DLF have been formulated and optimised. STP can prevent as well as treat bacterial infection within a wound whilst DLF can target the inflammatory phase of wound healing to relieve pain associated with injury. The optimised film has the potential to achieve more rapid wound healing.

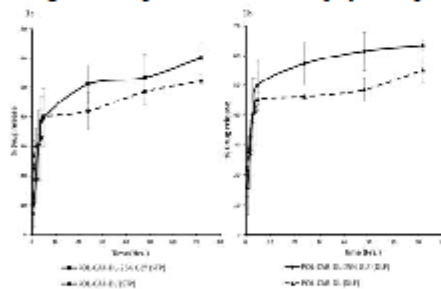


Figure 1. In vitro drug release profiles of STP and DLF from POL-CAR-BLK and POL-CAR-BLK-25%GLY.

Table 1. Summary of *in vitro* characterisation of POL-CAR films

Sample	No. of samples	Thickness (mm)	Adhesive (mN)		Antibacterial (mm)		% Drug loading	% Drug release	
			<i>Fmax</i>	W/OA	<i>E. coli</i>	<i>S. aureus</i>		STP	DLF
POL-CAR-BLK	10	0.09	1.23 ± 0.12	1.12 ± 0.11	5.0	5.0	52.11 ± 2.38	55.26 ± 4.26	
POL-CAR-BLK-25%GLY	10	0.09	1.52 ± 0.15	1.41 ± 0.14	10.0	10.0	89.78 ± 4.73	87.85 ± 9.05	
POL-CAR-DL	10	0.09	1.31 ± 0.13	1.20 ± 0.12	10.0	10.0	52.11 ± 2.38	55.26 ± 4.26	
POL-CAR-DL-25%GLY	10	0.09	1.60 ± 0.16	1.49 ± 0.15	10.0	10.0	89.78 ± 4.73	87.85 ± 9.05	
Reference STP	10	0.09	-	-	10.0	10.0	-	-	
Reference DLF	10	0.09	-	-	10.0	10.0	-	-	

## Preparation and characterization of Polyox™-carrageenan films containing antimicrobial and anti-inflammatory drugs for wound healing

H. Pawar<sup>1</sup>, J. Tetteh<sup>1</sup>, J.S. Boateng<sup>1</sup>.  
<sup>1</sup>School of Science, University of Greenwich at Medway, Kent, UK  
[ph26@gre.ac.uk](mailto:ph26@gre.ac.uk)



### INTRODUCTION

Solvent cast films prepared by combining natural and synthetic polymers is of particular significance due to their biocompatibility. This significance lies in the minimisation of the negative characteristics of each individual polymer whilst maximising the optimum properties of each in the resulting combined matrix.

### MATERIALS AND METHODS

Films were prepared from gels containing two polymers; Polyox™ WSR301 (POL) and carrageenan (CAR) in a 75/25 weight ratio and loaded with 30%w/w STP and 10%w/w DLF. Glycerol (GLY) (25% w/w) was added as plasticizer and the gels dried in an oven at 40°C for 18 hrs. The blank (BLK) and drug loaded (DL) films (POL-CAR-BLK, POL-CAR-25%GLY-BLK, POL-CAR-DL, POL-CAR-25%GLY-DL) were characterised by SEM, XRD, FTIR and *in vitro* drug release studies.

### RESULTS AND DISCUSSION

SEM of POL-CAR (BLK and DL) films containing 25% GLY and POL-CAR-BLK films showed smooth and homogeneous surface which reduced the characteristic spherulitic crystallisation of POL (Fig 1).

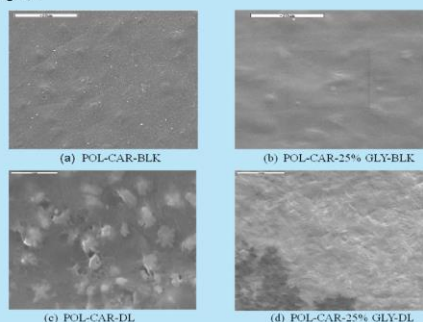


Fig.1. SEM images of films (a) POL-CAR-BLK (b) POL-CAR-25% GLY-BLK (c) POL-CAR-DL (d) POL-CAR-25% GLY-DL

XRD patterns (Fig 2) of POL-CAR-BLK films showed a reduction in the crystallisation of POL by interruption of POL chain interactions due to formation of hydrogen bonds between ether group of POL and the side chain groups of CAR. POL-CAR-25%GLY-BLK films showed a reduction in crystallinity due to the interpenetration of GLY into the POL-CAR crosslinking. POL-CAR-DL films showed high crystallinity due to the physical crosslinking of drugs and polymers, but this was decreased with the 25% w/w GLY. However, there were no distinct peaks of DLF and STP in the XRD spectra suggesting molecular dispersion of both drugs within the film.

FTIR spectra of the blended films showed significant differences in the region of C-O-C asymmetric stretch. The results show that the films have undergone a transition resulting in a band shift to lower wave number. POL showed C-O-C asymmetric stretch at 1099 cm<sup>-1</sup> which was shifted to 1097 cm<sup>-1</sup> due to weak hydrogen

bonding interaction between the POL and CAR.

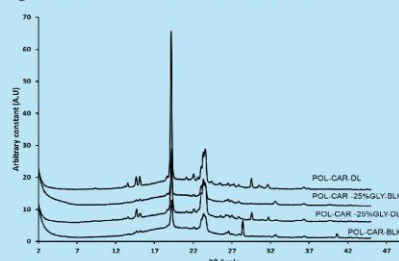


Fig. 2. XRD patterns of the films, from bottom POL-CAR-BLK, POL-CAR-25% GLY-DL, POL-CAR-25% GLY-BLK, POL-CAR-DL.

It was observed that the cumulative drug release from POL-CAR-25%GLY-DL films was higher (60.03 ± 5.56% STP, 63.39 ± 1.92% DLF) than the POL-CAR-DL (52.11 ± 2.38% STP and 55.26 ± 4.26% DLF). This may be due to the high miscibility of GLY with water involving the opening of channels in the films which facilitates solvent (dissolution medium) uptake, leading to an enhancement in the drug release from plasticized POL-CAR films [1]

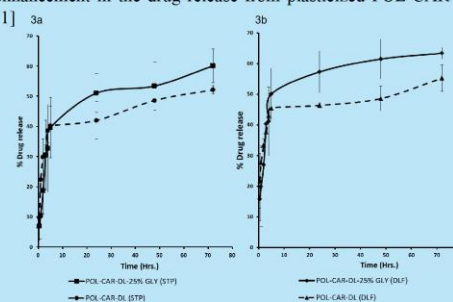


Fig. 3. *In vitro* drug release profiles of (a) STP and (b) DLF from POL-CAR-DL and POL-CAR-DL-25% GLY films. showing plot of mean percent cumulative release (n = 3; ± SD) against time.

### CONCLUSIONS

Films prepared from POL-CAR with 25% w/w GLY containing STP and DLF may have potential to be used as drug delivery film dressing to prevent and treat infections as well as reduce inflammation and pain. The ultimate result will be to allow more rapid wound healing.

### ACKNOWLEDGMENTS

The authors would like to acknowledge Dr. Ian Slipper for his help with SEM, XRD analyses.

### REFERENCES

- [1] E.P. Azevedo, T.D.P. Saldanha, M.V.M. Navarro, A.C. Medeiros, M.F. Ginani, F.N. Raffin, *Journal of Applied Polymer Science* 102 (2006) 3462.

**PREPARATION AND EVALUATION OF STREPTOMYCIN AND DICLOFENAC LOADED MUCOADHESIVE FILMS FOR WOUND HEALING**

H. V. Pawar<sup>1</sup>, J. Tetteh<sup>1</sup>, J. Boateng<sup>1</sup>; <sup>1</sup>School Of Science, University Of Greenwich, Chatham, KENT

Topic: Basic

Category: Wound Infection

Keywords: Polymer Blend, Solvent Cast Films, Wound Healing, Mucoadhesion, Antibacterial Study, In Vitro Drug Release

Solvent cast films comprising a synthetic [polyethylene oxide - Polyox™ WSR301 (POL)] and natural [carrageenan (CAR)] polymers together with streptomycin (anti-microbial) combined with diclofenac (anti-inflammatory) for synergistic action, with the aim of achieving enhanced wound healing effects have been prepared. The films containing different ratios of POL and CAR, plasticised with glycerol were characterised by swelling and hydration capacity, scanning electron microscopy (SEM), differential scanning calorimetry (DSC), texture analysis for mechanical properties and *in vitro* mucoadhesive properties. *In vitro* antibacterial studies using disk diffusion test and drug release profiles with Franz diffusion cell were conducted. SEM studies of unplasticized blank films showed presence of spherulitic crystals of POL with homogeneous interpenetrating polymer network. Both blank (BLK) and drug loaded (DL) films showed homogeneous morphology. DSC results of pure streptomycin and diclofenac showed a melt peak at 146.77°C and 293.96°C respectively, however this peak was absent in DL films indicating molecular dispersion of the drug. Films containing 25% w/w glycerol exhibited significantly ( $n=3$ ,  $P<0.001$ ) high work of adhesion, stickiness and cohesiveness with high hydration and swelling index corresponding to unplasticized films. BLK films containing glycerol showed higher tensile strength (TS) (1.1-12.3 MPa) than DL films (0.7-9.5 MPa). Film plasticized with 25 % w/w glycerol (1.00 MPa TS, 1031% elongation at break) revealed soft and tough formulation. Antibacterial studies showed that diclofenac and streptomycin significantly ( $n=3$ ,  $P<0.01$ ) increased zone of inhibition (ZOI) in *Escherichia coli*, *Staphylococcus aureus* and *Pseudomonas aeruginosa* in contrast to their individual ZOIs. Plasticized films showed significantly ( $n=2$   $P<0.0318$ ) higher cumulative % drug release of streptomycin and diclofenac (60.07±1.56%, 63.39±1.92% respectively) compared to unplasticized films (52.11±1.34%, 55.26±2.25%) within 72 hrs. Films prepared from POL and CAR containing streptomycin and diclofenac, have potential to prevent and treat wound infections and targets inflammatory phase of wound healing to relieve pain.

# Preparation and optimization of mucoadhesive films for local wound healing applications

H.V. Pawar<sup>1</sup>, J. Tetteh<sup>1</sup>, J.S. Boateng<sup>1</sup>  
 School of Science, University of Greenwich at Medway, Chatham Maritime, Kent ME4 4TB, UK



## Introduction

Several drug delivery systems including gels are currently used for treating infected wounds. This suffers from leakage, messiness and low residence time with poor contact with wound surfaces. This problem may be resolved using mucoadhesive films, which can help to improve wound healing and reduce the dosage frequency. This project involves the formulation and characterization of streptomycin loaded films prepared from polyox and carrageenan.

## Materials & Methods

Mucoadhesive films were prepared by solvent casting technique. In brief, 1% Polyox 301 (POL), 0.5% Carrageenan NF 812 (CAR) and glycerol (GLY) were dissolved in distilled water with constant stirring at 70°C. The temperature was reduced to 40°C during drug incorporation to avoid streptomycin degradation. The gel was poured into Petri dishes and dried at 40°C. The optimization of films was carried by varying the concentration of GLY and tested on texture analyzer. The optimized film was loaded with 20 % w/w of streptomycin and characterized by using SEM, XRD and DSC.

## Results & Discussion

Surface morphology of the films by SEM, is shown in figure 1. Blank films had a relatively rough surface with presence of white patches on the surface of film, but addition of streptomycin significantly affected the surface morphology of film. Films with 20%w/w drug loading had a homogeneous and smoother surface as compared to blank film. This may be due to molecular dispersion of streptomycin into the polymer matrix.

XRD data of films showed that the base peak of the POL disappeared with increased concentration of GLY. It also revealed that increasing the plasticizer concentration is responsible for the amorphous nature of the final film matrix. The characteristic peak (2θ) was observed for non plasticized drug loaded films for streptomycin at 9.2°, 14°, 19.2°, 23.1°, 26°, 28.4°, 29.2°, 32.8° but this was less intense for the plasticized films.



**Figure 1:** SEM image of film containing POL: CAR:GLY (2:1:1) with (A) Blank film (B) 20 % w/w of streptomycin

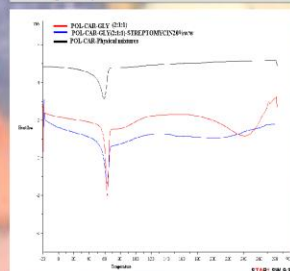


**Figure 2:** DSC curve of Polyox Carrageenan films with GLY and streptomycin and their physical mixtures.

## Results and Discussion

DSC curves of physical mixtures of POL-CAR and GLY and streptomycin containing films are shown in figure 2. The physical mixture had endothermic peak at 66.3°C which was similar to streptomycin loaded and blank films. Addition of GLY showed a broad peak at 238.0°C and an exothermic peak at 290.8°C which disappeared after addition of streptomycin. This indicates that streptomycin was molecularly dispersed in to plasticized polymeric films.

## Conclusions

Solvent cast POL-CAR films plasticized with GLY has optimum mechanical properties and streptomycin was uniformly dispersed into films and has great potential for wound healing applications.

## Acknowledgments

The authors would like to thank Colorcon, UK for providing HPMC and POL and to Dr Ian Slipper for his help with the SEM and XRD experiments

## References

[1] Radebaugh G.W, Murtha J.L, Julian T. N, Bondi J. N, "Methods for evaluating the puncture and shear properties of pharmaceutical polymeric films" *Int. J. Pharm*; **45** (1988) 39-46.

## Contact details

Mr. HARSHAVARDHAN PAWAR  
 University of Greenwich at Medway  
 School of Science ( Grenville Building)

Central Avenue  
 Chatham  
 Kent ME4 4TB  
 Tel: 020-8331-7570  
 E-mail: [ph26@gre.ac.uk](mailto:ph26@gre.ac.uk)

**Table 1:** Mechanical properties of plasticized films with different concentrations of GLY.

Type of films	GLY conc. (% w/w)	Tensile strength N/mm <sup>2</sup>	Elongation at break (%)	Young's Modulus (MPa)
Soft and weak	10	0.17	81.27	490.26
Hard and brittle	25	0.12	73.77	247.10
Soft and tough	50	0.07	96.07	231.16
Hard and tough	75	0.05	92.37	188.51

## Preparation and characterization of novel mucoadhesive films comprising polyox for wound healing applications.



H. Pawar<sup>1</sup>, J. Tetteh<sup>1</sup>, J.S. Boateng<sup>1</sup>.

<sup>1</sup>School of Science, University of Greenwich at Medway, Kent, UK

### INTRODUCTION

Solvent cast films from mucoadhesive polymers can be used as drug delivery carriers to moist surfaces such as wounds [1]. This paper describes the formulation and characterisation of polyox (POL) films modified with four different mucoadhesive hydrophilic polymers [three natural-sodium alginate (SA), carrageenan (CAR), chitosan (CS) and one semi-synthetic hydroxypropylmethylcellulose (HPMC)]. These solvent cast films have potential for wound healing application.

### MATERIALS AND METHODS

The films were prepared by solvent casting technique in ratios of 2:1 for POL to each of the other polymers. Briefly, polyox (POL) was hydrated in distilled water with constant stirring and heating, at 70°C. In a separate beaker, the other polymers (SA, CS, CAR, HPMC) were dissolved individually. The two gels were mixed to form a homogeneous gel. Gels were poured into Petri dishes, allowed to set and dried in an oven at 40°C. The films were characterised using SEM, DSC and XRD.

### RESULTS AND DISCUSSION

SEM was used to study the surface morphology of the solvent cast films (Fig 1A-1D). The POL-HPMC films had a smooth surface with POL-CAR films exhibiting homogeneous but rough surface. Films comprising POL-CS showed a rough surface with few visible crystals whilst surface crystallisation increased with SA. The presence of crystals on the SA and CS films caused discontinuities in the polymeric sheet.

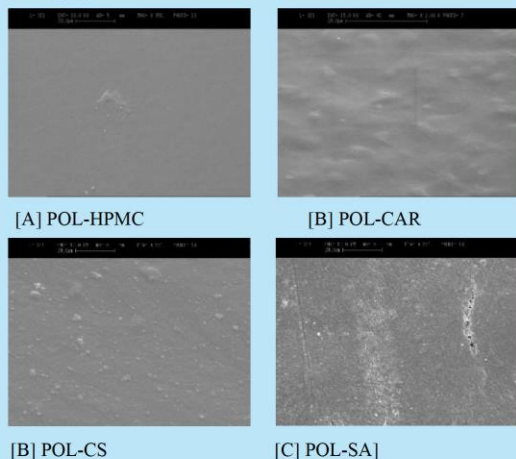


Fig.1.SEM images of the four different films of POL with other polymers

XRD analysis showed that POL is a semi-crystalline polymer with strong peaks at 2θ of 19.1° and 23.5° and a series of smaller peaks at 2θ of 13.4°, 14.6°, 26.1°, 32.5°, 36.1° and 39.3°. Narrow and weaker peaks at 23.5° and 19.1° were observed in POL-HPMC, POL-SA and POL-CS films compared to the pure POL.

Crystalline peaks associated with POL were absent or of low intensity in the POL-CAR films.. These findings suggest that CAR was partially miscible with the polyox, resulting in a decrease in POL crystallinity. Thermal properties of the films were also investigated using DSC. The melting point of pure POL was observed at 70.4°C. Films of POL with HPMC, SA, CAR and CS showed a depressed POL melt peak in the range of ~ 61°C - 65°C and with continuous heating, an exothermic (recrystallization) peak at 161.5°C, 160.7°C, 166.7°C and 172.4°C respectively. The benefit of the presence of the modifying hydrophilic polymers in POL films is reinforced by the significant depression of its melting point. A larger peak width of POL-CAR film revealed the reduction and broadening of the POL melting which could be due to the presence of less crystalline material and these results support the observations from the XRD.

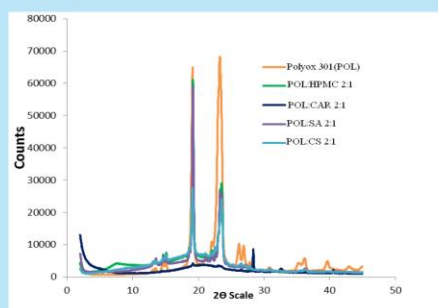


Fig.2 . X-Ray diffractograms of pure POL, POL-HPMC, POL-CAR, POL-SA, POL-CS films.

### CONCLUSIONS

The result of this study demonstrates that POL - CAR and POL - HPMC films (less crystalline with homogeneous surface) were successfully prepared by the solvent casting technique. These films will be characterised and tested as potential dressings for drug delivery to wounds.

### ACKNOWLEDGMENTS

The authors will like to thank Colorcon, UK for providing HPMC and POL and to Dr Ian Slipper for his help with the SEM and XRD experiments.

### REFERENCES

[1] A. De Ascentiis, J.L. deGrazia, C.N. Bowman, P. Colombo, N. Peppas, "Mucoadhesion of poly (2-hydroxyethyl methacrylate) is improved when linear poly (ethylene oxide) chains are added to polymer network". *J. Controlled Release*, **33** (1995), 197-201.

### Contact details

Mr. HARSHAVARDHAN PAWAR  
University of Greenwich at Medway  
School of Science ( Grenville Building)

Central Avenue  
Chatham Maritime  
Kent ME4 4TB

Tel: 020-8331-7570  
E-mail: [ph26@gre.ac.uk](mailto:ph26@gre.ac.uk)  
[pawarhv\\_21@yahoo.com](mailto:pawarhv_21@yahoo.com)

## Preparation and optimization of PMAA-PEG-Chitosan nanoparticles for oral drug delivery

H. Pawar, D. Douroumis, J. S. Boateng.

School of Science, University of Greenwich at Medway, Chatham Maritime, ME4 4TB, UK  
Ph836@gre.ac.uk

### INTRODUCTION

The aim of the study was to formulate spherical, bioadhesive nanoparticles for oral drug delivery system using a range of polymerisation approaches. Nanoparticles prepared from a combination of methacrylic acid (MAA), polyethylene glycol (PEG) and chitosan (CS) seems to be promising strategy for the oral drug delivery system. Such polymer complexes possess ideal mucoadhesive property [1].

### MATERIALS AND METHOD

Materials used included, MAA, PEG (MW 3,350), CS, ethylene glycol dimethacrylate (EDMA). Potassium per sulphate was used as initiator and model drug metoprolol was employed. Spherical nanoparticles were successfully prepared by the ionic gelation method (IGM) which involved mixing 2gm MAA, 0.05gm PEG, 0.2 gm EDMA and 0.02 gm chitosan in 300 ml of distilled water with constant stirring. After 15 minutes the polymer initiator was added to the solution, temperature was increased to 60°C and reaction continued for 6 hrs. The resulting suspension was left to settle down overnight, filtered with sintered glass and then freeze dried. The nanoparticles were evaluated by using Mastersizer<sup>®</sup>, SEM, DSC and XRD. Selected optimised nanoparticles with smallest particle sizes were loaded with metoprolol at two different concentrations (20 and 40 %). *In vitro* dissolution studies were carried out in USP dissolution bath for drug loaded particles.

### RESULT AND DISCUSSION

Table 1. Varying parameters during formulation development

Fn No.	Description	Particle Size (µm)
F1	Initial Formula	39±3 µm
F2	Increased water quantity (2X)	40±3 µm
F3	Use of glycol chitosan	300±3 µm
F4	Increased polymer initiator (5X)	130±10 µm
F5	Increased PEG and decreased chitosan concentration	62±2 µm
F6	Homogenisation	145±5 µm

The formulation development is summarised in table 1. Data obtained from SEM analysis revealed that particles obtained from preliminary formulation were in the micrometer size range, due to aggregates of spherical nanoparticles. Therefore the IGM approach was the method of choice for preparing nanoparticles for drug

loading. DSC analysis showed no melt peak whilst XRD data showed no intense peak indicating molecular dispersion of the metoprolol in polymer matrix.

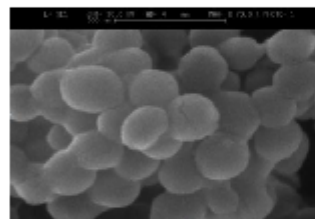


Fig. 1. SEM image of nanoparticles

Drug incorporation of 20.68% and 29.30% were achieved respectively for the two different metoprolol concentrations initially loaded. Dissolution studies were carried out in acidic and basic pH by using 0.1N HCl and phosphate buffer of pH6.8. The drug release profile illustrates that both formulations have immediate and high percent of drug release in the acidic medium whereas slow and prolonged release was achieved at alkaline pH.

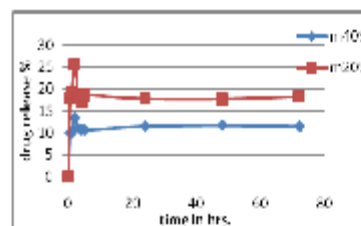


Fig. 2. Drug release profiles of formulations.

### CONCLUSION

IGM was successfully implemented for the preparation of smooth, spherical nanoparticles suitable for oral drug delivery. In dissolution studies, acidic medium showed immediate release due to the drastic swelling of polymers. Although prolonged drug release was seen in alkaline pH, extent of release was low. Hence further studies on extent of drug release in alkaline media are being carried out.

### ACKNOWLEDGEMENTS

The authors will like to thank Dr Ian Slipper for his help with SEM and XRD experiments.

### REFERENCE

S. Sajjosh, K. Bouchemal, C.P. Sharma, and C. Vauthier, "Surface functionalised polymethacrylic acid based hydrogel microparticles for oral drug delivery" *Eur. J. Pharm Biopharm.*, 74 (2010) 209-218.